

STUDIES OF SN/B BISMETALIC ARENES,
ELECTRONIC-DRIVEN AROMATIC C-H BORYLATION CATALYZED BY
IR-ELECTRON DEFICIENT BIPYRIDINE LIGANDS, AND
DESYMMETRIZATION OF DIBORYL AROMATICS

By

Hao Li

A DISSERTATION

Submitted to
Michigan State University
in partial fulfillment of the requirements
for the degree of

Chemistry - Doctor of Philosophy

2016

ABSTRACT

STUDIES OF SN/B BISMETALIC ARENES, ELECTRONIC-DRIVEN AROMATIC C-H BORYLATION CATALYZED BY IR-ELECTRON DEFICIENT BIPYRIDINE LIGANDS, AND DESYMMETRIZATION OF DIBORYL AROMATICS

By

Hao Li

Ir-catalyzed C-H activation/borylation was first reported in 1999.¹ Within two decades this methodology evolved into a synthetic protocol to install a boron group on a pre-functionalized benzene or heterocycle.² Earlier studies have characterized many features of this methodology. The Ir-catalyzed C-H activation/borylation tolerates a wide variety of functionalities pre-installed on the aryl or heteroaryl substances. It was also both predicted computationally and proven experimentally that the Ir-catalyzed C-H activation/borylation favors more acidic C-H bonds.³ Also demonstrated experimentally, steric effects govern the regioselectivity of the Ir-catalyzed C-H activation/borylation in most cases.⁴

My studies covered these topics: 1. Synthesis of boron/tin bimetallic arenes and chemoselective Suzuki coupling of these compounds;⁵ 2. Electronics driven regioselective Ir-catalyzed C-H activation/borylation of fluorinated benzenes.⁶ And 3. Desymmetrization of symmetrically diborylated benzenes.⁷

Copyright by
HAO LI
2016

To
My family, friends, professors, and colleagues

TABLE OF CONTENTS

LIST OF TABLES	vii
----------------------	-----

LIST OF FIGURES	viii
-----------------------	------

Chapter 1 Synthesis And Suzuki Coupling Of B/Sn Bimetallic Arenes.....1

1.1 Introduction.....	1
1.2 Proposed pathways to bimetallic arenes.....	5
1.3 Selective suzuki coupling of the b/sn bimetallic arenes.....	9
1.4 Experimental section.....	12
1.5 Summary	21

Chapter 2 Electronics Driven Regioselective Ir-Catalyzed C-H

Activation/Borylation Of Fluorinated Benzenes..... 22

2.1 Introduction.....	22
2.2 Screening borylation conditions	31
2.3 Ligand effects hypothesis	33
2.4 Searching for new ligands.....	34
2.5 Results and discussions.....	37
2.6 Tandem borylation-Suzuki coupling.....	41
2.7 Kinetics study of the borylations with electron deficient ligands.....	42
2.7.1 Preparation of stock solutions.....	43
2.7.2 Preparation of stock solutions.....	44
2.7.3 Preparation of stock solutions.....	46
2.7.4 Preparation of stock solutions.....	49
2.7.5 Preparation of stock solutions.....	51
2.7.6 Preparation of stock solutions.....	53
2.7.7 Preparation of stock solutions.....	55
2.8 Probing the ligand decomposition	57
2.9 Degradation of ttfbpy during borylation.....	60
2.10 Borylation under a H ₂ atmosphere.....	61
2.11 Temperature effect or borylation reagent effect	65
2.12 Summary	66
2.13 Experimental.....	67

Chapter 3 Desymmetrization Of Diboryl Aromatics..... 86

3.1 Introduction.....	86
3.2 Synthesis of the (PinB)Ar(BF ₃)Cs salts.....	90
3.2.1 Desymmetrizing 2,2'-(5-bromo-2-fluoro-1,3-phenylene)bis(BPin)	90
3.2.2 Desymmetrizing 2,2'-(5-methoxy-2-fluoro-1,3-phenylene)bis(BPin).....	91

3.3 Synthesis of the (PinB)Ar(BMida)	92
3.4 Summary	102
APPENDIX.....	104
REFERENCES.....	224

LIST OF TABLES

Table 1. Attempts of borylation of arylstannanes	6
Table 2. Stannylation of bromophenyl boronic esters	8
Table 3. Base screening for selective Suzuki couplings of B/Sn bismetallic arenes	10
Table 4. Selective Suzuki coupling of 2a-f with 8	11
Table 5. Borylation screening	32
Table 6. Borylation screening with bpy(CF ₃) _x ligands	38
Table 7. Borylation of 12a by HBPIn	41
Table 8. Tandem borylation-Suzuki coupling	42
Table 9. Summary of kinetic studies at high concentration	49
Table 10. First order kinetic behavior of borylation of 12a	53
Table 11. Results of kinetic studies of the borylation of 12c	56
Table 12. Desymmetrizing 2,2'-(5-methoxy-2-fluoro-1,3-phenylene)bis(BPin).....	91

LIST OF FIGURES

Figure 1. Different types of bifunctional cross coupling partners	1
Figure 2. Knochel's cross-coupling cascade synthesis of mepanipyrim	2
Figure 3. One pot C-N/C-C bond formations sequence.....	2
Figure 4. Synthesis and Stille coupling of 1,4-B/Sn diene compound.....	3
Figure 5. Synthesis and Stille coupling of a 1,4-B/Sn benzene	3
Figure 6. Staubitz's Sn/B thiophene building block and Stille/Suzuki CCR's sequence	4
Figure 7. Wang's Sandmeyer-type borylation-reduction-stannylation sequence on nitro-aniline and their Stille/Suzuki CCR's	4
Figure 8. Chmeoselective Suzuki coupling of B/Sn bismetallic diene	5
Figure 9. Proposed routes to m-B/Sn bismetallic arenes	6
Figure 10. Synthesis of B/Sn bismetallic arenes via Pd catalyzed stannylation.....	7
Figure 11. Synthesis of 2a via Zn mediated stannylation.....	7
Figure 12. Attempts of stannylation on bromoheteroaryl boronic esters.....	9
Figure 13. Suzuki couplings of 1f and 2f with various electrophiles	12
Figure 14. Structure of fludrocortisone.....	22
Figure 15. Ritter's fluoride derived late stage fluorination, and applications on complicated molecules	23
Figure 16. Borylation of fluorobenzenes or fluorination of aromatic boronic acids and/or esters	24
Figure 17. General Scheme of Balz-Shiemann reaction.....	24
Figure 18. Fluorination with DAST.....	25
Figure 19. An example of asymmetric electrophilic fluorination.....	25

Figure 20. Palladium catalyzed electrophilic C-H fluorinations	25
Figure 21. Lithiation/borylation at cryogenic condition and its possible risk	26
Figure 22. General scheme of a Suzuki-Miyaura coupling reaction	27
Figure 23. Ingelsohn's electrophilic aromatic borylation	27
Figure 24. Sandmeyer type borylation of ortho fluoroanilines	28
Figure 25. Pt-catalyzed C-H activation/borylation on fluorobenzene	28
Figure 26. Borylation ortho to F on a 1,4-substituted benzene	28
Figure 27. Possible synthetic routes for regioselective borylation on 1-fluoro-3-chloro- benzene derivatives	29
Figure 28. Regiochemical outcomes in borylation of 1,3-disubstituted benzenes	30
Figure 29. Ligands used for screening	31
Figure 30. Literature synthesis of bis- and tetra- CF ₃ substituted bipyridines	34
Figure 31. Improving the synthesis of 4,4-bistrifluoromethyl bipyridine (btfbpy)	35
Figure 32. Proton NMR of the mixture of reduction products, aliphatic part	36
Figure 33. Proton NMR of the mixture of reduction products, aromatic part	36
Figure 34. ¹⁹ F NMR of the mixture of reduction products	37
Figure 35. Improving the synthesis of 4,4',5,5'-tetratetrafluoromethyl bipyridine (ttfbpy) ..	38
Figure 36. Resurrecting the borylation	39
Figure 37. Borylation by HBPIn	40
Figure 38. Synthesis of pre-assembled catalyst	43
Figure 39. Kinetic study of the borylation of 12a	43
Figure 40. First order fitting for the reaction described in 2.7.1	44
Figure 41. ¹⁹ F NMR of the CF ₃ region, from bottom to top: 0.0, 1.0, 2.3, 3.5, 4.8, 6.0 hours after substrate (12a) was added	45

Figure 42. Kinetic study of the borylation of 12a	45
Figure 43. 1st order fitting for the reaction described in 2.7.2	46
Figure 44. ¹⁹ F NMR of the CF ₃ region, from bottom to top: 0.0, 1.0, 2.3, 3.5, 4.8, 6.0 hours after substrate (12a) was added.....	47
Figure 45. Kinetic study of the borylation of 12a	47
Figure 46. 1 st order fitting for the reaction described in 2.7.3	48
Figure 47. ¹⁹ F NMR of the CF ₃ region, from bottom to top: 0.0, 1.0, 2.3, 3.5, 4.8, 6.0 hours after substrate (12a) was added.....	48
Figure 48. Kinetic study of the borylation of 12a	49
Figure 49. First order fitting for the reaction described in 2.7.4.....	50
Figure 50. ¹⁹ F NMR of the CF ₃ region, from bottom to top: 0.0, 1.0, 2.3, 3.5, 4.8, 6.0 hours after substrate (12a) was added.....	51
Figure 51. Kinetic study of the borylation of 12a	51
Figure 52. First order fitting for the reaction described in 2.7.5.....	51
Figure 53. ¹⁹ F NMR of the CF ₃ region, from bottom to top: 0.0, 1.0, 2.3, 3.5, 4.8, 6.0 hours after substrate (12a) was added.....	53
Figure 54. Kinetic study of the borylation of 12c	54
Figure 55. First order fitting for the reaction described in 2.7.6.....	54
Figure 56. Kinetic study of borylation of 12c	55
Figure 57. First order fitting for the reaction described in 2.7.7.....	56
Figure 58. ¹ H NMR of the preassembled catalyst (15) treated by B ₂ Pin ₂ and HBPIn in THF- <i>d</i> ₈ , top: Compound 15 , mid: Compound 15 and 5 equiv B ₂ Pin ₂ after 4 h at 298 K, bottom: Additional 5 equiv HBPIn added, then after 4 h at 298 K	57
Figure 59. ¹¹ B NMR of the preassembled catalyst (15) treated by B ₂ Pin ₂ and HBPIn in THF- <i>d</i> ₈ , top: Compound 15 , mid: Compound 15 and 5 equiv B ₂ Pin ₂ after 4 h at 298 K, bottom: Additional 5 equiv HBPIn added, then after 4 h at 298 K.....	58

Figure 60. ^{19}F NMR of the preassembled catalyst (15) treated by B_2Pin_2 and HBPIn in THF- d_8 , top: Compound 15 , mid: Compound 15 and 5 equiv B_2Pin_2 after 4 h at 298 K, bottom: Additional 5 equiv HBPIn added, then after 4 h at 298 K.....	59
Figure 61. Borylation of 12a by stoichiometric 15	59
Figure 62. Borylation of 12c by stoichiometric Ir and ttfbpy	60
Figure 63. Borylation of 12c with stoichiometric Ir and ttfbpy, top: Before heating, mid: 4.5 h Heating, bottom: 9 h Heating.....	61
Figure 64. H_2 influence on borylation.....	62
Figure 65. Conversions of the borylation of 12a with HBPIn affected by H_2	62
Figure 66. Regioselectivity of the borylation of 12a with HBPIn affected by H_2	63
Figure 67. H_2 influence on borylation.....	63
Figure 68. Borylation of 12a by HBPIn affected by H_2	64
Figure 69. Borylation of 12a by HBPIn affected by H_2	64
Figure 70. Borylation of 12a by HBPIn with btfbpy at high temperature	65
Figure 71. Borylation of 12a by HBPIn at high temperature.....	66
Figure 72. Borylation with B_2Pin_2 at higher temperature.	67
Figure 73. Borylation of substrate 12d	73
Figure 74. Suginome's B(dan) protection groups.....	86
Figure 75. Molander's exploitation of ArBF_3M salts	86
Figure 76. Burk's exploitation of Mida protected boron	87
Figure 77. Two approaches toward unsymmetric diborates	88
Figure 78. Desymmetrizing $\text{Ar}(\text{BPin})_2$ by H_2Mida	88
Figure 79. Desymmetrizing $\text{Ar}(\text{BPin})_2$ via $\text{Ar}(\text{BPin})\text{BF}_3\text{M}$ salt	89
Figure 80. Desymmetrizing 2,2'-(5-bromo-2-fluoro-1,3-phenylene)bis(BPin)	89

Figure 81. Desymmetrizing 2,2'-(5-methoxy-2-fluoro-1,3-phenylene)bis(BPin) in water.....	91
Figure 82. ^1H NMR of PhBF_3Cs in CD_3CN	92
Figure 83. ^{11}B NMR of PhBF_3Cs in CD_3CN	93
Figure 84. ^{19}F NMR of PhBF_3Cs in CD_3CN	94
Figure 85. ^{11}B NMR after adding 1 equiv TMSCl	94
Figure 86. ^{19}F NMR after adding 1 equiv TMSCl	95
Figure 87. ^{11}B NMR after adding 2 equiv TMSCl	95
Figure 88. Activation of PhBF_3Cs by TMSCl	95
Figure 89. Formation of PhBF_3^- after adding Na_2Mida	96
Figure 90. Protection of PhBF_2 by Mida ligand in DMSO	96
Figure 91. ^{19}F NMR after adding 2 equiv TMSCl	96
Figure 92. ^1H NMR of the crude product of Figure 90 in DMSO-d_6	97
Figure 93. ^{11}B NMR of the crude product of Figure 90 in DMSO-d_6	98
Figure 94. Optimization of the reaction conditions	99
Figure 95. Attempted transformation of 17a	100
Figure 96. Stepwise transformation of 17a and 17b	100
Figure 97 ^{119}Sn NMR of compound 2a	105
Figure 98 ^{11}B NMR of compound 2a	106
Figure 99 ^{13}C NMR of compound 2a	107
Figure 100 ^1H NMR of compound 2a	108
Figure 101 ^{119}Sn NMR of compound 2b	109
Figure 102 ^{11}B NMR of compound 2b	110
Figure 103 ^{13}C NMR of compound 2b	111

Figure 104 ^{19}F NMR of compound 2b	112
Figure 105 ^1H NMR of compound 2b	113
Figure 106 ^{119}Sn NMR of compound 2c	114
Figure 107 ^{11}B NMR of compound 2c	115
Figure 108 ^{13}C NMR of compound 2c	116
Figure 109 ^1H NMR of compound 2c	117
Figure 110 ^{119}Sn NMR of compound 2d	118
Figure 111 ^{11}B NMR of compound 2d	119
Figure 112 ^{13}C NMR of compound 2d	120
Figure 113 ^1H NMR of compound 2d	121
Figure 114 ^{119}Sn NMR of compound 2e	122
Figure 115 ^{11}B NMR of compound 2e	123
Figure 116 ^{13}C NMR of compound 2e	124
Figure 117 ^1H NMR of compound 2e	125
Figure 118 ^{119}Sn NMR of compound 2f	126
Figure 119 ^{11}B NMR of compound 2f	127
Figure 120 ^{13}C NMR of compound 2f	128
Figure 121 ^{19}F NMR of compound 2f	130
Figure 122 ^1H NMR of compound 2f	130
Figure 123 ^{119}Sn NMR of compound 4a	131
Figure 124 ^{13}C NMR of compound 4a	132
Figure 125 ^1H NMR of compound 4a	133
Figure 126 ^{119}Sn NMR of compound 4b	134

Figure 127 ^{13}C NMR of compound 4b	135
Figure 128 ^{19}F NMR of compound 4b	136
Figure 129 ^1H NMR of compound 4b	137
Figure 130 ^{119}Sn NMR of compound 4c	138
Figure 131 ^{13}C NMR of compound 4c	139
Figure 132 ^1H NMR of compound 4c	140
Figure 133 ^{119}Sn NMR of compound 4d	141
Figure 134 ^{13}C NMR of compound 4d	142
Figure 135 ^1H NMR of compound 4d	143
Figure 136 ^{119}Sn NMR of compound 4e	144
Figure 137 ^{13}C NMR of compound 4e	145
Figure 138 ^1H NMR of compound 4e	146
Figure 139 ^{119}Sn NMR of compound 4f	147
Figure 140 ^{13}C NMR of compound 4f	148
Figure 141 ^{19}F NMR of compound 4f	149
Figure 142 ^1H NMR of compound 4f	150
Figure 143 ^{119}Sn NMR of compound 5	151
Figure 144 ^{13}C NMR of compound 5	152
Figure 145 ^1H NMR of compound 5	153
Figure 146 ^{119}Sn NMR of compound 7	154
Figure 147 ^{13}C NMR of compound 7	155
Figure 148 ^1H NMR of compound 7	156
Figure 149 ^{13}C NMR of compound 11	157

Figure 150 ^{19}F NMR of compound 11	158
Figure 151 ^1H NMR of compound 11	159
Figure 152 ^1H NMR of mixture of compounds 13d and 13d'	160
Figure 153 ^{11}B NMR of mixture of compounds 13d and 13d'	161
Figure 154 ^{13}C NMR of mixture of compounds 13d and 13d'	162
Figure 155 ^{19}F NMR of mixture of compounds 13d and 13d'	163
Figure 156 ^1H NMR of mixture of compounds 13e and 13e'	164
Figure 157 ^{11}B NMR of mixture of compounds 13e and 13e'	165
Figure 158 ^{13}C NMR of mixture of compounds 13e and 13e'	166
Figure 159 ^{19}F NMR of mixture of compounds 13e and 13e'	167
Figure 160 ^1H NMR of mixture of compounds 13f and 13f'	168
Figure 161 ^{11}B NMR of mixture of compounds 13f and 13f'	169
Figure 162 ^{13}C NMR of mixture of compounds 13f and 13f'	170
Figure 163 ^{19}F NMR of mixture of compounds 13f and 13f'	171
Figure 164 ^1H NMR of mixture of compounds 13a and 13a'	172
Figure 165 ^{11}B NMR of mixture of compounds 13a and 13a'	173
Figure 166 ^{13}C NMR of mixture of compounds 13a and 13a'	174
Figure 167 ^{19}F NMR of mixture of compounds 13a and 13a'	175
Figure 168 ^1H NMR of mixture of compounds 13c and 13c'	176
Figure 169 ^{11}B NMR of mixture of compounds 13c and 13c'	177
Figure 170 ^{13}C NMR of mixture of compounds 13c and 13c'	178
Figure 171 ^{19}F NMR of mixture of compounds 13c and 13c'	179
Figure 172 ^1H NMR of mixture of compounds 13b and 13b'	180

Figure 173 ¹¹ B NMR of mixture of compounds 13b and 13b'	181
Figure 174 ¹³ C NMR of mixture of compounds 13b and 13b'	182
Figure 175 ¹⁹ F NMR of mixture of compounds 13b and 13b'	183
Figure 176 ¹ H NMR of compound 14a	184
Figure 177 ¹³ C NMR of compound 14a	185
Figure 178 ¹⁹ F NMR of compound 14a	186
Figure 179 ¹ H NMR of compound 14a'	187
Figure 180 ¹³ C NMR of compound 14a'	188
Figure 181 ¹⁹ F NMR of compound 14a'	189
Figure 182 ¹ H NMR of mixture of compounds 14b and 14b'	190
Figure 183 ¹⁹ F NMR of mixture of compounds 14b and 14b'	191
Figure 184 ¹ H NMR of compound 14b'	192
Figure 185 ¹³ C NMR of compound 14b'	193
Figure 186 ¹⁹ F NMR of compound 14b'	194
Figure 187 ¹ H NMR of compound 14c	195
Figure 188 ¹³ C NMR of compound 14c	196
Figure 189 ¹⁹ F NMR of compound 14c	197
Figure 190 ¹ H NMR of compound 14c'	198
Figure 191 ¹³ C NMR of compound 14c'	199
Figure 192 ¹⁹ F NMR of compound 14c'	200
Figure 193 ¹ H NMR of compound 14d	201
Figure 194 ¹³ C NMR of compound 14d	202
Figure 195 ¹⁹ F NMR of compound 14d	203

Figure 196 ^1H NMR of compound 14d'	204
Figure 197 ^{13}C NMR of compound 14d'	205
Figure 198 ^{19}F NMR of compound 14d'	206
Figure 199 ^1H NMR of mixture of compounds 14e and 14e'	207
Figure 200 ^{13}C NMR of mixture of compounds 14e and 14e'	208
Figure 201 ^{19}F NMR of mixture of compounds 14e and 14e'	209
Figure 202 ^1H NMR of mixture of compounds 14f and 14f'	210
Figure 203 ^1H NMR of mixture of compounds 14f and 14f'	211
Figure 204 ^{19}F NMR of mixture of compounds 14f and 14f'	212
Figure 205 ^1H NMR of mixture of compounds 17a and 18a	213
Figure 206 ^{11}B NMR of mixture of compounds 17a and 18a	214
Figure 207 ^{19}F NMR of mixture of compounds 17a and 18a	215
Figure 208 ^1H NMR of compound 17b	216
Figure 209 ^{13}C NMR of compound 17b	217
Figure 210 ^1H NMR of compound 19a	218
Figure 211 ^{13}C NMR of compound 19a	219
Figure 212 ^1H NMR of compound 19b	220
Figure 213 ^{11}B NMR of compound 19b	221
Figure 214 ^{13}C NMR of compound 19b	222
Figure 215 ^{19}F NMR of compound 19b	223

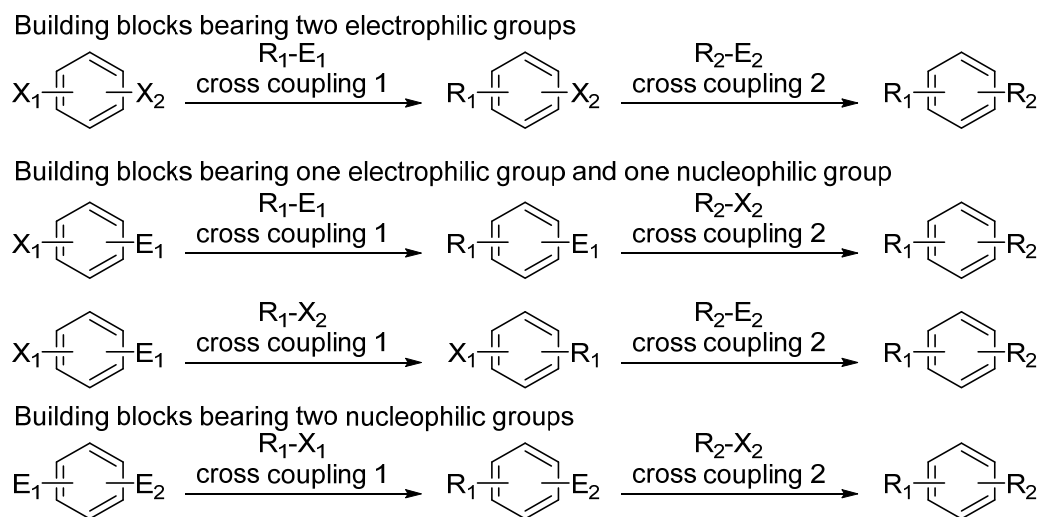
Chapter 1 Synthesis and Suzuki Coupling of

B/Sn Bimetallic Arenes

1.1 Introduction

Transition metal catalyzed cross-coupling reactions are powerful tools for C-C bond formations.⁸ Suzuki couplings⁹ and Stille couplings¹⁰ have found wide applications in the synthesis of both simple and complex molecules. Molecules that bear two functional groups that can participate in a sequence of controlled tandem two-step cross couplings are potential powerful building blocks for organic synthesis. One can consider there to be three different models of such building blocks: Molecules with two nucleophilic groups, molecules with one nucleophilic group and one electrophilic group, and molecules with two electrophilic groups (**Figure 1**).

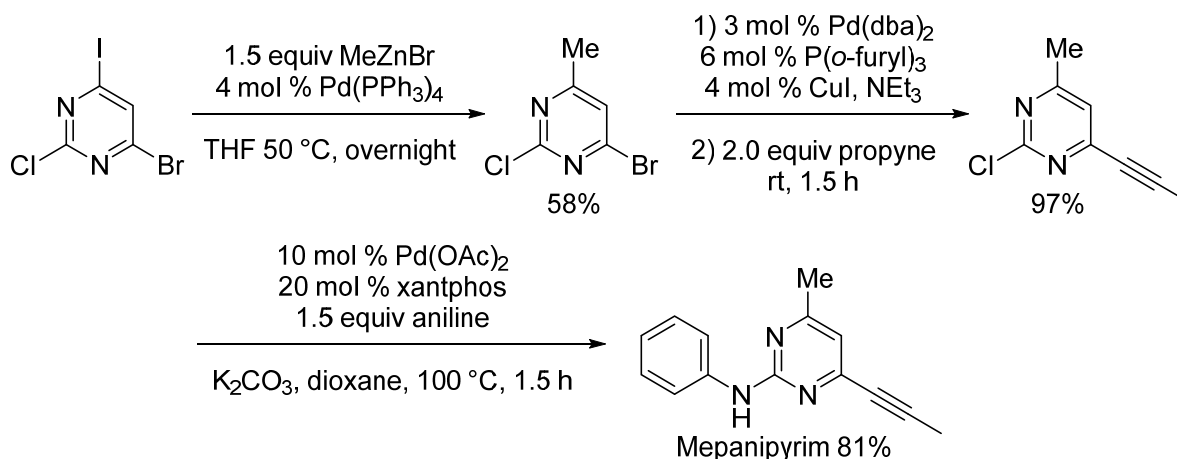
Figure 1. Different types of bifunctional cross coupling partners



The electrophilic partners of transition metal catalyzed cross-coupling reactions typically display a sequence of reactivity of I > Br >= OTf >> Cl.¹¹ Based on this order, electrophile selective cross couplings have been realized.¹² One brilliant cascade of Negishi, Sonagashira, and Buchwald-

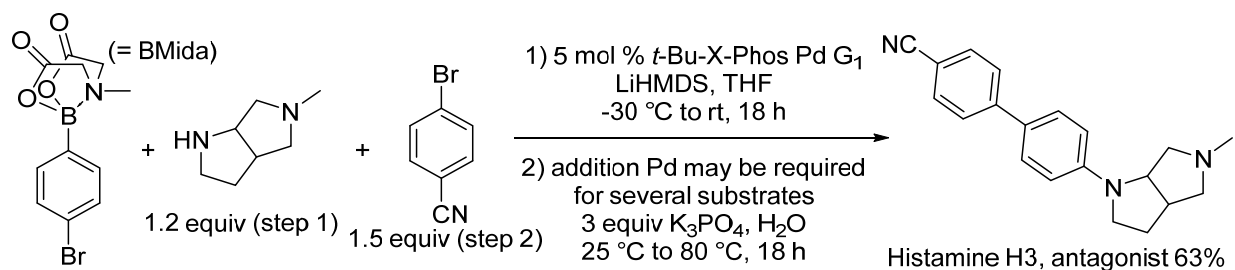
Hartwig cross-couplings with a chloro-bromo-iodopyrimidine led to the synthesis of mepaniprym, as demonstrated in **Figure 2**.

Figure 2. Knochel's cross-coupling cascade synthesis of mepaniprym



In contrast nucleophile-selective cross-coupling reactions are less developed. Several examples of Buchwald-Hartwig cross-coupling reactions on a bromobenzene bearing a boron group exist. Jonathan Grob and his team demonstrated a one pot strategy of Buchwald-Hartwig and Suzuki cross-coupling reactions for C-N and C-C bond formations (**Figure 3**).¹³ Several examples involving boron groups of different reactivity will be discussed in Chapter 3.

Figure 3. One pot C-N/C-C bond formations sequence



Hetero-bimetallic compounds bearing both boron and tin have served as versatile synthetic building blocks. The laboratories of Carboni,¹⁴ Coleman,¹⁵ Snieckus,¹⁶ and Burke¹⁷ (one example is illustrated in **Figure 4**) are among those to have developed preparations of boron/tin (B/Sn)

bissubstituted dienes and trienes. These bismetallated species can undergo preferential Stille reaction by running the Pd-catalyzed cross-coupling in the absence of base. The remaining boronic ester then can undergo a second cross-coupling under standard Suzuki conditions.

Figure 4. Synthesis and Stille coupling of 1,4-B/Sn diene compound

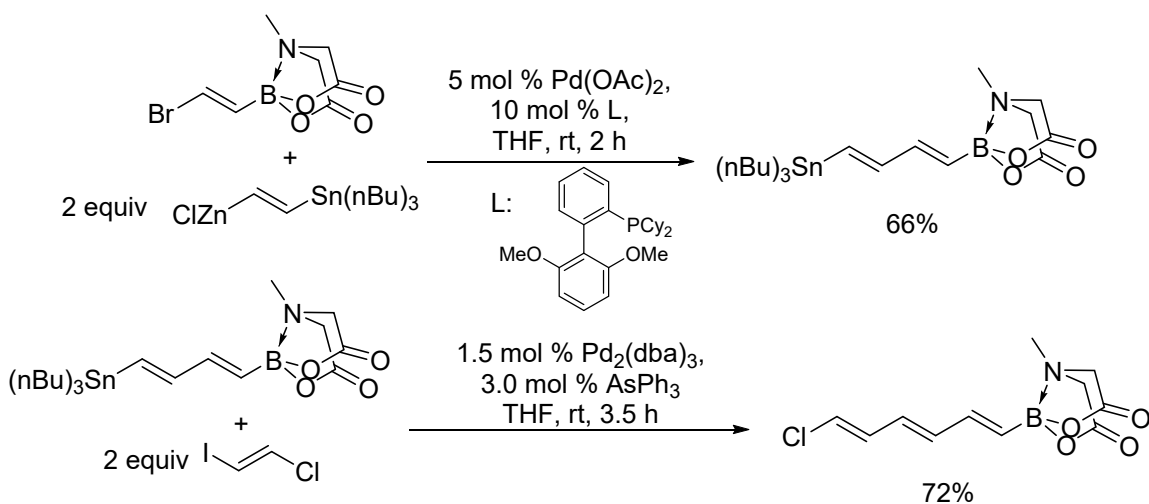
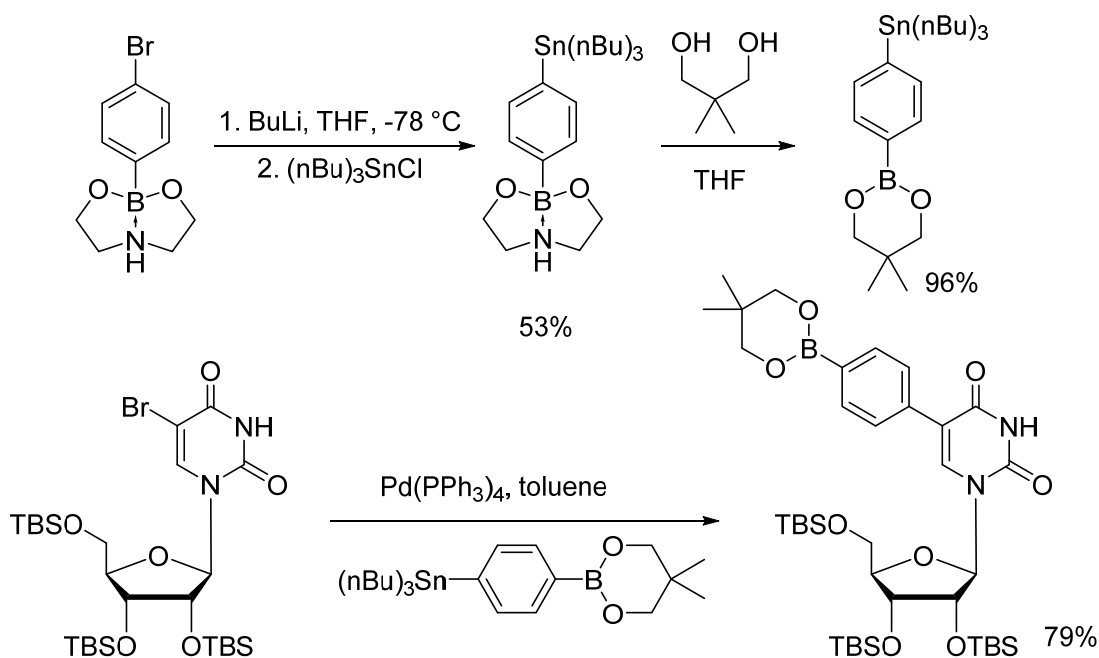


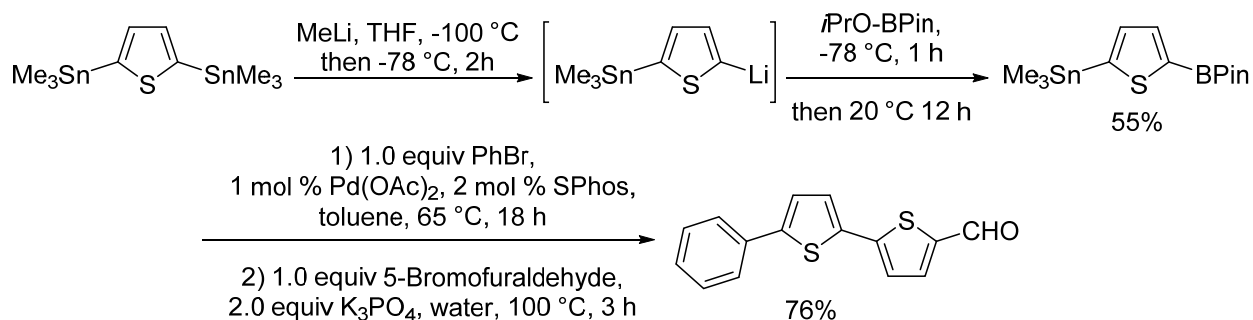
Figure 5. Synthesis and Stille coupling of a 1,4-B/Sn benzene



Besides the diene and triene bimetallic molecules discussed above, Yamamoto reported the

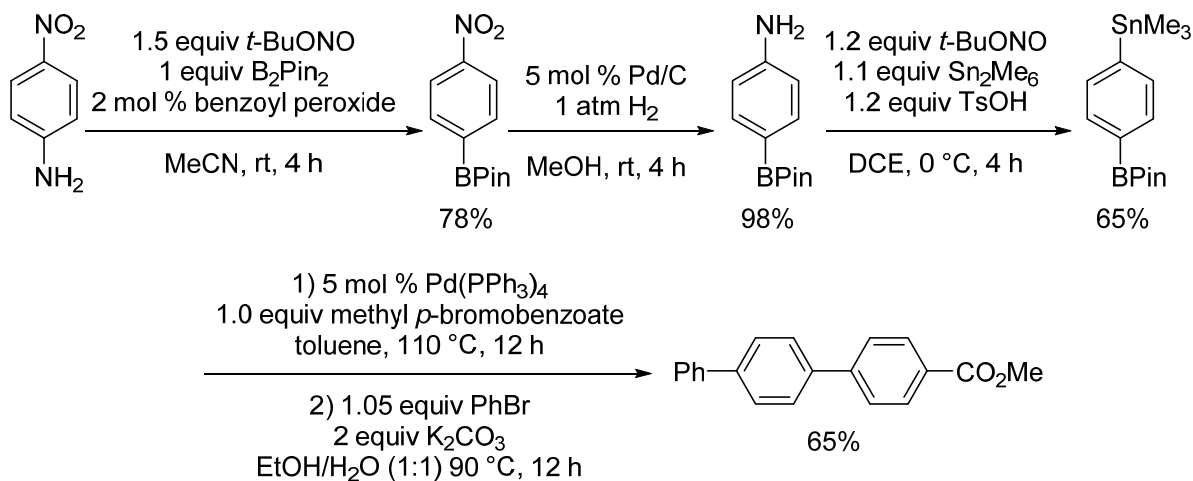
preparation and Stille reaction of a 1,4-B/Sn substituted benzene in 1989 (as shown in Figure 5),¹⁸ but few applications of this chemistry followed.

Figure 6. Staubitz's Sn/B thiophene building block and Stille/Suzuki CCR's sequence



In recent years, Staubitz and her group developed an interesting chemistry that desymmetrized a 1,4-distannyl thiophene and demonstrated the Stille /Suzuki CCR's (cross coupling reactions) sequence of this building block (Figure 6).¹⁹

Figure 7. Wang's Sandmeyer-type borylation-reduction-stannylation sequence on nitroaniline and their Stille/Suzuki CCR's

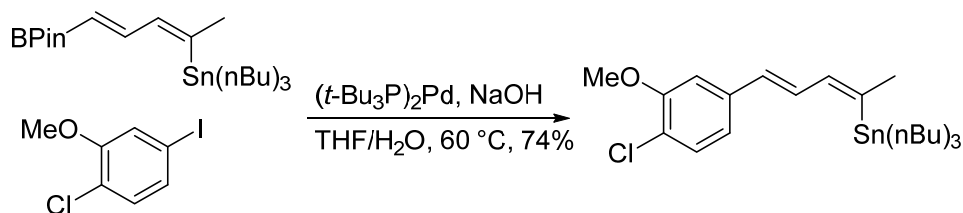


Wang and his group reported a sequence of two Sandmeyer type reactions to introduce (t-Bu)₃Sn and BPin groups onto a nitro aniline derivative, provided other existing functional groups survive the Sandmeyer conditions and the Pd catalyzed hydrogenation (reduction of nitro group to amino

for the second Sandmeyer transformation). They then demonstrated a Stille/Suzuki CCR's sequence as shown in **Figure 7**.²⁰

Such successive Stille/Suzuki cross-couplings have proven quite useful in target synthesis.²¹ In contrast, B/Sn bismetallic substrates have rarely been made to undergo a complementary Suzuki/Stille cross-coupling sequence. Coleman described a single example of a trisubstituted vinyl tin moiety surviving the Suzuki coupling of a coexisting *E*-vinyl boronic ester.²² In this case, the cross-coupling preference is likely due to sterics about the vinylstannane slowing down the Stille or the presence of water accelerating the Suzuki, as shown in **Figure 8**.²³

Figure 8. Chemoselective Suzuki coupling of B/Sn bismetallic diene



1.2 Proposed pathways to bismetallic arenes

Owing to the ability of organotins to undergo not only Stille reactions, but transmetallations, Sn/halogen exchanges and other useful transformations,²⁴ we sought to clearly establish a universal protocol for performing a selective Suzuki coupling on similar B/Sn bismetallic compounds. We were jointly interested in evaluating the ability of Ir-catalyzed borylations^{25,26} to function on aryl stannanes. Furthermore, given the halogen tolerance of Ir-catalyzed borylations, we recognized that Pd-mediated stannylation of the corresponding halo-substituted arylboronic ester would provide an equally direct route to stannylated aryl boronic esters. Thus, we set out to explore both approaches as illustrated in **Figure 9**.

Figure 9. Proposed routes to m-B/Sn bismetallic arenes

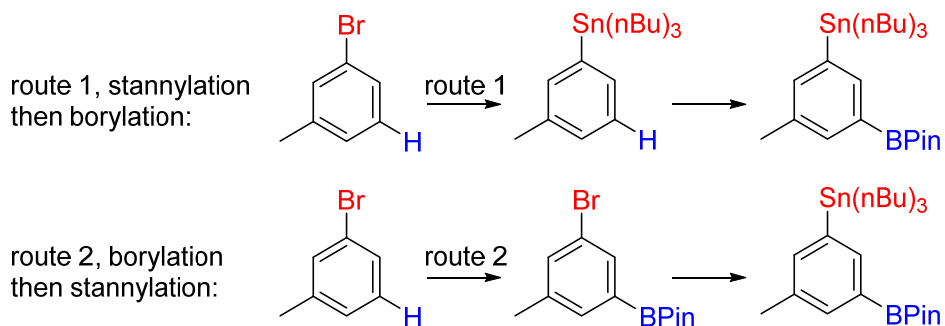


Table 1. Attempts of borylation of arylstannanes

R = CH₃, CN, CF₃ not found

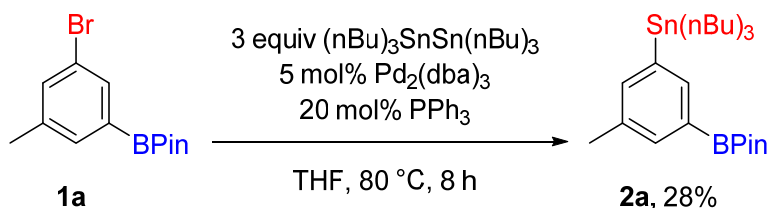
entry	aryl stannane	recovered SM ^a	entry	aryl stannane	recovered SM
1		75%	3		82%
2		88%	4		87%

^aIsolated by column chromatography.

Unfortunately the attempted borylations of several 3'-substituted phenylstannanes as well as tributylstannylthiophene only gave recovered starting materials (75–88%) and none of the desired products (**Table 1**). To gain insight into these failures, we attempted to borylate an equal mixture of 3-tributylstannyltoluene and 3-bromotoluene. Monitoring the reaction by ¹¹B NMR never gave any indication of C-B bond formation. Furthermore, a stoichiometric reaction of Ir(COE)(dtbpy)(BPIn)₃ complex²⁷ with 3-stannyl-trifluorotoluene gave no borylation by ¹¹B NMR, but the disappearance of the starting stannane by ¹¹⁹Sn NMR. Given these NMR data and the highly reactive nature of thiophenes and 3-bromotoluene in most Ir-catalyzed borylations, we

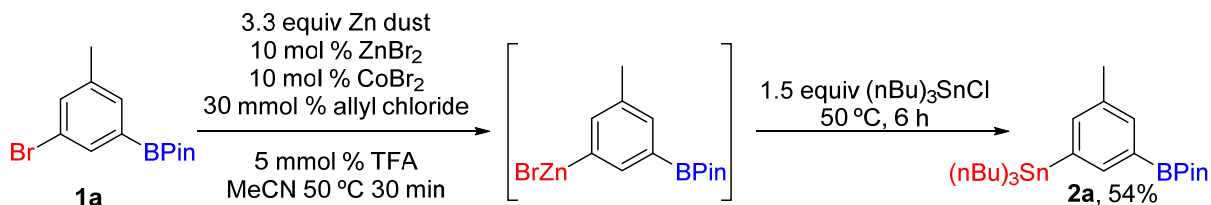
concluded that the presence of a R_3Sn group reacts with the active Ir(III) species in a way that shuts down catalysis.

Figure 10. Synthesis of B/Sn bismetallic arenes via Pd catalyzed stannylation



With route 1 proving unsuccessful, route 2 was brought to trial. Compound **1a** was readily prepared from 3-bromotoluene, however Pd-catalyzed coupling with hexabutylditin afforded the desired product **2a** in a disappointing 28% isolated yield (**Figure 10**). This low yield was a consequence of unwanted coupling of the substrate with the aryl tin product.

Figure 11. Synthesis of **2a** via Zn mediated stannylation



Seeking a higher yielding approach to stannylated aryl boronic esters, our attention was drawn to Gosmini's report describing the Zn(II)/Co(II) mediated stannylation of aryl iodides and bromides.²⁸ Although no examples of halogenated arylboronic esters were described in that work, the functional group tolerance noted argued in favor of us testing the methodology on **1a**. We were gratified when this stannylation protocol (**Figure 11**) afforded a synthetically useful yield of **2a** (54%) and exhibited none of the typical incompatibility between organozinc species and aryl boronates.²⁹

Table 2. Stannylation of bromophenyl boronic esters

Reaction scheme showing the stannylation of bromophenyl boronic esters **1a-1f** to products **2a-2f** and byproducts **3c-d**. Conditions: 1) 3.3 equiv Zn dust, 10 mol % ZnBr₂, 10 mol % CoBr₂, 30 mmol % allyl chloride, 5 mmol % TFA, MeCN, 50 °C, 30 min; 2) 1.5 equiv (nBu)₃SnCl, 50 °C, 6 h.

entry	product ^b	byproduct	entry	product ^b	byproduct
1	 2a Me 54%	-	4	 2d MeO 50%	 3d MeO 1/18 ^c
2	 2b F ₃ C 50%	-	5	 2e Cl 61%	-
3	 2c NC 55%	 3c NC 6%	6	 2f F 62%	-

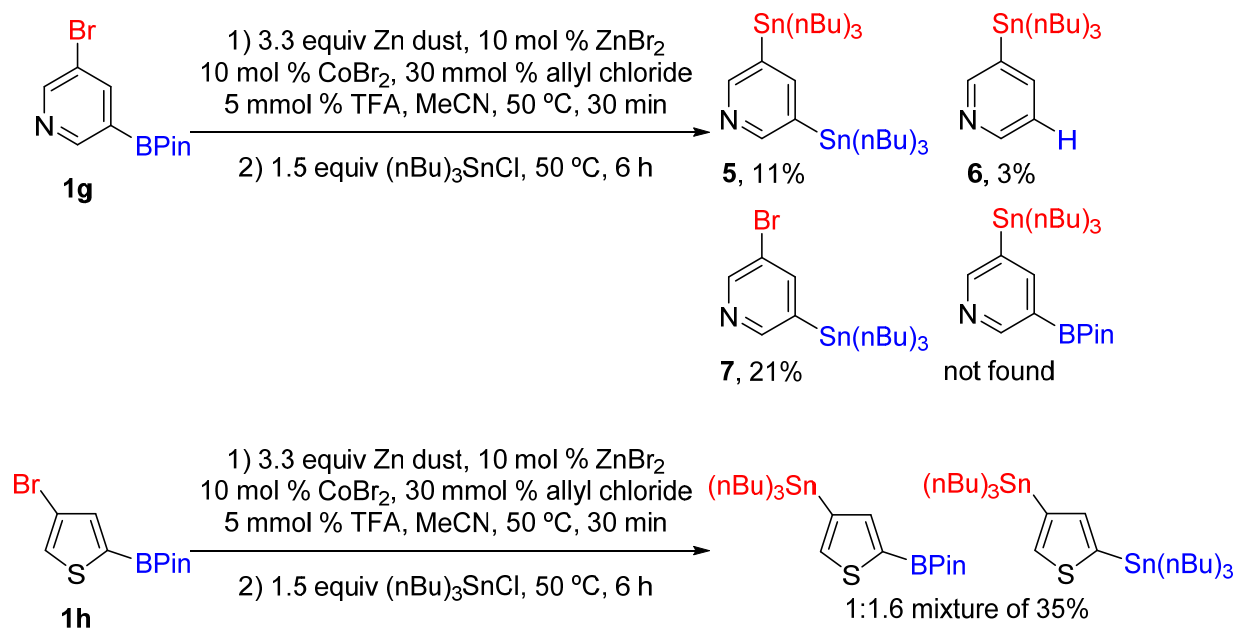
^aSame condition as described in **Scheme 2**. ^bIsolated yields.

^cUnseparable mixture with **2d**

Encouraged by this result, several bromoarenes were borylated under Ir-catalysis and then subjected to the Zn(II)/Co(II) stannylation conditions (Zn dust (3.3 equiv), ZnBr₂ (10 mol %), CoBr₂ (10 mol %), then allyl chloride (30 mol %), TFA (50 mol %), then substrate, then *n*-Bu₃SnCl (1.5 equiv)). We were able to perform this stannylation on a variety of substrates. Electron rich, neutral, and poor arenes all afforded the B/Sn products in synthetically useful isolated yields. Furthermore, potentially reactive functionality (e.g. CN and Cl) remained intact under the reaction conditions (**Table 1.2**). In contrast to arenes, the two heteroarenes studied proved more troublesome. While substrates **1c** and **1d** (entries 3 and 4) afforded minor amounts of distannylated byproducts, the reaction of 4-bromo-2-borylated thiophene **1g** gave a 1:1.6 ratio of the desired B/Sn product and the 2,4-bis(tributyltin)thiophene in 35% yield. Moreover, 5-bromo-3-borylated

pyridine **1h** afforded none of the desired product and actually favored B/Sn exchange over Br/Sn exchange (Figure 12).

Figure 12. Attempts of stannylation on bromoheteroaryl boronic esters



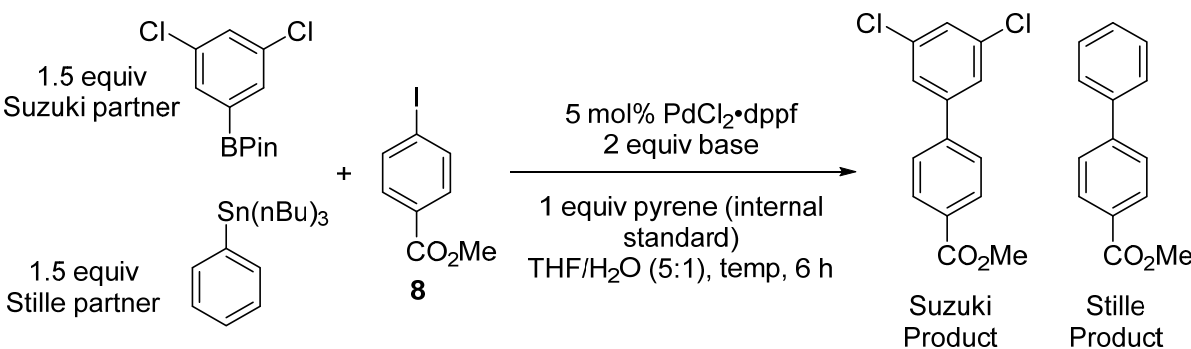
The observed B/Sn exchange products presumably arise from a boron-zinc followed by zinc-tin transmetallations. Bolm has describe similar B/Zn exchanges on aryl boronic acids.²¹ However, Gosmini successfully stannylated 4-bromobenzaldehyde,^{20(b)} suggesting that the organozinc species generated from these two processes may exhibit distinct reactivity profiles. Certainly the heteroaryl boronic esters studied are more prone undergo boron-zinc transmetallations relative to their aryl counterparts.

1.3 Selective Suzuki coupling of the B/Sn bismetallic arenes

These troubled substrates aside, the borylation/stannylation sequence gave us a set B/Sn metallated arenes that could be used to identify conditions that afford selective Suzuki couplings. The search for suitable conditions commenced with a screening of various bases. As the presence of water is known to accelerate Suzuki reactions,¹⁵ we explored wet THF in the reactions. Our aim was to

determine conditions that afforded high yields of the Suzuki product and recovered stannane. During the screening, we noticed that triethylamine provided poor chemoselectivity, but strong inorganic bases provided satisfactory differentiation, favoring the Suzuki coupling over Stille coupling. Importantly the stannyl group survived the condition.³⁰ As expected, the coupling reaction performed better with heating than at room temperature. We chose the conditions in entry 4 to further test for the selective Suzuki coupling of the B/Sn compounds (**Table 3**).

Table 3. Base screening for selective Suzuki couplings of B/Sn bismetallic arenes



entry	base	T(°C)	iodide	B ^a	Sn ^a	Su ^b	St ^b
1	TEA	80	4.8%	68.0%	42.6%	33.5%	46.4%
2	K ₃ PO ₄	rt ^c	39.5%	35.5%	92.3%	52.3%	4.8%
3	K ₂ CO ₃	80	0.7%	9.2%	96.5%	71.6%	1.1%
4	KOH	80	0.7%	16.5%	96.8%	97.9%	1.5%
5	KF	80	1.5%	9.7%	80.3%	88.1%	8.5%

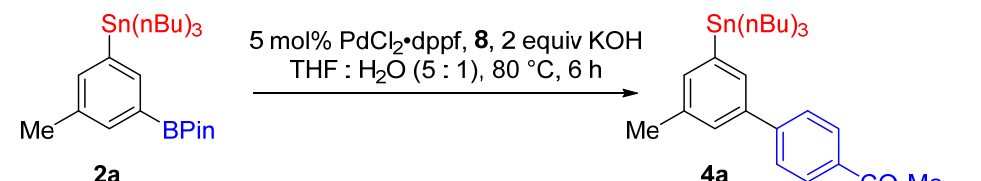
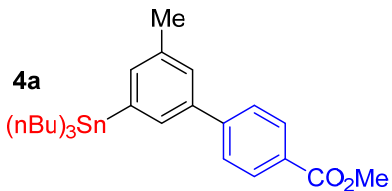
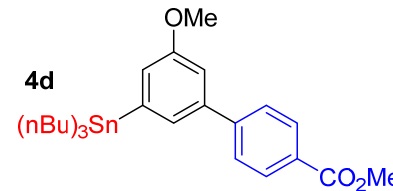
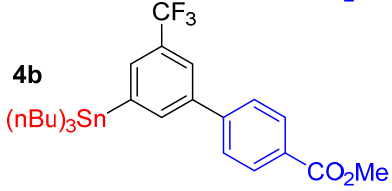
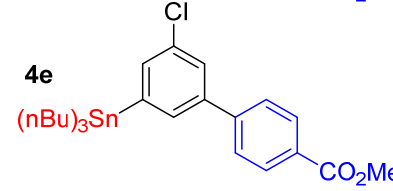
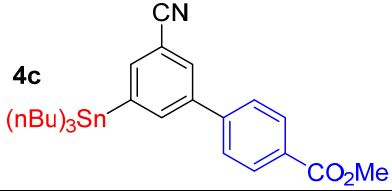
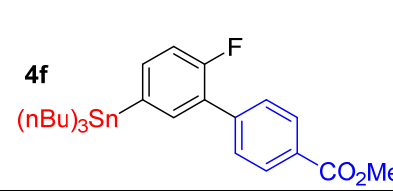
^aRecovery based on B or Sn starting material ^bGC yield based on iodide ^c24 hour reaction

Conditions: 0.2 mmol scale reactions in a mixture of 2 mL THF and 0.4 mL water were carried out in closed tube purged with N₂, and all reagents are added together in one batch. After 6 h, the reaction was cooled down quickly in ice-water bath, and diluted by ~10 mL Et₂O, then ~1.5 mL of the organic layer was passed through a short plug of MgSO₄ into a GC sample vial for quantitative determinations

The reaction of 1.5 equivalents of **2a** with methyl *p*-iodobenzoate (**8**) and 2 equiv KOH in THF/water clearly favored the Suzuki coupling, affording **4a** in 85% yield based on the limiting reagent **8**. In as much as the B/Sn metallated arenes will often be the more precious coupling partner, we examined the reaction with lower loads of **2a**. While 1:1 ratio of **2a** and **8** gave **4a** in

59% yield, using 1.2 equivalents of **2a** provided a good balance of yield and stoichiometry. Thus, a series of other B/Sn metallated arenes with variety of substituents ranging from strong EWG such as CF₃ or CN, to strong EDG such as OMe, were tested with **8** (Table 4), and gave moderate to high yields of the selective Suzuki coupling products.

Table 4. Selective Suzuki coupling of 2a-f with 8

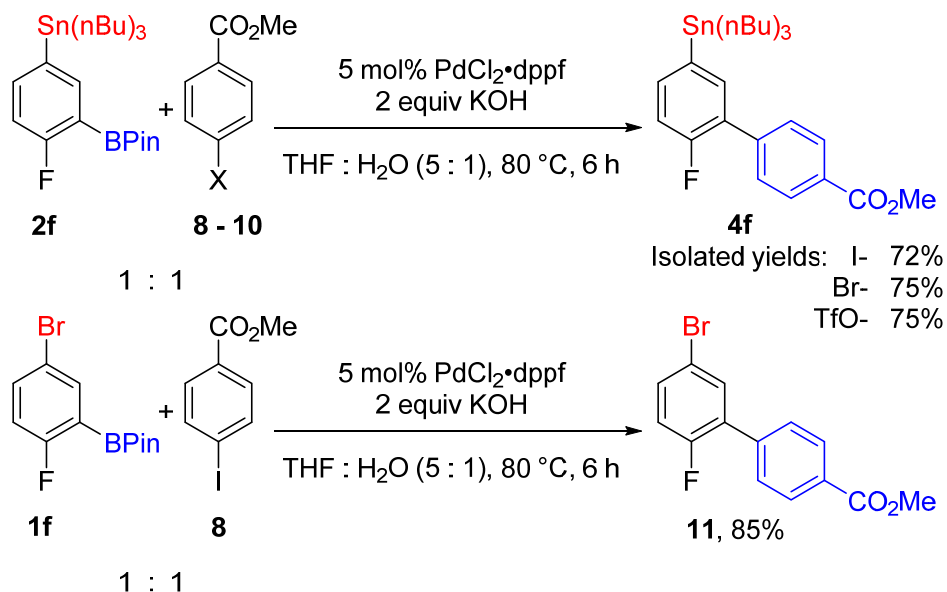
 <p style="text-align: center;">2a → 4a</p>	<p>5 mol% PdCl₂·dppf, 8, 2 equiv KOH THF : H₂O (5 : 1), 80 °C, 6 h</p>	<p>4a</p> <p>57% based on 2a, 85% based 8</p> <p>62% based on 2a, 81% based 8</p> <p>59%</p>			
1.5 equiv 2a					
1.2 equiv 2a					
1.0 equiv 2a					
entry	product	yield (%)	entry	product	yield (%)
1	 <p>4a</p>	57 ^a 62 ^b 59 ^c	4	 <p>4d</p>	57
2	 <p>4b</p>	77 ^b	5	 <p>4e</p>	76
3	 <p>4c</p>	81 ^b	6	 <p>4f</p>	72

^aIsolated yield based on 1.5 equiv **2a** used. ^bIsolated yield based on 1.2 equiv **2x** used. ^cIsolated yield based on 1.0 equiv **2x** used.

So as to benchmark this approach to stannylated biaryls, we looked to synthesize **4f** by cross-coupling **1f** with the iodide **8**, bromide **9**, and triflate **10**. As illustrated in Figure 13, **1f** successfully coupled with iodide **8** to give **11** with little evidence of polyphenylene formation. In

contrast, polymerization of **1f** predominated the attempted cross-couplings with **9** or **10**, which afforded none of Suzuki product **10**. Meanwhile, **2f** was smoothly coupled with **8**, **9** and **10** giving selective Suzuki product **4f** in 72–75% yield, corresponding to 45–47% overall yields (two steps) from **1f**.

Figure 13. Suzuki couplings of 1f and 2f with various electrophiles



1.4 Experimental section

General Methods: All substrates were purified before use. Aryl halides were refluxed over CaH_2 , distilled, and degassed. Pinacolborane (HBPin) was purchased from Aldrich, stirred over PPh_3 overnight, vacuum transferred into an air free flask and brought into the glove box. Bis(pinacolato)diboron (B_2Pin_2) was purchased from various sources and was used without purification. 1,1'-Bis(diphenylphosphino)ferrocene dichloropalladium (II) ($\text{Pd}(\text{dppf})\text{Cl}_2$) was purchased from Aldrich and used as received. 4,4'-Di-*t*-butyl-2,2'-bipyridine (dtbpy) was purchased from Aldrich and was sublimed before use. (η^5 -Indenyl)(cyclooctadiene)iridium

$\{(\text{Ind})\text{Ir}(\text{COD})\}$ and $\text{bis}(\eta^4\text{-1,5-cyclooctadiene})\text{-di-}\mu\text{-methoxy-diiridium(I)}$ $\{\text{Ir}(\text{OMe})(\text{COD})\}_2$ were prepared per literature procedures.^{1,2}

All reactions were carried out in oven-dried flasks, magnetically stirred, and monitored by Varian CP-3800 GC-FID (column type: WCOT Fused silica 30m×0.25mm ID coating CP-SIL 8 CB). GC-FID method: 70 °C, 2 min.; 20 °C/min, 50 min.; 250 °C, 20 min.; 1.8 mL/min flow rate. All yields are of isolated materials and are average of at least two runs.

All compounds were characterized by ^1H NMR, ^{13}C NMR, ^{11}B NMR, ^{119}Sn NMR and ^{19}F NMR, IR spectroscopy, and low resolution mass spectroscopy. ^1H and ^{13}C NMR spectra were recorded on a Varian VXR-500, or Varian Unity-500-plus spectrometer (499.74 and 125.67 MHz respectively) or Varian Inova-600 (599.81 and 150.84 MHz respectively) and referenced to residual solvent signals. ^{11}B spectra were recorded on a Varian VXR-300 operating at 96.29 MHz and were referenced to neat $\text{BF}_3\cdot\text{Et}_2\text{O}$ as the external standard. ^{19}F spectra were recorded on a Varian Inova-300 operating at 282.36 MHz and were referenced to neat CFCl_3 as the external standard. ^{119}Sn NMR spectra were recorded on a Varian VXR-500, or Varian Unity-500-plus spectrometer (operating at 186.42 MHz), or Varian Inova-600 (operating at 223.66 MHz). All coupling constants are apparent J values measured at the indicated field strength. GC-MS data were obtained using a Varian Saturn 220 GC/MS (column type: WCOT Fused silica 30m×0.25mm ID coating CP-SIL 8 CB). High-resolution mass spectra were obtained at Michigan State University Mass Spectrometry Service Center with a JOEL-AX505 mass spectrometer (resolution 7000). Melting points were measured on Thomas-Hoover capillary melting apparatus and are uncorrected.

General Procedure for Preparation of B/Sn-Bimetallic Compounds: Zn dust (220 mg, 3.3 mmol), ZnBr₂ (22.5 mg, 0.1 mmol), and CoBr₂ (21.9 mg, 0.1 mmol) were charged into a 10 mL round bottom flask. Then 1 mL MeCN was added, followed by allyl chloride (24 μ L, 0.3 mmol) and TFA (3.7 μ L, 0.05 mmol). At this moment, the color of the solution turned from cobalt blue to a reddish brown. The mixture was stirred at room temperature for 5 min. Then the aryl bromide (1.0 mmol) was added. The flask was then connected to a condenser and the reaction mixture was stirred in a 50 °C pre-heated oil bath for 30 min. The solution usually turned to colorless or pale yellow. Tri-*n*-butyltin chloride (489 mg, 1.5 mmol) was then added in one batch. After 6 h heating, the reaction mixture is then filtered through a short plug with silica gel and purified by column chromatography or bulb to bulb distillation.

General Procedure for Selective Suzuki Couplings of B/Sn-Bimetallic Compounds: Boron-tin compound (0.2 mmol), methyl *p*-iodobenzoate (0.2 mmol) and PdCl₂·dppf (0.01 mmol) were mixed in an air free flask with 2 mL THF. The mixture was then degassed and the flask was filled with nitrogen. 1M NaOH solution (0.4 mL) prepared with water freshly sparged by nitrogen was then added to the flask. The reaction mixture was then heated in an 80 °C oil bath for 6 h. The crude reaction mixture was washed through a basic alumina short plug and then purified by silica gel chromatography.

Tributyl(3-methyl-5-(4,4,5,5-tetramethyl-1,3,2-dioxaborolan-2-yl)phenyl)stannane (2a):

Compound **1a** was subjected to the general procedure for preparation of B/Sn-Bimetallic compounds, and purified by a silica gel column with hexanes : EtOAc 20 : 1, to give a colorless oil, 54% yield. ¹H NMR (500 MHz, CDCl₃) δ 7.69 (br, 1 H), 7.57 (br, 1 H), 7.36 (br, 1 H), 2.33 (s, 3 H), 1.53 (m, 6 H), 1.34 (m, 18 H), 1.05 (m, 6 H), 0.89 (t, J = 7.3 Hz, 9 H); ¹³C NMR (125 MHz, CDCl₃) δ 141.0, 140.2, 139.8, 136.3, 135.2, 83.6, 29.1, 27.4, 24.8, 21.3, 13.7, 9.5; ¹¹B NMR

(160 MHz, CDCl₃) δ 30.9; ¹¹⁹Sn NMR (186 MHz, CDCl₃) δ -43.6 (s); HRMS (ESI+) calculated 451.1830 for [C₂₁H₃₆BO₂Sn]⁺ (M-nBu)⁺, found 451.1833. IR neat: 2958, 2926, 2871, 2854, 1354, 1146 cm⁻¹.

Tributyl(3-(4,4,5,5-tetramethyl-1,3,2-dioxaborolan-2-yl)-5-(trifluoromethyl)phenyl)-

stannane (2b): Compound **1b** was subjected to the general procedure for preparation of B/Sn-Bismetallic and compounds, purified by a silica gel column with hexanes : EtOAc 20 : 1 to give a colorless oil, 50% yield. ¹H NMR (500 MHz, CDCl₃) δ 8.06 (s, 1H), 8.00 (s, 1H), 7.78 (s, 1H), 1.56 (m, 6H), 1.36 (m, 18H), 1.12 (m, 6H), 0.90 (t, *J* = 7.3 Hz, 9H); ¹³C NMR (125 MHz, CDCl₃) δ 146.0, 142.4, 135.2 (q, *J*_{C-F} = 3.6 Hz), 131.0 (q, *J*_{C-F} = 3.6 Hz), 129.3 (129.7 ppm, 129.4 ppm, 129.2 ppm, 128.9 ppm, q, *J*_{C-F} = 31 Hz), 124.8 (128.0 ppm, 125.8 ppm, 123.6 ppm, 121.5 ppm, q, *J*_{C-F} = 273 Hz), 84.1, 29.0, 27.3, 24.8, 13.6, 9.7; ¹¹B NMR (160 MHz, CDCl₃) δ 30.4; ¹¹⁹Sn NMR (186 MHz, CDCl₃) δ -38.9 (q, *J*_{Sn-F} = 2.8 Hz); ¹⁹F NMR (282 MHz, CDCl₃) δ -65.5; HRMS (ESI+) calculated 505.1548 for [C₂₁H₃₃BF₃O₂Sn]⁺ (M-nBu)⁺, found 505.1556. IR neat: 2959, 2928, 2873, 2854, 1486, 1323, 1126 cm⁻¹.

3-(4,4,5,5-tetramethyl-1,3,2-dioxaborolan-2-yl)-5-(tributylstannyl)benzonitrile (2c):

Compound **1c** was subjected to the general procedure for preparation of B/Sn-Bismetallic compounds, and purified by a silica gel column with hexanes : EtOAc 10 : 1 to give a colorless oil, 55% yield. ¹H NMR (500 MHz, CDCl₃) δ 8.02 (t, *J* = 1.1 Hz, 1H), 7.98 (dd, *J* = 2.0, 1.0 Hz, 1H), 7.76 (dd, *J* = 2.0, 1.0 Hz, 1H), 1.49 (m, 6H), 1.31 (m, 18H), 1.08 (m, 6H), 0.87 (t, *J* = 7.3 Hz, 9H); ¹³C NMR (125 MHz, CDCl₃) δ 146.4, 143.1, 141.9, 137.8, 119.5, 111.6, 84.3, 28.9, 27.2, 24.8, 13.6, 9.7; ¹¹B δ (160 MHz, CDCl₃) 30.2; ¹¹⁹Sn (186 MHz, CDCl₃) δ -37.4. HRMS (ESI+)

calculated 520.2409 for $[\text{C}_{25}\text{H}_{43}\text{BNO}_2\text{Sn}]^+$ ($\text{M}+\text{H}$) $^+$, found 520.2420. IR neat: 2957, 2927, 2872, 2854, 2227, 1587, 1426, 1352, 1144, 705 cm^{-1} .

Tributyl(3-methoxy-5-(4,4,5,5-tetramethyl-1,3,2-dioxaborolan-2-yl)phenyl)stannane (2d):

Compound **1d** was subjected to the general procedure for preparation of B/Sn-Bismetallic compounds, and purified by a silica gel column with hexanes : EtOAc 20 : 1 to give a colorless oil, 50% yield, with small amount of impurity **3d**. Analytical pure **2d** can be accessed by Kugelrohr distillation, at 150 °C, 0.2 mmHg, as a colorless oil ^1H NMR (500 MHz, acetone- d_6) δ 7.46 (t, J = 0.8 Hz, 1H), 7.20 (dd, J = 2.7, 0.8 Hz, 1H), 7.15 (dd, J = 2.7, 0.8 Hz, 1H), 3.80 (s, 3H), 1.59 (m, 6H), 1.36 (m, 18H), 1.11 (m, 6H), 0.89 (t, J = 7.3 Hz, 9H); ^{13}C NMR (125 MHz, acetone- d_6) δ 159.7, 143.0, 135.9, 126.3, 119.3, 84.6, 55.3, 28.1, 25.3, 14.0, 10.2; ^{11}B (160 MHz, acetone- d_6) δ 32 (br); ^{119}Sn (186 MHz, acetone- d_6) δ -39.6; IR neat 2956, 2935, 2879, 2871, 1352, 1146 cm^{-1} ; HRMS (ESI+) calculated: 467.1774 for $[\text{C}_{21}\text{H}_{36}\text{BO}_3\text{Sn}]^+$ ($\text{M} - n\text{-Bu}$) $^+$, found 467.1787.

Tributyl(3-chloro-5-(4,4,5,5-tetramethyl-1,3,2-dioxaborolan-2-yl)phenyl)stannane (2e):

Compound **1e** was subjected to the general procedure for preparation of B/Sn-Bismetallic compounds, and purified by a silica gel column with hexanes : EtOAc 20 : 1 to give a colorless oil, 61% yield. ^1H NMR (500 MHz, CDCl_3) δ 7.75 - 7.65 (m, 2H), 7.46 (dd, J = 2.3, 0.9 Hz, 1H), 1.51 (m, 6H), 1.31 (m, 18H), 1.06 (m, 6H), 0.87 (t, J = 7.3 Hz, 9H); ^{13}C NMR (125 MHz, CDCl_3) δ 143.9, 140.4, 138.6, 84.0, 29.0, 27.3, 24.8, 13.6, 9.1; ^{11}B (160 MHz, CDCl_3) δ 30.16; ^{119}Sn (186 MHz, CDCl_3) δ -37.4. IR neat: 2957, 2925, 2871, 2843, 1342 1145 cm^{-1} ; HRMS (ESI+) calculated: 471.1279 for $[\text{C}_{20}\text{H}_{33}\text{BClO}_2\text{Sn}]^+$ ($\text{M} - n\text{-Bu}$) $^+$ found 471.1285.

Tributyl(4-fluoro-3-(4,4,5,5-tetramethyl-1,3,2-dioxaborolan-2-yl)phenyl)stannane (2f):

Compound **1f** was subjected to the general procedure for preparation of B/Sn-Bismetallic

compounds, and purified by a silica gel column with hexanes : EtOAc 20 : 1 to give a colorless oil, 60% yield. ^1H NMR (600 MHz, CDCl_3) δ 7.78 (dd, $J = 6.8, 1.5$ Hz, 2H), 7.49 (ddd, $J = 8.1, 6.6, 1.5$ Hz, 1H), 6.98 (dd, $J = 10.0, 8.1$ Hz, 1H), 1.52 (m, 6H), 1.32 (m, 18H), 1.04 (m, 6H), 0.88 (t, $J = 7.3$ Hz, 9H); ^{13}C NMR (151 MHz, CDCl_3) δ 167.7 (d, $J_{\text{C-F}} = 251$ Hz), 144.6 (d, $J_{\text{C-F}} = 6.3$ Hz), 141.1 (d, $J_{\text{C-F}} = 7.5$ Hz), 136.0 (d, $J_{\text{C-F}} = 4.6$ Hz), 114.9 (d, $J_{\text{C-F}} = 21.9$ Hz); ^{11}B (192 MHz, CDCl_3) δ 30.2; ^{119}Sn (224 MHz, CDCl_3) δ -39.0, ^{19}F (282 MHz, CDCl_3) -101.7 (m). IR neat: 2958, 2924, 2872, 2840, 1447, 1379, 1266, 1149, 740 cm^{-1} ; HRMS (ESI+) calculated: 455.1574 for $[\text{C}_{20}\text{H}_{33}\text{BFO}_2\text{Sn}]^+$ ($\text{M} - n\text{-Bu}$) $^+$, found 455.1587.

Methyl 3'-methyl-5'-(tributylstannyl)-[1,1'-biphenyl]-4-carboxylate (4a) 1.0 equiv **2a** was subjected to the general condition for selective Suzuki coupling and purified by a silica gel column with hexanes : EtOAc 5 : 1 to give a 59% yield of **4a** as a colorless oil. ^1H NMR (500 MHz, CDCl_3) δ 8.09 (AA'BB', $J = 8.3, 2.0, 1.7$ Hz, 2H), 7.63 (AA'BB', $J = 8.3, 2.0, 1.7$ Hz, 2H), 7.47 (m, 1H), 7.34 (m, 1H), 7.29 (m, 1H), 3.93 (s, 3H), 2.41 (s, 3H), 1.57 (m, 6H), 1.35 (m, 6H), 1.09 (m, 6H), 0.90 (t, $J = 7.3$ Hz, 9H); ^{13}C NMR (125 MHz, CDCl_3) δ 167.0, 146.3, 142.8, 139.4, 137.7, 137.0, 132.2, 130.0, 128.6, 127.9, 127.1, 52.1, 29.1, 27.4, 21.5, 13.7, 9.6; ^{119}Sn (186 MHz, CDCl_3) δ -41.7; HRMS (ESI+) calculated 517.2129 for $[\text{C}_{27}\text{H}_{41}\text{O}_2\text{Sn}]^+$ ($\text{M} + \text{H}$) $^+$ found 517.2133. IR neat: 2956, 2926, 2853, 1727, 1277 cm^{-1} .

Methyl 3'-(tributylstannyl)-5'-(trifluoromethyl)-[1,1'-biphenyl]-4-carboxylate (4b) 1.2 equiv **2b** was subjected to the general condition for selective Suzuki coupling and purified by a silica gel column with hexanes : EtOAc 5 : 1 to give a 77% yield of **4b** as a colorless oil. ^1H NMR (500 MHz, CDCl_3) δ 8.13 (AA'BB', $J = 8.8, 2.0, 1.7$ Hz, 2H), 7.82 (m, 1H), 7.74 (m, 1H), 7.69 (m, 1H), 7.64 (AA'BB', $J = 8.8, 2.0, 1.7$ Hz, 2H), 3.94 (s, 3H), 1.56 (m, 6H), 1.34 (m, 6H), 1.13 (m, 6H), 0.89

(t, $J = 7.3$ Hz, 9H), ^{13}C NMR (125 MHz, CDCl_3) δ 166.8, 144.7, 144.6, 139.8, 138.3 (m), 132.1 (m), 130.4 (q, $J_{\text{C-F}} = 31.4$ Hz), 130.2 (d, $J = 3.2$ Hz), 129.4, 127.2 (m), 124.4 (q, $J_{\text{C-F}} = 273.1$ Hz), 123.7, 52.2 (q, $J_{\text{C-F}} = 2.9$ Hz), 29.0, 27.3, 12.6, 9.8; ^{119}Sn (186 MHz, CDCl_3) δ -37.2; ^{19}F (282 MHz, CDCl_3) δ -64.3; HRMS (ESI+) calculated 513.1063 for $[\text{C}_{23}\text{H}_{28}\text{F}_3\text{O}_2\text{Sn}]^+$ ($\text{M} - n\text{-Bu}$) $^+$ found 513.1063. IR neat: 2958, 2928, 2873, 2854, 1728, 1611, 1334, 1279, 1200, 1137 cm^{-1} .

Methyl 3'-cyano-5'-(tributylstannyl)-[1,1'-biphenyl]-4-carboxylate (4c) 1.2 equiv **2c** was subjected to the general condition for selective Suzuki coupling and purified by a silica gel column with hexanes : EtOAc 5 : 1 to give a 81% yield of **4c** as a colorless oil. ^1H NMR (500 MHz, CDCl_3) δ 8.13 (AA'BB', $J = 8.8, 2.0, 1.7$ Hz, 2H), 7.84 (dd, $J = 1.9, 0.8$ Hz, 1H), 7.77 (t, $J = 1.8$ Hz, 1H), 7.72 (dd, $J = 1.9, 0.8$, 1H), 7.59 (AA'BB', $J = 8.8, 2.0, 1.7$ Hz, 2H), 3.93 (s, 3H), 1.53 (m, 6H), 1.53 (m, 6H), 1.12 (m, 6H), 0.88 (t, $J = 7.3$ Hz, 9H); ^{13}C NMR (125 MHz, CDCl_3) δ 166.7, 165.5, 145.3, 13.8, 140.0, 139.0 (d, $J = 14.5$ Hz), 130.3, 130.2, 129.7, 127.1, 119.2, 112.6, 52.2, 29.0, 27.3, 13.6, 9.9; ^{119}Sn (186 MHz, CDCl_3) δ -33.63; IR neat: 2957, 2926, 2871, 2852, 2227, 1726, 1610, 1461, 1436, 1278, 1190, 1112, 1018, 908, 774, 697 cm^{-1} ; HRMS (ESI+) calculated: 470.1137 for $[\text{C}_{23}\text{H}_{28}\text{NO}_2\text{Sn}]^+$ ($\text{M} - n\text{-Bu}$) $^+$ found 470.1146.

Methyl 3'-methoxy-5'-(tributylstannyl)-[1,1'-biphenyl]-4-carboxylate (4d) 1.0 equiv **2d** was subjected to the general condition for selective Suzuki coupling and purified by a silica gel column with hexanes : EtOAc 5 : 1 to give a 57% yield of **4d** as a colorless oil. ^1H NMR (500 MHz, CDCl_3) δ 8.09 (AA'BB' $J = 8.6, 2.0, 2.0$ Hz, 2H), 7.63 (AA'BB' $J = 8.6, 2.0, 2.0$ Hz, 2H), 7.24 (b, 1H), 7.03 (m, 2H), 3.93 (s, 3H), 3.86 (s, 3H), 1.56 (m, 6H), 1.34 (m, 6H), 1.08 (m, 6H), 0.88 (t, $J = 7.3$ Hz, 9H); ^{13}C NMR (125 MHz, CDCl_3) δ 167.0, 159.3, 146.0, 144.4, 140.8, 130.0, 128.9, 127.6, 127.2, 121.7, 112.3, 55.2, 52.1, 29.1, 27.3, 13.7, 9.7; ^{119}Sn (186 MHz, CDCl_3) δ -37.6; IR neat:

2954, 2912, 2871, 2856, 1726, 1609, 1581, 1462, 1436, 1276, 1210, 1111, 773, 699 cm^{-1} ; HRMS (ESI+) calculated: 475.1290 for $[\text{C}_{23}\text{H}_{31}\text{O}_3\text{Sn}]^+$ (M - *n*-Bu)⁺ found 475.1299.

Methyl 3'-chloro-5'-(tributylstannyl)-[1,1'-biphenyl]-4-carboxylate (4e) 1.0 equiv **2e** was subjected to the general condition for selective Suzuki coupling and purified by a silica gel column with hexanes : EtOAc 5 : 1 to give a 76% yield of **4e** as a colorless oil ^1H NMR (500 MHz, CDCl_3) δ 8.10 (AA'BB', $J = 8.5, 2.0, 1.5$ Hz, 2H), 7.60 (AA'BB', $J = 8.5, 2.0, 1.5$ Hz, 2H), 7.50 (dd, $J = 1.7, 0.6$ Hz, 1H), 7.49 (t, $J = 1.8$ Hz, 1H), 7.41 (dd, $J = 2.0, 0.7$ Hz, 1H), 3.93 (s, 3H) 1.54 (m, 6H), 1.33 (m, 6H), 1.09 (m, 6H), 0.89 (t, $J = 7.3$ Hz, 9H); ^{13}C NMR (125 MHz, CDCl_3) δ 166.9, 145.5, 144.7, 141.1, 135.4, 134.7, 133.0, 129.3, 127.1, 52.2, 29.0, 27.3, 13.6, 9.8; ^{119}Sn (186 MHz, CDCl_3) δ -34.9; IR neat: 2956, 2921, 2871, 2851, 1725, 1610, 1462, 1436, 1276, 1104, 851, 774, 741, 965 cm^{-1} ; HRMS (ESI+) calculated: 479.0794 for $[\text{C}_{22}\text{H}_{28}\text{ClO}_2\text{Sn}]^+$ (M - *n*-Bu)⁺ found 479.0797.

Methyl 2'-fluoro-5'-(tributylstannyl)-[1,1'-biphenyl]-4-carboxylate (4f) 1.0 equiv **2f** was subjected to the general condition for selective Suzuki coupling and purified by a silica gel column with hexanes : EtOAc 5 : 1 to give a 72% yield of **4f** as a colorless oil. ^1H NMR (600 MHz, CDCl_3) δ 8.11 (AA'BB', $J = 8.8, 2.0, 1.5$ Hz, 2H), 7.62 (dd, $J = 8.4, 1.6$ Hz, 2H), 7.48 (dd, $J = 8.6, 1.3$ Hz, 1H), 7.34 (ddd, $J = 7.8, 5.6, 1.5$ Hz, 1H), 7.13 (dd, $J = 11.5, 8.1$ Hz, 1H), 3.93 (s, 3H) 1.55 (m, 6H), 1.34 (m, 6H), 1.08 (m, 6H), 0.89 (t, $J = 7.3$ Hz, 9H); ^{13}C NMR (151 MHz, CDCl_3) δ 166.9, 160.1 (d, $J_{\text{C-F}} = 249.1$ Hz), 140.9, 138.3 (d, $J_{\text{C-F}} = 2.3$ Hz), 137.7 (d, $J_{\text{C-F}} = 6.9$ Hz), 137.6 (d, $J_{\text{C-F}} = 4.6$ Hz), 129.6, 129.1, 129.0 (d, $J_{\text{C-F}} = 2.9$ Hz), 127.6 (d, $J_{\text{C-F}} = 11.5$ Hz), 115.8 (d, $J_{\text{C-F}} = 20.7$ Hz), 52.1, 29.0, 27.3, 13.6, 9.7; ^{119}Sn (224 MHz, CDCl_3) δ -37.3; ^{19}F NMR (282 MHz, CDCl_3) δ -116.8 (m); IR neat: 2956, 2922, 2871, 2850, 1762, 1612, 1482, 1463, 1363, 178, 1112, 817, 776, 740, 703 cm^{-1} ; HRMS (ESI+) calculated: 463.1090 for $[\text{C}_{22}\text{H}_{28}\text{FO}_2\text{Sn}]^+$ (M - *n*-Bu)⁺ found 463.1099.

3,5-Bis(tributylstannyl)pyridine (5) and **3,5-Bis(tributylstannyl)pyridine (7)**: Compound **1g** was subjected to the general procedure for preparation of B/Sn-Bismetallic compounds, and purified by a silica gel column with hexanes : EtOAc 20 : 1 to give compound **5** as a colorless oil, 11% yield. ^1H NMR (600 MHz, CDCl_3) δ 8.47 (d, $J = 1.5$ Hz, 2H), 7.75 (t, $J = 1.5$ Hz, 1H); 1.52 (m, 12H), 1.31 (m, 12H), 1.06 (m, 12H), 0.86 (t, $J = 7.3$ Hz, 18H); ^{13}C NMR (151 MHz, CDCl_3) δ 155.3, 152.4, 136.8, 29.0, 27.3, 13.6, 9.6; ^{119}Sn (224 MHz, CDCl_3) δ -41.7; HRMS (ESI+) calculated: 652.2604 for $[\text{C}_{29}\text{H}_{58}\text{N}^{116}\text{Sn}_2]^+$ (M+H) $^+$ found 652.2625. and compound **7** as a colorless oil 21% yield ^1H NMR (600 MHz, CDCl_3) δ 8.55 (d, $J = 2.4$ Hz, 1H), 8.46 (d, $J = 1.1$ Hz, 1H); 7.81 (dd, $J = 2.4, 1.1$ Hz, 1H); 1.51 (m, 6H), 1.31 (m, 6H), 1.09 (m, 6H), 0.87 (t, $J = 7.3$ Hz, 9H); ^{13}C NMR (151 MHz, CDCl_3) δ 153.8, 150.1, 145.9, 139.5, 122.0, 28.9, 27.3, 13.6, 9.8; ^{119}Sn (224 MHz, CDCl_3) δ -36.4; HRMS (ESI+) calculated: 444.0642 for $[\text{C}_{17}\text{H}_{31}\text{BrN}^{116}\text{Sn}]^+$ (M+H) $^+$ found 444.0657.

Methyl 5'-bromo-2'-fluoro-[1,1'-biphenyl]-4-carboxylate (11): 1.0 equiv **1f** was subjected to the general condition for selective Suzuki coupling and purified by a silica gel column with hexanes : EtOAc 5 : 1 to give a 85% yield of **11** as a white solid. ^1H NMR (500 MHz, CDCl_3) δ 8.09 (d, $J = 8.8$ Hz, 1H), 7.56 (m, overlapping, 3H); 7.43 (ddd, $J = 8.8, 4.3, 2.6$ Hz, 1H); 7.04 (dd, $J = 10.1, 8.7$ Hz, 1H), 3.92 (s, 3H, OMe); ^{13}C NMR (125 MHz, CDCl_3) δ 166.6 (C=O), 158.7 (159.7 ppm, 157.7 ppm, d, $J = 249$ Hz, C-F), 138.8, 133.2 (d, $J = 3.4$ Hz), 132.4 (d, $J = 8.2$ Hz), 129.9 (d, $J = 14$ Hz), 129.8, 128.9 (d, $J = 3.4$ Hz), 118.0 (118.1 ppm, 117.9 ppm, d, $J = 24$ Hz), 116.9 (d, $J = 3.4$ Hz), 52.2; ^{19}F NMR (282 MHz, CDCl_3) δ -116.8 (m); HRMS (ESI+) calculated: 307.9848 for $[\text{C}_{14}\text{H}_{10}^{79}\text{BrFO}_2]^+$ (M) $^+$ found 307.9818. IR neat: 3063, 2954, 2922, 2852, 1720, 1480, 1282, 1110, 804 cm^{-1} .

1.5 Summary

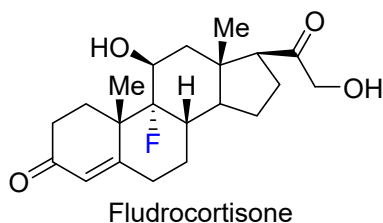
We found that Ir catalyzed C-H activation/borylation is not compatible with aryl tin compounds. But we were able to synthesis variety of B/Sn bimetallic compounds via Zn mediated stannylation of aryl bromides bearing a BPin group. This method was somewhat problematic with heterocyclic substrates. Finally, we found conditions for the selective Suzuki coupling of these B/Sn bimetallic compounds where the stannyl group survived.

Chapter 2 Electronics Driven Regioselective Ir-Catalyzed C-H

Activation/Borylation of Fluorinated Benzenes

2.1 Introduction

Figure 14. Structure of fludrocortisone

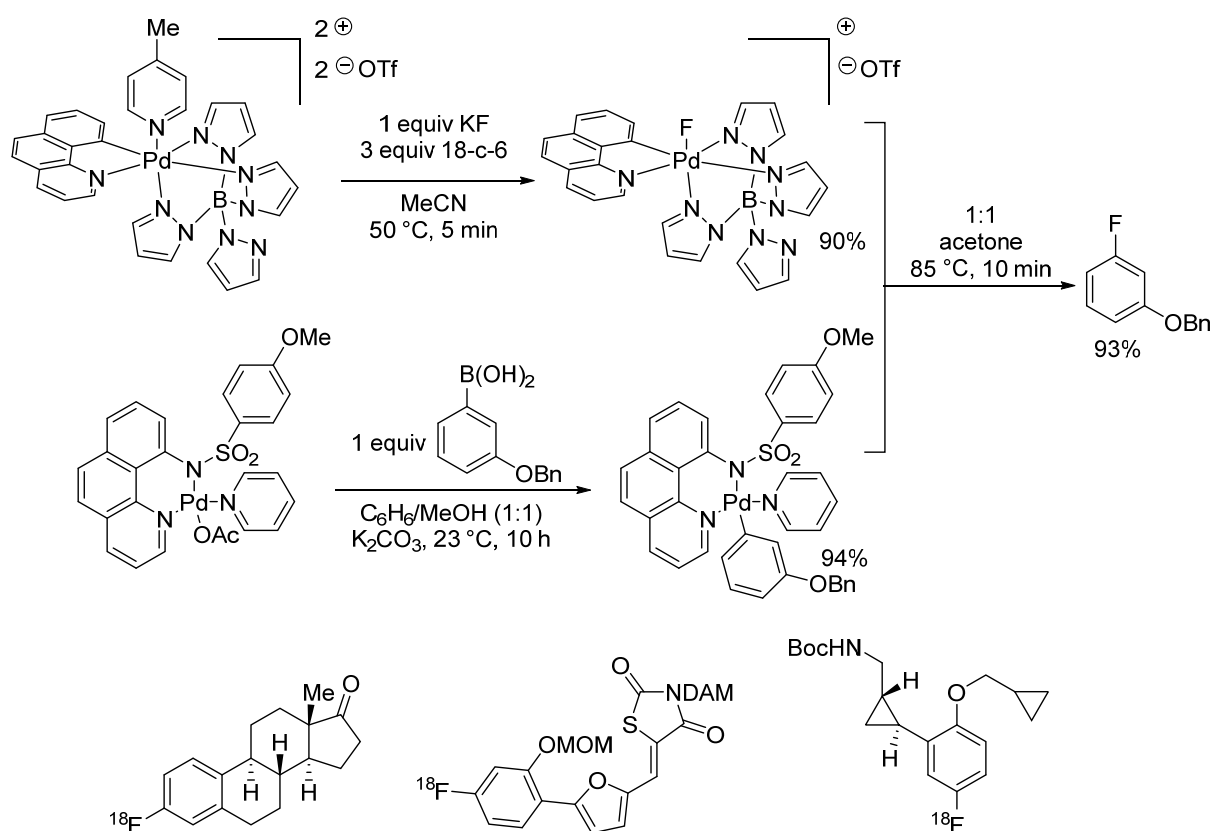


Ever since the introduction of fludrocortisone (**Figure 14**),³¹ the first fluorine-containing drug, fluorinated compounds have been intensively interesting to chemists studying bio-active molecules and medicines. As summarized in this review,³² the electronegativity, size, omniphobicity/lipophilicity, and electrostatic interactions of fluorine or fluorine containing functional groups can lead to dramatic differences in reactivity, stereochemistry, and bioavailability. Liu and others reviewed 40 fluorinated or fluorine containing new drugs introduced into the market in the decade from 2001 to 2011,³³ covering compounds that include anticancer drugs, drugs acting on the central nervous system, drugs affecting the cardiovascular system, drugs for infectious diseases, eye care drugs, drugs acting on the genitourinary system, respiratory system drugs, antidiabetes drugs, gastrointestinal tract drugs, endocrine system drugs, nutrition affecting drugs.

The preparation of fluorinated or fluorine containing organic molecules may take two routes: Late stage fluorination of organic molecules, or construction of the molecule with fluorinated building blocks. New methods have been developed in recent years for the late stage fluorination of

complicated organic molecules.³⁴ In Ritter's work, an octahedron Pd(IV) fluoride was formed, and its fluoride transferred to a Ar-Pd(II) species generated from a corresponding aryl boronic acid. This proceeds via an S_N2 mechanism by Pd(II) attacking on F, to give an Ar-Pd(IV)-F intermediate, which then affords the fluoroarene via a reductive elimination (**Figure 15**). This method avoids direct contact between strongly oxidative fluorinating species and potentially sensitive substrates.

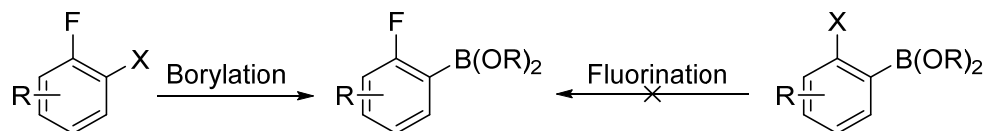
Figure 15. Ritter's fluoride derived late stage fluorination, and applications on complicated molecules



Due to stability of C-F bonds under most reaction conditions, construction of complicated molecules with fluorine containing building blocks is very attractive. We are interested in fluorinated aromatic boronic acids and/or esters, especially, *o*-fluoro boronic acids/esters. While late stage introduction of fluorine is attractive on paper, chemoselectivity in such fluorinations remains a challenge. In contrast, many simple fluorinated aromatics and heteroaromatics are

already commercially available. Fluorine does not require to be protected during further applications of boronic acids or esters in various transformations, especially Suzuki coupling reactions. Thus relatively simple fluorinated boronic acid or ester building blocks may enable introduction of fluorinated aromatics into complex molecules by multi-step synthesis. We proposed two routes for the synthesis of such compounds (**Figure 16**): the borylation of fluorobenzenes and the fluorination of aromatic boronic acids and/or esters.

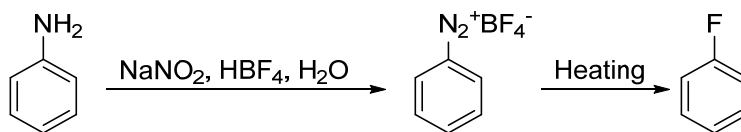
Figure 16. Borylation of fluorobenzenes or fluorination of aromatic boronic acids and/or esters



Although the fluorination of an aromatic boron compound was not found in a literature search. The chemistry of introducing fluorine into a small molecule has a long history. Regio- and chemoselective fluorinations have been performed in these ways:³⁵

1) The Balz-Schiemann reaction was reported as early as 1927. A recent look into this chemistry gave it new life.³⁶ Nonetheless, the reaction requires the formation of potentially dangerous diazonium salts $\text{ArN}_2^+\text{BF}_4^-$ and requires an amino group on the benzene ring (**Figure 17**).

Figure 17. General Scheme of Balz-Schiemann reaction



2) Nucleophilic fluorination, especially with aminosulfuranes such as DAST (**Figure 18**).³⁷ A drawback of this method is that those reagents are toxic and corrosive.

3) Electrophilic fluorination,³⁸ where nucleophiles such as enolates or electron-rich aromatic rings attack fluorines attached on a good leaving group (**Figure 19**).

Figure 18. Fluorination with DAST

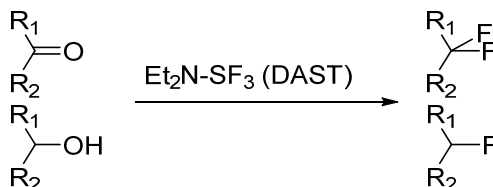
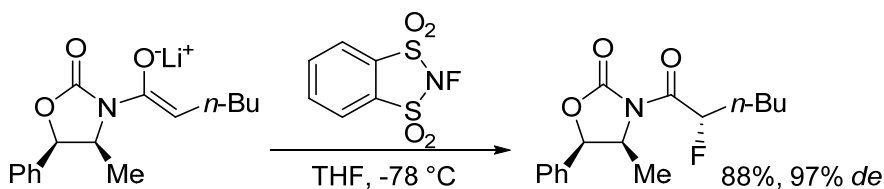
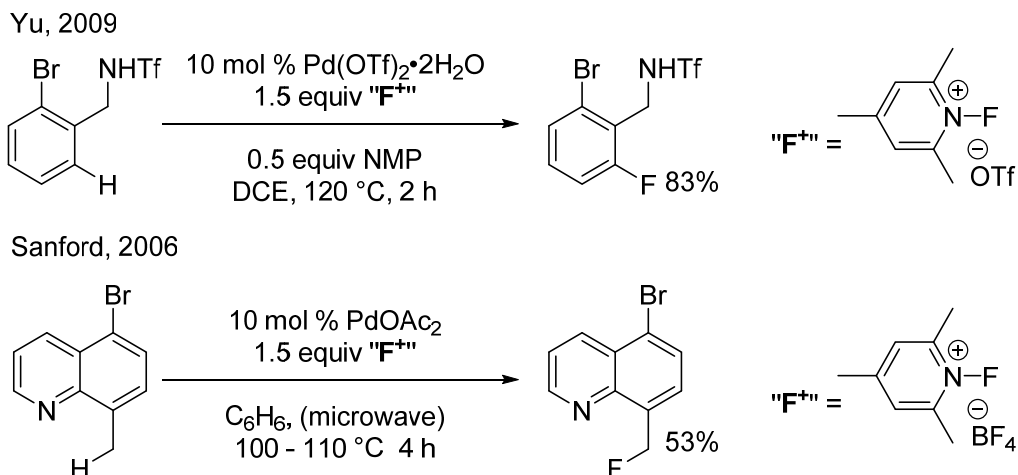


Figure 19. An example of asymmetric electrophilic fluorination



Yu, and Sanford have developed palladium catalyzed electrophilic C-H fluorinations. Their methods rely on activation of C-H bonds by palladium catalyst to generate a nucleophilic organometallic intermediate, which picks up an electrophilic fluorine from fluorinated reagents.³⁹ The reactions go through a Pd (II)-Pd(IV) catalytic cycle, allowing the survival of a bromine (**Figure 20**).

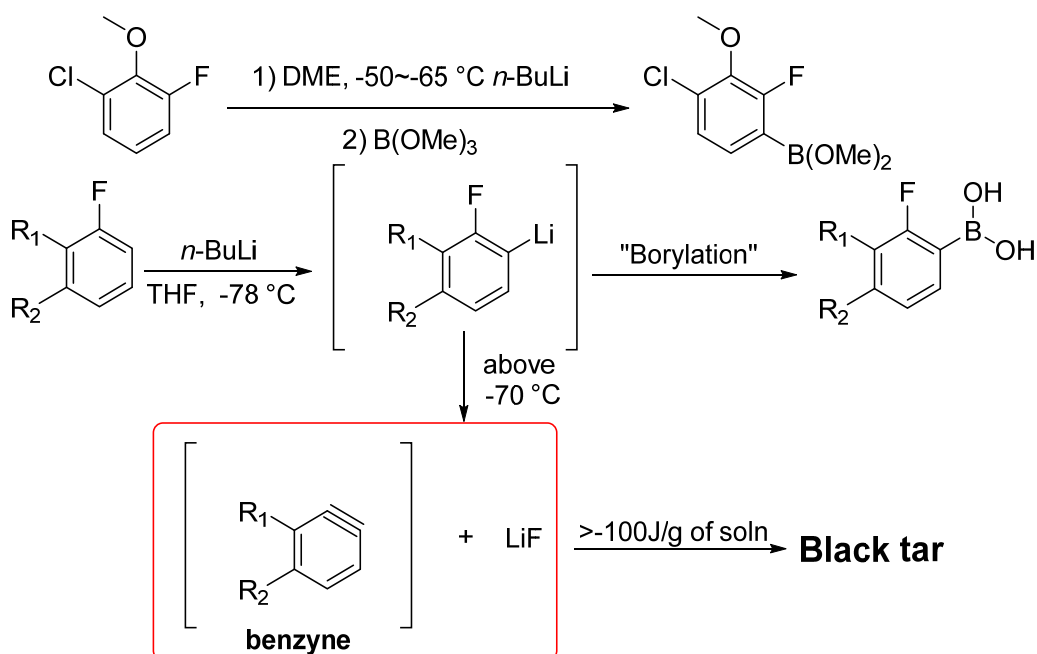
Figure 20. Palladium catalyzed electrophilic C-H fluorinations



These fluorination methodologies mentioned above all involve conditions unfavorable for the survival of aryl boronic esters, such as formation of HF, application of strong Lewis base nucleophiles, and transition metal catalysts.

The introduction of a boryl group ortho to fluorine on a benzene ring has been achieved in different ways.

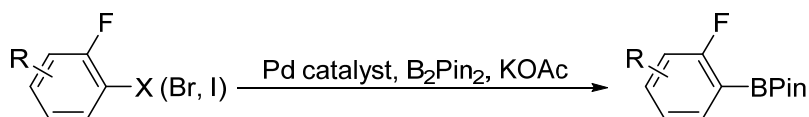
Figure 21. Lithiation/borylation at cryogenic condition and its possible risk



1) C-H/X lithium exchange: Due to the electronegativity of F, ortho C-H bond acidity is increased. Thus a strong base such as *n*-BuLi may lithiate the position ortho to fluorine. Quenching the litho salts with B(OMe)₃ can give the corresponding boronic esters (**Figure 21**).⁴⁰ Some drawbacks are associated with these reactions. These H-Li exchange or Br-Li exchange reactions require cryogenic temperature conditions. Chilling a large size industrial reactor to cryogenic temperature and maintaining it at such temperature is energy intensive and requires specially built reactors. Alkyl lithium solutions at industry scale also pose safety issues. Furthermore, even at cryogenic

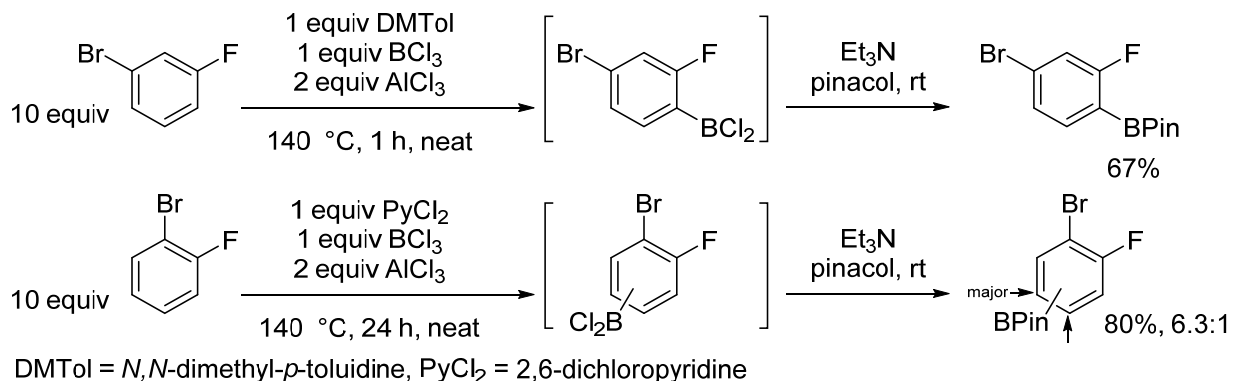
temperature, the formation of benzyne from the elimination of LiF is possible.⁴¹ In this specific example, the *o*-lithiofluorobenzene intermediate tends to form benzyne above -70 °C in THF. The resulting benzyne tends to polymerize to form a black tar via an exothermic process. The heat released from this process naturally facilitates more benzyne formation. Another concern is that such reaction conditions may also require protection of many functional groups. Lastly, the corresponding bromo starting material may be expensive or inaccessible.

Figure 22. General scheme of a Suzuki-Miyaura coupling reaction



2) Suzuki-Miyaura coupling reactions: As demonstrated in **Figure 22**, Pd-catalyzed borylations proceed under mild conditions. However those reactions again require arylhalides, which in addition to their accessibility can be toxic.

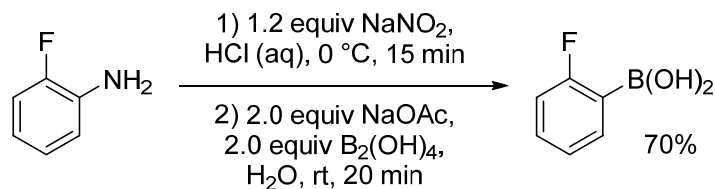
Figure 23. Ingelsohn's electrophilic aromatic borylation



3) Electrophilic aromatic borylation: Ingelsohn and his team reported the electrophilic borylation of benzene rings.⁴² The reaction of 1,3-substituted fluorobenzenes selectively borylates ortho to fluorine, however, the 1,2-substituted fluorobenzenes give a mixture, favoring para to fluorine (**Figure 23**). A significant drawback of this protocol is the need to use a large excess of

fluoroaromatics to suppress di-borylation. A few other examples of similar reactions are also known.⁴³

Figure 24. Sandmeyer type borylation of ortho fluoroanilines



4) Sandmeyer-type borylation: Sandmeyer reactions convert corresponding ortho fluoroanilines nicely into desired fluoroaryl boronic acids (**Figure 24**).⁴⁴ Similar reactions were also mentioned in Chapter 1. Again, such reactions involve potentially explosive diazonium salt intermediates.

Figure 25. Pt-catalyzed C-H activation/borylation on fluorobenzene

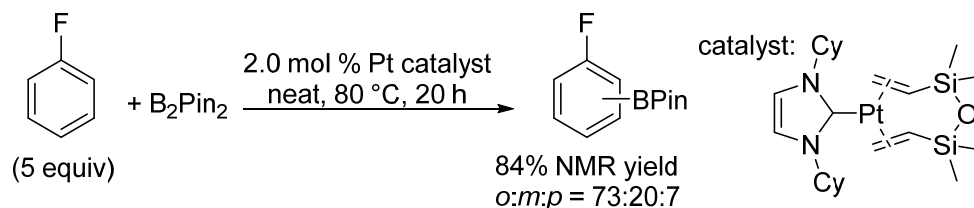
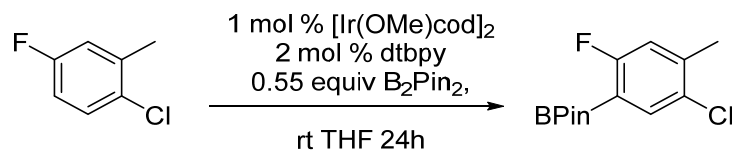


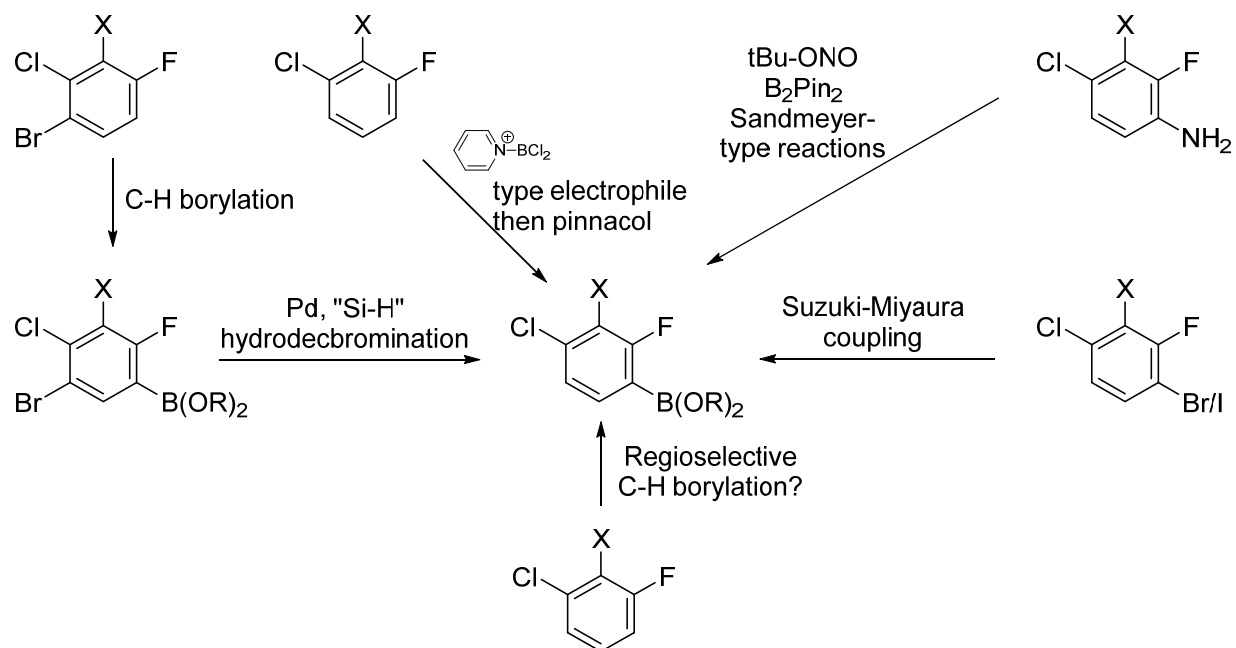
Figure 26. Borylation ortho to F on a 1,4-substituted benzene



5) Pt-catalyzed C-H activation/borylation: Tobisu and Chatani developed a method for aromatic C-H activation/borylation catalyzed Pt-NHC complexes (**Figure 25**).⁴⁵ These catalysts favor borylation of C-H bonds ortho to the fluorine and are less sensitive to steric effects, and therefore can borylate very hindered C-H bonds. A large excess of the arene substrate is used in this reaction, but the borylations of heteroaromatic substrates catalyzed by these platinum complexes are carried out with stoichiometric amount of borylation reagent and substrate.

6) Ir-catalyzed C-H activation/borylation was first reported in 1999.⁴⁶ Within two decades this methodology evolved into a widely used synthetic protocol to install a boron group on an unfunctionalized benzene or heterocycle.⁴⁷ Early studies of Ir-catalyzed C-H activation/borylation showed that on substituted benenes the regiochemistry favors the least hindered C-H site. Later, several recent works demonstrated substituent directed regioselectivity.⁴⁸ Due to the relatively small size of F, borylation ortho to fluorine is achievable, especially in a 1,4-disubstituted case, such as that illustrated in **Figure 26**.

Figure 27. Possible synthetic routes for regioselective borylation on 1-fluoro-3-chlorobenzene derivatives



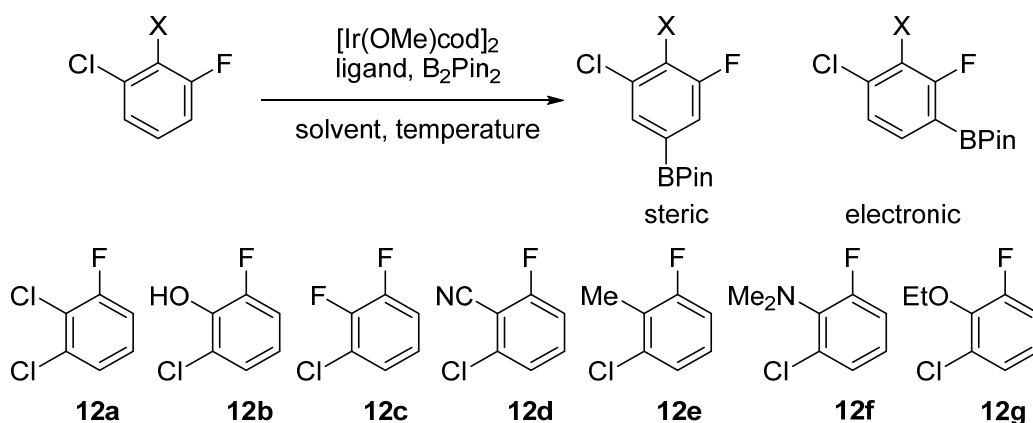
In our project, we were interested in borylation ortho to F on 1-fluoro-3-chlorobenzene derivatives. Based on our knowledge of the literature, several possible synthetic routes were considered (**Figure 27**). The Suzuki-Miyaura coupling and borylation-hydrodebromination require a pre-existing bromine at certain positions on the benzene ring. Sandmeyer type borylations require the

existence of an NH₂ at ortho to F. The region chemical outcome of the electrophilic borylations can be dramatically affected by the –X group.

However the possibility for a regioselective borylation that is governed by the electronic features of the substrate remains largely uncharted. To probe this possibility, we started with the borylation of substituted 1,3-fluorochlorobenzenes. Such substrates present a competition between a generally more reactive C-H bond ortho to F (the electronic product),⁴⁹ and a sterically unhindered C-H bond (the steric product), as shown in **Figure 28**.

As described in the literature, several substrates listed in **Figure 28** can be borylated ortho- to F via lithiation at cryogenic temperatures, followed by quenching with the corresponding boronic electrophiles. This route benefits from the high regioselectivity of ortho- deprotonation of fluorobenzenes, however, there are the previously described drawbacks. Ir catalyzed C-H activation/borylation, on the other hand, performs at room temperature or mild heating, and is known to tolerate many functional groups.

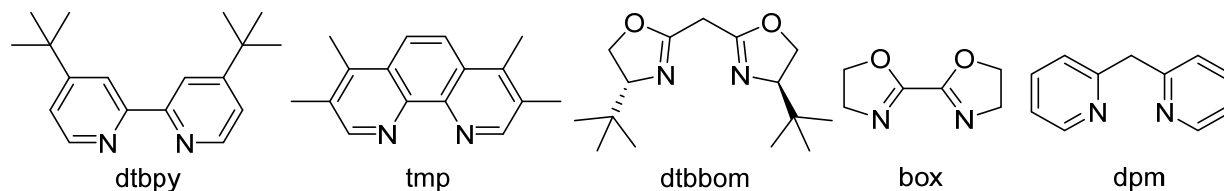
Figure 28. Regiochemical outcomes in borylation of 1,3-disubstituted benzenes



The goal of the study is to better understand factors that affect the regioselectivity and chemical yields of such borylations. Eventually we aim to be able to uncover the conditions that will enable

selective borylations to either electronic or steric products. Several different ligands were used in the screening, as listed in **Figure 29**.

Figure 29. Ligands used for screening



2.2 Screening borylation conditions

The borylations of these substrates under different combinations of ligands, solvents⁵⁰ and temperatures were carried out with the assistance of high throughput techniques. The screening reactions were analyzed by ¹⁹F NMR. The full analysis of these results are detailed in **Table 5**. The most profound factors affecting the borylation regioselectivities are the substrate and ligand effects. Clearly observed is a trend for electron donating substituents to favor electronic products and *vice versa*. Also, the BOX ligand favors electronic products more than any other ligands. Temperature, does not affect the regioselectivity significantly, but of course does affect reactivity. The heated reactions, in most cases gave higher conversions than their room temperature counterparts. Solvent choice also affects mainly reactivity rather than selectivity. As one might expect, reactions in polar NMP gave lower conversions than those in less polar solvents, namely cyclohexane, THF, and Hünig's base. Notably, the reactivity of the BOX ligand also depended on its solubility in the corresponding solvent.

Table 5. Borylation screening

1 mol % [Ir(OMe)cod]₂
2 mol % ligand

1 equiv B₂Pin₂
solvent, temperature

BPin Steric (st) Electronic (ele)

entry	X	ligand	solvent	T (°C)	t (h)	conversion ^a	st/ele	entry	X	ligand	solvent	T (°C)	t (h)	conversion ^a	st/ele
1	Me	dtbpy	CyH	r.t.	12	66%	73 : 27	47	F	tmp	Hünig's base	60	6	69%	39 : 61
2	OEt	dtbpy	CyH	r.t.	12	54%	50 : 50	48	CN	tmp	Hünig's base	60	6	70%	67 : 33
3	NMe ₂	dtbpy	CyH	r.t.	12	49%	56 : 44	49	Me	BOX	Hünig's base	60	6	20%	45 : 55
4	Cl	dtbpy	CyH	r.t.	12	58%	53 : 47	50	OEt	BOX	Hünig's base	60	6	28%	17 : 83
5	F	dtbpy	CyH	r.t.	12	74%	39 : 61	51	NMe ₂	BOX	Hünig's base	60	6	26%	28 : 72
6	CN	dtbpy	CyH	r.t.	12	57%	70 : 30	52	Cl	BOX	Hünig's base	60	6	42%	21 : 79
7	Me	tmp	CyH	r.t.	12	51%	73 : 27	53	F	BOX	Hünig's base	60	6	42%	12 : 88
8	OEt	tmp	CyH	r.t.	12	78%	53 : 47	54	CN	BOX	Hünig's base	60	6	53%	45 : 55
9	NMe ₂	tmp	CyH	r.t.	12	85%	59 : 41	55	Me	dpm	Hünig's base	60	6	50%	65 : 35
10	Cl	tmp	CyH	r.t.	12	90%	57 : 43	56	OEt	dpm	Hünig's base	60	6	56%	47 : 53
11	F	tmp	CyH	r.t.	12	85%	59 : 41	57	NMe ₂	dpm	Hünig's base	60	6	58%	56 : 44
12	CN	tmp	CyH	r.t.	12	67%	70 : 30	58	Cl	dpm	Hünig's base	60	6	88%	58 : 42
13	Me	dtbpy	CyH	60	6	61%	73 : 27	59	F	dpm	Hünig's base	60	6	86%	40 : 60
14	OEt	dtbpy	CyH	60	6	74%	52 : 48	60	CN	dpm	Hünig's base	60	6	75%	63 : 37
15	NMe ₂	dtbpy	CyH	60	6	66%	57 : 43	61	Me	bom	Hünig's base	60	6	2%	-
16	Cl	dtbpy	CyH	60	6	69%	57 : 43	62	OEt	bom	Hünig's base	60	6	1%	-
17	F	dtbpy	CyH	60	6	82%	44 : 56	63	NMe ₂	bom	Hünig's base	60	6	1%	-
18	CN	dtbpy	CyH	60	6	74%	68 : 32	64	Cl	bom	Hünig's base	60	6	1%	-
19	Me	tmp	CyH	60	6	75%	72 : 28	65	F	bom	Hünig's base	60	6	2%	-
20	OEt	tmp	CyH	60	6	55%	56 : 44	66	CN	bom	Hünig's base	60	6	N.R.	-
21	NMe ₂	tmp	CyH	60	6	79%	64 : 36	67	Me	dtbpy	Hünig's base	r.t.	12	10%	70 : 30
22	Cl	tmp	CyH	60	6	67%	57 : 43	68	OEt	dtbpy	Hünig's base	r.t.	12	19%	46 : 54
23	F	tmp	CyH	60	6	85%	57 : 43	69	NMe ₂	dtbpy	Hünig's base	r.t.	12	10%	58 : 42
24	CN	tmp	CyH	60	6	78%	71 : 29	70	NMe ₂	dtbpy	Hünig's base	r.t.	12	51%	55 : 45
25	Me	BOX ^b	CyH	60	6	2%	-	71	F	dtbpy	Hünig's base	r.t.	12	54%	33 : 67
26	OEt	BOX	CyH	60	6	2%	-	72	CN	dtbpy	Hünig's base	r.t.	12	30%	60 : 40
27	NMe ₂	BOX	CyH	60	6	2%	-	73	Me	tmp	Hünig's base	r.t.	12	N.R.	-
28	Cl	BOX	CyH	60	6	3%	-	74	OEt	tmp	Hünig's base	r.t.	12	N.R.	-
29	F	BOX	CyH	60	6	3%	-	75	NMe ₂	tmp	Hünig's base	r.t.	12	N.R.	-
30	CN	BOX	CyH	60	6	15%	58 : 42	76	Cl	tmp	Hünig's base	r.t.	12	N.R.	-
31	Me	dpm	CyH	60	6	26%	63 : 37	77	F	tmp	Hünig's base	r.t.	12	N.R.	-
32	OEt	dpm	CyH	60	6	35%	43 : 57	78	CN	tmp	Hünig's base	r.t.	12	N.R.	-
33	NMe ₂	dpm	CyH	60	6	45%	54 : 46	79	Me	BOX	Hünig's base	r.t.	12	N.R.	-
34	Cl	dpm	CyH	60	6	75%	57 : 43	80	OEt	BOX	Hünig's base	r.t.	12	N.R.	-
35	F	dpm	CyH	60	6	66%	36 : 64	81	NMe ₂	BOX	Hünig's base	r.t.	12	N.R.	-
36	CN	dpm	CyH	60	6	25%	63 : 37	82	Cl	BOX	Hünig's base	r.t.	12	N.R.	-
37	Me	dtbpy	Hünig's base	60	6	75%	73 : 27	83	F	BOX	Hünig's base	r.t.	12	N.R.	-
38	OEt	dtbpy	Hünig's base	60	6	78%	53 : 47	84	CN	BOX	Hünig's base	r.t.	12	N.R.	-
39	NMe ₂	dtbpy	Hünig's base	60	6	75%	59 : 41	85	Me	dpm	Hünig's base	r.t.	12	N.R.	-
40	Cl	dtbpy	Hünig's base	60	6	86%	57 : 43	86	OEt	dpm	Hünig's base	r.t.	12	N.R.	-
41	F	dtbpy	Hünig's base	60	6	93%	40 : 60	87	NMe ₂	dpm	Hünig's base	r.t.	12	N.R.	-
42	CN	dtbpy	Hünig's base	60	6	88%	66 : 34	88	Cl	dpm	Hünig's base	r.t.	12	N.R.	-
43	Me	tmp	Hünig's base	60	6	47%	75 : 25	89	F	dpm	Hünig's base	r.t.	12	N.R.	-
44	OEt	tmp	Hünig's base	60	6	64%	54 : 46	90	CN	dpm	Hünig's base	r.t.	12	N.R.	-
45	NMe ₂	tmp	Hünig's base	60	6	49%	54 : 46	91	Me	dtbpy	NMP	60	6	45%	72 : 28
46	Cl	tmp	Hünig's base	60	6	63%	57 : 43	92	OEt	dtbpy	NMP	60	6	44%	59 : 41

Table 5 (cont'd)

entry	X	ligand	solvent	T (°C)	t (h)	conversion ^a	st/ele	entry	X	ligand	solvent	T (°C)	t (h)	conversion ^a	st/ele
93	NMe ₂	dtbpy	NMP	60	6	46%	67 : 33	119	F	tmp	THF	r.t.	12	51%	37 : 63
94	Cl	dtbpy	NMP	60	6	36%	62 : 38	120	CN	tmp	THF	r.t.	12	68%	76 : 24
95	F	dtbpy	NMP	60	6	40%	31 : 69	121	Me	dpm	THF	60	6	13%	73 : 27
96	CN	dtbpy	NMP	60	6	9%	10 : 90	122	OEt	dpm	THF	60	6	14%	66 : 34
97	Me	dpm	NMP	60	6	10%	78 : 22	123	NMe ₂	dpm	THF	60	6	14%	67 : 33
98	OEt	dpm	NMP	60	6	11%	57 : 43	124	Cl	dpm	THF	60	6	66%	63 : 37
99	NMe ₂	dpm	NMP	60	6	9%	70 : 30	125	F	dpm	THF	60	6	62%	42 : 58
100	Cl	dpm	NMP	60	6	21%	64 : 36	126	CN	dpm	THF	60	6	15%	72 : 28
101	F	dpm	NMP	60	6	22%	45 : 55	127	Me	BOX	THF	60	6	12%	45 : 55
102	CN	dpm	NMP	60	6	10%	64 : 36	128	OEt	BOX	THF	60	6	15%	25 : 75
103	Me	BOX	THF	r.t.	12	N.R.	-	129	NMe ₂	BOX	THF	60	6	12%	37 : 63
104	OEt	BOX	THF	r.t.	12	2%	-	130	Cl	BOX	THF	60	6	24%	33 : 67
105	NMe ₂	BOX	THF	r.t.	12	N.R.	-	131	F	BOX	THF	60	6	22%	23 : 77
106	Cl	BOX	THF	r.t.	12	15%	20 : 80	132	CN	BOX	THF	60	6	30%	55 : 45
107	F	BOX	THF	r.t.	12	15%	9 : 91	133	Me	tmp	THF	60	6	46%	74 : 26
108	CN	BOX	THF	r.t.	12	19%	39 : 61	134	OEt	tmp	THF	60	6	61%	54 : 46
109	Me	dtbpy	THF	r.t.	12	47%	75 : 25	135	NMe ₂	tmp	THF	60	6	66%	62 : 38
110	OEt	dtbpy	THF	r.t.	12	71%	51 : 49	136	Cl	tmp	THF	60	6	74%	61 : 39
111	NMe ₂	dtbpy	THF	r.t.	12	65%	57 : 43	137	F	tmp	THF	60	6	85%	41 : 59
112	Cl	dtbpy	THF	r.t.	12	79%	57 : 43	138	CN	tmp	THF	60	6	64%	74 : 26
113	F	dtbpy	THF	r.t.	12	84%	37 : 63	139	Me	dtbpy	THF	60	6	75%	74 : 26
114	CN	dtbpy	THF	r.t.	12	84%	80 : 20	140	OEt	dtbpy	THF	60	6	52%	57 : 43
115	Me	tmp	THF	r.t.	12	50%	74 : 26	141	NMe ₂	dtbpy	THF	60	6	63%	61 : 39
116	OEt	tmp	THF	r.t.	12	50%	49 : 51	142	Cl	dtbpy	THF	60	6	59%	61 : 39
117	NMe ₂	tmp	THF	r.t.	12	46%	60 : 40	143	F	dtbpy	THF	60	6	86%	47 : 53
118	Cl	tmp	THF	r.t.	12	53%	59 : 41	144	CN	dtbpy	THF	60	6	72%	67 : 33

a. Conversion based on boron atoms.

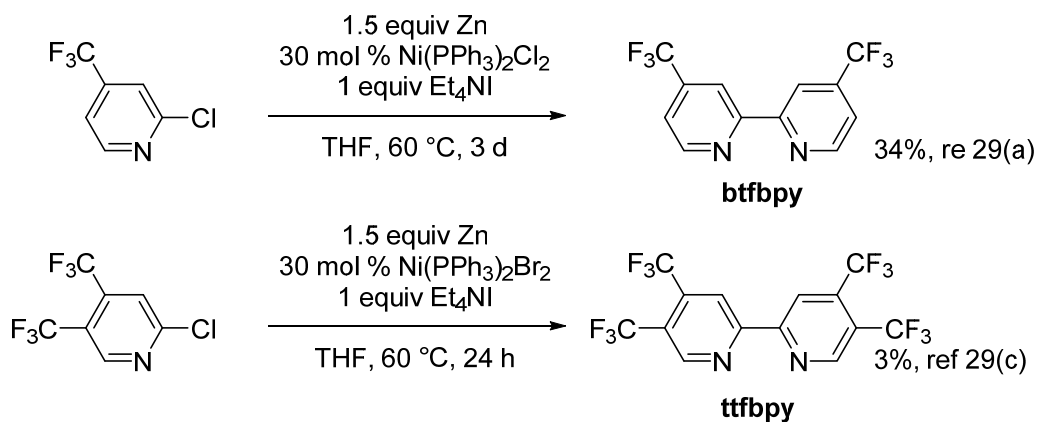
b. Box ligand is not well dissolved in cyclohexane.²

2.3 Ligand effects hypothesis

Earlier research showed that electron rich ligands are more effective borylation catalysts (due to the proton transfer characteristics of the C-H activation transition state). Because of their high reactivity in activating C-H bonds, the regioselectivity is mostly dictated by steric effects. We hypothesized that if the ligands were electron poor, then the reactivity of the C-H bond itself might become a driving force of the reaction regioselectivity. Based on this argument, we believed a suitable ligand for selective borylation ortho to fluorine should be an electron deficient molecule that would discriminate C-H bonds based on their relative acidity, provided there is insignificant steric hindrance at that C-H bond.

2.4 Searching for new ligands

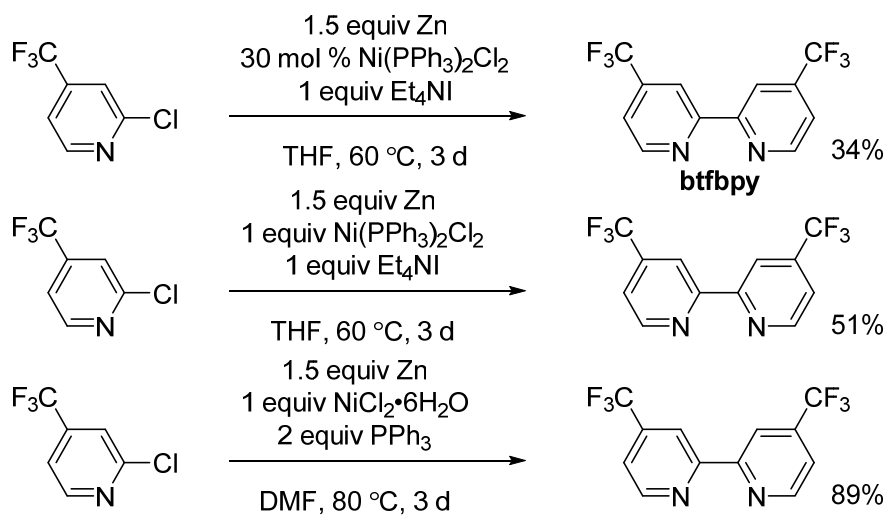
Figure 30. Literature synthesis of bis- and tetra- CF₃ substituted bipyridines



The tetrahydrodiboxazole (BOX) ligand fits into our criteria for an ortho to F selective ligand, as it is electron poorer than dtbpy or tmp, and is not sterically hindered. Also, in practice the BOX ligand favored electronic products with most of the substrates. However BOX gave lower conversions and formation of large amount of borates (B(OR)₃, ~ 22 ppm) were observed in the ¹¹B NMR of the reaction crude. We considered the relatively open bite angle (N-Ir-N angle) of a BOX-Ir complex might lead to less efficient L-Ir binding.⁵¹ Thus we looked into bipyridines with electron withdrawing substituents. Such ligands might inherit the good geometry of bipyridine parent model, but the electron deficient rings could still favor the electronic product. We proposed two tentative structures, 4,4'-bistrifluoromethyl bipyridine (btfbpy) and 4,4',5,5'-tetrakis(trifluoromethyl) bipyridine (ttfbpy) for exploration. The synthesis of both ligands were described in the literature, but these synthesis suffered from relatively low yields, especially the latter, as illustrated in **Figure 30**.⁵² Thus we sought to improve the yields by modifying the conditions.⁵³ We started with the synthesis of btfbpy. Naturally, we began by increasing Ni catalyst load to equal that of the substrate, and we observed a significant increase in the yield (**Figure 31**). We then considered a different reaction set up, namely NiCl₂ and PPh₃ instead of the pre-assembled catalyst.

The reaction was performed in DMF. Since the Ni salt was hydrated, we used DMF without drying. We at first had feared the water be problematic, but it turned out not to inhibit the success. The reaction was followed by GC-MS until the starting material was fully consumed, and in the end 89% isolated yield was achieved (**Figure 31**).

Figure 31. Improving the synthesis of 4,4-bistrifluoromethyl bipyridine (btfbpy)



We next applied these conditions to the synthesis of ttfbpy. We observed a 31% isolated yield, as opposed to the 3% literature yield.⁵² We attempted to further optimize the conditions by doubling the zinc load to 3 equivalents. After 48 hours of heating, GC-MS indicated full consumption of the starting material, but the desired product was not found. Instead, a peak with *m/e* 374 was found, which could be bpy(CF₃)₃CH₃. We partially separated from the crude, a mixture of two proposed byproducts. In the ¹H NMR (**Figure 32 and 33**), we observed two methyl peaks at 2.56 and 2.61 ppm 3:1 ratio. In the ¹⁹F NMR (**Figure 34**) we observed a set of peaks at -59.2 ppm, -61.7 ppm and -64.1 ppm (1:1:1) overlapping with another set of peaks at -59.2 ppm and -61.7 ppm (1:2). It was most likely that the excessive Zn lead to the reduced byproduct, Based on the proposed structure, an isolated yield of 18% was achieved.

Figure 32. Proton NMR of the mixture of reduction products, aliphatic part

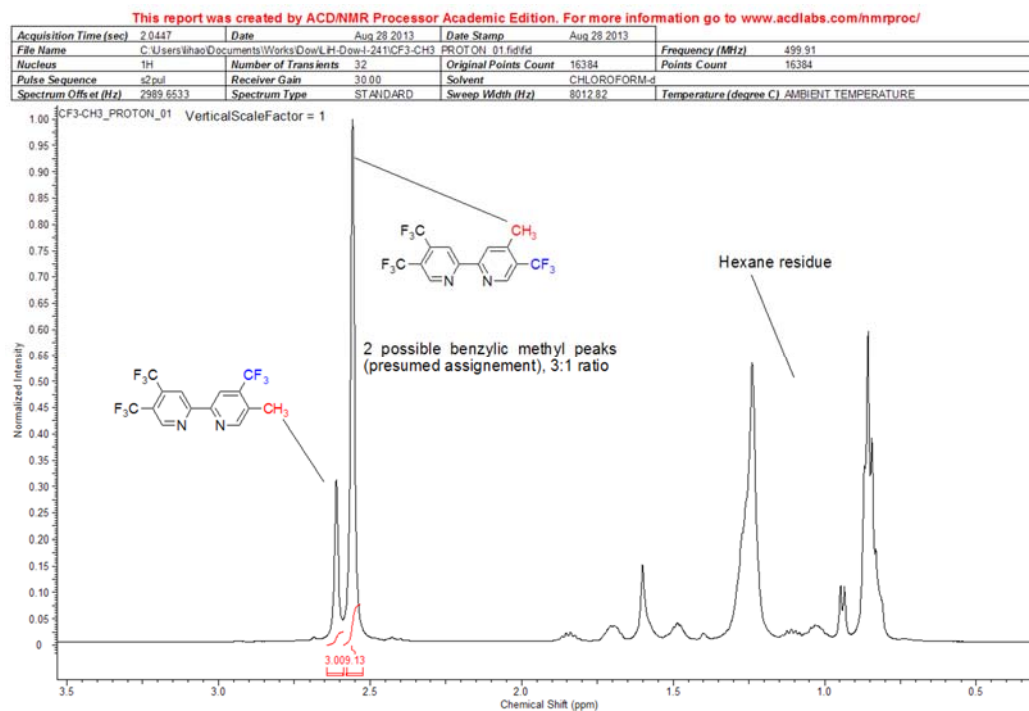


Figure 33. Proton NMR of the mixture of reduction products, aromatic part

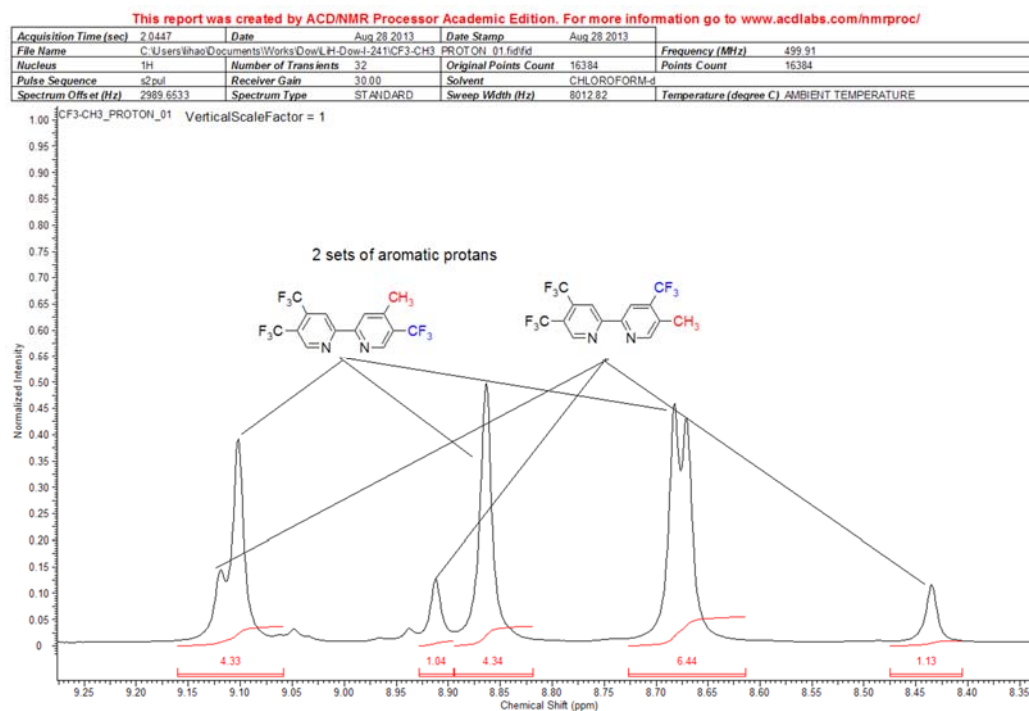
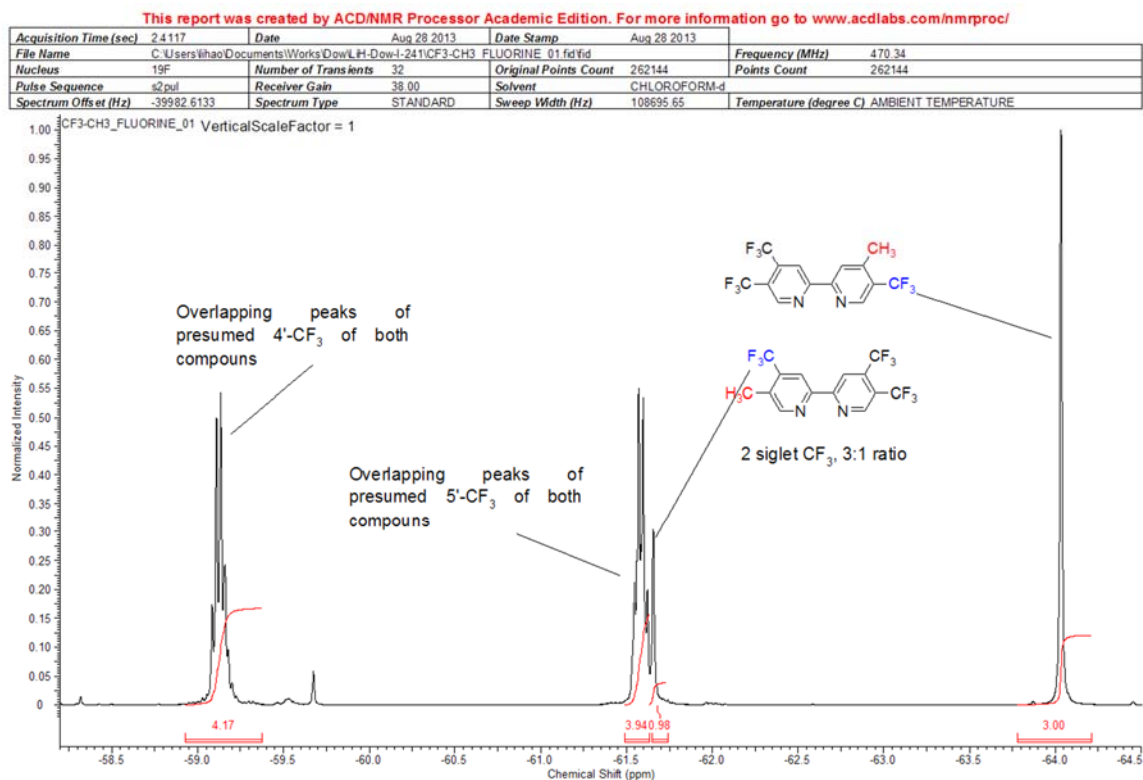


Figure 34. ^{19}F NMR of the mixture of reduction products



When we reduced the load of Zn to 1 equivalent, the byproducts were no longer seen by GC-MS, but the desired product was observed. A 71% isolated was achieved on 1 mmol scale, and 67% isolated yield on 10 mmol scale (**Figure 35**). These ligands were reported as borylation catalyst, and borylation catalysts are usually electron rich ligands, however electron deficient ligands were used in published borylation reactions by Ishiyama.^{25 (b)}

2.5 Results and discussions

We subjected both new ligands to high throughput screening and the results are listed in **Table 7**. We were pleased to find that the regioselectivity in those reactions significantly switched towards the electronic products. The conversions with electron rich substrates were lower, but moderate with electron poor substrates.

Figure 35. Improving the synthesis of 4,4',5,5'-tetratrifluoromethyl bipyridine (ttfbpy)

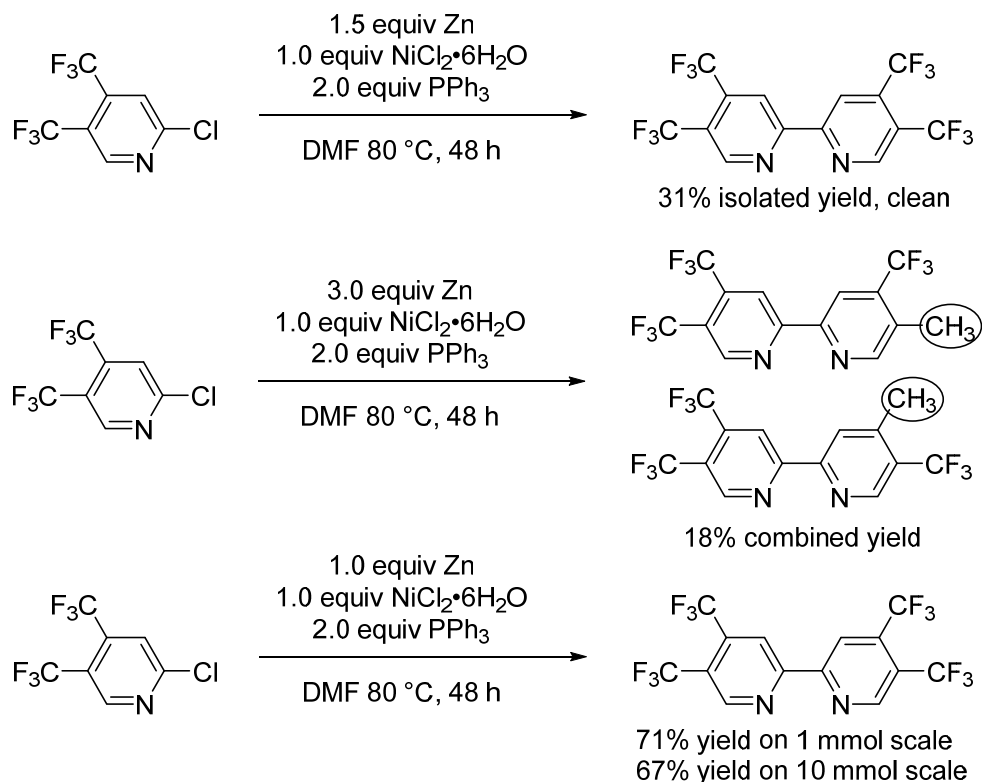


Table 6. Borylation screening with bpy(CF₃)_x ligands

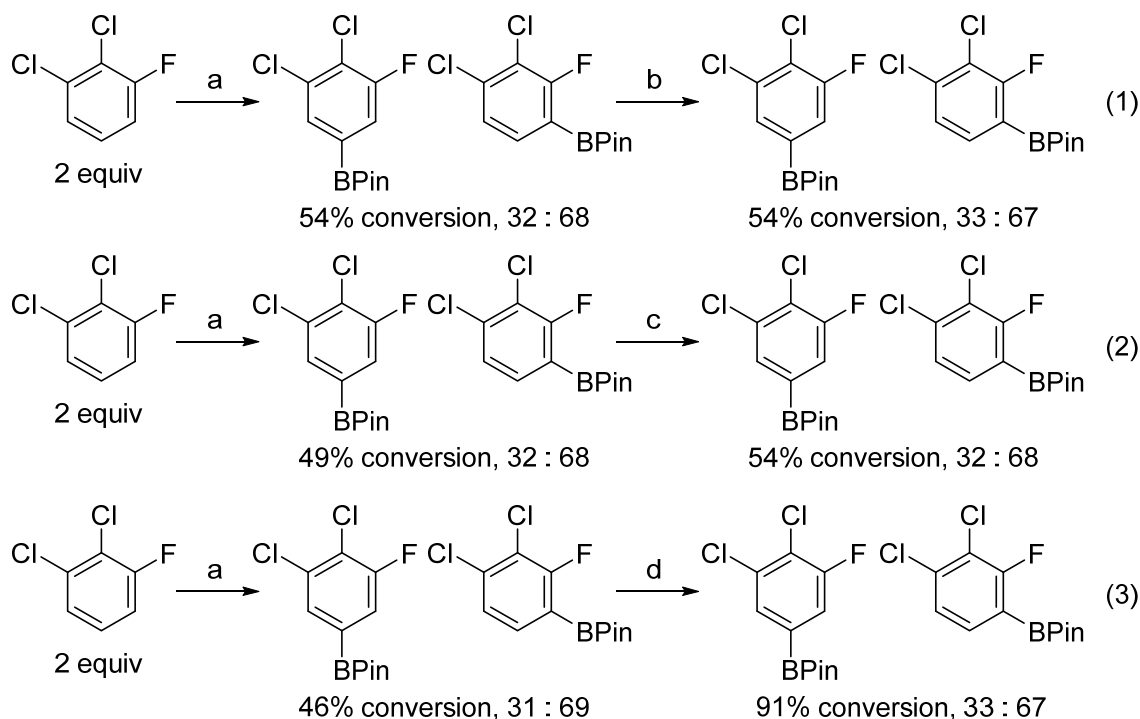
entry	X	ligand	conversion ^a	st/ele ^a	entry	X	ligand	conversion ^a	st/ele ^a
1	Me	btfbpy	28%	42 : 58	7	Me	ttfbpy	12%	52 : 48
2	OEt	btfbpy	45%	48 : 52	8	OEt	ttfbpy	12%	43 : 57
3	NMe ₂	btfbpy	49%	35 : 65	9	NMe ₂	ttfbpy	32%	32 : 68
4	Cl	btfbpy	57%	35 : 65	10	Cl	ttfbpy	77%	32 : 68
5	F	btfbpy	57%	21 : 79	11	F	ttfbpy	64%	18 : 82
6	CN	btfbpy	63%	37 : 63	12	CN	ttfbpy	74%	33 : 67

^aConversion based on boron atoms.

We found out the borylation of 1,2-dichloro-3-fluorobenzene (**12a**) with btfbpy as ligand can also be carried out at room temperature, but the reaction stops at 50% conversion based on boron atom equivalent, ¹¹B NMR of the crude reaction mixture showed the formation of borylation products

and HBPin. The reaction seems to be only consuming B₂Pin₂, but not the HBPin generated *in situ* after the borylation with B₂Pin₂. We set up a group of reactions to exam whether adding more B₂Pin₂ or catalyst can push the reaction further (**Figure 36**).

Figure 36. Resurrecting the borylation

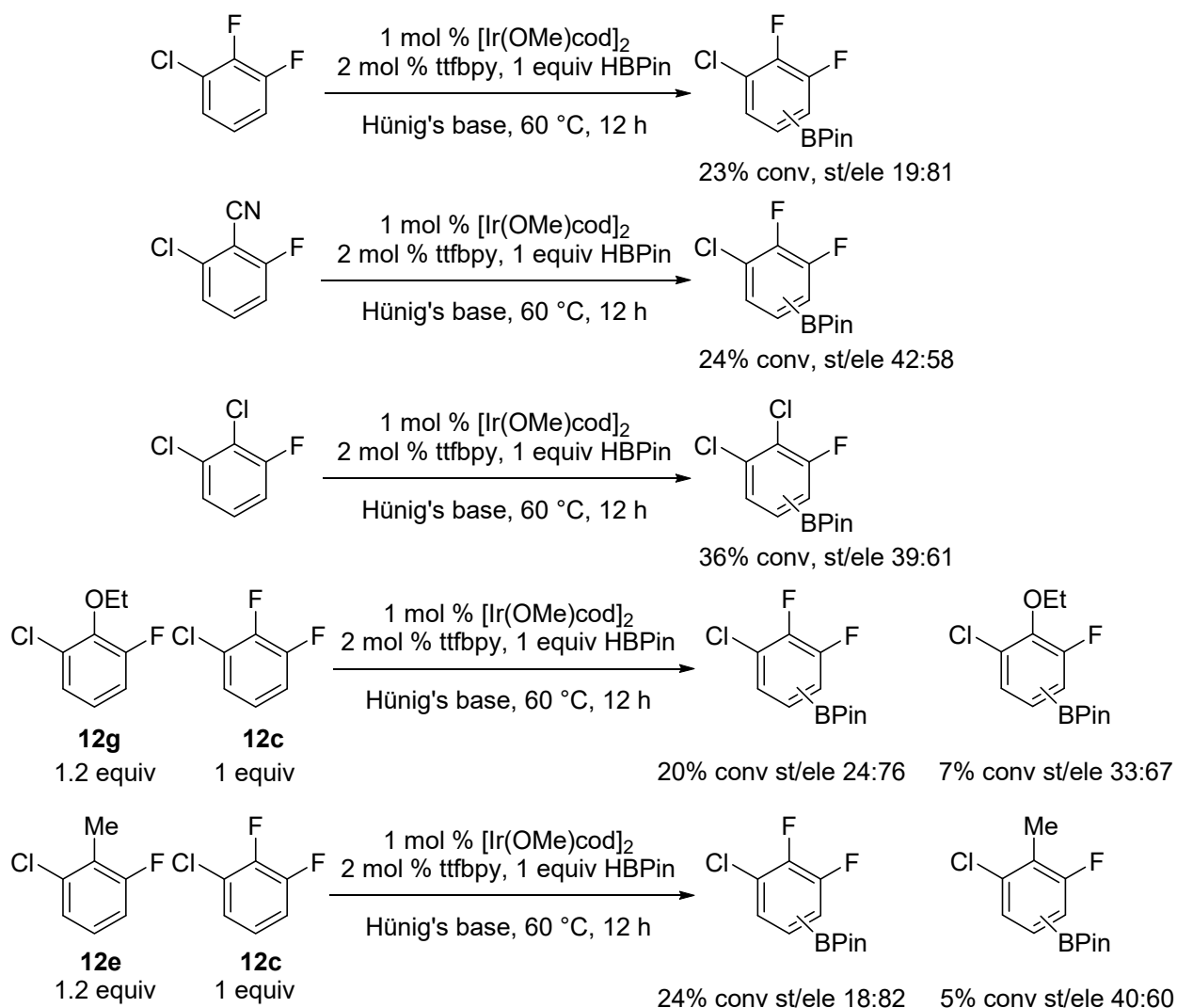


a. 1 mol % [Ir(OMe)cod]₂, 2 mol % btfbpy, 1 equiv B₂Pin₂, dodecane (GC internal standard), Hünig's base, rt, 4 h. b. rt 4 h. c. additional 1 mol % [Ir(OMe)cod]₂ and 2 mol % btfbpy, rt, 4 h. d. additional 1 equiv B₂Pin₂, rt, 40 h

Three reactions were set up parallel. All three proceeded to around 50% conversion at room temperature after 4 hours. As a control group, reaction (1) was allowed to go for another 4 hours. No progress in the reaction was observed and the ratio of the products remained the same. To reaction (2) additional catalyst was added after the reaction reached 50% conversion. The additional Ir and ligands did not push the reaction further. To reaction (3) an additional 1 equiv of B₂Pin₂ lead to further borylation, which eventually achieved 91% conversion after 40 hours. This suggests under such conditions only one boron of the B₂Pin₂ is utilized for the borylation. Note

that in **Table 7**, electron poor substrates went over 50% conversion (entries 10, 11, and 12), suggesting *in situ* HBPIn was consumed in these borylations. Borylations by HBPIn were then compared among several substrates as shown in **Figure 37**.

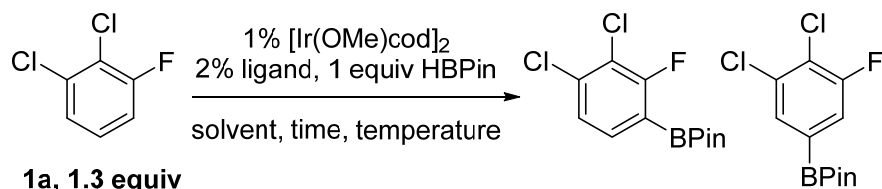
Figure 37. Borylation by HBPIn



The presence of **12e** or **12g** did not shut down the borylation of **12c** with HBPIn, however they gave very low conversions. Generally the borylations by HBPIn with these ligands are not practical, especially with electron rich substrates. We then further tested borylations of another substrate (1,2-dichloro-3-fluorobenzene, **12a**) by HBPIn with ttfbpy as the ligand, and with different combinations

of temperature/solvent (**Table 8**). The results show that the combination of electron deficient ligand and HBPIn is inefficient for the borylations.

Table 7. Borylation of 12a by HBPIn

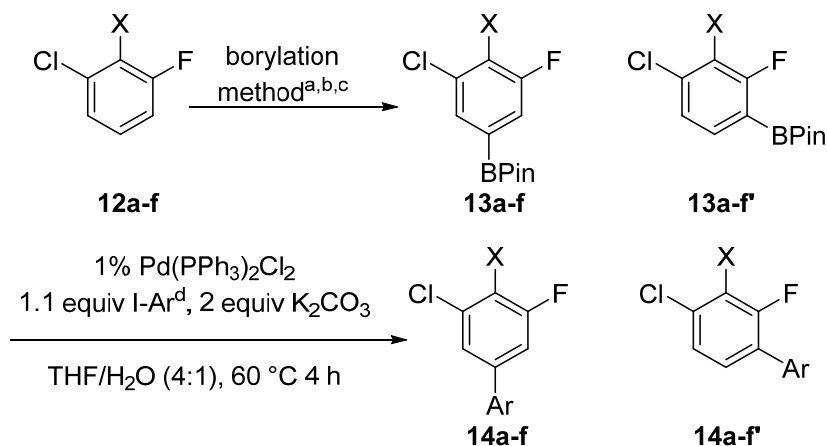


entry	solvent	ligand	temp	time	conversion ^a	st/ele ^a
1	THF	dtbpy	rt	12 h	trace	-
2	THF	tmp	rt	12 h	trace	-
3	THF	btfbpy	rt	12 h	trace	-
4	THF	dtbpy	80 °C	12 h	72%	72 : 28
5	THF	tmp	80 °C	12 h	45%	66 : 34
6	THF	btfbpy	80 °C	12 h	14%	33 : 67
7	NMP	btfbpy	rt	12 h	trace	-
8	Hünig's Base	btfbpy	rt	12 h	trace	-
9	Hünig's Base	btfbpy	80 °C	12 h	11%	34 : 66

^aConversion based on boron atoms.

2.6 Tandem borylation-Suzuki coupling

The application of electron deficient ligands greatly improved the yield of electronic products that are difficult to obtain under conversional Ir-catalyzed borylation conditions. However, even in our best cases, we only achieved a 1:4 ratio of products. As it was hard for us to separate those products, we reasoned that perhaps if these boronic ester intermediate could be transformed to more easily separated products, this methodology could still be of synthetic value. We decided to subject mixture of borylation products to Suzuki conditions aiming to generate a more stable and separable final product. We borylated several substrates with dtbpy (4,4'-di-tert-butylbipyride), btfbpy (4,4'-bistrifluoromethylbipyride) and ttfbpy (4,4',5,5'-tetrakis(trifluoromethyl)bipyride). The reaction crude was partially purified to give a mixture of two borylation products that could be subjected to a Suzuki coupling. This purification was necessary to avoid deborylation catalyzed by Ir residue during the Suzuki coupling. The results of our attempts are listed in **Table 9**, but it should be noted that some of the Suzuki regioisomeric mixtures were still difficult to be separated.

Table 8. Tandem borylation-Suzuki coupling

entry	-X	borylation conversion and 13/13' ratio ^e	Suzuki crude yield and 14/14' ratio ^f	Suzuki isolated yield ^e
1 ^a	Cl	93% (33 : 67)	99% (33 : 67)	15% 14a , 30% 14a'
2 ^a	OH	96% (31 : 69)	84% (29 : 71)	3% 14b , 48% mixture (26 : 74)
3 ^b	F	85% (18 : 82)	85% (15 : 85)	7% 14c , 41% 14c'
4 ^b	CN	80% (36 : 64)	68% (32 : 68)	8% 14d , 17% 14d'
5 ^c	Me	87% (75 : 25)	88% (81 : 19)	59% mixture (72 : 28)
6 ^c	NMe ₂	94% (61 : 39)	70% (66 : 34)	30% mixture (62 : 38)

a. 1% [Ir(OMe)cod]₂, 2% btfbpy, 1.0 equiv B₂Pin₂, Hünig's Base, rt, 12 h
 b. 1% [Ir(OMe)cod]₂, 2% ttfbpy, 0.5 equiv B₂Pin₂, Hünig's Base, 60 °C 6 h
 c. 1% [Ir(OMe)cod]₂, 2% dtbpy, 0.5 equiv B₂Pin₂, THF, 60 °C 6 h
 d. Methyl 4-iodobenzoate; e. Based on substrate; f. Based on borylated materials

2.7 Kinetics study of the borylations with electron deficient ligands

To further investigate these electron deficient ligands, we performed kinetic studies. We synthesized a pre-assembled catalyst Ir(Bpin)₃btfbpy(coe) (**15**) using a protocol similar to literature method of making Ir(Bpin)₃dtbpy(coe) (**Figure 38**).^{25 (b)}

We set up kinetic studies using pre-assembled catalyst (**15**). We decided to monitor the reaction by ¹⁹F NMR, as fluorine NMR gives fewer but well distinguished peaks for the starting material, products and also the catalyst. We fixed the concentration of starting material, varied the concentration of between 5 to 10 equivalents. While this looks to be a narrower range than typical setups for pseudo-first order studies, we were limited by solubility of B₂Pin₂ and the minimum concentration of catalyst **15** needed to afford reliable NMR integration. We considered this to be

acceptable as Ishiyama and Hartwig operated in an even narrower range of excess B_2Pin_2 (between 1.5 and 2.4 equivs).^{25 (b)}

Figure 38. Synthesis of pre-assembled catalyst

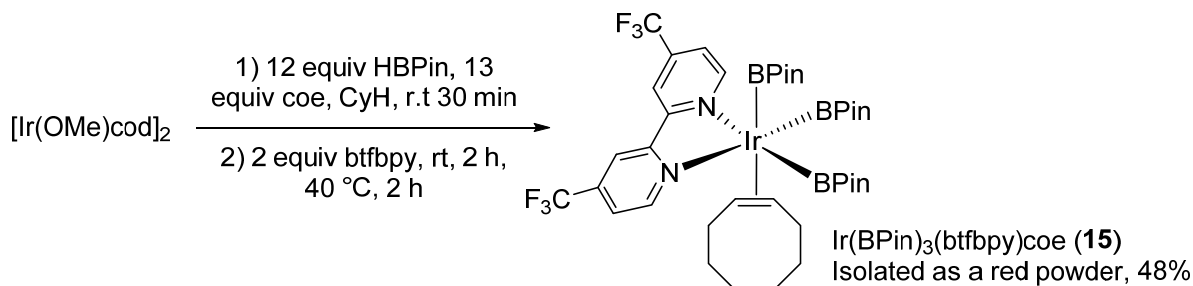
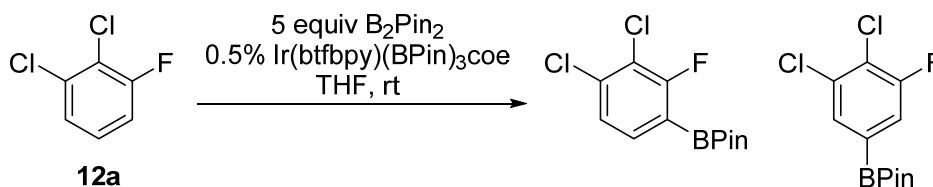


Figure 39. Kinetic study of the borylation of 12a

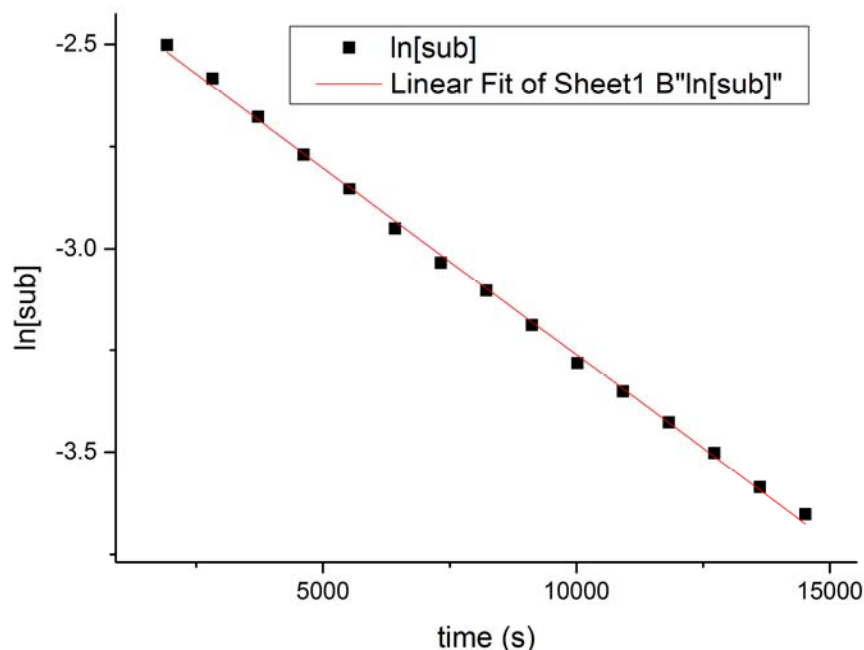


2.7.1 Preparation of stock solutions: 1. In a nitrogen glovebox, a stock solution was prepared with $Ir(Bpin)_3btfbpy(coe)$ (**15**, 24 mg, 0.025 mmol), and C_6F_6 (218 mg, 1.17 mmol) in THF in a 10.00 mL volumetric flask. The volumetric flask was filled to the 10.00 mL line. 2. Another stock solution was prepared with B_2Pin_2 (1.299 g, 5.114 mmol) and 2.000 mL of the stock solution prepared in step 1 (0.005 mmol Ir, 0.234 mmol C_6F_6) in THF in a 10.00 mL volumetric flask. This volumetric flask was filled to the 10.00 mL line. The total amount of THF was 7.623 g (105.71 mmol).

A 1.000 mL stock solution prepared in step 2 (0.511 mmol B_2Pin_2 , 0.0005 mmol **15**, 0.0215 mmol C_6F_6) was transferred into an NMR tube and sealed with a rubber cap. After tuning and gradient shimming, substrate **12a** (11.7 μ L, 0.100 mmol) was added. Precise concentration of **12a** and catalyst can be determined by NMR. *NMR sample:* B_2Pin_2 0.511 mol/L, determined by NMR: **12a**

0.103 mol/L, **15** 5.7×10^{-4} mol/L, THF 10.57 mol/L. The reaction (**Figure 39**) was followed by ^{19}F NMR every 15 min for 12 h. The concentrations of each species, **12a**, **13a**, **13a'**, and **15** were calculated by NMR integration. Data up to 75% conversion (two half-lives) were used for rate law fitting. first order fitting: $R^2=0.999$, $k_{\text{obs}}=1.02 \times 10^{-4} \text{ s}^{-1}$ (**Figure 40**).

Figure 40. First order fitting for the reaction described in 2.7.1



We also looked into the CF_3 region (about -50 to -70 ppm) of the ^{19}F NMR spectra obtained from the experiment (**Figure 41**). Several new peaks developed in this area, suggesting the original pre-assembled catalyst was decomposing. This was also observed in several other experiments, described in the following paragraphs.

2.7.2 Preparation of stock solutions: 1. In a nitrogen glovebox, a stock solution was prepared with $\text{Ir}(\text{Bpin})_3\text{btpy}(\text{coe})$ (**15**, 24 mg, 0.025 mmol), and C_6F_6 (200 mg, 1.07 mmol) in THF in a 10.00 mL volumetric flask. The volumetric flask was filled to the 10.00 mL line. 2. Another stock solution was prepared with B_2Pin_2 (1.905g, 7.501 mmol) and 2.000 mL of the stock solution

prepared in step 1 (0.005 mmol **15**, 0.215 mmol C₆F₆) in THF in a 10.00 mL volumetric flask. This volumetric flask was filled to the 10.00 mL line. The total amount of THF was 7.068 g (98.02 mmol).

Figure 41. ¹⁹F NMR of the CF₃ region, from bottom to top: 0.0, 1.0, 2.3, 3.5, 4.8, 6.0 hours after substrate (**12a**) was added.

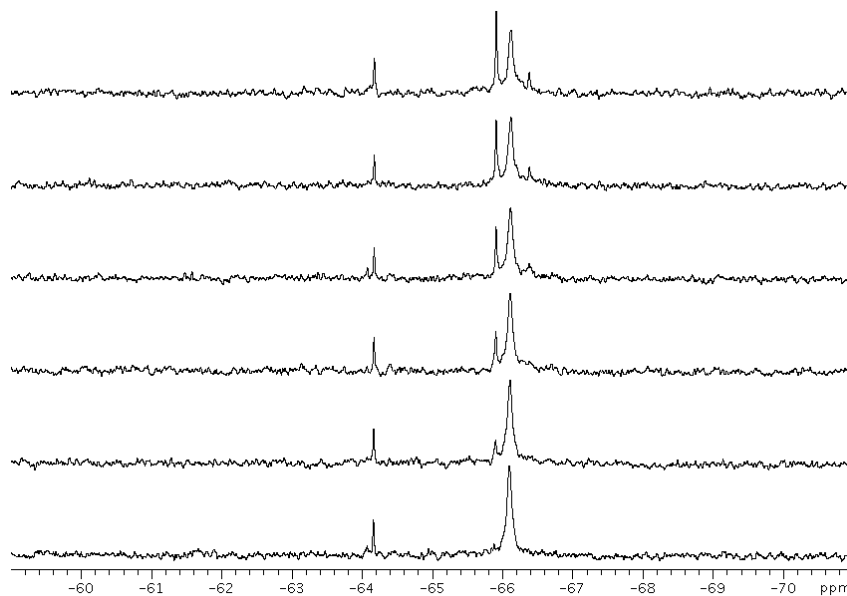
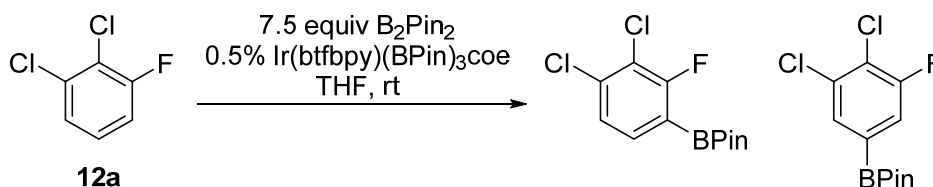


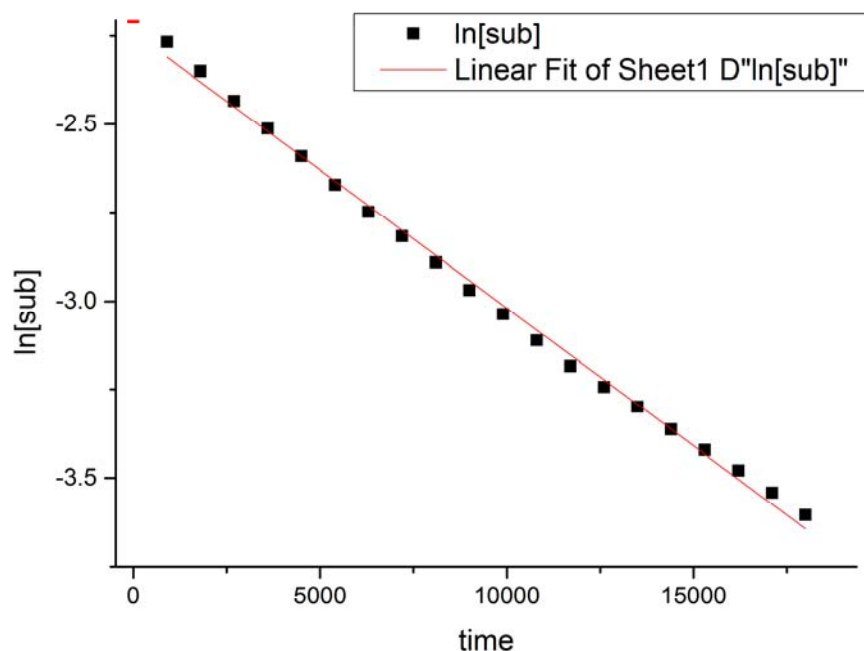
Figure 42. Kinetic study of the borylation of 12a



A 1.000 mL stock solution prepared in step 2 (0.750 mmol B₂Pin₂, 0.0005 mmol Ir, 0.0215 mmol C₆F₆) was transferred into an NMR tube and sealed with a rubber cap. After tuning and gradient shimming, substrate, **12a** (11.7 μL, 0.100 mmol) was added. Precise concentration of substrate and catalyst can be determined by NMR. *NMR sample*: B₂Pin₂ 0.750 mol/L, determined by NMR: **12a** 0.114 mol/L, **15** 5.7×10⁻⁴ mol/L, THF 9.80 mol/L. The reaction (**Figure 42**) was followed by

^{19}F NMR every 15 min for 12 h. The concentrations of each species, **12a**, **13a**, **13a'**, and **15** were calculated by NMR integration. Data up to 75% conversion (two half-lives) were used for rate law fitting. First order fitting: $R^2=0.996$, $k_{\text{obs}}=7.80\times 10^{-5} \text{ s}^{-1}$ (**Figure 43**). Again, we observed the degradation of catalysts, as shown in **Figure 44**.

Figure 43. 1st order fitting for the reaction described in 2.7.2



2.7.3 Preparation of stock solutions: 1. In a nitrogen glovebox, a stock solution was prepared with $\text{Ir}(\text{Bpin})_3\text{btfbpy}(\text{coe})$ (**15**, 24 mg, 0.025 mmol), and C_6F_6 (197 mg, 1.06 mmol) in THF in a 10.00 mL volumetric flask. The volumetric flask was filled to the 10.00 mL line. 2. Another stock solution was prepared with B_2Pin_2 (2.548g, 10.03 mmol) and 2.000 mL of the stock solution prepared in step 1 (0.005 mmol Ir, 0.212 mmol C_6F_6) in THF in a 10.00 mL volumetric flask. This volumetric flask was filled to the 10.00 mL line, total amount of THF was 6.484g (89.92 mmol).

Figure 44. ^{19}F NMR of the CF_3 region, from bottom to top: 0.0, 1.0, 2.3, 3.5, 4.8, 6.0 hours after substrate (**12a**) was added.

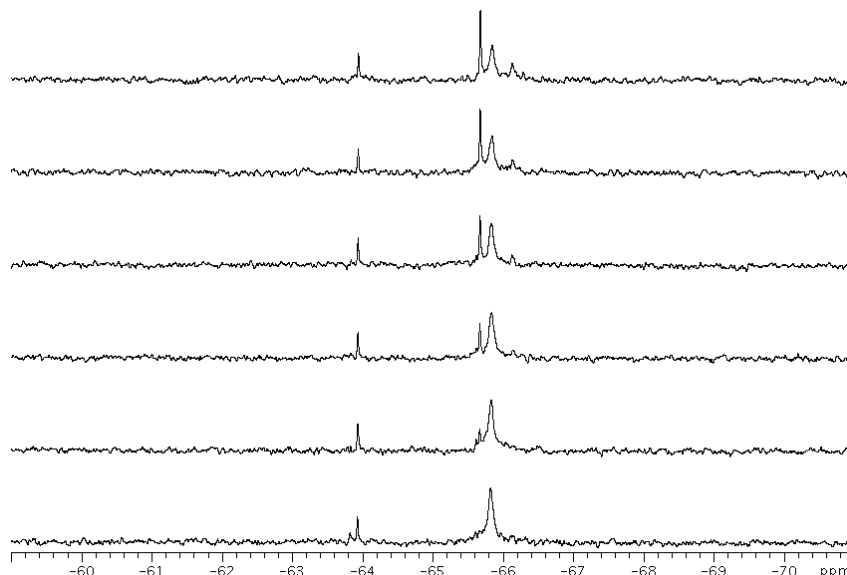
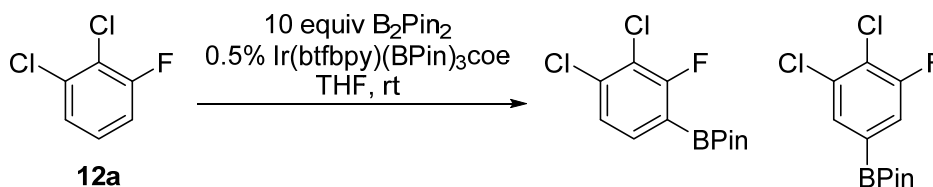


Figure 45. Kinetic study of the borylation of 12a



A 1.000 mL stock solution prepared in step 2 (1.003 mmol B_2Pin_2 , 0.0005 mmol **15**, 0.0212 mmol C_6F_6) was transferred into an NMR tube and sealed with a rubber cap. After tuning and gradient shimming, substrate, **12a** (11.7 μL , 0.100 mmol) was injected. Precise concentration of substrate and catalyst can be determined by NMR. *NMR sample*: B_2Pin_2 1.00 mol/L, determined by NMR: **12a** 0.109 mol/L, **15** 5.7×10^{-4} mol/L, THF 8.99 mol/L. The reaction (**Figure 45**) was followed by ^{19}F NMR, every 15 min for 12 h. The concentrations of each species, **12a**, **13a**, **13a'**, and **15** were calculated by NMR integration. Data up to 75% conversion (two half-lives) were used for rate law fitting. First order fitting: $R^2=0.990$, $K_{\text{obs}}=6.24 \times 10^{-5} \text{ s}^{-1}$ (**Figure 46**). Again, we observed the degradation of catalysts, as shown in **Figure 47**.

Figure 46. 1st order fitting for the reaction described in 2.7.3

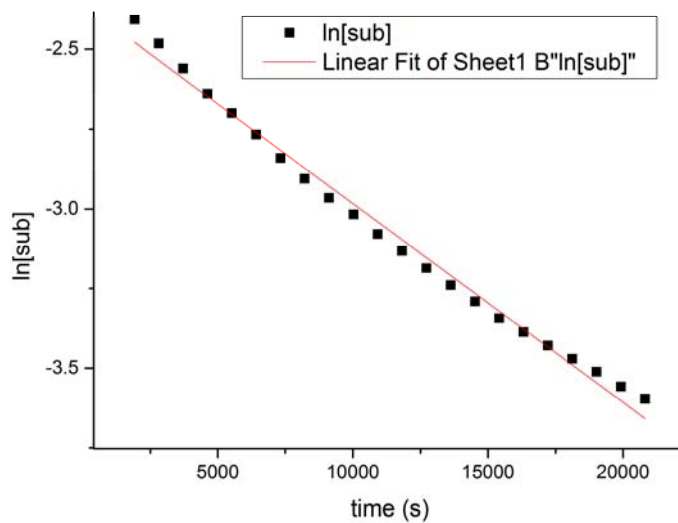
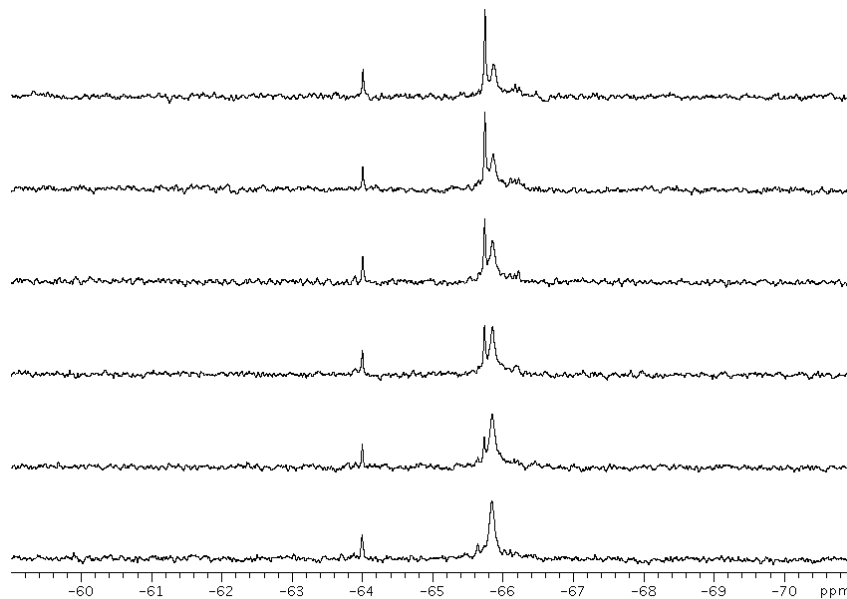


Figure 47. ¹⁹F NMR of the CF₃ region, from bottom to top: 0.0, 1.0, 2.3, 3.5, 4.8, 6.0 hours after substrate (12a) was added



The results of these kinetic runs are summarized in **Table 10**. Seemingly, the reactions demonstrated a decreasing reaction rate and conversion, as the B₂Pin₂ initial concentration increases. Comparing Figures **41**, **44**, and **47**, we also noticed that the preassembled catalyst was

gradient shimming, substrate (**12a** 1.2 μL , 0.010 mmol) was added. Precise concentration of substrate and catalyst can be determined by NMR. *NMR sample*: B_2Pin_2 0.1 mol/L, determined by NMR: **12a** 0.011 mol/L, **15** 5.3×10^{-4} mol/L, THF 11.8 mol/L. The reaction (**Figure 48**) was followed by ^{19}F NMR, every 15 min for 12 h. The concentrations of each species, **12a**, **13a**, **13a'**, and **15** were calculated by NMR integration. Data up to 75% conversion (two half-lives) were used for rate law fitting. First order fitting of 0-75% conversion: $R^2=0.999$, $K_{\text{obs}}=1.02 \times 10^{-4} \text{ s}^{-1}$ (**Figure 49**). As observed the CF_3 region of the ^{19}F NMR spectra the degradation of catalyst seemed to be suppressed at lower reaction concentrations (**Figure 50**).

Figure 49. First order fitting for the reaction described in 2.7.4

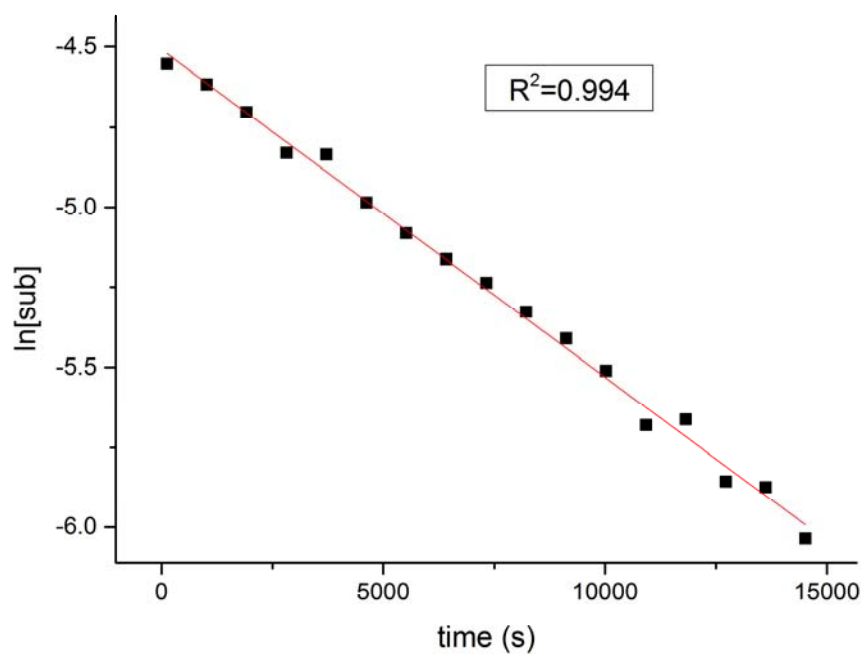
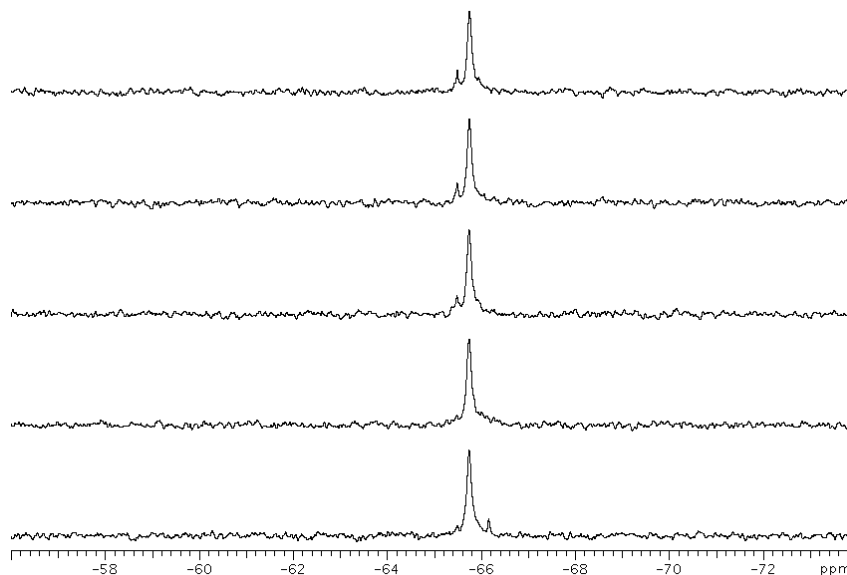


Figure 50. ^{19}F NMR of the CF_3 region, from bottom to top: 0.0, 1.0, 2.3, 3.5, 4.8, 6.0 hours after substrate (**12a**) was added



2.7.5 Preparation of stock solutions: 1. In a nitrogen glovebox, a stock solution was prepared with $\text{Ir}(\text{Bpin})_3\text{btfbpy}(\text{coe})$ (**15**, 24 mg, 0.025 mmol), and C_6F_6 (22.7 mg, 0.122 mmol) in THF in a 10.00 mL volumetric flask. The volumetric flask was filled to the 10.00 mL line. 2. Another stock solution was prepared with B_2Pin_2 (127 mg, 0.5 mmol) and 2.000 mL of the stock solution prepared in step 1 (0.005 mmol **15**, 0.0244 mmol C_6F_6) in THF in a 10.00 mL volumetric flask. This volumetric flask was filled to the 10.00 mL line, total amount of THF was 8.693 g (120.6 mmol). A 1.000 mL stock solution prepared in step 2 (0.010 mmol B_2Pin_2 , 0.0005 mmol **15**, 0.0024 mmol C_6F_6) was transferred into an NMR tube and sealed with a rubber cap.

Figure 51. Kinetic study of the borylation of 12a

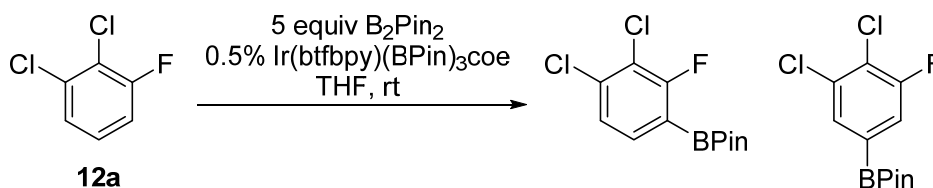
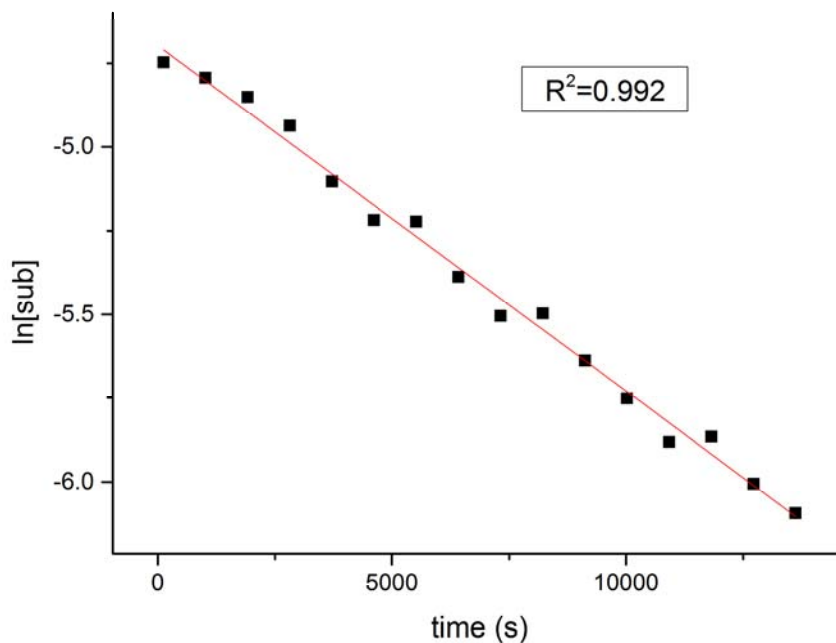


Figure 52. First order fitting for the reaction described in 2.7.5



After tuning and gradient shimming, substrate (**12a**, 1.2 μL , 0.010 mmol) was added. Precise concentration of substrate and catalyst can be determined by NMR. *NMR sample*: B_2Pin_2 0.050 mol/L, determined by NMR: **12a** 0.0094 mol/L, catalyst 5.2×10^{-4} mol/L, THF 12.1 mol/L. The reaction (**Figure 51**) was followed by ^{19}F NMR every 15 min for 12 h. The concentrations of each species, **12a**, **13a**, **13a'**, and **15** were calculated by NMR integration. Data up to 75% conversion (two half-lives) were used for rate law fitting. First order fitting of 0-75% conversion: $R^2=0.999$, $K_{\text{obs}}=1.03 \times 10^{-4} \text{ s}^{-1}$ (**Figure 52**). As observed in the CF_3 region on ^{19}F NMR spectra the degradation of the catalyst seemed to be suppressed at lower reaction concentrations (**Figure 53**).

As summarized in **Table 11**, the reaction demonstrated a 0-order kinetic behavior of B_2Pin_2 which would be expected at lower concentrations without ligand decomposition. We also studied the kinetics of the borylation of **12c**.

Figure 53. ^{19}F NMR of the CF_3 region, from bottom to top: 0.0, 1.0, 2.3, 3.5, 4.8, 6.0 hours after substrate (12a) was added

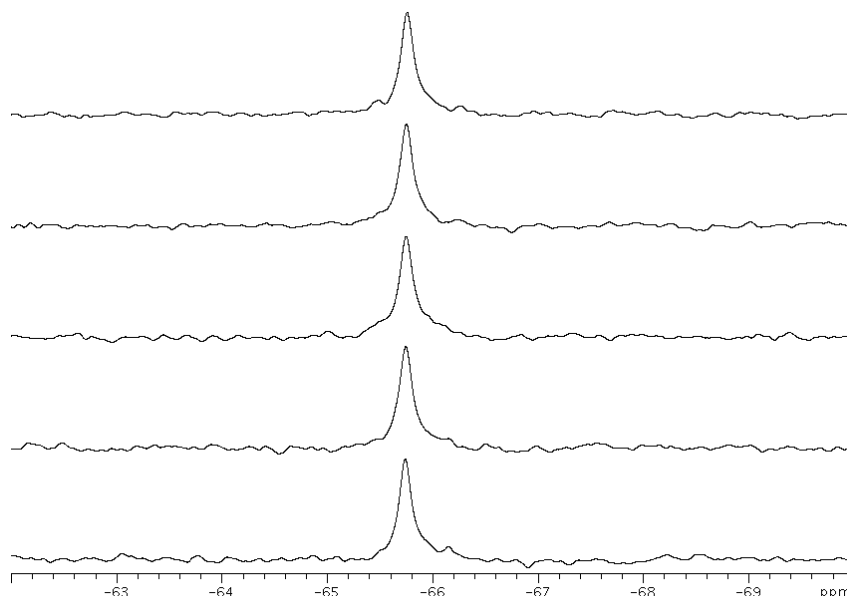
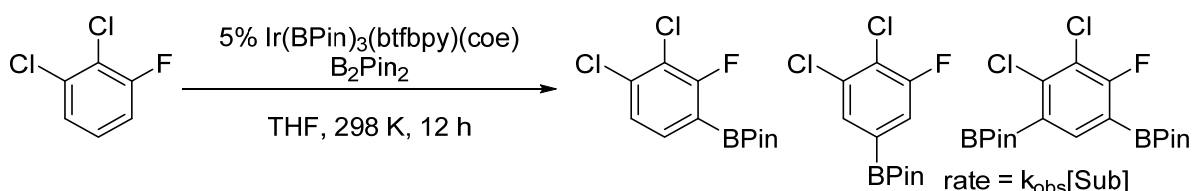


Table 10. First order kinetic behavior of borylation of 12a



entry	$[\text{sub}]_0$	$[\text{B}_2\text{Pin}_2]_0$	$[\text{Ir}]_0$	conversion	$k_{\text{obs}}(\text{s}^{-1})^{\text{a}}$
1	0.0094M	0.050M	5.2E-4M	97%	1.03E-4
2	0.011M	0.100M	5.3E-4M	97%	1.02E-4

a. based on first 75% conversion (two half-lives)

2.7.6 Preparation of stock solutions: 1. In a nitrogen glovebox, a stock solution was prepared with $\text{Ir}(\text{Bpin})_3\text{btfbpy}(\text{coe})$ (**15**, 24 mg, 0.025 mmol), and C_6F_6 (20.4 mg, 0.110 mmol) in THF in a 10.00 mL volumetric flask. The volumetric flask was filled to the 10.00 mL line. 2. Another stock solution was prepared with B_2Pin_2 (127 mg, 0.5 mmol) and 2.000 mL of the stock solution prepared in step 1 (0.005 mmol **15**, 0.022 mmol C_6F_6) in THF in a 10.00 mL volumetric flask. This

volumetric flask was filled to the 10.00 mL line. The total mass of stock solution was 8812 mg, so that total amount of THF was 8.677 g (120.3 mmol).

Figure 54. Kinetic study of the borylation of 12c

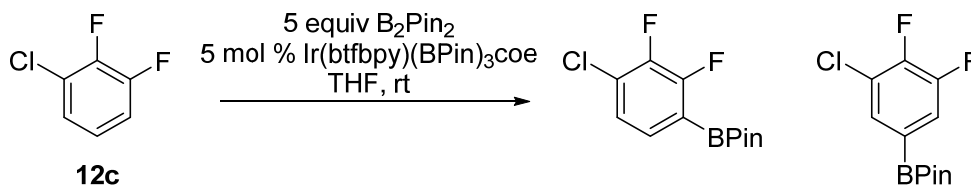
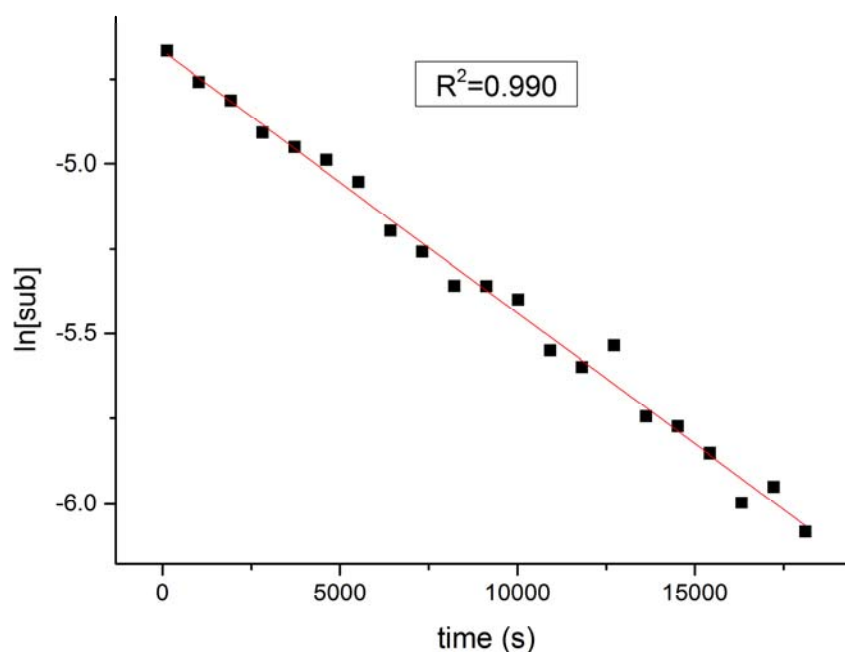


Figure 55. First order fitting for the reaction described in 2.7.6

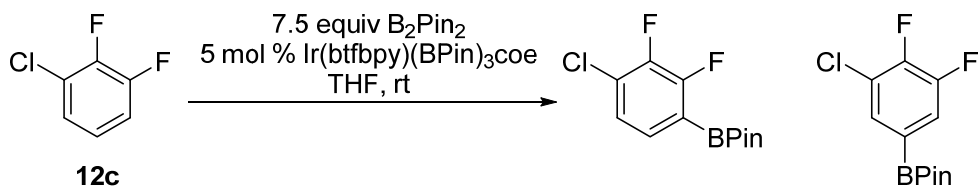


A 1.000 mL stock solution prepared in step 2 (0.0500 mmol B_2Pin_2 , 0.0005 mmol **15**, 0.022 mmol C_6F_6) was transferred into an NMR tube and sealed with a rubber cap. After tuning and gradient shimming, substrate (**12c** 0.9 μ L, 0.0100 mmol) was added. Precise concentration of substrate and catalyst can be determined by NMR. *NMR sample*: B_2Pin_2 0.050 mol/L, determined by NMR: **12c** 0.0099 mol/L, **15** 5.2×10^{-4} mol/L, THF 12.0 mol/L. The reaction (**Figure 54**) was followed by ^{19}F

NMR, every 15 min for 12 h. The concentrations of each species, **12c**, **13c**, **13c'**, and **15** were calculated by NMR integration. Data up to 75% conversion (two half-lives) were used for rate law fitting. First order fitting of 0-75% conversion: $R^2=0.990$, $K_{\text{obs}}=7.71 \times 10^{-5} \text{ s}^{-1}$ (**Figure 55**).

2.7.7 Preparation of stock solutions: 1. In a nitrogen glovebox, a stock solution was prepared with $\text{Ir}(\text{Bpin})_3\text{btfbpy}(\text{coe})$ (**15**, 25 mg, 0.025 mmol), and C_6F_6 (23.3 mg, 0.125 mmol) in THF in a 10.00 mL volumetric flask. The volumetric flask was filled to the 10.00 mL line. 2. Another stock solution was prepared with B_2Pin_2 (190 mg, 0.748 mmol) and 2.000 mL of the stock solution prepared in step 1 (0.005 mmol **15**, 0.025 mmol C_6F_6) in THF in a 10.00 mL volumetric flask. This volumetric flask was filled to the 10.00 mL line. The total mass of stock solution was 8780 mg, so that total amount of THF was 8.580 g (119.0 mmol). A 1.000 mL stock solution prepared in step 2 (0.075 mmol B_2Pin_2 , 0.0005 mmol **15**, 0.025 mmol C_6F_6) was transferred into an NMR tube and sealed with a rubber cap. After tuning and gradient shimming, substrate (**12c** 0.9 μL , 0.01 mmol) was added. Precise concentration of substrate and catalyst can be determined by NMR. **NMR sample:** B_2Pin_2 0.075 mol/L, determined by NMR: **12c** 0.0085 mol/L, **15** 5.0×10^{-4} mol/L, THF 11.9 mol/L. The reaction (**Figure 56**) was followed by ^{19}F NMR, every 15 min for 12 h. The concentrations of each species, **12c**, **13c**, **13c'**, and **15** were calculated by NMR integration. Data up to 75% conversion (two half-lives) were used for rate law fitting. First order fitting of 0-75% conversion: $R^2=0.994$, $K_{\text{obs}}=7.78 \times 10^{-5} \text{ s}^{-1}$ (**Figure 57**)

Figure 56. Kinetic study of borylation of 12c



The results of the kinetic studies of the borylation of **12c** are summarized in **Table 12**. The

borylations also demonstrated first order behavior against substrate and 0 order against B_2Pin_2 . Compared to the borylation of **12a**, a difference of reaction rate due to substrate effect is clearly observed, but too few substrates were tested to draw any conclusions based on the trend.

Figure 57. First order fitting for the reaction described in 2.7.7

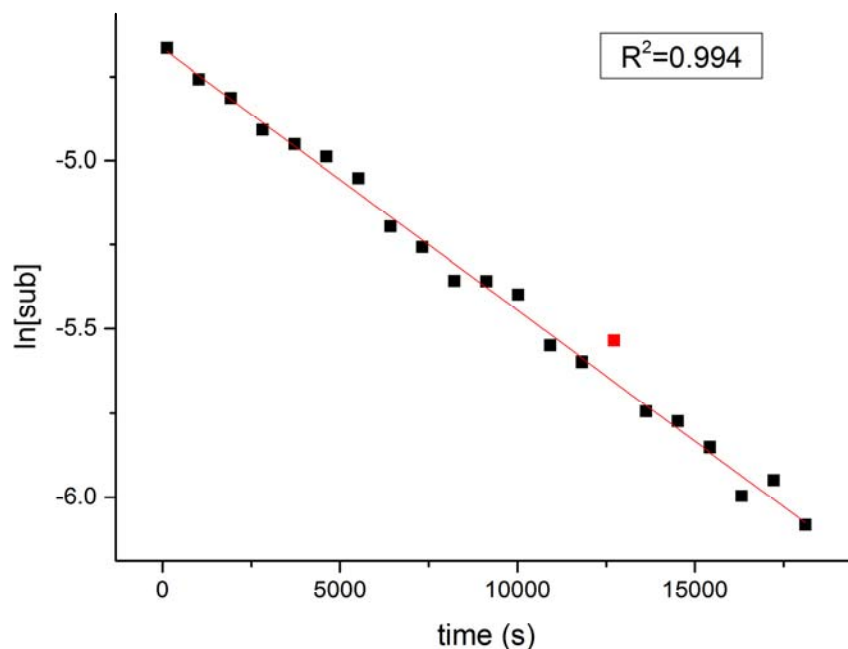
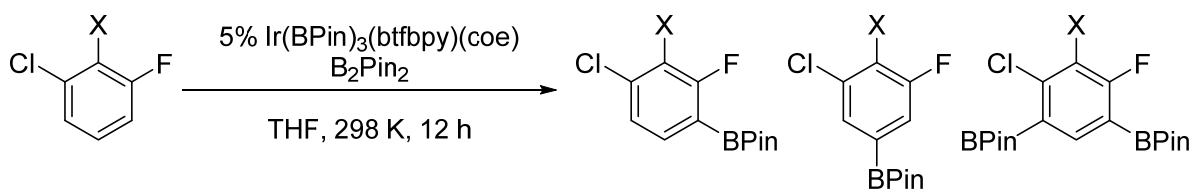


Table 11. Results of kinetic studies of the borylation of 12c



entry	X	[sub] ₀	rate = $k_{obs}[Sub]$		conversion	$k_{obs}(s^{-1})^a$
			[B_2Pin_2] ₀	[Ir] ₀		
1	F	0.0099M	0.050M	5.2E-4M	98%	7.71E-5
2	F	0.0085M	0.075M	5.0E-4M	97%	7.78E-5
3	Cl	0.011M	0.100M	5.3E-4M	97%	1.02E-4

a. based on first 75% conversion (two half-lives)

2.8 Probing the ligand decomposition

During the kinetic studies, we noticed the decomposition of the preassembled catalyst and formation of other species. Also we noted that this phenomenon is more significant at higher reaction concentrations. At first we believed it to be an interaction between the Ir catalyst and B₂Pin₂ or HBPin. To test this, we mixed the preassembled catalyst **15** and B₂Pin₂ or HBPin in THF-d₈, as illustrated in **Figures 58, 59** and **60**.

Figure 58. ¹H NMR of the preassembled catalyst (**15**) treated by B₂Pin₂ and HBPin in THF-d₈, top: Compound **15**, mid: Compound **15** and 5 equiv B₂Pin₂ after 4 h at 298 K, bottom: Additional 5 equiv HBPin added, then after 4 h at 298 K

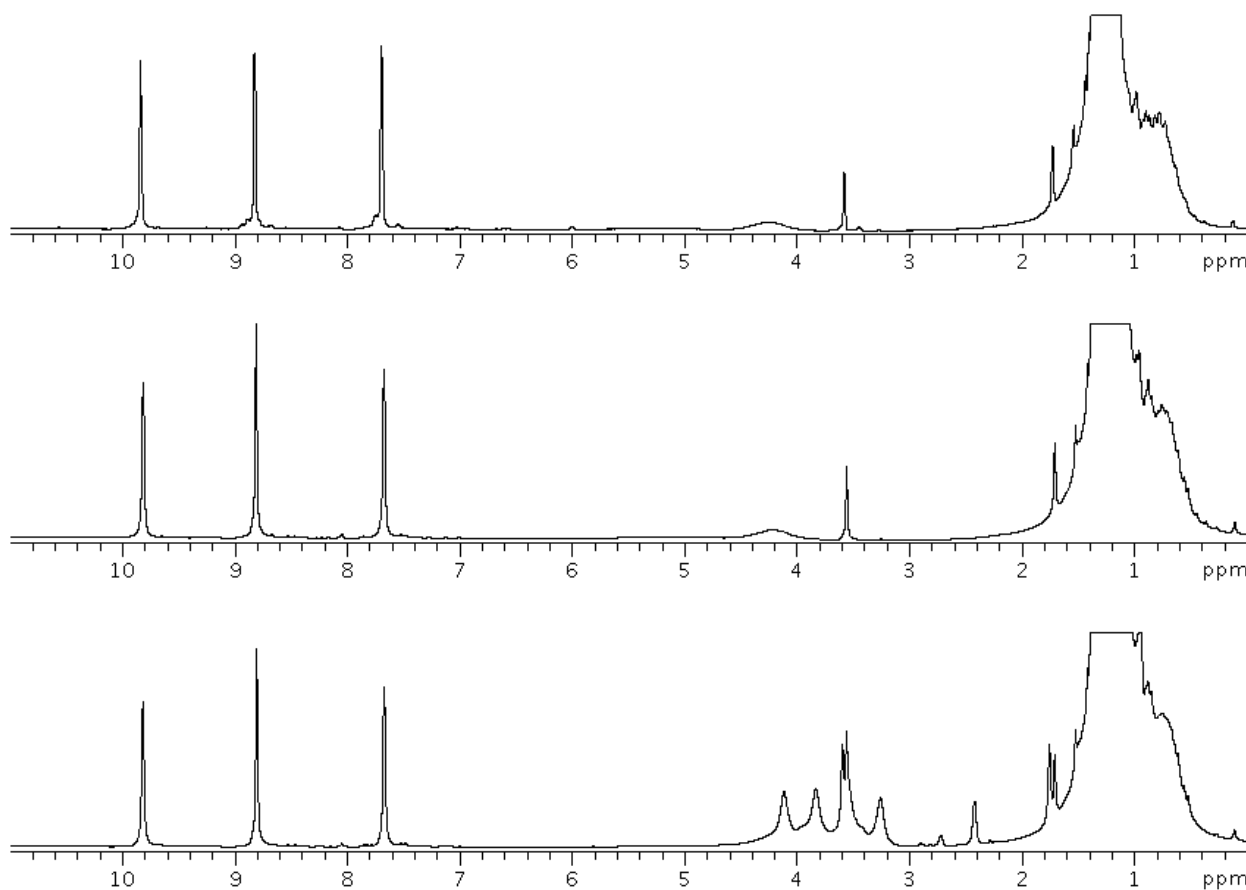
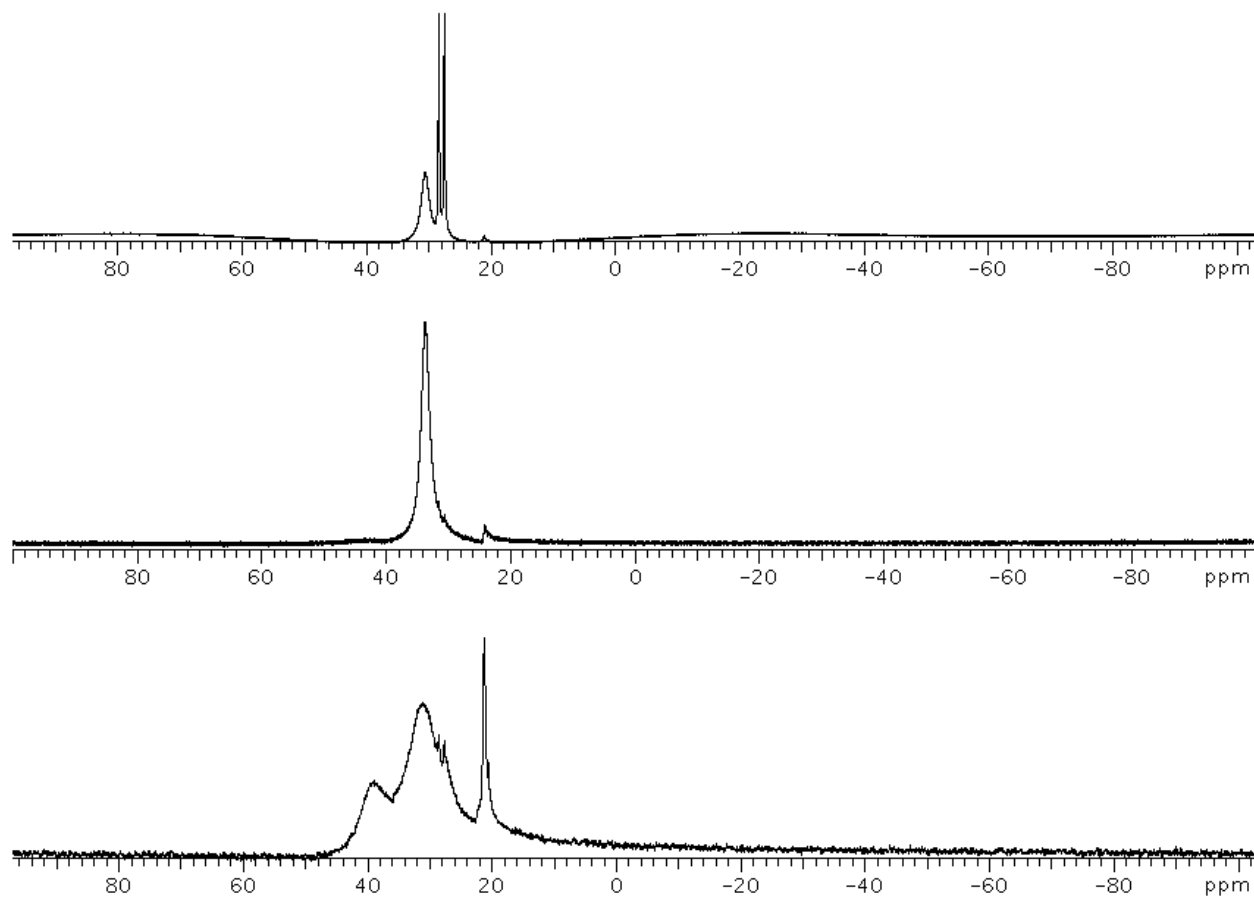


Figure 59. ^{11}B NMR of the preassembled catalyst (**15**) treated by B_2Pin_2 and HBPIn in $\text{THF-}d_8$, top: Compound **15**, mid: Compound **15** and 5 equiv B_2Pin_2 after 4 h at 298 K, bottom: Additional 5 equiv HBPIn added, then after 4 h at 298 K



After treating **15** with 5 equiv B_2Pin_2 at r.t for 4 hours, we did not observe any noticeable change in the aromatic region of the ^1H NMR and the ^{19}F NMR of the preassembled catalyst. Neither had we found any change to the B_2Pin_2 peak in ^{11}B NMR. After an additional 5 equiv HBPIn was added and kept at r.t for another 4 h. Again we did not observe any noticeable change in the aromatic region of the ^1H NMR and the ^{19}F NMR of the preassembled catalyst. Neither had we found any change to the HBPIn peak in ^{11}B NMR. This ruled out the decomposition of catalyst resulting from an interaction of HBPIn or B_2Pin_2 with the preassembled catalyst (**15**)

Figure 60. ^{19}F NMR of the preassembled catalyst (**15**) treated by B_2Pin_2 and HBPiIn in $\text{THF-}d_8$, top: Compound **15**, mid: Compound **15** and 5 equiv B_2Pin_2 after 4 h at 298 K, bottom: Additional 5 equiv HBPiIn added, then after 4 h at 298 K

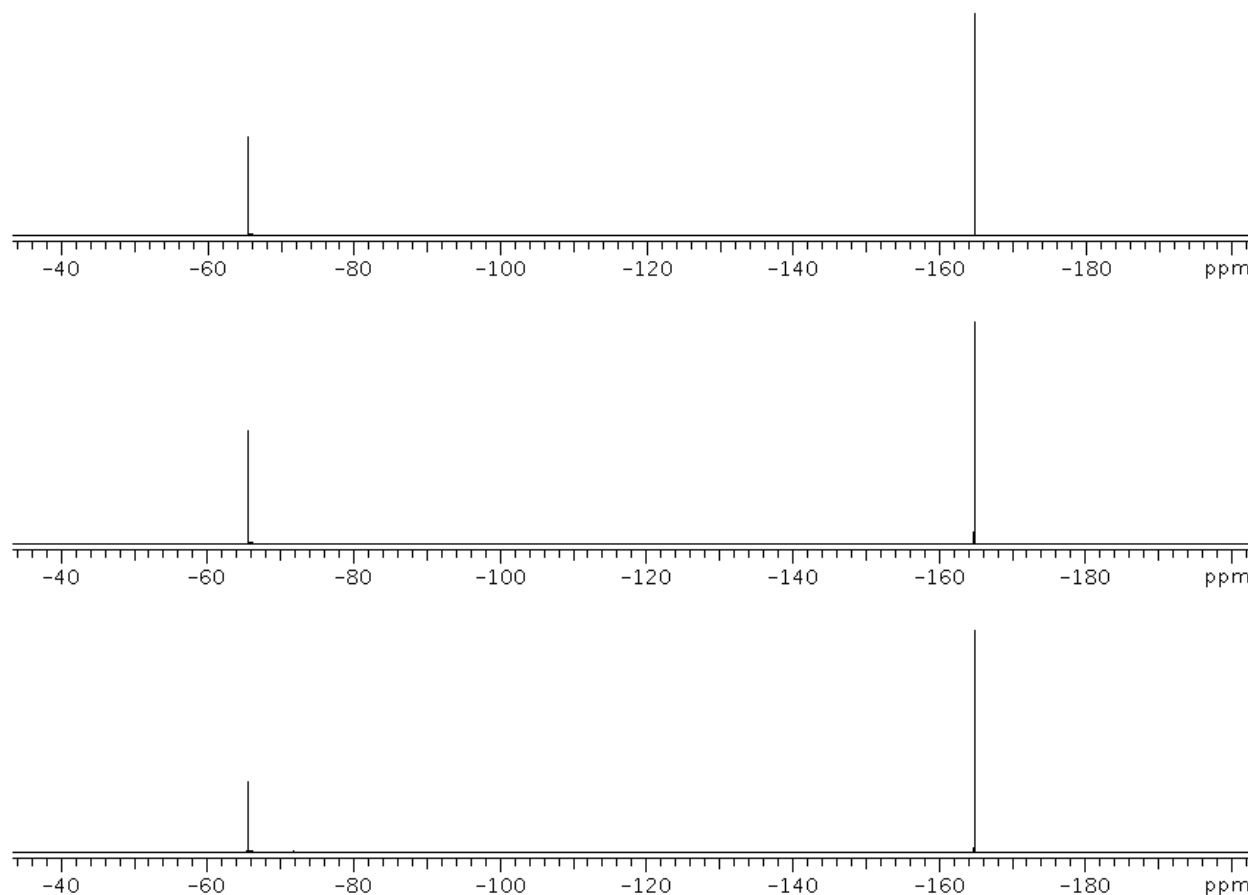
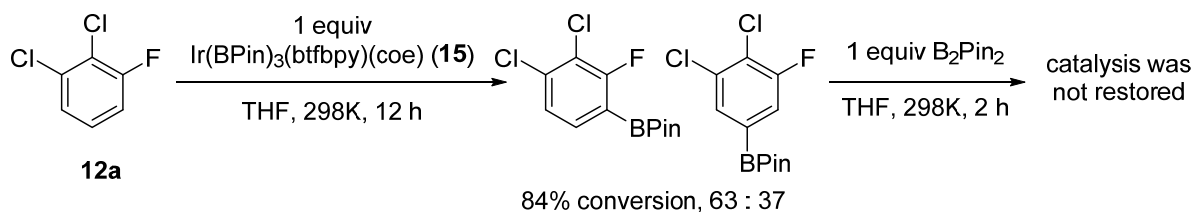


Figure 61. Borylation of **12a** by stoichiometric **15**

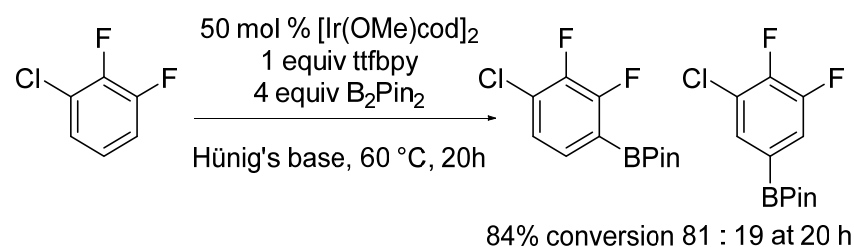


We then set up a borylation of **12a** with the stoichiometric preassembled catalyst **15** (**Figure 61**). By ^{19}F NMR, the CF_3 peak area became messy and after 12 h, 84% conversion was achieved. At this time, 1 equiv B_2Pin_2 was added, but we did not observe the restoration of peak for compound **15** restored. These observations suggest the decomposition is due to a side reaction or side

reactions of the borylation intermediates. The reaction could most likely be bimolecular, since the decomposition of the catalyst is more severe at higher reaction concentrations.

2.9 Degradation of ttfbpy during borylation

Figure 62. Borylation of 12c by stoichiometric Ir and ttfbpy

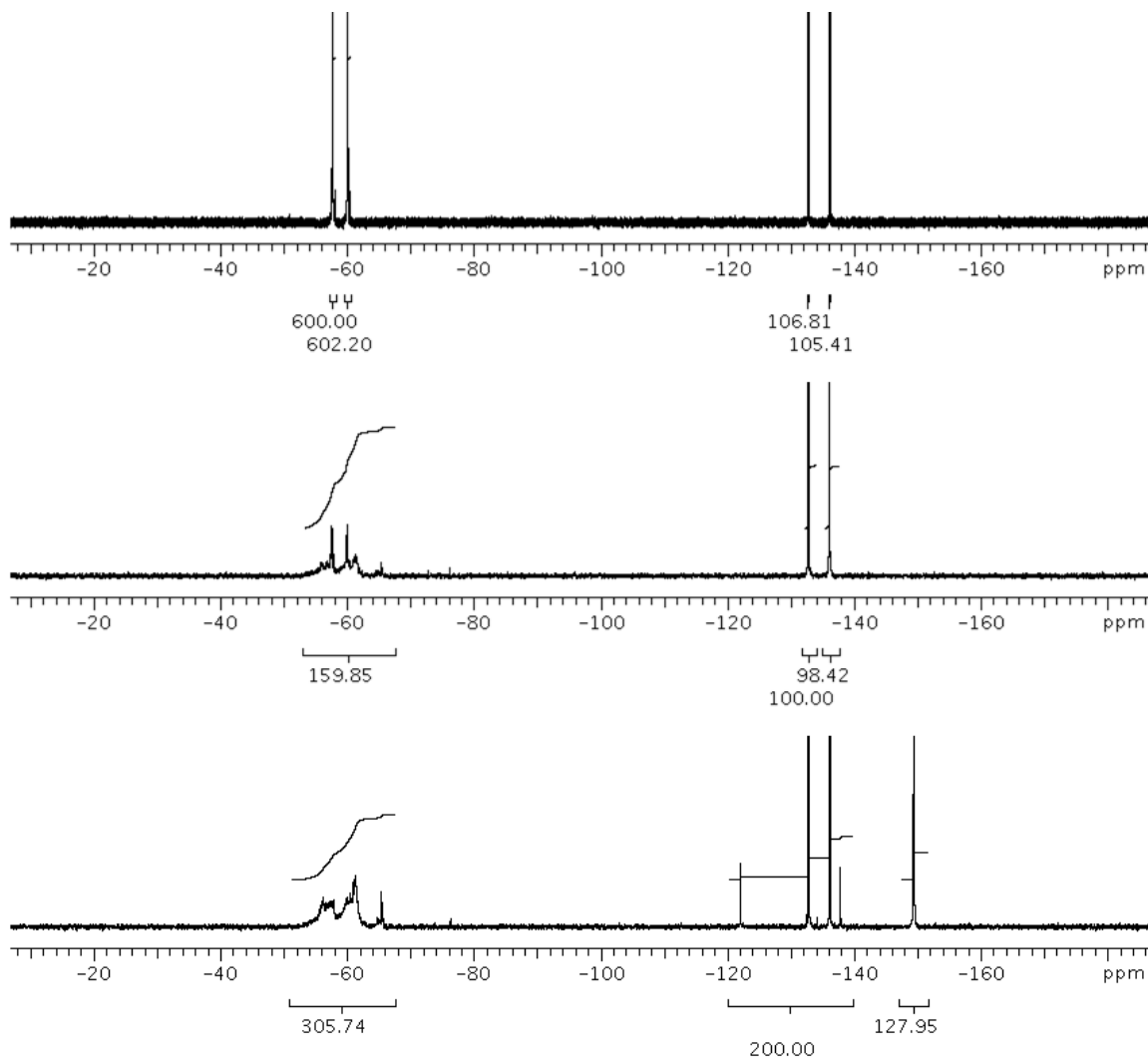


While studying the borylations catalyzed with ttfbpy ligand, we noticed that the reactions were often displayed an induction period. Furthermore for successful borylations, signals for the ligand's CF₃'s were never observed in the ¹⁹F NMR of the reaction crude. To probe these phenomena, we borylated **12c** with stoichiometric Ir and ttfbpy (**Figure 62**), and monitored the reaction by both ¹¹B and ¹⁹F NMR.

We found after that only the reaction was heated for 4.5 h, the consumption of the B₂Pin₂ started. At that time the original ligand CF₃ peak had disappeared and three broad peaks were observed in typical CF₃ area by ¹⁹F NMR. The total integration of the ¹⁹F NMR CF₃ area shrank to about 13% that of the original. After 9 h, the total integration of the ¹⁹F NMR CF₃ area increased to 25% that of the original and we found a sharp peak at -149 ppm, likely F-BPin, with an integration equal to 11% of the original ligand. At this point, 10% conversion of the expected borylation was observed by ¹⁹F NMR (**Figure 63**). By ¹¹B NMR, we observed the formation of a peak at 22 ppm, likely F-BPin. We observed further increases in the integration of the F-BPin peak in both ¹⁹F and ¹¹B NMR, but the total integration of the three broad peaks in the CF₃ area remained the same. Unfortunately we were not able to isolate the residue of the ligand, but based on our past

observation of the ttfbpy ligand being reduced by Zn metal,⁵² we hypothesized that the ligand might be reduced by B₂Pin₂ or HBPin.

Figure 63. Borylation of 12c with stoichiometric Ir and ttfbpy, top: Before heating, mid: 4.5 h Heating, bottom: 9 h Heating



2.10 Borylation under a H₂ atmosphere

We also looked into the mechanism of the borylations, especially the role of HBPin and H₂ in the borylations. We setup the reaction as following (**Figure 64**): In a nitrogen atmosphere glove box, [Ir(OMe)cod]₂ (6.6 mg, 0.01 mmol), and dtbpy (5.4 mg, 0.02 mmol) were dissolved in Hünig's

base 2.0 mL, HBPIn (146 μ L, 1.0 mmol) was added and well mixed. Compound **12a** (152 μ L, 1.3 mmol) was added. A portion of the reaction mixture was then sealed in an NMR tube and reaction was followed by ^{19}F NMR every 15 min. Another reaction was prepared in this same way, and a portion of the reaction mixture was sealed into a thick wall screw-capped NMR tube and then charged with 100 PSI H_2 gas, and the reaction was followed by ^{19}F NMR every 15 min.

Figure 64. H_2 influence on borylation

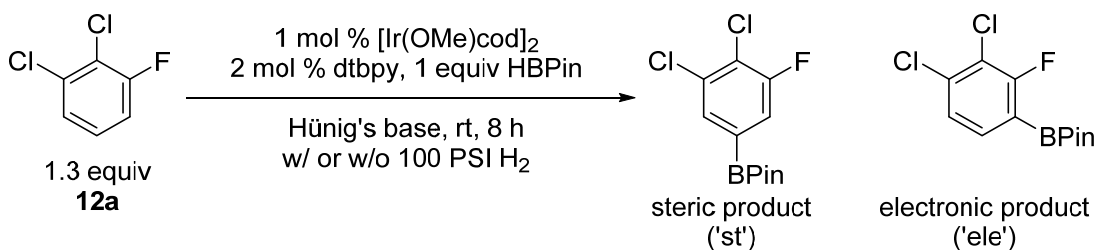
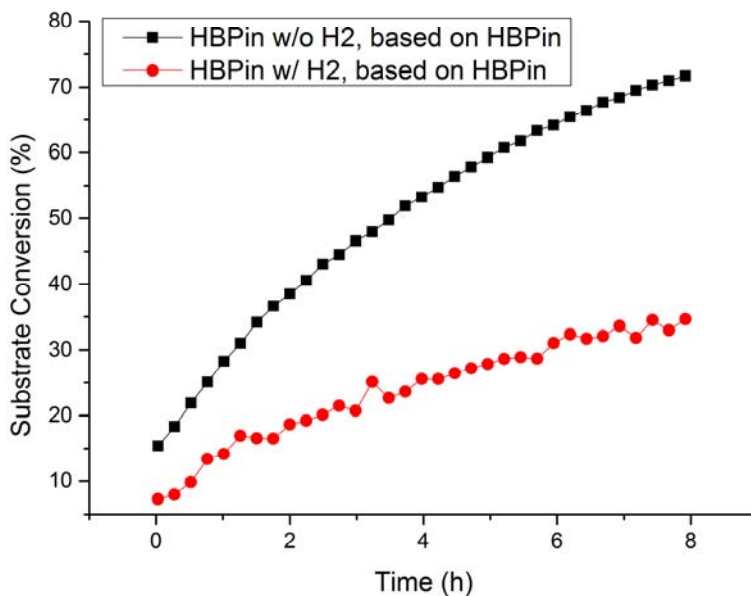


Figure 65. Conversions of the borylation of 12a with HBPIn affected by H_2



The borylation slowed down (**Figure 65**, conversions are based on HBPIn), but the regioselectivity was not much affected (**Figure 66**).

Figure 66. Regioselectivity of the borylation of 12a with HBPIn affected by H₂

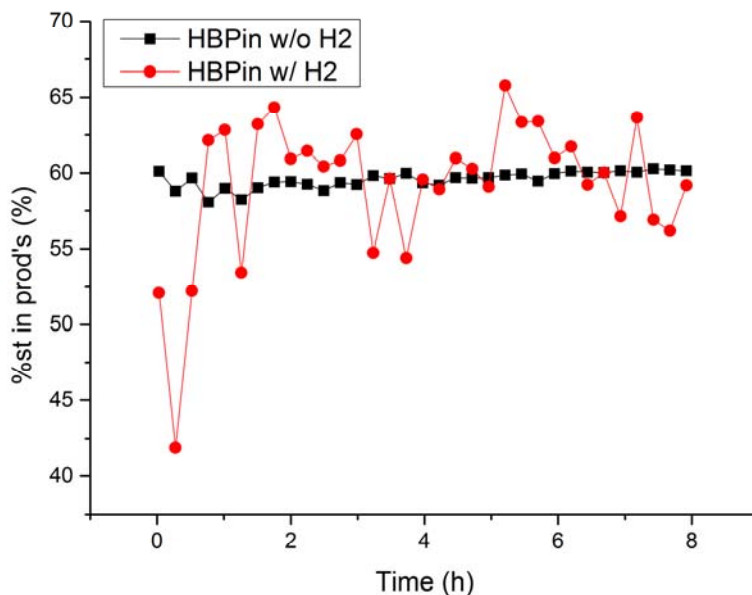
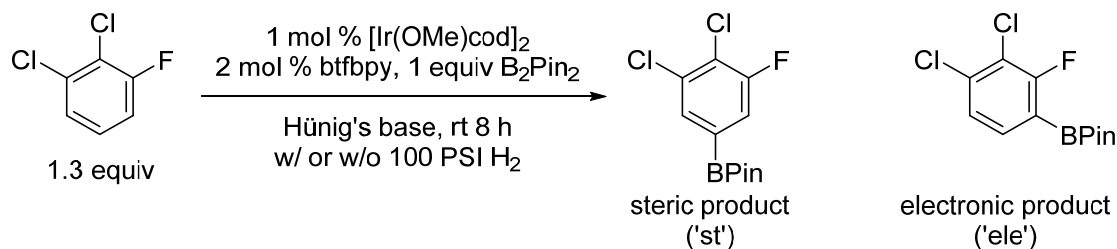


Figure 67. H₂ influence on borylation



We also looked into how H₂ effects on borylation with B₂Pin₂. In a nitrogen atmosphere glove box, [Ir(OMe)cod]₂ (6.6 mg, 0.01 mmol), B₂Pin₂ (254 mg, 1.0 mmol), and btfbpy (5.8 mg, 0.02 mmol) were dissolved in Hünig's base (2.0 mL) and well mixed. Compound **12a** (152 μL, 1.3 mmol) was added. A portion of the reaction mixture was then sealed into a NMR tube and the reaction was followed on ¹⁹F NMR every 15 min. Another reaction was prepared in this same way and a part of the reaction mixture was sealed into a thick wall screw-capped NMR tube and then charged with 100 PSI H₂ gas. The reaction was followed on ¹⁹F NMR every 15 min. (Figure 67).

Figure 68. Borylation of 12a by HBPIn affected by H₂

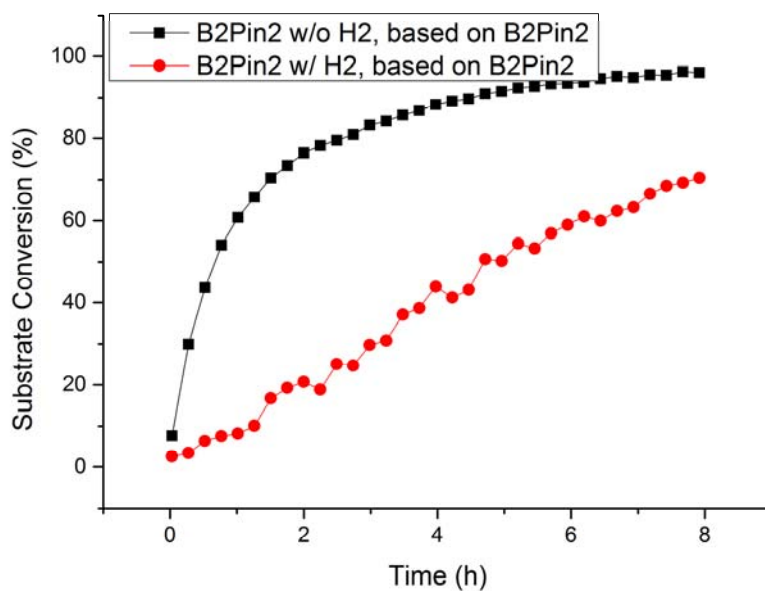
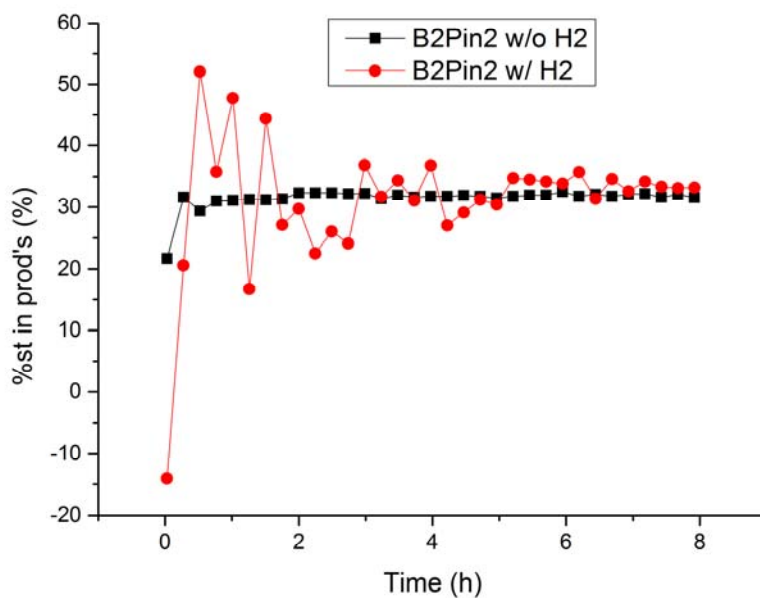


Figure 69. Borylation of 12a by HBPIn affected by H₂



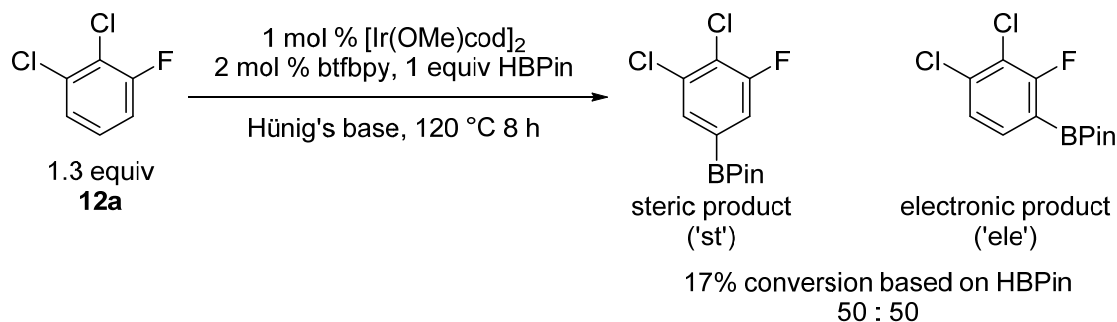
The reaction is setup as shown in **Figure 67**. Even without generating H₂ as a byproduct, the reaction was slow with the presence of H₂ (**Figure 68**), but the regioselectivity was not much affected (**Figure 69**).

Unexpectedly, the presence of H₂ gas slowed down the rate of borylation reactions that do not generate H₂ as a by-product. However the regioselectivity of the reaction was not affected. These data suggest that H₂ might bind with one of the Ir species in the catalytic cycle to hinder the recovery of the catalyst, but the form of active catalyst does not change.

2.11 Temperature effect or borylation reagent effect

We also tried to push borylations with HBPIn using btfbpy as the ligand. The reaction at room temperature was extremely slow, but could be accelerated upon heating. The reaction was setup as follows: In a nitrogen atmosphere glove box, [Ir(OMe)cod]₂ (6.6 mg, 0.01 mmol), dtbpy (5.4 mg, 0.02 mmol) were dissolved in Hünig's base 2.0 mL, HBPIn (146 μL, 1.0 mmol) was added and well mixed. Compound **12a** (152 μL, 1.3 mmol) was added. A part of the reaction mixture was then sealed into a J-Young NMR tube and reaction was followed by VT ¹⁹F NMR every 15 min at 120 °C. (**Figure 70**).

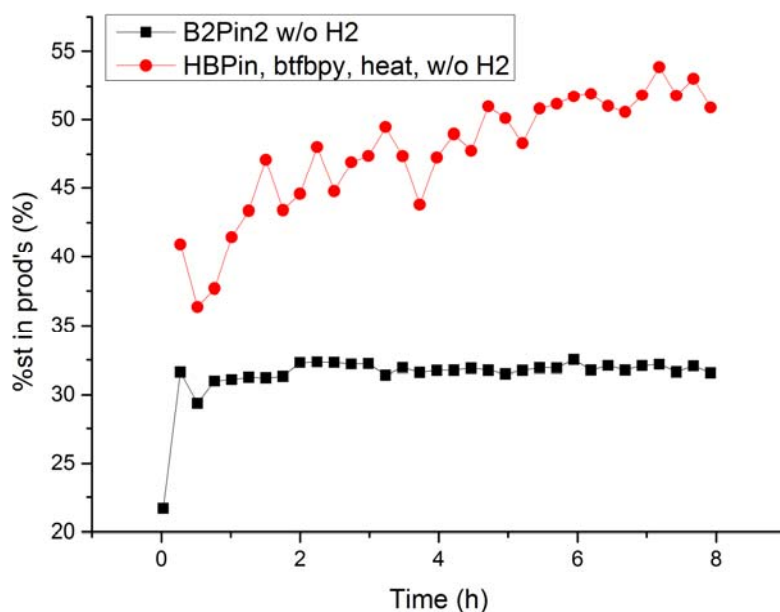
Figure 70. Borylation of 12a by HBPIn with btfbpy at high temperature



Less than 20% conversion was achieved after 8 hours, but what was immediately noticed was that the st/ele ratio changed over time and the ratio (50 : 50) achieved was different from that observed

with B₂Pin₂ at room temperature (33 : 67), as shown in **Figure 71**. We pondered whether this was a temperature effect or a reagent effect (HBPIn vs B₂Pin₂). So, another reaction was set up as follows: In a nitrogen atmosphere glove box, [Ir(OMe)cod]₂ (6.6 mg, 0.01 mmol), B₂Pin₂ (254 mg, 1.0 mmol), and btfbpy (5.8 mg, 0.02 mmol) were dissolved in Hünig's base (2.0 mL) and well mixed. Compound **12a** (152 μL, 1.3 mmol) was added. The reaction mixture was transferred into a screw-capped tube and heated at 120 °C for 1 h (**Figure 72**). The reaction was terminated at an early stage, where contribution from HBPIn borylation should be trivial. The ratio of the two products were similar to that of the borylation at room temperature suggesting a possible reagent effect.

Figure 71. Borylation of 12a by HBPIn at high temperature

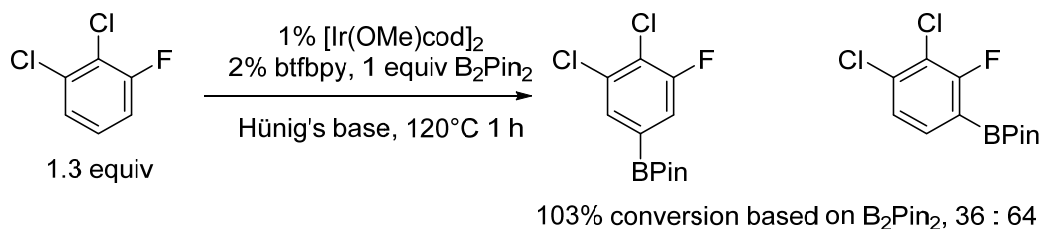


2.12 Summary

We probed electronic factors regulating the regioselectivity during the borylations of fluorobenzenes and established that electron deficient ligands favor borylation ortho to F. We

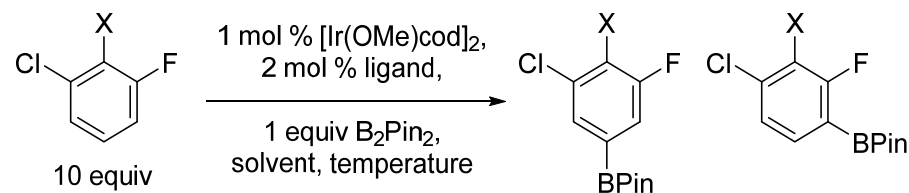
improved the synthesis of 4,4'-bistrifluoromethyl bipyridine (btfbpy) and 4,4',5,5'-tetrakis(trifluoromethyl) bipyridine (ttfbpy) and applied these compounds as borylation ligands. These ligands provided improved selectivity for the electronically controlled products, but gave lower yields with electron rich substrates and were not effective in borylation with HBPIn. We then looked into the kinetic profiles of the borylations with electron deficient ligands, finding them similar to that of the borylations with electron rich ligands, suggesting similar catalytic cycles. We noticed the degradation of catalyst during the borylation with ttfbpy, making a kinetic study of this ligand impossible. We also studied other aspects of the borylations, such as effect of the presence of H₂ gas, temperature, B₂Pin₂ vs HBPIn. We found the interesting phenomenon that in some cases borylation with HBPIn to give different products ratio compared to borylation with B₂Pin₂.

Figure 72. Borylation with B₂Pin₂ at higher temperature



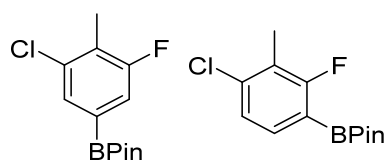
2.13 Experimental

Assignment and Characterization of Borylation Products⁵⁴

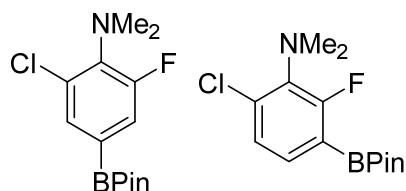


The borylations of the substrates were carried out on 0.1 mmol scale in a J-Young NMR tube to precisely determine conversions and isomeric product ratios in the reaction crude. Excess substrate was used to suppress possible diborylation. The general procedure for liquid substrates is shown

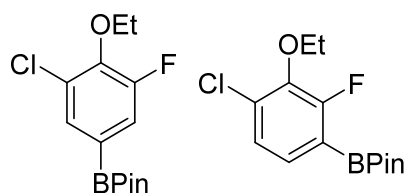
as follows: In a nitrogen atmosphere glove box, pinacol diborane (B_2Pin_2 , 254 mg, 1.0 mmol) was weighed into a 20 mL vial and dissolved in about 2 mL THF and then transferred to a 10 mL volumetric flask. The vial was then washed by 3×1 mL THF and the resulting solution was transferred to the same volumetric flask. The volumetric flask was then diluted to the 10 mL mark by adding more THF, giving a 0.10 M stock solution of B_2Pin_2 . $[Ir(OMe)cod]_2$ (33.1 mg, 0.050 mmol) was weighed into a 20 mL vial and dissolved in about 2 mL THF and transferred to a 10 mL volumetric flask. The vial was then washed by 3×1 mL THF and resulting solution was transferred to the same volumetric flask. The volumetric flask was then diluted to the 10 mL mark by more THF, giving a 0.0050 M stock solution of $[Ir(OMe)cod]_2$. Di(pyridin-2-yl)methane (dpm, 17.0 mg, 0.10 mmol) was weighed into a 20 mL vial and dissolved in about 2 mL THF and transferred to a 10 mL volumetric flask. The vial was then washed by 3×1 mL THF and resulting solution was transferred to the same volumetric flask. The volumetric flask was then diluted to the 10 mL mark by more THF, giving a 0.010 M stock solution of dpm. A J-Young NMR tube was charged with 200 μ L of the 0.0050 M stock solution of $[Ir(OMe)cod]_2$, then 1.0 mL of the 0.10 M stock solution of B_2Pin_2 was added, then 200 μ L of the 0.010 M stock solution of dpm was added. Finally, 121 μ L (1.0 mmol) 2-chloro-6-fluorotoluene was added. The J-Young NMR tube was capped and shaken to well mix the liquids, and then taken out of the glove box and heated in an oil bath at 80 $^{\circ}$ C. The reaction was observed by ^{19}F and ^{11}B NMR were taken until no further progress in borylation. The reaction mixture was then transferred to a 10 mL flask and all volatiles were removed by rotary evaporation, the residue was then purified by Kugelrohr distillation to give a mixture of borylated products.



Preparation of 2-(3-chloro-5-fluoro-4-methylphenyl)-4,4,5,5-tetramethyl-1,3,2-dioxaborolane (13e) and 2-(4-chloro-2-fluoro-3-methylphenyl)-4,4,5,5-tetramethyl-1,3,2-dioxaborolane (13e'):⁵⁵ Subjecting 2-chloro-6-fluorotoluene (121 μ L, 1.0 mmol) to the general procedure, with di(pyridin-2-yl)methane (17.0 mg, 0.10 mmol) as ligand and THF as solvent for 96 h at $^{\circ}$ C. Kugelrohr distillation (0.2 mmHg, 150 $^{\circ}$ C) afforded 49.3 mg (91% yield based on boron) of a 76:24 ratio of 2-(3-chloro-5-fluoro-4-methylphenyl)-4,4,5,5-tetramethyl-1,3,2-dioxaborolane and 2-(4-chloro-2-fluoro-3-methylphenyl)-4,4,5,5-tetramethyl-1,3,2-dioxaborolane as a white solid mixture. For 2-(3-chloro-5-fluoro-4-methylphenyl)-4,4,5,5-tetramethyl-1,3,2-dioxaborolane (major) ^1H NMR (500 MHz, acetone- d_6) δ 7.51 (s, 1H, overlapping with the other isomer), 7.30 (d, $J = 9.3$ Hz, 1H), 2.31 (d, $J = 2.5$ Hz, 3H), 1.34 (s, 12H, overlapping with the other isomer). ^{19}F NMR (470 MHz, acetone- d_6) δ -115.0 (dt, $J = 9.3, 2.5$ Hz). ^{13}C NMR (125 MHz, acetone- d_6) δ 162.3 (d, $J = 247.0$ Hz), 136.5 (d, $J = 4.8$ Hz), 132.0 (d, $J = 2.9$ Hz), 128.4 (d, $J = 20.0$ Hz), 120.2, (d, $J = 21.9$ Hz), 85.3, 25.2, 12.2 (d, $J = 4.3$ Hz). For 2-(4-chloro-2-fluoro-3-methylphenyl)-4,4,5,5-tetramethyl-1,3,2-dioxaborolane (minor) ^1H NMR (500 MHz, acetone- d_6) δ 7.51 (m, 1H, overlapping with the other isomer), 7.23 (d, $J = 8.3$ Hz, 1H), 2.23 (d, $J = 2.5$ Hz, 3H), 1.34 (s, 12H, overlapping with the other isomer). ^{19}F NMR (470 MHz, acetone- d_6) δ -102.4 (m). ^{13}C NMR (125 MHz, acetone- d_6) δ 166.9 (d, $J = 252.7$ Hz), 136.9 (d, $J = 6.7$ Hz), 135.8 (d, $J = 9.5$ Hz), 126.0 (d, $J = 3.8$ Hz), 125.0 (d, $J = 21.0$ Hz), 84.8, 25.2, 11.8 (d, $J = 4.8$ Hz).

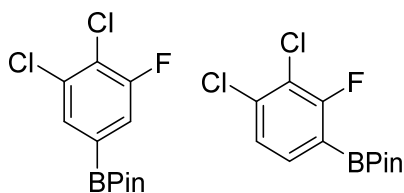


Preparation of 2-chloro-6-fluoro-N,N-dimethyl-4-(4,4,5,5-tetramethyl-1,3,2-dioxaborolan-2-yl)aniline (13f) and 6-chloro-2-fluoro-N,N-dimethyl-3-(4,4,5,5-tetramethyl-1,3,2-dioxaborolan-2-yl)aniline (13f'):⁵⁶ Subjecting 2-chloro-6-fluoro-N,N-dimethylaniline (148 μ L, 1.0 mmol) to the general procedure, with 4,4'-di-tert-butyl-2,2'-bipyridine (26.8 mg, 0.10 mmol) as ligand and THF as solvent for 6 h at 80 °C. Kugelrohr distillation (0.2 mmHg, 150 °C) afforded 53.8 mg (90% yield based on boron) of a 69:31 ratio of 2-chloro-6-fluoro-N,N-dimethyl-4-(4,4,5,5-tetramethyl-1,3,2-dioxaborolan-2-yl)aniline and 6-chloro-2-fluoro-N,N-dimethyl-3-(4,4,5,5-tetramethyl-1,3,2-dioxaborolan-2-yl)aniline as a colorless oil. For 2-chloro-6-fluoro-N,N-dimethyl-4-(4,4,5,5-tetramethyl-1,3,2-dioxaborolan-2-yl)aniline (major) ¹H NMR (500 MHz, CDCl₃) δ 7.51 (s, 1H), 7.28 (d, *J* = 12.2 Hz, 1H), 2.83 (d, *J* = 2.5 Hz, 6H), 1.26 (s, 12H). ¹⁹F NMR (470 MHz, CDCl₃) δ 120.2 (d, *J* = 11.6 Hz). For 6-chloro-2-fluoro-N,N-dimethyl-3-(4,4,5,5-tetramethyl-1,3,2-dioxaborolan-2-yl)aniline (minor) ¹H NMR (500 MHz, CDCl₃) δ 7.31 (dd, *J* = 7.8, 5.9 Hz, 1H), 7.08 (d, *J* = 7.8 Hz, 1H), 2.79 (d, *J* = 2.5 Hz, 6H), 1.30 (s, 12H). ¹⁹F NMR (470 MHz, CDCl₃) δ -108.4 (b). For the mixture ¹³C NMR (125 MHz, CDCl₃) δ 165.4 (d, *J* = 255.6 Hz), 159.7 (d, *J* = 250.8 Hz), 140.4 (d, *J* = 12.4 Hz), 137.7 (d, *J* = 16.2 Hz), 137.0 (d, *J* = 7.6 Hz), 132.0 (d, *J* = 2.9 Hz), 131.9, 131.8 (d, *J* = 10.5 Hz), 125.3 (d, *J* = 3.8 Hz), 121.0 (d, *J* = 20.0 Hz), 84.1, 83.9, 43.4 (d, *J* = 4.5 Hz), 43.2 (d, *J* = 4.8 Hz), 24.7



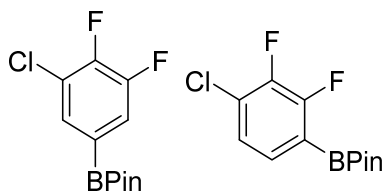
Preparation of 2-(3-chloro-4-ethoxy-5-fluorophenyl)-4,4,5,5-tetramethyl-1,3,2-dioxaborolane (13g) and 2-(4-chloro-3-ethoxy-2-fluorophenyl)-4,4,5,5-tetramethyl-1,3,2-dioxaborolane (13g'):⁵⁷ Subjecting 1-chloro-2-ethoxy-3-fluorobenzene (153 μ L, 1.0 mmol) to the

general procedure, with 4,4'-di-tert-butyl-2,2'-bipyridine (26.8 mg, 0.10 mmol) as ligand and THF as solvent for 12 h at 80 °C. Kugelrohr distillation (0.2 mmHg, 150 °C) afforded 53.5 mg (89% yield based on boron) of a 64:36 ratio of 2-(3-chloro-4-ethoxy-5-fluorophenyl)-4,4,5,5-tetramethyl-1,3,2-dioxaborolane and 2-(4-chloro-3-ethoxy-2-fluorophenyl)-4,4,5,5-tetramethyl-1,3,2-dioxaborolane as a colorless oil. For 2-(3-chloro-4-ethoxy-5-fluorophenyl)-4,4,5,5-tetramethyl-1,3,2-dioxaborolane (major) ¹H NMR (500 MHz, acetone-d₆) δ 7.52 (s, 1H), 7.37 (m, 1H, overlapping with the other isomer), 4.22 (q, *J* = 6.9 Hz, 2H), 1.38 (t, *J* = 6.9 Hz, 3H, overlapping with the other isomer), 1.33 (s, 12H, overlapping with the other isomer). ¹⁹F NMR (470 MHz, acetone-d₆) δ -129.3 (d, *J* = 10.0 Hz). For 2-(4-chloro-3-ethoxy-2-fluorophenyl)-4,4,5,5-tetramethyl-1,3,2-dioxaborolane (minor) ¹H NMR (500 MHz, acetone-d₆) δ 7.37 (m, 1H, overlapping with the other isomer), 7.24 (dd, *J* = 8.3, 1.4 Hz), 4.14 (q, *J* = 6.9 Hz, 2H), 1.38 (t, *J* = 6.9 Hz, 3H, overlapping with the other isomer), 1.34 (s, 12H, overlapping with the other isomer). ¹⁹F NMR (470 MHz, acetone-d₆) δ -117.9 (d, *J* = 5.0 Hz). For the mixture ¹³C NMR (125 MHz, acetone-d₆) δ 161.5 (d, *J* = 254.2 Hz), 156.8 (d, *J* = 248.9 Hz), 146.7 (d, *J* = 13.9 Hz), 144.3 (d, *J* = 15.7 Hz), 132.8 (d, *J* = 3.8 Hz), 132.4 (d, *J* = 3.1 Hz), 131.6 (d, *J* = 9.1 Hz), 126.1 (d, *J* = 3.6 Hz), 121.7 (d, *J* = 18.1 Hz), 85.3, 84.9, 70.9 (d, *J* = 5.1 Hz), 70.8 (d, *J* = 4.3 Hz), 25.2, 25.0, 15.9, 15.9.



Preparation of 2-(3,4-dichloro-5-fluorophenyl)-4,4,5,5-tetramethyl-1,3,2-dioxaborolane (13a) and 2-(3,4-dichloro-2-fluorophenyl)-4,4,5,5-tetramethyl-1,3,2-dioxaborolane (13a'): ⁵⁸

Subjecting 1,2-dichloro-3-fluorobenzene (117 μL , 1.0 mmol) to the general procedure, with 4,4'-di-tert-butyl-2,2'-bipyridine (26.8 mg, 0.10 mmol) as ligand and THF as solvent for 6 h at 80 $^{\circ}\text{C}$. Kugelrohr distillation (0.2 mmHg, 150 $^{\circ}\text{C}$) afforded 54.5 mg (94% yield based on boron) of a 60:40 ratio of 2-(3,4-dichloro-5-fluorophenyl)-4,4,5,5-tetramethyl-1,3,2-dioxaborolane and 2-(3,4-dichloro-2-fluorophenyl)-4,4,5,5-tetramethyl-1,3,2-dioxaborolane as a white solid. For 2-(3,4-dichloro-5-fluorophenyl)-4,4,5,5-tetramethyl-1,3,2-dioxaborolane (major) ^1H NMR (500 MHz, CD_3CN) δ 7.53 (s, 1H); 7.34 (dd, $J = 8.8, 1.5$ Hz, 1H), 1.28 (s, 12H). ^{19}F NMR (470 MHz, CD_3CN) δ -120.0 (d, $J = 8.3$ Hz). ^{13}C NMR (125 MHz, CD_3CN) δ 159.4 (d, $J = 250.8$ Hz), 134.3, 132.2 (d $J = 2.9$ Hz), 123.8 (d, $J = 20.0$ Hz), 120.8 (d, $J = 20.0$ Hz), 85.7, 25.2. For 2-(3,4-dichloro-2-fluorophenyl)-4,4,5,5-tetramethyl-1,3,2-dioxaborolane (minor) ^1H NMR (500 MHz, CD_3CN) δ 7.48 (dd, $J = 7.8, 5.9$ Hz, 1H); 7.25 (dd, $J = 7.8, 1.0$ Hz), 1.30 (s, 12H). ^{19}F NMR (470 MHz, CD_3CN) δ -100.7 (d, $J = 5.0$ Hz). ^{13}C NMR (125.72 MHz, CD_3CN) δ 163.4 (d, $J = 254.6$ Hz), 137.5, 135.5 (d, $J = 9.5$ Hz), 126.6 (d, $J = 3.8$ Hz), 121.1 (d, $J = 21.9$ Hz), 85.4, 25.2.



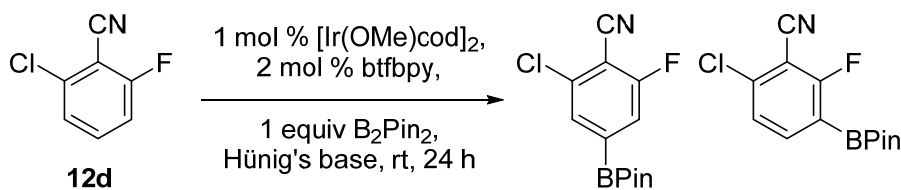
Preparation of 2-(3-chloro-4,5-difluorophenyl)-4,4,5,5-tetramethyl-1,3,2-dioxaborolane (13c) and 2-(4-chloro-2,3-difluorophenyl)-4,4,5,5-tetramethyl-1,3,2-dioxaborolane (13c'): ⁵⁹

Subjecting 1-chloro-2,3-difluorobenzene (93 μL , 1.0 mmol) to the general procedure, with 4,4'-di-tert-butyl-2,2'-bipyridine (26.8 mg, 0.10 mmol) as ligand and THF as solvent for 12 h at 80 $^{\circ}\text{C}$.

Kugelrohr distillation (0.2 mmHg, 150 °C) afforded 50.5 mg (92% yield based on boron) of a 55:45 ratio of 2-(3-chloro-4,5-difluorophenyl)-4,4,5,5-tetramethyl-1,3,2-dioxaborolane and 2-(4-chloro-2,3-difluorophenyl)-4,4,5,5-tetramethyl-1,3,2-dioxaborolane as a white solid. For 2-(3-chloro-4,5-difluorophenyl)-4,4,5,5-tetramethyl-1,3,2-dioxaborolane, ^1H NMR (500 MHz, CDCl_3) δ 7.58 (dt, $J = 6.9, 1.5$ Hz, 1H); 7.46 (m, 1H), 1.31 (s, 12H). ^{19}F NMR (470 MHz, CDCl_3) δ -134.5 (m, 1F), -135.9 (dd, $J = 21.6, 10.0$ Hz, 1F). For 2-(4-chloro-2,3-difluorophenyl)-4,4,5,5-tetramethyl-1,3,2-dioxaborolane, ^1H NMR (500 MHz, CDCl_3) δ 7.38 (m, 1H); 7.13 (m, 1H), 1.33 (s, 12H). ^{19}F NMR (470 MHz, CDCl_3) δ -125.5 (dd, $J = 21.6, 5.0$ Hz, 1F), -139.9 (dd, $J = 20.7, 5.8$ Hz, 1F). For the mixture ^{13}C NMR (125 MHz, CDCl_3) δ 155.0 (dd, $J = 255.7, 11.6$ Hz), 150.7 (dd, $J = 251.9, 12.0$ Hz), 149.0 (dd, $J = 254.5, 14.7$ Hz), 147.1 (dd, $J = 251.3, 16.5$ Hz), 131.8 (d, $J = 3.3$ Hz), 130.6 (dd, $J = 8.1, 5.2$ Hz), 125.6 (dd, $J = 14.4, 1.8$ Hz), 125.1, (dd, $J = 3.7, 1.5$ Hz), 122.3 (d, $J = 14.3$ Hz), 121.5 (d, $J = 15.7$ Hz), 84.6, 84.4, 24.8, 24.8.

The borylation of 2-chloro-6-fluorobenzonitrile (**12d**) was carried out in a slightly different way as showing in **Figure 73**.

Figure 73. Borylation of substrate 12d



Preparation of 2-chloro-6-fluoro-4-(4,4,5,5-tetramethyl-1,3,2-dioxaborolan-2-yl)benzonitrile (13d) and 6-chloro-2-fluoro-3-(4,4,5,5-tetramethyl-1,3,2-dioxaborolan-2-yl)benzonitrile (13d'):⁶⁰ In a nitrogen atmosphere glove box, bis(pinacolato)diboron (B_2Pin_2) (127 mg, 0.5 mmol), $[\text{Ir}(\text{OMe})\text{cod}]_2$ (3.3 mg, 0.005 mmol) were dissolved in 2 mL Hünig's base

in a 20 mL vial fitted with a stir bar. Btfbpy (2.9 mg, 0.01 mmol) was added. The resulting solution was stirred at room temperature for 1 h, to give a black color. 2-chloro-6-fluorobenzonitrile (77.5 mg, 0.5 mmol) was added. The reaction was stirred at room temperature for 24 h. GC-MS showed no substrate left and two monoborylated products formed. The volatiles were removed by rotary evaporation. The residue was then stirred with 10 mL water and 2 mL diethyl ether. The ether phase was separated and the water phase was extracted with approximately 2 mL diethyl ether \times 2. The combined ether solution was dried over MgSO₄, and the solvent was removed by rotary evaporation. The residue was purified by Kugelrohr distillation at 150 °C, 0.2 mmHg to give the regiochemical mixture of borylated products 105.1 mg (74% yield based on arene) of a 41:59 ratio of 2-chloro-6-fluoro-4-(4,4,5,5-tetramethyl-1,3,2-dioxaborolan-2-yl)benzonitrile and 6-chloro-2-fluoro-3-(4,4,5,5-tetramethyl-1,3,2-dioxaborolan-2-yl)benzonitrile as a white solid. For 2-chloro-6-fluoro-4-(4,4,5,5-tetramethyl-1,3,2-dioxaborolan-2-yl)benzonitrile (minor), ¹H NMR (500 MHz, CDCl₃) δ 7.67 (s, 1H); 7.47 (d, J = 8.3 Hz, 1H), 1.32 (s, 12H). ¹⁹F NMR (470 MHz, CD₃CN) δ -104.2 (d, J = 7.8 Hz). For 6-chloro-2-fluoro-3-(4,4,5,5-tetramethyl-1,3,2-dioxaborolan-2-yl)benzonitrile, ¹H NMR (500 MHz, CDCl₃) δ 7.86 (dd, J = 8.3, 6.4 Hz, 1H); 7.31 (d, J = 8.3 Hz, 1H), 1.31 (s, 12H). ¹⁹F NMR (470 MHz, CD₃CN) δ -92.2 (d, J = 4.2 Hz). For the mixture, ¹³C NMR (125 MHz, CDCl₃) δ 167.8 (d, J = 266.8 Hz), 163.1 (d, J = 263.0 Hz), 141.4 (d, J = 10.3 Hz), 140.6 (d, J = 2.1 Hz), 137.2, 131.1 (d, J = 3.3 Hz), 125.2 (d, J = 3.6 Hz), 119.7 (d, J = 18.1 Hz), 111.3 (d, J = 2.1 Hz), 104.9 (d, J = 18.1 Hz), 103.1 (d, J = 20.3 Hz), 85.1, 84.7, 24.8, 24.7.

Tandem borylation-Suzuki coupling

Tandem C-H activation/borylation and Suzuki coupling of 1,2-dichloro-3-fluorobenzene: In a nitrogen glove box, B₂Pin₂ (127 mg, 0.5 mmol) and [Ir(OMe)cod]₂ (6.6 mg, 0.01 mmol) were dissolved in 2 mL Hünig's base in a 20 mL vial fitted with a stir bar, giving a yellow solution.

Then btfbpy (5.8 mg, 0.02 mmol) was added and the mixture was stirred for 30 min. Substrate (117 μ L, 1.0 mmol) was added, and the mixture was stirred at room temperature for 12 h. ^{19}F NMR of crude material showed a 93% conversion of starting materials and 67:33 ratio of two products. The solvent was removed on a rotary evaporator, and the residue was partitioned between 50 mL deionized water and 20 mL EtOAc \times 3. The organic layer was then dried over Na_2SO_4 , and solvent was removed by rotary evaporator, the residue was then further purified on a Kugelrohr distillation at 0.2 mmHg, 150 $^\circ\text{C}$ to provide a mixture of 2-(3,4-dichloro-5-fluorophenyl)-4,4,5,5-tetramethyl-1,3,2-dioxaborolane and 2-(3,4-dichloro-2-fluorophenyl)-4,4,5,5-tetramethyl-1,3,2-dioxaborolane, (232 mg, 80% combined yield, 33:67). Methyl 4-iodobenzoate (260 mg, 0.99 mmol), K_2CO_3 (221 mg, 1.6 mmol) and $\text{Pd}(\text{PPh}_3)_2\text{Cl}_2$ (5.6 mg, 0.008 mmol) were weighed into a screw capped tube fitted with a stirbar. 1.6 mL of water was then added to dissolve the K_2CO_3 , and then the mixture from the Kugelrohr distillation was transferred to the screw capped tube dissolved in a total of 6.4 mL THF. The biphasic mixture was sparged with argon for 30 min before the vial was capped and heated in an oil bath at 60 $^\circ\text{C}$. After 4h, ^{19}F NMR of the reaction crude was taken, showing the Suzuki product of the ele boronate ester, and the Suzuki product of the st boronate ester (ratio of 67:33), and 1% unidentified peaks. The crude reaction was filtered through a basic alumina short plug and then washed by ethyl acetate. The solvents were then removed by rotary evaporation. and the residue was purified on a silica gel column with a mixture of hexane and diethyl ether (50:1). **Methyl 3',4'-dichloro-2'-fluoro-[1,1'-biphenyl]-4-carboxylate (14a')** was isolated as a white solid (mp 150-152 $^\circ\text{C}$), 89.7 mg (30% from starting arene). ^1H NMR (500 MHz, CDCl_3) δ 8.10 (AABB, observed $J = 8.5$ Hz, 2H), 7.56 (doublet of AABB, observed $J = 8.5, 1.7$ Hz, 2H), 7.34 (m, resolved into dd, coupling constants $J = 8.5, 1.5$ Hz, 1H), 7.28 (t, resolved into dd, coupling constants $J = 8.6, 7.3$ Hz, 1 H), 3.93 (s, 3H), ^{19}F NMR (470 MHz, CDCl_3) δ -112.9 (dd, resolved

into dq, $J = 7.5, 1.6$ Hz), ^{13}C NMR (126 MHz, CDCl_3) δ 166.6, 155.8 (d, $J = 253.2$ Hz), 138.6 (d, $J = 1.9$ Hz), 133.7, 129.9, 129.9, 128.8 (d, $J = 3.1$ Hz), 128.4 (d, $J = 4.1$ Hz), 127.8 (d, $J = 14.1$ Hz), 125.6 (d, $J = 4.3$ Hz), 121.7 (d, $J = 20.7$ Hz), 52.3. **Methyl 3',4'-dichloro-5'-fluoro-[1,1'-biphenyl]-4-carboxylate (14a)** was isolated as a white solid (mp 134-136 °C), 45.3 mg (15% from starting arene). ^1H NMR (500 MHz, CDCl_3) δ 8.09 (AABB, observed $J = 8.5$ Hz, 2H), 7.57 (doublet of AABB, observed $J = 8.5$, 2H), 7.50 (t, $J = 1.9$ Hz, 1H), 7.30 (dd, $J = 9.4, 2.0$ Hz, 1H), 3.93 (s, 3H), ^{19}F NMR (470 MHz, CDCl_3) δ -109.2 (dd, $J = 9.5, 1.6$ Hz), ^{13}C NMR (126 MHz, CDCl_3) δ 166.5, 159.0 (d, $J = 251.1$ Hz), 142.0 (d, $J = 2.4$ Hz), 140.2 (d, $J = 8.3$ Hz), 134.6 (d, $J = 1.4$ Hz), 130.4, 130.2, 126.8, 124.3 (d, $J = 3.1$ Hz), 120.4 (d, $J = 19.8$ Hz), 113.5 (d, $J = 22.7$ Hz), 52.3.

Tandem C-H activation/borylation and Suzuki coupling of 2-chloro-6-fluoro-phenol: In a nitrogen glove box, B_2Pin_2 (127 mg, 0.5 mmol) and $[\text{Ir}(\text{OMe})\text{cod}]_2$ (6.6 mg, 0.01 mmol) were dissolved in 0.5 mL THF, giving a yellow solution, then ttfbpy (8.6 mg, 0.02 mmol) was added, and the mixture was stirred in a 20 mL vial. Substrate (**12b**) (146 mg, 1.0 mmol) was dissolved in 1 mL THF in a 100 mL Schlenk flask, then HBPIn (160 μL , 1.1 mmol) was added, and the mixture was stirred for 30 min. Gas bubbles formed during this process. The previous mixture of Ir, ligand and B_2Pin_2 was then transferred into the Schlenk flask and washed by 0.35 mL THF \times 3, with the washings combined into the Schlenk flask. The Schlenk flask was then capped and transferred out of the glove box and connected onto an argon Schlenk line through a condenser. The Schlenk flask was then purged by argon flow for 5 min and then heated in an oil bath at 60 °C for 6 h, under argon. ^{19}F NMR of crude material showed a 96% conversion of starting materials and 69:31 ratio of two products. The reaction was cooled to room temperature and 1 mL of MeOH was added and stirred for 10 min. Gas bubbles were formed rapidly during this time. Crude NMR confirmed a

96% conversion of starting arene, with 69:31 ratio of the two products. THF and MeOH were removed on a rotary evaporator, and the residue was partitioned between 50 mL deionized water and 20 mL EtOAc \times 3. The organic layer was then dried over Na₂SO₄, and solvent was removed by rotary evaporator, the residue was then further purified by a Kugelrohr distillation at 0.2 mmHg, 150 °C providing a mixture of 2-chloro-6-fluoro-4-(4,4,5,5-tetramethyl-1,3,2-dioxaborolan-2-yl)phenol and 6-chloro-2-fluoro-3-(4,4,5,5-tetramethyl-1,3,2-dioxaborolan-2-yl)phenol, (165 mg, 61% combined yield, 69:31). Methyl 4-iodobenzoate (177 mg, 0.67 mmol), K₂CO₃ (169 mg, 1.2 mmol) and Pd(PPh₃)₂Cl₂ (4.3 mg, 0.0061 mmol) were weighed into a screw capped tube fitted with a stirbar. At this time 1.2 mL of water was then added to dissolve the K₂CO₃, and then the mixture from the Kugelrohr distillation was transferred to the screw capped tube by dissolved in a total of 4.8 mL THF. The biphasic mixture was sparged with argon for 30 min was capped and heated in an oil bath at 60 °C. After 4h, ¹⁹F NMR of the reaction crude was taken, showing peaks that integrated for 59% of the Suzuki product of the ele boronate ester, 23% of the Suzuki product of the st boronate ester (ratio of 71:29), 10% 2-chloro-6-fluoro-phenol and 8% unidentified peaks. The crude reaction was filtered through a basic alumina short plug and then washed by ethyl acetate. The solvents were then removed by rotary evaporation and the residue was purified on a silica gel column with a mixture of hexane and EtOAc (10:1), affording a very small amount of pure methyl 4'-chloro-2'-fluoro-3'-hydroxy-[1,1'-biphenyl]-4-carboxylate 8 mg (3% based on starting phenol), and a mixture of methyl 4'-chloro-2'-fluoro-3'-hydroxy-[1,1'-biphenyl]-4-carboxylate (major) and methyl 3'-chloro-5'-fluoro-4'-hydroxy-[1,1'-biphenyl]-4-carboxylate (minor) 135 mg (48% based on starting phenol, 73:27), making a combined yield of methyl 4'-chloro-2'-fluoro-3'-hydroxy-[1,1'-biphenyl]-4-carboxylate (major) and methyl 3'-chloro-5'-fluoro-4'-hydroxy-[1,1'-biphenyl]-4-carboxylate (minor) 143 mg (51% based on starting phenol, 75:25).

Methyl 4'-chloro-2'-fluoro-3'-hydroxy-[1,1'-biphenyl]-4-carboxylate (14b'): ^1H NMR (500 MHz, CDCl_3) δ ppm 8.09 (aabb, observed largest $J = 8.3$ Hz, 2H), 7.57 (dd, $J = 8.6, 1.7$ Hz, 2H), 7.19 (dd, $J = 8.3, 2.0$ Hz), 6.94 (dd, $J = 8.6, 7.6$ Hz, 1H), 5.63 (br. s, 1H), 3.93 (s, 3H). ^{19}F NMR (470 MHz, CDCl_3) δ ppm -138.9 (dd, $J = 7.5, 1.2$ Hz). ^{13}C NMR (126 MHz, CDCl_3) δ ppm 166.75 (s), 148.47 (dd, $J = 246.1, 1.0$ Hz), 141.08 (d, $J = 15.3$ Hz), 139.19 (d, $J = 1.9$ Hz), 129.81 (s), 129.66 (s), 128.83 (d, $J = 2.9$ Hz), 127.72 (d, $J = 11.4$ Hz), 124.62 (d, $J = 3.8$ Hz), 121.10 (d, $J = 2.9$ Hz), 52.26 (s).

Unseparated mixture of methyl 4'-chloro-2'-fluoro-3'-hydroxy-[1,1'-biphenyl]-4-carboxylate (major) and methyl 3'-chloro-5'-fluoro-4'-hydroxy-[1,1'-biphenyl]-4-carboxylate (**14b** & **14b'**) (minor) ^1H NMR (500 MHz, CDCl_3) δ ppm 8.11 – 8.06 (overlapping of the two compounds), 7.59 – 7.53 (overlapping of the two compounds), 7.39 (t, $J = 2.0$ Hz, minor 1H), 7.28 (dd, $J = 11.0, 2.2$ Hz, minor 1H), 7.19 (dd, $J = 8.6, 1.7$ Hz, major 1H), 6.93 (dd, $J = 8.3, 7.3$ Hz, major 1H), 3.93 (s, major, 3H), 3.92 (s, minor, 3H). ^{19}F NMR (470 MHz, CDCl_3) δ ppm -133.6 (dd, $J = 11.0, 1.4$ Hz, minor) -138.9 (dd, $J = 7.7, 1.5$ Hz, major)

Tandem C-H activation/borylation and Suzuki coupling of 1-chloro-2,3-difluorobenzene (12c): In a nitrogen glove box, B_2Pin_2 (127 mg, 0.5 mmol) and $[\text{Ir}(\text{OMe})\text{cod}]_2$ (6.6 mg, 0.01 mmol), and ttfbpy (8.5mg, 0.02 mmol) were mixed in a Schlenk flask fitted with a stirbar in 2.0 mL Hünig's base, and stirred for 1 h at room temperature. 1-Chloro-2,3-difluorobenzene (93 μL , 1.0 mmol) was then added. The Schlenk flask was then connected to an argon manifold through a water condenser outside the glovebox and heated in a 60 °C oil bath for 6 h. ^{19}F NMR was taken of the crude reaction mixture, showing 85% conversion of the starting material, and 82:18 ratio of the two products. Solvent was then removed by rotary evaporation. Kugelrohr distillation at 0.2 mmHg, 150 °C provided a mixture of 2-(4-chloro-2,3-difluorophenyl)-4,4,5,5-tetramethyl-1,3,2-

dioxaborolane and 2-(3-chloro-4,5-difluorophenyl)-4,4,5,5-tetramethyl-1,3,2-dioxaborolane as colorless oil (solidified in the fridge, 217 mg, 79% yield combined, 82:18 ratio). Methyl 4-iodobenzoate (228 mg, 0.87 mmol), K₂CO₃ (218 mg, 1.58 mmol) and Pd(PPh₃)₂Cl₂ (5.5 mg, 0.008 mmol) were weighed into a screw capped tube fitted with a stirbar. Water (1.6 mL) was then added to dissolve the K₂CO₃ and then the mixture of 2-(4-chloro-2,3-difluorophenyl)-4,4,5,5-tetramethyl-1,3,2-dioxaborolane and 2-(3-chloro-4,5-difluorophenyl)-4,4,5,5-tetramethyl-1,3,2-dioxaborolane was transferred to the screw capped tube by being dissolved in a total of 6.4 mL THF. The biphasic mixture was sparged with argon for 30 min before the tube was capped and heated in an oil bath 60 °C. After 4h, GC-MS showed a small amount of bromide left, no boronate esters left, and an overlapped peak of Suzuki coupling products. ¹⁹F NMR of the reaction crude was taken, showing peaks that integrated for 72% of the Suzuki product of the major boronate ester, 13% of the Suzuki product of the minor boronate ester (ratio of 85:15), and 15% for unidentified peaks. The crude reaction was filtered through a basic alumina short plug and then washed by ethyl acetate. The solvents were then removed by rotary evaporation, and the residue was purified by a silica gel column with a mixture of hexane and diethyl ether (20:1), affording **methyl 3'-chloro-4',5'-difluoro-[1,1'-biphenyl]-4-carboxylate (14c)** as a white solid, mp 104 °C, (21 mg, 0.074 mmol, 7% isolated yield based on 1-Chloro-2,3-difluorobenzene) ¹H NMR (500 MHz in CDCl₃) δ 8.09 (AA'BB', *J* = 8.6, 2H), 7.55 (AA'BB', *J* = 8.6 Hz, 2H), 7.41 (dt, *J* = 5.9, 2.0 Hz, 1H), 7.31 (ddd, *J* = 10.5, 6.6, 2.2 Hz, 1H), 3.93 (s, 3H). ¹⁹F NMR (470 MHz, CDCl₃) δ -137.5 (ddd, *J* = 20.7, 10.7, 2.1 Hz, 1F), -139.2 (dt, *J* = 20.8, 6.2 Hz, 1F). ¹³C NMR (126 MHz, CDCl₃) δ 166.6, 151.1 (dd, *J* = 251.8, 13.4 Hz), 146.0 (dd, *J* = 251.8, 15.3 Hz), 142.2, 136.8 (dd, *J* = 7.6, 4.8 Hz), 130.3, 129.9, 126.9, 124.2 (d, *J* = 2.9 Hz), 123.2 (dd, *J* = 14.3, 1.9 Hz), 114.6 (d, *J* = 18.1 Hz), 52.3. **Methyl 4'-chloro-2',3'-difluoro-[1,1'-biphenyl]-4-carboxylate (14c')** as a

white solid, mp 101 °C, (117 mg, 0.41 mmol, 41% isolated yield based on 1-chloro-2,3-difluorobenzene) ^1H NMR (500 MHz in DMSO- d_6) δ 8.08 (AA'BB', J = 8.8, 2H), 7.74 (doublet of an AA'BB', J = 8.8, 1.6 Hz, 2H), 7.57 (ddd, J = 8.7, 6.9, 2.0 Hz, 1H), 7.47 (ddd, J = 8.7, 7.3, 2.0 Hz, 1H), 3.89 (s, 3H). ^{19}F NMR (470 MHz, CDCl_3) δ -137.5 (ddd, J = 20.5, 6.4, 2.1 Hz, 1F), -139.0 (ddq, J = 20.4, 7.0, 1.7 Hz, 1F). ^{13}C NMR (126 MHz, CDCl_3) δ 166.6, 148.5 (dd, J = 253.7, 13.4 Hz) 147.7 (dd, J = 251.8, 15.3 Hz) 138.3, 130.0, 129.9, 128.8 (d, J = 3.8 Hz), 128.7 (d, J = 10.5 Hz), 125.2 (d, J = 4.8 Hz), 124.6 (t, J = 2.9 Hz), 122.2 (d, J = 15.3 Hz), 52.3.

Tandem C-H activation/borylation and Suzuki coupling of 2-chloro-6-fluorobenzonitrile

(12d): In a nitrogen glove box, B_2Pin_2 (127 mg, 0.5 mmol) and $[\text{Ir}(\text{OMe})\text{cod}]_2$ (6.6 mg, 0.01 mmol), and ttfbpy (8.5mg, 0.02 mmol) were mixed in a Schlenk flask fitted with a stirbar in 2.0 mL Hünig's base and the mixture was stirred for 1 h at room temperature. 2-chloro-6-fluorobenzonitrile (156 mg, 1.0 mmol) was then added. The Schlenk flask was then connected to an argon manifold through a water condenser outside the glovebox and heated in a 60 °C oil bath for 6 h. ^{19}F NMR was taken of the crude reaction, showing 80% conversion of the starting material and a 64:36 ratio of the two products. Solvent was then removed by rotary evaporation. Kugelrohr distillation at 0.2 mmHg, 150 °C provided a mixture of 6-chloro-2-fluoro-3-(4,4,5,5-tetramethyl-1,3,2-dioxaborolan-2-yl)benzonitrile and 2-chloro-6-fluoro-4-(4,4,5,5-tetramethyl-1,3,2-dioxaborolan-2-yl)benzonitrile and 2-chloro-6-fluorobenzonitrile as a white solid (213 mg, 64:4:32, 74% yield of borylated products). Methyl 4-iodobenzoate (213 mg, 0.81 mmol), K_2CO_3 (204 mg, 1.48 mmol) and $\text{Pd}(\text{PPh}_3)_2\text{Cl}_2$ (5.2 mg, 0.0074 mmol) were weighed into a screw capped tube fitted with a stirbar. Water (1.5 mL) was then added to dissolve the K_2CO_3 , and then the mixture from the Kugelrohr distillation result was transferred to the screw capped tube by being dissolved in a total of 6.0 mL THF. The biphasic mixture was sparged with argon for 30 min before

the tube was capped and heated in an oil bath 60 °C. After 4h, GC-MS showing no boronate esters left and two overlapped peaks of Suzuki coupling products. ¹⁹F NMR of the reaction crude was taken, showing peaks that integrated for 46% of the Suzuki product of the major boronate ester, 22% of the Suzuki product of the minor boronate ester (ratio of 68:32), and 13% unborylated arene, and 19% for unidentified peaks. The crude reaction was filtered through a basic alumina short plug and then washed by ethyl acetate. The solvents were then removed by rotary evaporation, and the residue was purified on a silica gel column with a mixture of hexane and EtOAc (5:1), affording **2-chloro-6-fluoro-3-(4,4,5,5-tetramethyl-1,3,2-dioxaborolan-2-yl)benzotrile (14d')** as a white solid, mp 209-211 °C, (49 mg, 0.17 mmol, 17% isolated yield based on 2-chloro-6-fluorobenzotrile) ¹H NMR (500 MHz in CDCl₃) δ 8.14 (AA'BB', *J* = 8.3, 2H), 7.62 (AA'BB', *J* = 8.3 Hz, 2H), 7.56 (t, *J* = 1.5 Hz, 1H), 7.36 (dd, *J* = 9.3, 1.5 Hz, 1H), 3.94 (s, 3H). ¹⁹F NMR (470 MHz, CDCl₃) δ -102.2 (dd, *J* = 9.5, 0.8 Hz). ¹³C NMR (126 MHz, CDCl₃) δ 166.2, 163.9 (d, *J* = 262.3 Hz), 147.2 (d, *J* = 8.6 Hz), 141.1, 138.3 (d, *J* = 2.9 Hz), 131.3, 130.6, 127.2, 124.4 (d, *J* = 2.9 Hz), 113.3 (d, *J* = 20.0 Hz), 111.2, 102.4 (d, *J* = 18.1 Hz), 52.4. **6-chloro-2-fluoro-4-(4,4,5,5-tetramethyl-1,3,2-dioxaborolan-2-yl)benzotrile (14d)** was isolated as a white solid, mp 148-150 °C, (23 mg, 0.08 mmol, 8% isolated yield based on 2-chloro-6-fluorobenzotrile) ¹H NMR (500 MHz in DMSO-*d*₆) δ 8.18 (AA'BB', *J* = 8.3, 2H), 7.63 (t, *J* = 8.3 Hz, 1H), 7.56 (d of AA'BB', *J* = 8.3, 2.0 Hz, 2H), 7.41 (dd, *J* = 8.3, 1.0 Hz, 1H), 3.94 (s, 3H). ¹⁹F NMR (470 MHz, CDCl₃) δ -106.6 (dt, *J* = 8.3, 1.7 Hz). ¹³C NMR (126 MHz, CDCl₃) δ 166.4, 160.6 (d, *J* = 264.2 Hz), 137.3 (br, s), 137.0 (d, *J* = 1.9 Hz), 135.2 (d, *J* = 5.7 Hz), 130.6, 130.1, 128.8 (d, *J* = 2.9 Hz), 127.7 (d, *J* = 13.4 Hz), 126.0 (d, *J* = 3.8 Hz), 111.2, 104.2 (d, *J* = 19.1 Hz), 52.4. A mixed fraction of the two (**14d** & **14d'**) (46 mg, 0.12 mmol, 12% of the first product, 0.04 mmol, 4% for the second product) was also isolated.

Tandem C-H activation/borylation and Suzuki coupling of 2-chloro-6-fluorotoluene (12e): In a nitrogen glove box, B₂Pin₂ (127 mg, 0.5 mmol) and [Ir(OMe)cod]₂ (6.6 mg, 0.01 mmol), and ttfbpy (8.5mg, 0.02 mmol) were mixed in a Schlenk flask fitted with a stirbar in 2.0 mL THF base, and the mixture was stirred for 1 h at room temperature. 2-chloro-6-fluorotoluene (131 μ L, 1.0 mmol) was then added. The Schlenk flask was then connected to an argon manifold through a water condenser outside the glovebox and heated in a 60 °C oil bath for 6 h. ¹⁹F NMR was taken of the crude reaction, showing 87% conversion of the starting material, and a 25:75 ratio of the two products. Solvent was then removed by rotary evaporation. Kugelrohr distillation at 0.2 mmHg, 150 °C provided a mixture of 6-chloro-2-fluoro-3-(4,4,5,5-tetramethyl-1,3,2-dioxaborolan-2-yl)toluene and 2-chloro-6-fluoro-4-(4,4,5,5-tetramethyl-1,3,2-dioxaborolan-2-yl)toluene as a white solid (222 mg, 26:74, 82% yield of borylated products). Methyl 4-iodobenzoate (236 mg, 0.90 mmol), K₂CO₃ (407 mg, 1.62 mmol) and Pd(PPh₃)₂Cl₂ (5.8 mg, 0.0082 mmol) were weighed into a screw capped tube fitted with a stirbar. Water (2.0 mL) was then added to dissolve the K₂CO₃, and then the mixture from the Kugelrohr distillation was transferred to the screw capped tube by being dissolved in a total of 8.0 mL THF. The biphasic mixture was sparged with argon for 30 min before the tube was capped and heated in an oil bath 60 °C. After 4h, GC-MS showed no boronate esters left, and two overlapped peaks of Suzuki coupling products. ¹⁹F NMR of the reaction crude was taken, showed peaks that integrated for 16% of the Suzuki product of the ele boronate ester, 71% of the Suzuki product of the st boronate ester (ratio of 18:82), and 13% unidentified peaks. The crude reaction was filtered through a basic alumina short plug and then washed by ethyl acetate. The solvents were then removed by rotary evaporation, and the residue was purified on a silica gel column with a mixture of hexane and EtOAc (5:1). The two products came out as one fraction. Several different combinations of solvents were tried, but no separation was achieved. The

resulting 164 mg (0.59 mmol, 59% combined yields, based on substrate, 28:72) was isolated as a white solid. ^1H NMR (500 MHz in CDCl_3) δ 8.08 (d, $J = 8.3$ Hz, 2H overlapping of two products), 7.58 (d, $J = 8.3$ Hz, 2H, the steric product), 7.56 (d, $J = 8.3$ Hz, 2H, the electronic product), 7.42 (s, 1H, the steric product), 7.22-7.18 (m, overlapping), 3.92 (s, 3H, overlapping of two products), 2.36 (d, $J = 2.0$ Hz, 3H, the electronic product), 2.33 (d, $J = 2.0$ Hz, 3H, the steric product), ^{13}C NMR (126 MHz, CDCl_3) δ 166.7, 166.6, 161.5 (d, $J = 247.0$ Hz), 158.0 (d, $J = 249.9$ Hz), 142.9 (d, $J = 2.9$ Hz), 139.8, 139.4 (d, $J = 9.0$ Hz), 136.0 (d, $J = 7.6$ Hz), 135.2 (d, $J = 5.7$ Hz), 130.2, 129.6, 129.6, 129.3, 128.8 (d, $J = 2.9$ Hz), 127.8 (d, $J = 3.8$ Hz), 126.7, 126.3 (d, $J = 14.3$ Hz), 124.8 (d, $J = 3.8$ Hz), 124.6 (d, $J = 20.0$ Hz), 123.7 (d, $J = 19.1$ Hz), 123.2 (d, $J = 3.8$ Hz), 112.2 (d, $J = 24.8$ Hz), 52.1, 12.5 (d, $J = 5.7$ Hz), 11.7 (d, $J = 3.8$ Hz), ^{19}F NMR (470 MHz, CDCl_3) δ -112.3 (d, $J = 10.0$ Hz, the steric product), -116.4 (m, the electronic product)

Tandem C-H activation/borylation and Suzuki coupling of 2-chloro-6-fluoro-*N,N*-dimethylaniline (12f): In a nitrogen glove box, B_2Pin_2 (127 mg, 0.5 mmol) and $[\text{Ir}(\text{OMe})\text{cod}]_2$ (6.6 mg, 0.01 mmol), and dtbpy (5.4 mg, 0.02 mmol) were mixed in a Schlenk flask fitted with a stirbar in 2.0 mL THF. 2-Chloro-6-fluoro-*N,N*-dimethylaniline (153 μL , 1.0 mmol) was then added. The Schlenk flask was then connected to an argon manifold through a water condenser outside the glovebox and heated in a 60 $^\circ\text{C}$ oil bath for 6 h. ^{19}F NMR was taken of the crude reaction, showing 94% conversion of the starting material, and a 38:62 ratio of the two products. Solvent was then removed by rotary evaporation. Kugelrohr distillation at 0.2 mmHg, 150 $^\circ\text{C}$ provided a mixture of 6-chloro-2-fluoro-*N,N*-dimethyl-3-(4,4,5,5-tetramethyl-1,3,2-dioxaborolan-2-yl)aniline and 2-chloro-6-fluoro-*N,N*-dimethyl-4-(4,4,5,5-tetramethyl-1,3,2-dioxaborolan-2-yl)aniline as a colorless oil (199 mg, 29:71, 66% yield of borylated products). Methyl 4-iodobenzoate (192 mg, 0.73 mmol), K_2CO_3 (184 mg, 1.33 mmol) and $\text{Pd}(\text{PPh}_3)_2\text{Cl}_2$ (4.7 mg,

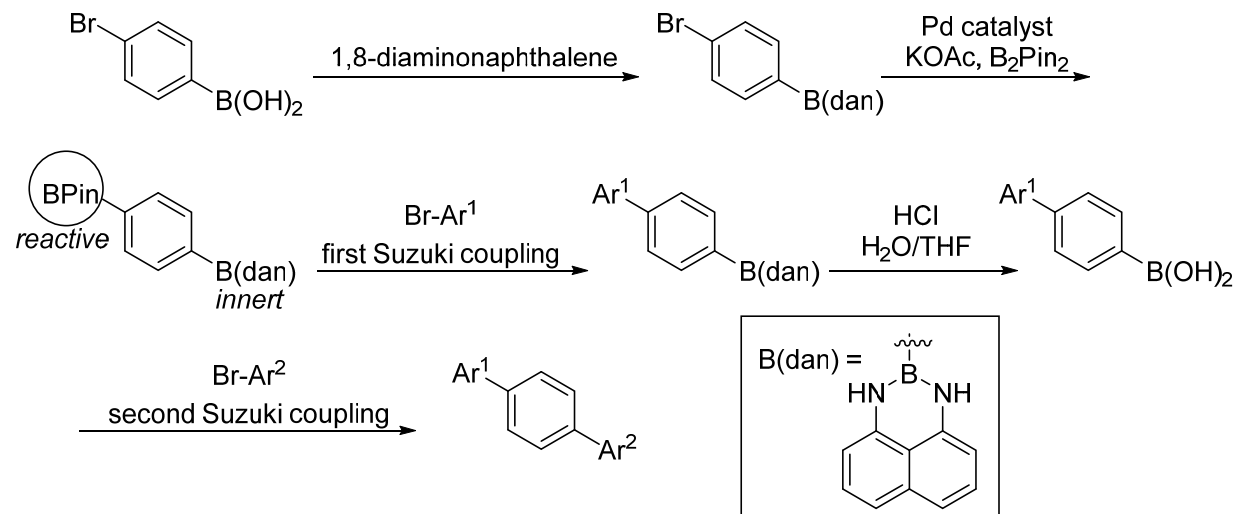
0.0066 mmol) were weighed into a screw capped tube fitted with a stirbar. Water (1.3 mL) was then added to dissolve the K_2CO_3 , and then the mixture from the Kugelrohr distillation was transferred to the screw capped tube by being dissolved in a total of 5.2 mL THF. The biphasic mixture was sparged with argon for 30 min before the tube was capped and heated in an oil bath 60 °C. After 4h, GC-MS showing no boronate esters left, and two peaks of Suzuki coupling products. ^{19}F NMR of the reaction crude was taken, showing peaks that integrated for 24% of the Suzuki product of the ele boronate ester, 46% of the Suzuki product of the st boronate ester (ratio of 34:66), and 30% unidentified peaks. The crude reaction mixture was filtered through a basic alumina short plug and then washed by ethyl acetate. The solvents were then removed by rotary evaporation, and the residue was purified on a silica gel column with a mixture of hexane and EtOAc (10:1). However, the two products came out as one fraction. Several different combinations of solvents were tried, but no separation was achieved. The resulting 92 mg (0.30 mmol, 30% combined yields, based on substrate, 38:62) of products was isolated as a white solid. 1H NMR (500 MHz in $CDCl_3$) δ 8.07 (d, 2H overlapping of two products, unable to determine coupling constant), 8.05 (d, 2H overlapping of two products, unable to determine coupling constant), 7.54 (d, $J = 8.3$ Hz, 2H overlapping of two products), 7.40 (t, $J = 1.7$ Hz, 1H, the steric product), 7.21-7.15 (m, overlapping), 7.04 (t, $J = 7.81$ Hz, 1H, the electronic product), 3.91 (s, 3H, overlapping of two products), 3.91 (s, 3H, overlapping of two products), 2.89 (d, $J = 2.5$ Hz, 6H, overlapping of two products), 2.88 (d, $J = 2.5$ Hz, 6H, overlapping of two products). ^{13}C NMR (126 MHz, $CDCl_3$) δ 166.7, 166.6, 160.5 (d, $J = 248.9$ Hz), 157.9 (d, $J = 253.7$ Hz), 142.7 (d, $J = 1.9$ Hz), 139.7, 138.4 (d, $J = 13.4$ Hz), 137.6 (d, $J = 12.4$ Hz), 136.4 (d, $J = 9.5$ Hz), 133.3 (d, $J = 7.6$ Hz), 133.1 (d, $J = 6.7$ Hz), 129.3 (d, $J = 3.8$ Hz), 128.9 (d, $J = 2.9$ Hz), 128.0 (d, $J = 13.4$ Hz), 125.6 (d, $J = 3.8$ Hz), 125.5 (d, $J = 4.8$ Hz), 124.2 (d, $J = 2.9$ Hz), 113.9 (d, $J = 22.9$ Hz), 52.1 (s), 43.4-43.3

(m), ^{19}F NMR (470 MHz, CDCl_3) δ -118.1 (br, d, $J = 12.4$ Hz, the steric product), -123.1 (s, br, the electronic product).

Chapter 3 Desymmetrization of Diboryl Aromatics

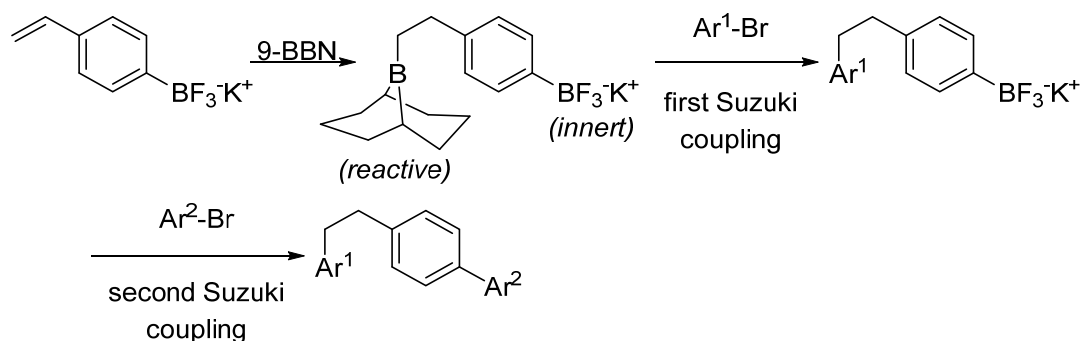
3.1 Introduction

Figure 74. Suginome's B(dan) protection groups



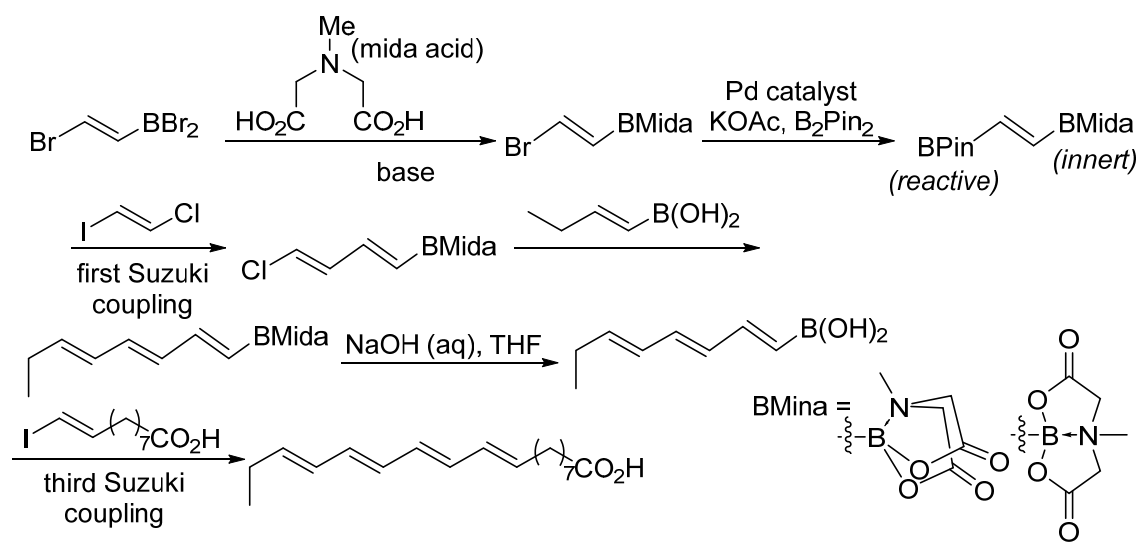
Differentiation of symmetric functionality is a widely used synthetic strategy, because the value of the unsymmetrical compounds that result is almost always greater than that of the symmetrical precursors. One class of compound where desymmetrization has met with limited success is boronic esters and acids. Solutions to this problem could have broad appeal because boronic acids and esters are synthons for a broad range of chemical functionality, and are widely used in cross coupling reactions like Suzuki-Miyaura cross-couplings.

Figure 75. Molander's exploitation of ArBF₃M salts



There have been numerous attempts to differentiate two or more boron atoms in a molecule.⁶¹ Success on this front has been relatively recent with noteworthy reports from the laboratories of Suginome (**Figure 76**),⁶² Molander (**Figure 75**),⁶³ and Burke (**Figure 76**).⁶⁴ In these examples, the key to differentiating the boron sites is to install those sequentially using orthogonal transformations that are chemically compatible. It is important to note that this approach requires starting materials in which the carbon positions where boron will ultimately reside are chemically distinct, and in no case has this been achieved from a symmetric starting material.

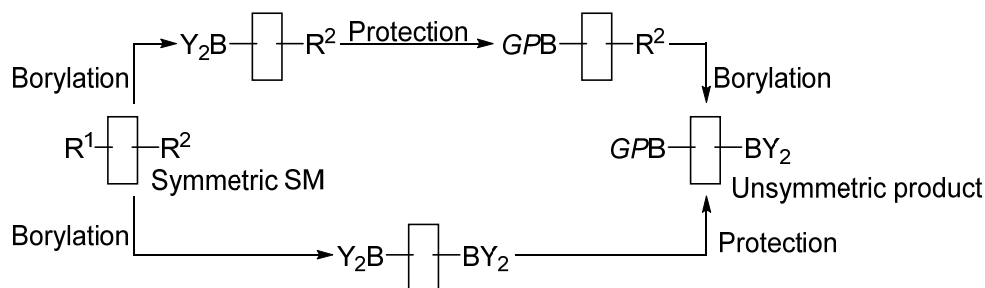
Figure 76. Burk's exploitation of Mida protected boron



Our interest in this problem originated in Ir-catalyzed C–H borylation chemistry, where a significant number of substrates yield diborylated products where the boron sites are chemically equivalent. If these positions could be selectively transformed, C–H borylation would provide a simple protocol for desymmetrizing C–H bonds. Two approaches for preparing differentiated diborylated compounds are borylation/protection/ borylation and diborylation/desymmetrization, as shown in **Figure 77**. The former strategy has an additional step and the protecting group must be compatible with Ir-catalyzed borylation. Both approaches require selectivity for one of two

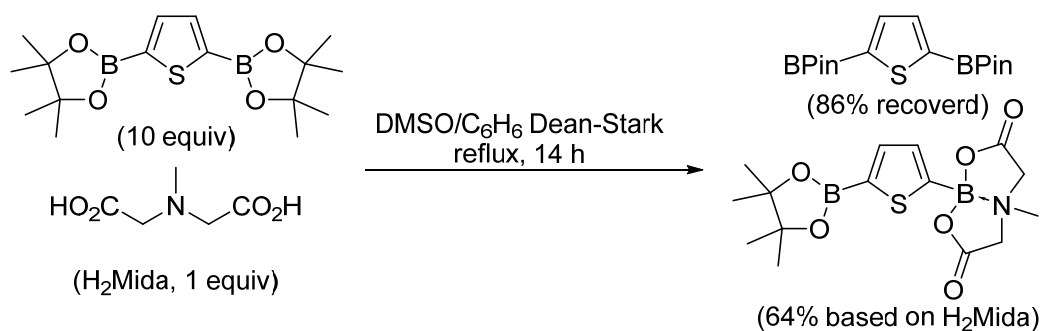
symmetric sites. The borylation/protection/borylation route requires that diborylation be avoided in the first step, while the diborylation/ desymmetrization strategy calls for a selective monoprotection of the symmetric diboronate.

Figure 77. Two approaches toward unsymmetric diborates



For evaluation of the diborylation/protection route, Burke's MIDA protecting group was used exclusively.⁶⁵ It is conceivable that BF_3K or dan (1,8-diamidonaphthalene) protecting groups could be used, but our decision was based on (i) the expectation that transesterification of the pin groups to MIDAs could be achieved by reacting ArBpin compounds with MIDAH_2 , and (ii) product purification would be aided by the differences in solubilities of ArBpin , ArBMIDA , and MIDAH_2 .

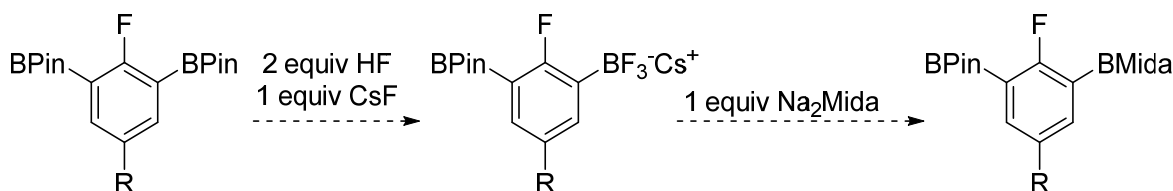
Figure 78. Desymmetrizing $\text{Ar}(\text{BPin})_2$ by H_2Mida



Previously Smith's group found that such symmetrically diborylated compounds could be desymmetrized by protecting one of the two borons by methylimidodiacetic acid (Mida ligand or Mida acid, or H_2Mida), by reaction of diborylated compounds and H_2Mida at high temperature.

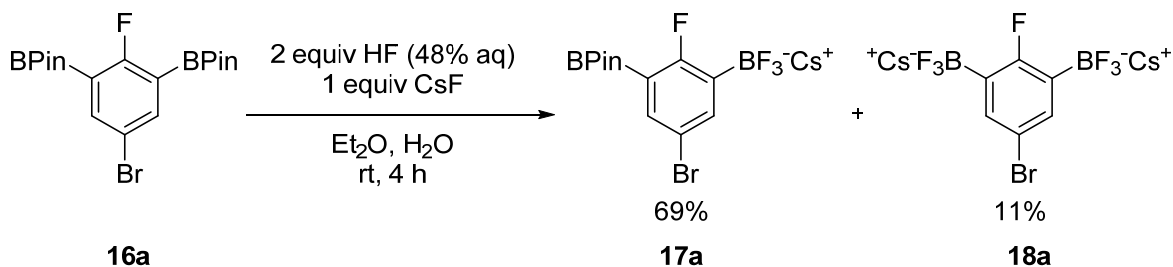
To avoid formation of $\text{Ar}(\text{BMida})_2$ products, a large excess of the $\text{Ar}(\text{BPin})_2$ compound was required, though the starting material could be recovered (**Figure 78**).

Figure 79. Desymmetrizing $\text{Ar}(\text{BPin})_2$ via $\text{Ar}(\text{BPin})\text{BF}_3\text{M}$ salt



We considered if it would be possible to convert one of the two BPin's into a $-\text{BF}_3\text{M}$ salt by treating the $\text{Ar}(\text{BPin})_2$ compounds with a 2:1 mixture of HF/MF, activating the $-\text{BF}_3\text{M}$ salt with a silicon reagent such as TMSCl would give a $-\text{BF}_2$ group as a reactive intermediate, which could be protect with Na_2Mida under mild conditions (**Figure 79**). Although this route adds one more step to the protection, it does not require the use of large excess of diborylated material. This could be very convenient, especially for bench top scale reactions.

Figure 80. Desymmetrizing 2,2'-(5-bromo-2-fluoro-1,3-phenylene)bis(BPin)



The key step of this transformation is the first step, where the desymmetrization of the diborylated compounds takes place. The formation of ArBF_3Cs salts by treating $\text{ArB}(\text{OR})_2$ or $\text{ArB}(\text{OH})_2$ with a mixture of HF (conc. aq) and CsF was first published by Matterson⁶⁶ and has found application in many transformations. However, preventing the transformation of both BPin group might still issue a challenge to our proposed transformations.

3.2 Synthesis of the (PinB)Ar(BF₃)Cs salts.

We started by adopting Matteson's method:

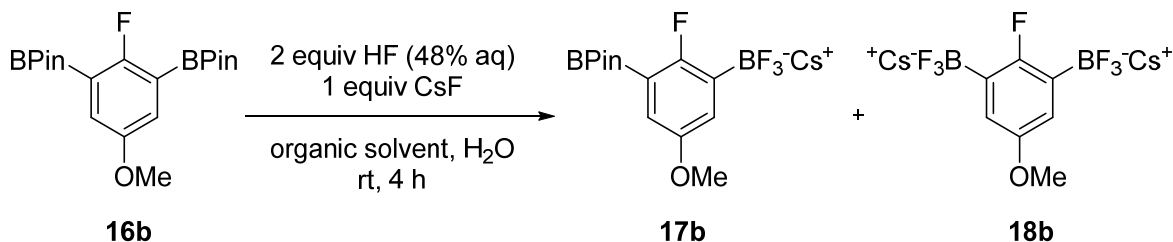
3.2.1 Desymmetrizing 2,2'-(5-bromo-2-fluoro-1,3-phenylene)bis(BPin)

CsF (1.52 g, 10 mmol) was weighed into a Teflon flask fitted with a stirbar and HF (830 mg, 48% aq, 20 mL) was weighed in a plastic syringe and injected into the Teflon flask. The mixing of HF and CsF resulted in a solution and the process was exothermic. The Teflon flask was then cooled in an ice bath to room temperature or below. Diborylated arene **16a** (4.27g, 10 mmol) dissolved in 20 mL of Et₂O (distilled to remove antioxidant) was added in one dose. The flask was then sealed and the reaction mixture was stirred at room temperature for 4 hours. This resulted in a large amount of white solid, which was filtered out and washed with a large amount of Et₂O, giving a white solid 4.04 g, 69% yield of the desired product **17a**, and 11% of the undesired by-product **18a** as mixture (ratio based on NMR's), as shown in **Figure 80**. Mp of this solid is not available, for it starts to decompose above 220 °C. Compound **17a**: ¹H NMR (300 MHz, DMSO-*d*₆) δ ppm 7.49 (dd, *J* = 4.5, 3.0 Hz, 1H) 7.39 (dd, *J* = 4.8, 2.9 Hz, 1H), 1.28 (s, 12H). ¹¹B NMR (96 MHz, CD₃CN) δ ppm 30.5 (br. s., 1B), 2.5 (q, *J* = 45.0 Hz, 1B), ¹⁹F NMR (282 MHz, CD₃CN) δ ppm -97.3 (br. s.), -137.8 (m). Compound **18a**, ¹H NMR (300 MHz, DMSO-*d*₆) δ ppm 7.09 (d, *J* = 4.7 Hz, 2H), 1.28 (s, 12H). ¹¹B NMR (96 MHz, CD₃CN) δ ppm 2.49 (q, *J* = 45.0 Hz, 1B), ¹⁹F NMR (282 MHz, CD₃CN) δ ppm -102.7 (br. s.), -136.0 (m.).

The crude product (1.97 g) was stirred with dry CH₃CN and filtered. The CH₃CN was removed from the solution by a rotary evaporator, to give a white solid, which was then dried in Abderhaldron's drying pistol to give 1.01 g of purer **17a** (100:3 by ¹H NMR) Mp of this solid is not available, for it starts to decompose above 220 °C.

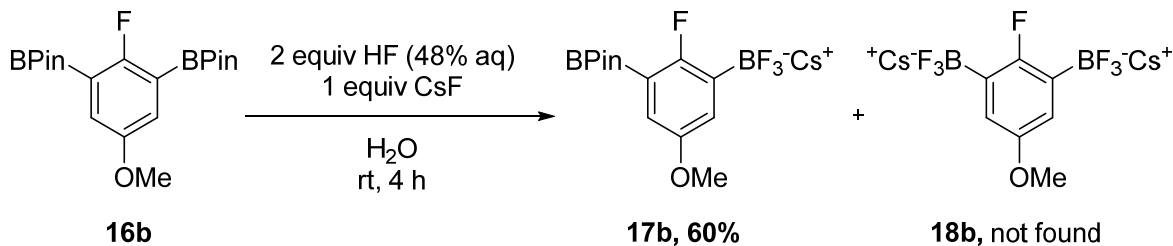
3.2.2 Desymmetrizing 2,2'-(5-methoxy-2-fluoro-1,3-phenylene)bis(BPin)

Table 12. Desymmetrizing 2,2'-(5-methoxy-2-fluoro-1,3-phenylene)bis(BPin)



entry	solvent	17b	18b
1	Et ₂ O	15%	33%
2	THF	24%	28%
3	hexanes	0	44%

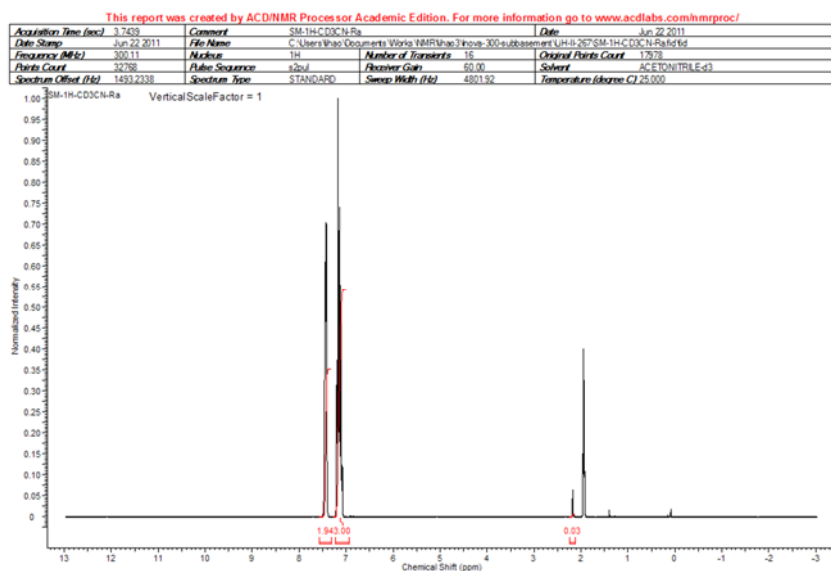
Figure 81. Desymmetrizing 2,2'-(5-methoxy-2-fluoro-1,3-phenylene)bis(BPin) in water



When **16b** was treated by the same procedure, the reaction favored the undesired di-salt **18b**. We then tried to run the reaction with different organic solvents, reasoning that the solubility of **17b** might play a role in promoting or suppressing formation of **18b**. The results are summarized in **Table 13**. At first, we anticipated that in a less polar solvent, **17b** might precipitate faster and thus reduce the chance of further fluorinated into **18b**. However, the experiments showed absolutely the opposite selectivity trend, with THF giving slightly better selectivity and hexanes giving only **18b**. These results suggest, once the (PinB)Ar(BF₂•HF) intermediate forms, the higher concentration of Cs⁺ helps the precipitation of **17b** and preventing formation of **18b**. Based on this argument, we tested the reaction without organic solvent (**Figure 81**). Compound **16b** (3.78 g, 10

mmol) and CsF (1.52 g, 10 mmol) was weighed into a Teflon flask fitted with a stir bar, and 20 mL of deionized water was added. HF (830 mg, 48% aq. 20 mmol) was weighed in a plastic syringe and added to the flask dropwise. The mixture was stirred at room temperature for 4 h, giving a white solid. This solid was then transferred to a glass flask with help of CH₃CN. Water was removed by azeotropy with CH₃CN. The dried solid was washed by 100 mL of hot and dry CH₃CN 3 times and the liquid phases were filtered out and combined. CH₃CN was removed on a rotary evaporator to give a white solid, which was then washed by 150 mL hot hexanes to give pure **17b** 2.71g 60% yield. Compound **17b**: ¹H NMR (500 MHz, DMSO-*d*₆) δ ppm 6.96 (t, *J* = 3.9 Hz, 1H) 6.76 (t, *J* = 3.7 Hz, 1H) 3.66 (s, 3H) 1.27 (s, 12H) ¹³C NMR (126 MHz, DMSO-*d*₆) δ ppm 164.4 (d, *J* = 239.7 Hz) 153.8 123.3 (d, *J* = 14.8 Hz) 116.5 (d, *J* = 8.4 Hz), 83.0, 55.1, 24.6.

Figure 82. ¹H NMR of PhBF₃Cs in CD₃CN

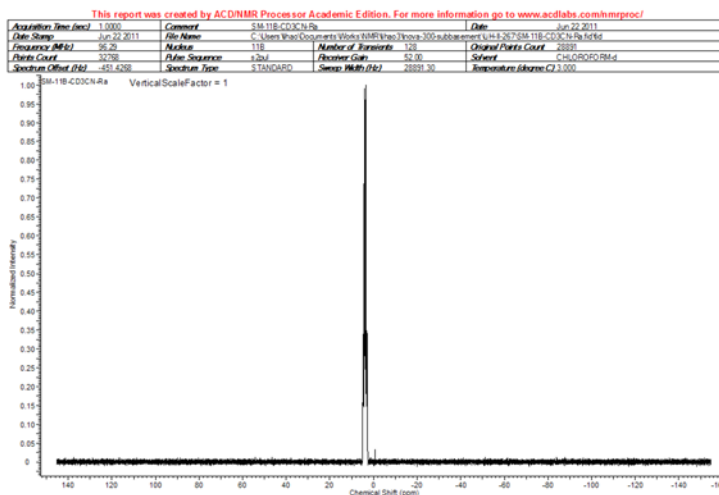


3.3 Synthesis of the (PinB)Ar(BMida).

We tested the protection conditions by using PhBF₃Cs. PhBF₃Cs was dried in an Abderhalden's drying pistol and CD₃CN was distilled over P₂O₅. PhBF₃Cs (29 mg, 0.1 mmol) was dissolved in 1 mL CD₃CN in a nitrogen glove box and transferred into an NMR tube that was sealed by a rubber

cap. NMRs were taken, showing the pure starting material with a trace water. ^{11}B NMR showed the ArBF_3^- at 3.9 ppm as a quartet with $J = 55$ Hz, resulting from coupling with the 3F's and the rigid tetrahedron structure. By ^{19}F NMR, the ArBF_3^- was observed at -136.8 ppm as quartet with $J = 55$ Hz, resulting from coupling with the B, as illustrated in **Figures 82, 83** and **84**.

Figure 83. ^{11}B NMR of PhBF_3Cs in CD_3CN



With the NMR data of the starting material secure, we next set out to establish the ability of TMSCl to activate the ArBF_3 salts. Toward this end, TMSCl (distilled over CaH_2 , 12.5 μL , 0.1 mmol) was injected through a micro syringe. CsCl precipitations started to form and 30 min later we observed formation of TMSF (-157 ppm, m) and a chemical shift change in the ^{11}B and ^{19}F NMR's. By ^{11}B NMR, the quartet at 3.9 ppm was gone, instead, we saw a broad singlet at 12.8 ppm, suggesting a relaxed planar B center, as illustrated in **Figure 85**.

Figure 84. ^{19}F NMR of PhBF_3Cs in CD_3CN

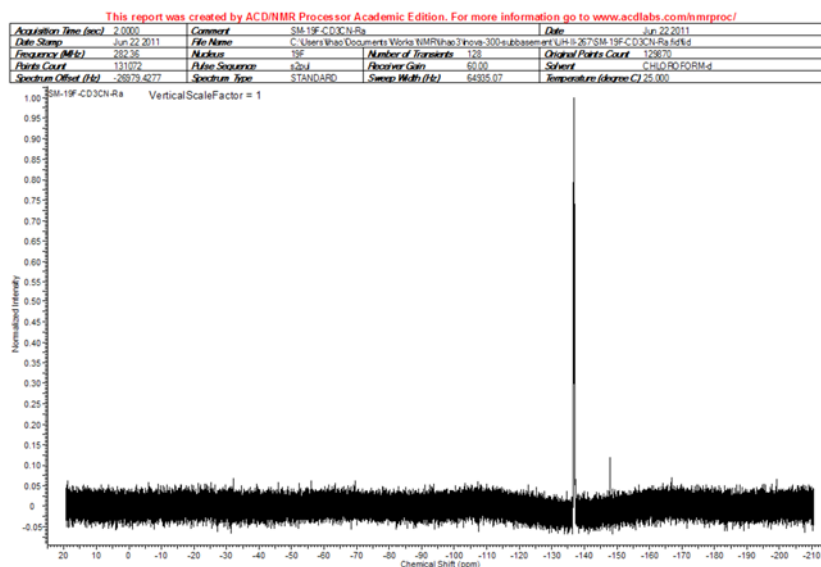
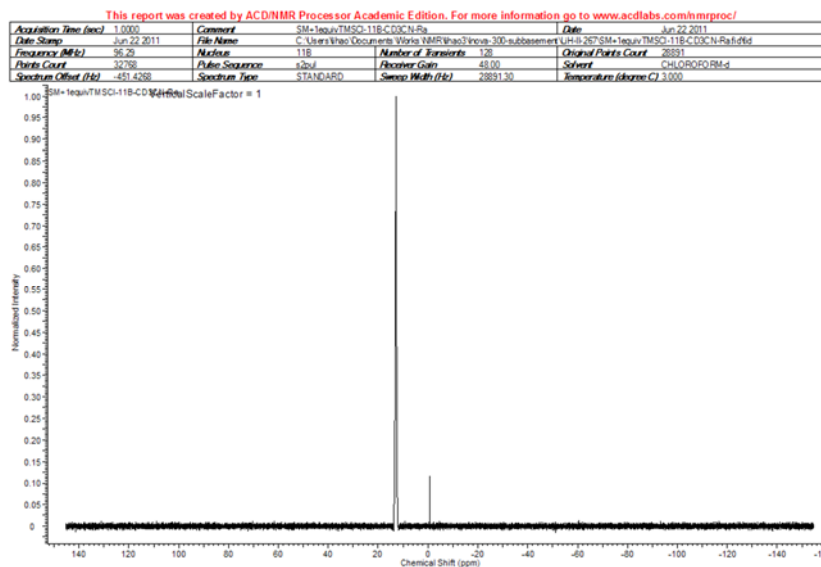


Figure 85. ^{11}B NMR after adding 1 equiv TMSCl



By ^{19}F NMR, we observed formation of TMSF , and PhBF_2 , as illustrated in **Figure 86**, PhBF_3Cs still existed. So, another dose of TMSCl ($12.5 \mu\text{L}$, 0.1 mmol) was injected, and by ^{11}B NMR, we observed that the boron peak shifted further down field to 14.5 ppm , as shown in **Figure 87**. By ^{19}F NMR, we observed a broad single peak at -116.5 ppm that integrated into two fluorines if the TMSF (-155 ppm) was normalized as one fluorine, as shown in **Figure 88**.

Figure 86. ^{19}F NMR after adding 1 equiv TMSCl

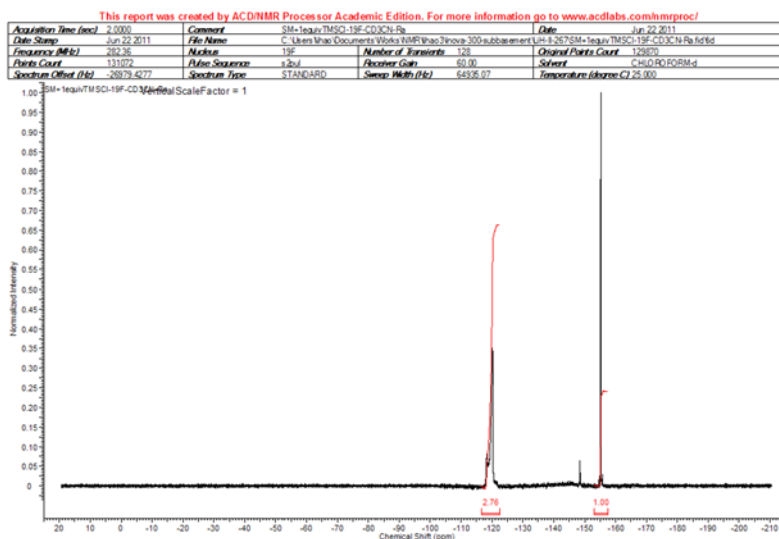
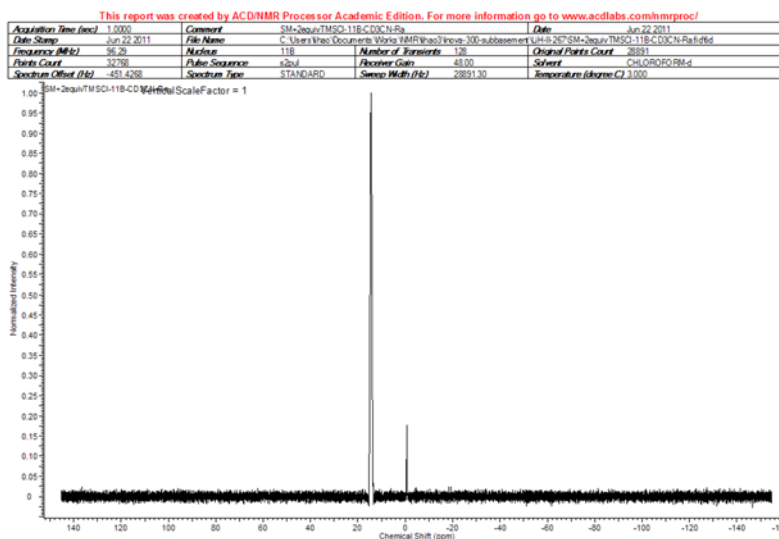
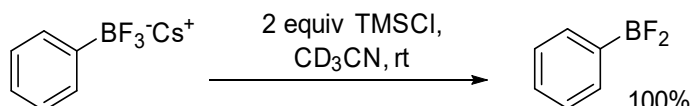


Figure 87. ^{11}B NMR after adding 2 equiv TMSCl



Our conclusion based on these NMR data was that by treatment with TMSCl, the ArBF_3Cs salt lost one fluorine to give ArBF_2 . Two equiv of TMSCl is enough to push the equilibrium to the end, as illustrated in Figure 88. Activation of the ArBF_3Cs by TMSCl was successful.

Figure 88. Activation of PhBF_3Cs by TMSCl



The clear liquid phase of this NMR sample was transferred by a syringe with long needle and injected into a flask charged with Na₂Mida (19 mg, 0.1 mmol) and a stir bar. The mixture was stirred at room temperature for 6 h, and was then transferred back into another NMR tube. Only open chain Mida ligand was observed, but the PhBF₂ species remained largely untouched with a small amount of PhBF₃⁻ “revived”. We proposed a possible mechanism in **Figure 89**.

Figure 89. Formation of PhBF₃⁻ after adding Na₂Mida

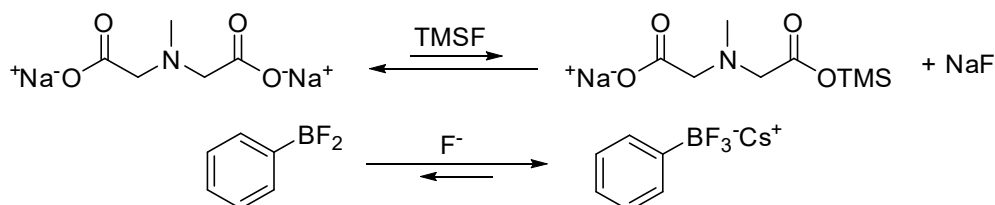


Figure 90. Protection of PhBF₂ by Mida ligand in DMSO

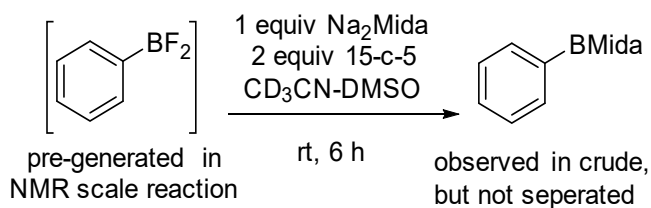
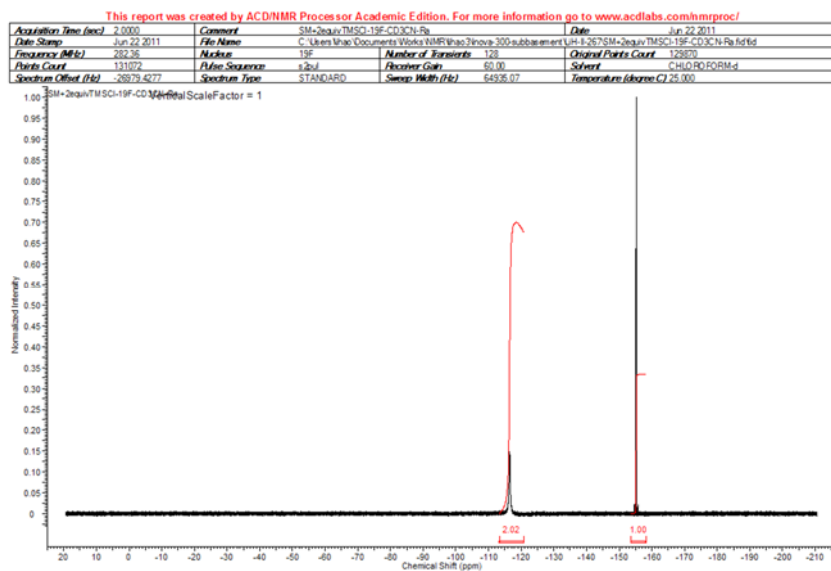
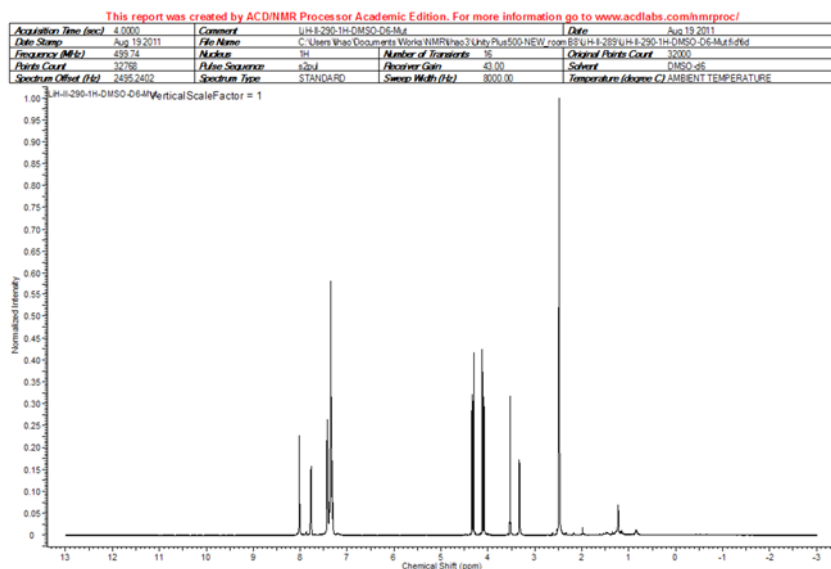


Figure 91. ¹⁹F NMR after adding 2 equiv TMSCl



The same reaction was repeated several times, resulting in the same observation. At first, we thought the poor solubility of Na₂Mida in CH₃CN might be the possible problem. We decided to use a combination of dry DMSO and 15-c-5 to help the process. We performed the formation of PhBF₂ as elaborated above in an NMR tube and monitored the process by NMR. The clear liquid phase of the NMR reaction was transferred into a flask charged with Na₂Mida (19 mg, 0.1 mmol), and 15-c-5 (40 μL, 0.2 mmol) dissolved in 1 mL of DMSO (dry) and a stir bar. The reaction was stirred at room temperature (**Figure 88**). After 6 hours, the solvent of the reaction was removed by vacuum distillation and NMR spectra of the 12 mg residue were collected in DMSO-*d*₆. By ¹H NMR of the crude material, two peaks at 4.32 ppm and 4.09 ppm integrated into two protons each, and demonstrated ²J H-H coupling 17 Hz, which is a finger print of –BMida group. By ¹¹B NMR, a major peak was observed at 12 ppm marching the –BMida group, as illustrated (**Figures 91 and 92**).

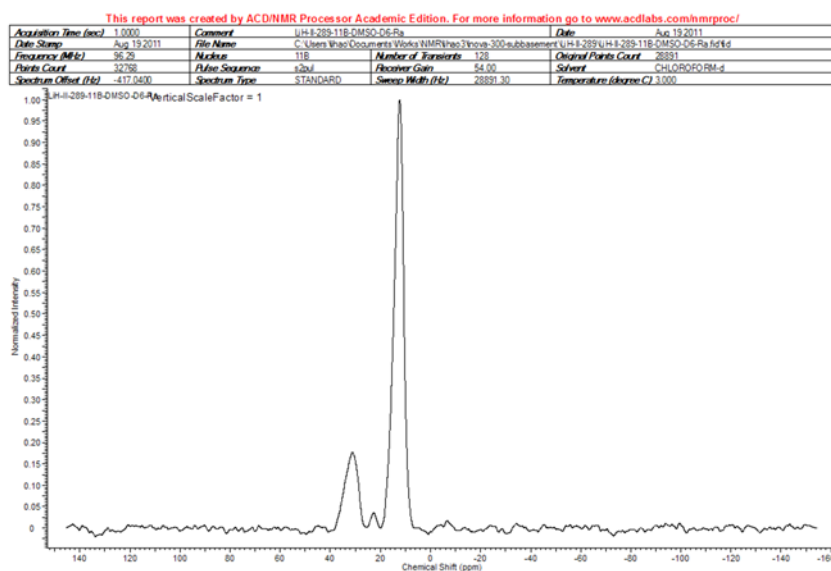
Figure 92. ¹H NMR of the crude product of Figure 90 in DMSO-*d*₆



Encouraged by these results, we decided to follow the protections steps by NMR. We set up an experiment where PhBF₂ was pre-generated in the same way as elaborated above. The clear liquid

phase of the NMR sample was then transferred into another NMR tube charge with Na₂Mida (19 mg, 0.1 mmol), and 15-c-5 (40 μL, 0.2 mmol) dissolved in 1 mL of DMSO-d₆ (dry). As expected, we observed formation of PhBF₃⁻ by both ¹¹B and ¹⁹F NMR, presumably via the mechanism proposed in **Figure 89**. After 1 h at room temperature, however we did not observe any formation of desired PhBMida. Dissappointed, we stopped the experiment, and distilled out all solvents and volatiles, to obtain about 11 mg residue. We dissolved this residue in DMSO-*d*₆, to see if we got the PhBF₃M. Strikingly, the ¹H and ¹¹B NMRs suggested that the residue was that of almost pure PhBMida. So the problem was solved: The 10-15 min of heating during the distillation of DMSO promoted the reaction!

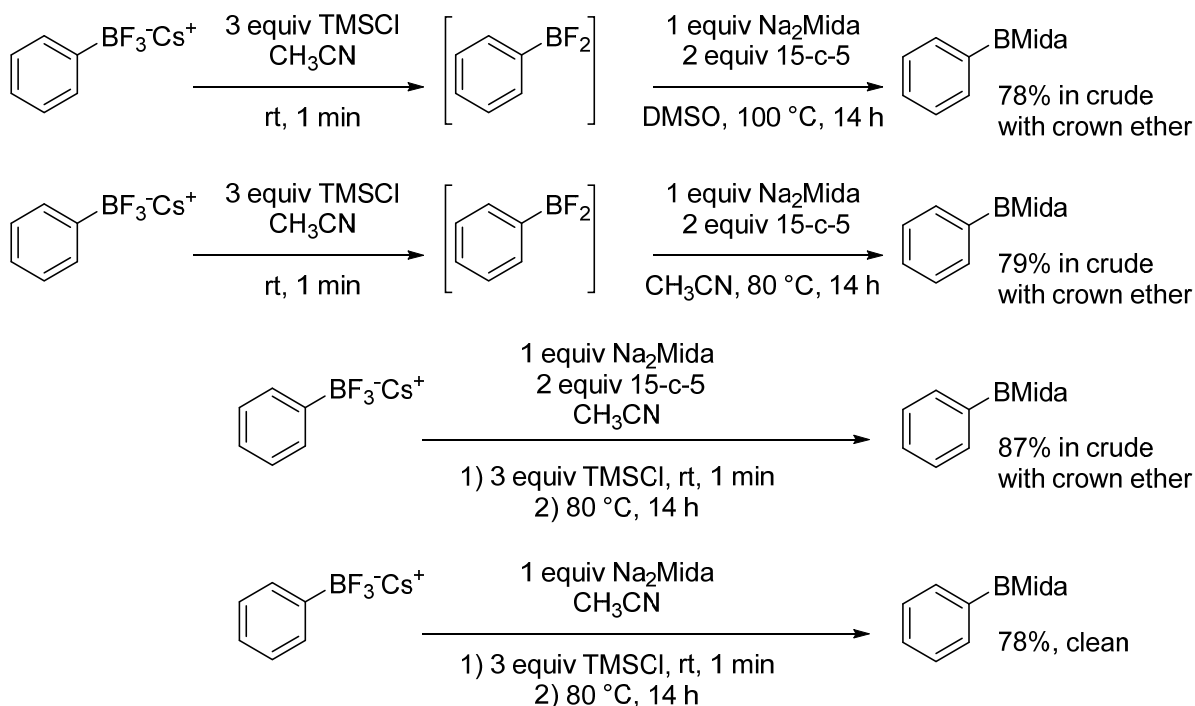
Figure 93. ¹¹B NMR of the crude product of **Figure 90** in DMSO-*d*₆



To confirm this finding, we performed a small scale transformation of PhBF₃Cs to PhBMida: In a 25 mL round bottom flask (A), PhBF₃Cs (28 mg, 0.1 mmol) was dissolved in 1 mL dry CH₃CN. In a 25 mL round bottom flask (B), and Na₂Mida (19 mg, 0.1 mmol), 15-c-5 (40 μL, 0.2 mmol) were dissolved in 1 mL of dry DMSO. To flask A, TMSCl (distilled, 38 μL, 0.3 mmol) was injected and swirled for 1 min. The clear liquid phase of flask A was then cannulated into flask B. A white

solid formation was observed. Flask B was the attached to a condenser and then heated in an oil bath at 100 °C under nitrogen, for 14 h. The reaction crude was distilled under vacuum to remove DMSO and the residue was partitioned between water and EtOAc. The organic phases were dried over Na₂SO₄. Removal of EtOAc on a rotary evaporator gave 18 mg of residue. By NMR a 10:4 mixture of desired PhBMida and the crown ether (about 78% yield in crude materials) were observed. This reaction was successful and relatively clean, as shown in **Figure 94**. We further optimized the reaction conditions. Using CH₃CN as solvent for second step gave a crude product yield of 79% contaminated by crown ether. Running the reaction in one-pot gave a crude product yield of 87% also contaminated by crown ether. Performing the one-pot transformation without crown ether gave 78% of clean product without column purification.

Figure 94. Optimization of the reaction conditions



We thereby applied the optimized conditions to **17a** as shown in **Figure 95**. The reaction gave a complex mixture, and no desired product was found in the crude. We rolled back to a stepwise reaction, as shown in **Figure 96**.

Figure 95. Attempted transformation of 17a

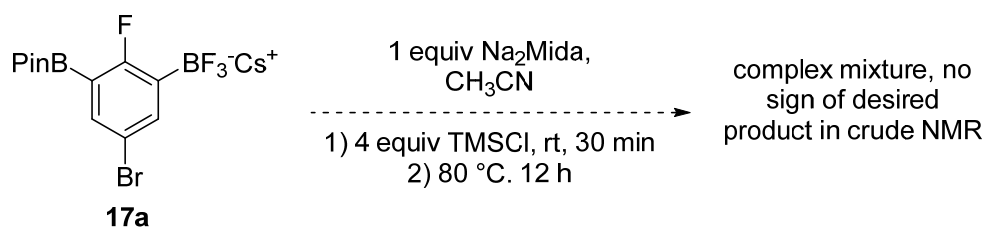
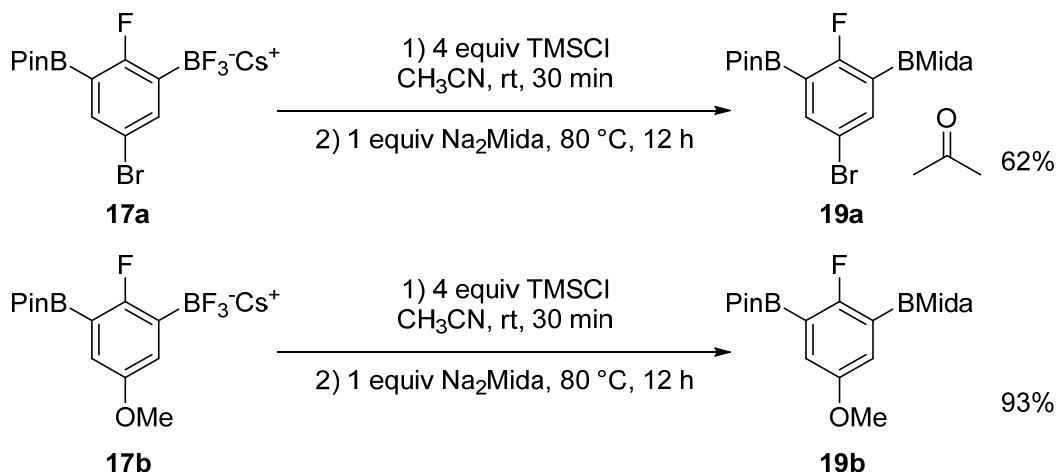


Figure 96. Stepwise transformation of 17a and 17b



Synthesis of compound **19a** (**Figure 94** reaction 1): In a nitrogen glove box, compound **17a** (dried, 500 mg, 1.00 mmol) was weighed into a 20 mL vial fitted with a stir bar. The substrate was dissolved in 5 mL dry CH₃CN. The vial was then sealed by a rubber septum. Na₂Mida (dry, 191 mg, 1.00 mmol) was weighed into a 50 mL round bottom flask fitted with a stir bar and capped by a rubber septum. Outside the glove box, to the vial with **17a** dissolved in CH₃CN, TMSCl (freshly distilled, 0.50 mL, 4.0 mmol) was injected, and the mixture was stirred at room temperature for 30 min. Then the slurry was then entirely cannulaed into the round bottom flask with Na₂Mida. The

flask was then attached to a condenser and the mixture was stirred at room temperature under nitrogen for 5 min, and then heated in an oil bath at 80 °C for 12 h. The resulting slurry was filtered, and the solids was washed by CH₃CN. The combined solution phases was evaporated on a rotary evaporator to give a crude material. The crude material was then passed through a silica gel short plug by EtOAc and solvent was removed to give pure product. The product was transferred by acetone to into a 20 mL vial to be finally pumped dry, resulting in an adduct of the desired product with one acetone molecule. Unsuccessful attempts to remove the acetone including column separation lead to some loss of the product, giving 318 mg, 62% yield, as a white solid, decomposes above 250 °C. Compound **19a**: ¹H NMR (600 MHz, CD₃CN) δ ppm 7.76 - 7.81 (m, 2H), 4.14 (dd, *J* = 17.1, 1.3 Hz, 2H), 3.95 (d, *J* = 17.4 Hz, 2H), 2.68 (s, 3H), 2.09 (s, 6H), 1.33 (s, 12H). ¹³C NMR (151 MHz, CD₃CN) δ ppm 207.9, 170.5 (d, *J* = 246.2 Hz) 169.5, 142.1 (d, *J* = 10.4 Hz) 141.7 (d, *J* = 9.8 Hz) 118.1 (d, *J* = 2.3 Hz) 85.7, 64.2 (d, *J* = 2.9 Hz) 31.3, 25.5. Consistent with Smith group's previous NMR data.

Synthesis of compound **19b** (**Figure 94** reaction 2): In a nitrogen glove box, compound **17b** (dried, 45 mg, 0.1 mmol) was weighed into a 20 mL vial fitted with a stir bar. The substrate was dissolved in 5 mL dry CH₃CN. The vial was then sealed by a rubber septum. Na₂Mida (dry, 191 mg, 1.00 mmol) was weighed into a 50 ml round bottom flask fitted with a stir bar and capped by a rubber septum. Outside the glove box, to the vial with **17a** dissolved in CH₃CN, TMSCl (freshly distilled, 0.50 mL, 4.0 mmol) was injected, and the mixture was stirred at room temperature for 30 min. Then the slurry was then entirely cannulaed into the round bottom flask with Na₂Mida. The flask was then attached to a condenser and the mixture was stirred at room temperature under nitrogen for 5 min, and then heated in an oil bath at 80 °C for 12 h. The resulting slurry was filtered, and the solids was washed by CH₃CN. The combined solution phases was evaporated on a rotary

evaporator to give a crude material. The crude material was then passed through a silica gel short plug by EtOAc and solvent was removed to give pure product. The substrate was dissolved in 5 mL dry CH₃CN. The vial was then sealed by a rubber septum. Na₂Mida (dry, 191 mg, 1.00 mmol) was weighed into a 50 ml round bottom flask fitted with a stir bar and capped by a rubber septum. Outside the glove box, to the vial with **17a** dissolved in CH₃CN, TMSCl (freshly distilled, 0.50 mL, 4.0 mmol) was injected, and the mixture was stirred at room temperature for 30 min. Then the slurry was then entirely cannulaed into the round bottom flask with Na₂Mida. The flask was then attached to a condenser and the mixture was stirred at room temperature under nitrogen for 5 min, and then heated in an oil bath at 80 °C for 12 h. The resulting slurry was filtered, and the solids was washed by CH₃CN. The combined solution phases was evaporated on a rotary evaporator to give a crude material. The crude material was then passed through a silica gel short plug by EtOAc and solvent was removed to give pure product. The product was transferred by CH₃CN to into a 20 mL vial to be finally pumped dry, afford 38 mg, 93% yield, as a white solid, decomposes above 250 °C. Compound **19b**: ¹H NMR (600 MHz, CD₃CN) δ ppm 7.13 - 7.25 (m, 2H) 4.13 (dd, *J* = 17.1, 1.3 Hz, 2H) 3.94 (d, *J* = 17.3 Hz, 2H) 3.78 (s, 3H) 2.66 (s, 3H) 1.32 (s, 12H). ¹¹B NMR (97 MHz, CD₃CN) δ ppm 30.9 (br. s., 1B) 11.6 (br. s., 1B), ¹³C NMR (151 MHz, CD₃CN) δ ppm 169.7, 165.7 (d, *J* = 237.5 Hz) 156.7, 124.8 (d, *J* = 9.9 Hz) 123.1 (d, *J* = 9.9 Hz) 85.3, 64.2 (d, *J* = 2.8 Hz) 56.7, 49.0 (d, *J* = 1.1 Hz) 25.5. ¹⁹F NMR (283 MHz, CD₃CN) δ ppm -105.4 (s)

3.4 Summary

In this project, we explored the potential of desymmetrizing Ar(BPin)₂, diboryl compounds, via a (PinB)Ar(BF₃CS) intermediate. We established and optimized the reaction conditions for the transformation from Ar(BPin)₂ to the (PinB)Ar(BF₃CS), minimizing the formation of undesired

bisalts $\text{Ar}(\text{BF}_3\text{Cs})_2$. Then we looked into the mechanism of the transformation from the PhBF_3M salt to the PhBMida compound, including the formation of the key intermediate PhBF_2 , and the protection of difluoroboryl by Mida ligand. We established and optimized a clean one-pot protocol for this transformation that does not require column purification to obtain the product with decent purity. We applied this method to $\text{Ar}(\text{BPin})_2$, finding it problematic. We then applied the method in a stepwise manner, leading to high yield of the clean product with high purity without the aid of column purification.

APPENDIX

NMR spectra

Figure 97 ^{119}Sn NMR of compound 2a

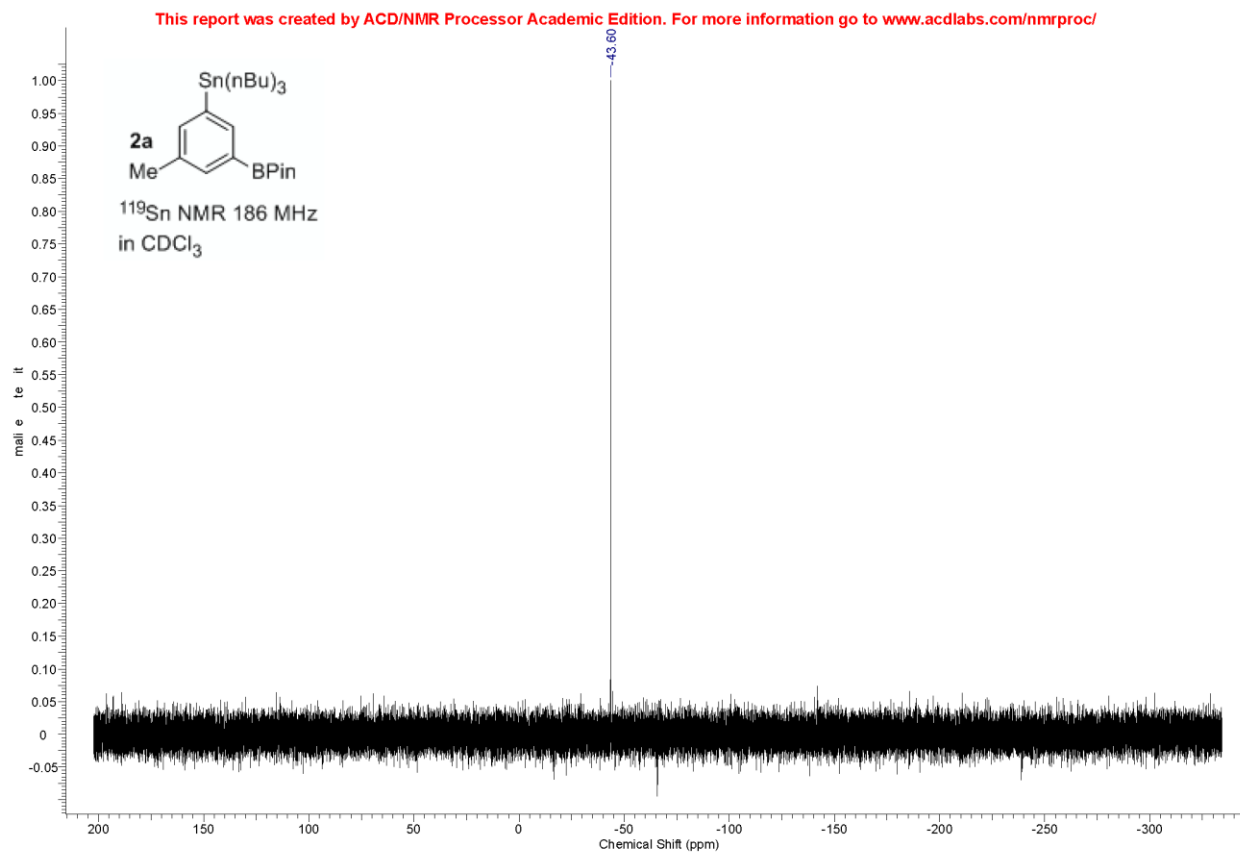


Figure 98 ^{11}B NMR of compound 2a

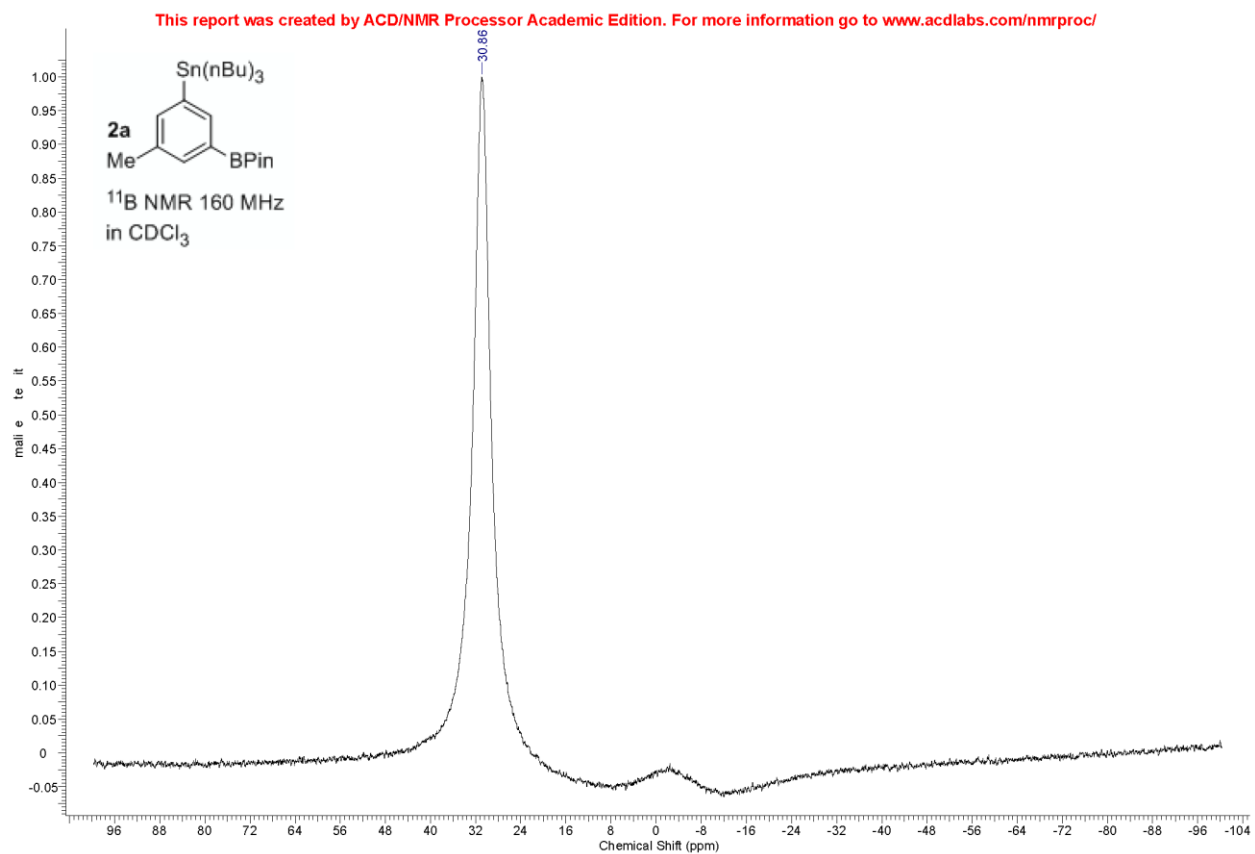


Figure 99 ^{13}C NMR of compound 2a

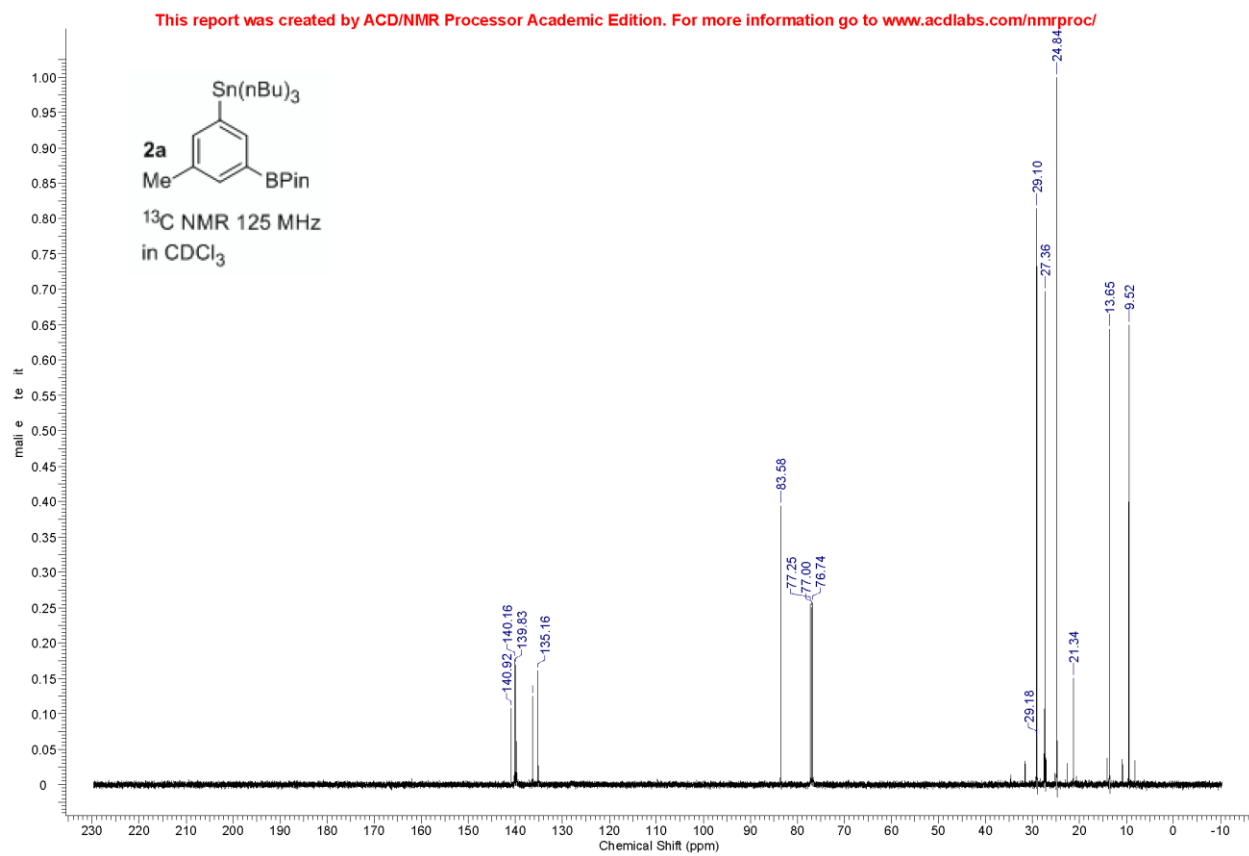


Figure 100 ^1H NMR of compound 2a

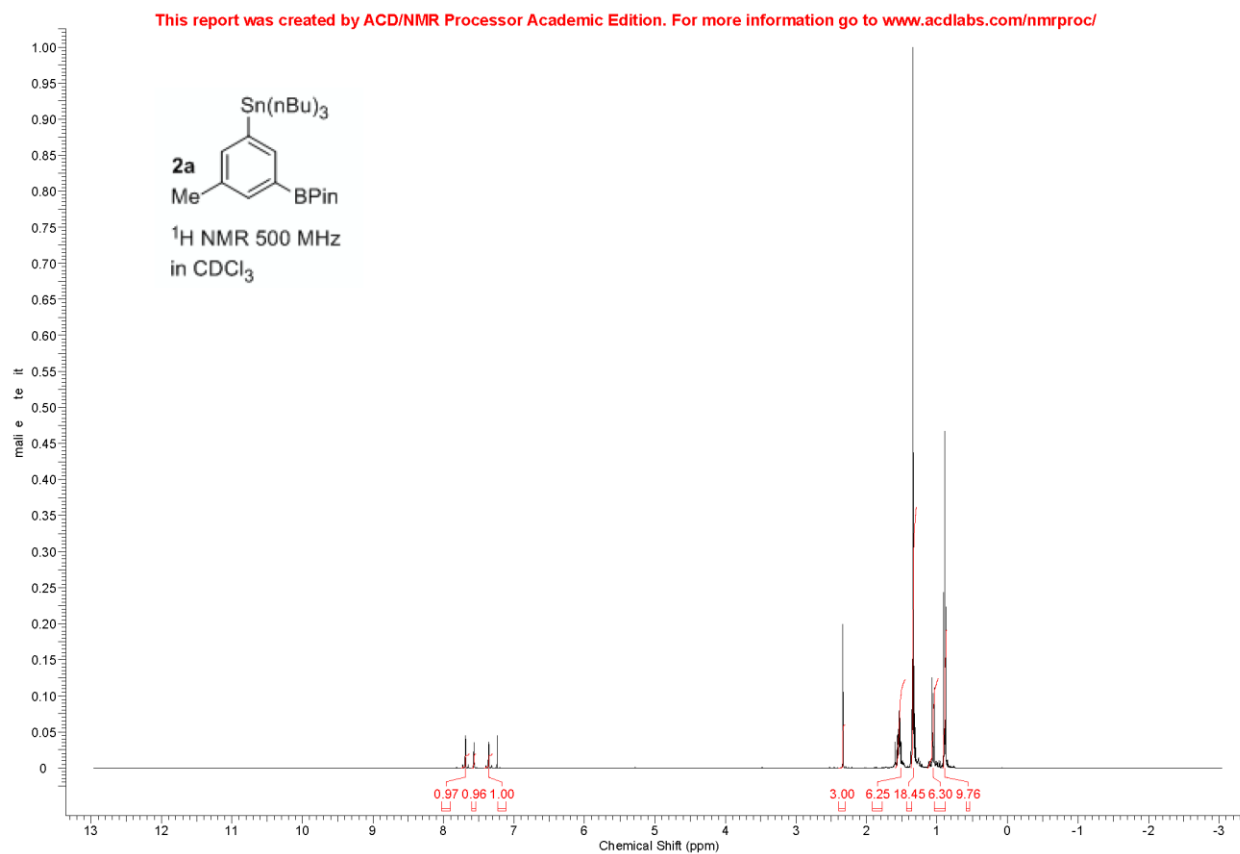


Figure 101 ^{119}Sn NMR of compound 2b

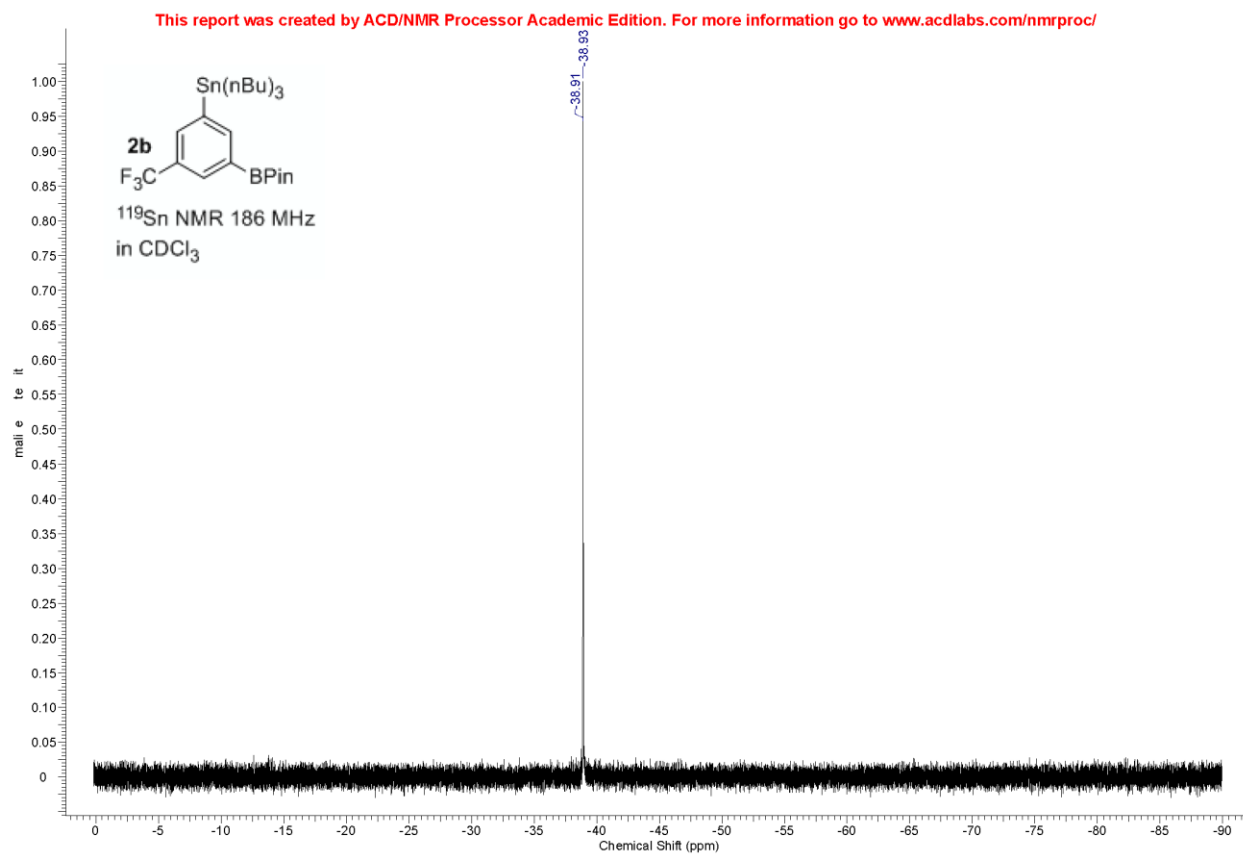


Figure 102 ^{11}B NMR of compound **2b**

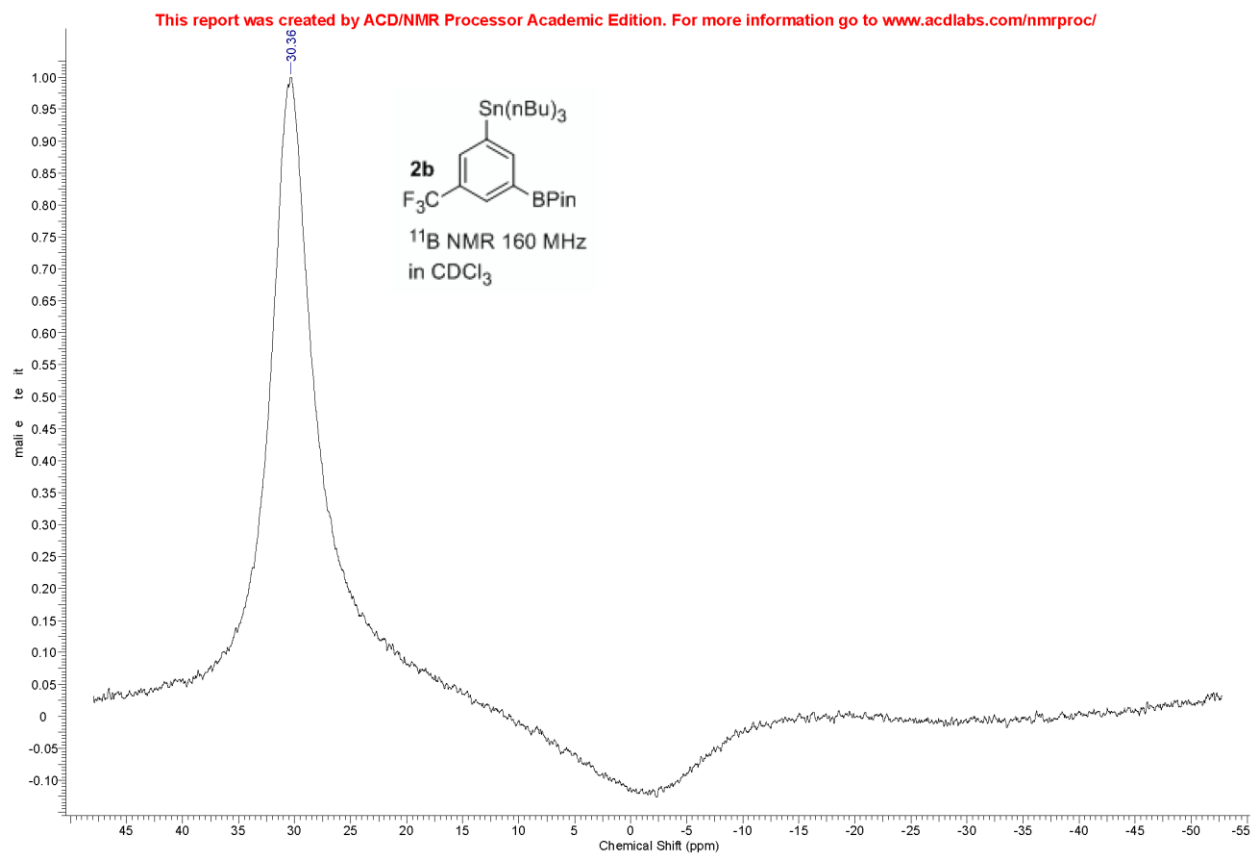


Figure 103 ^{13}C NMR of compound 2b

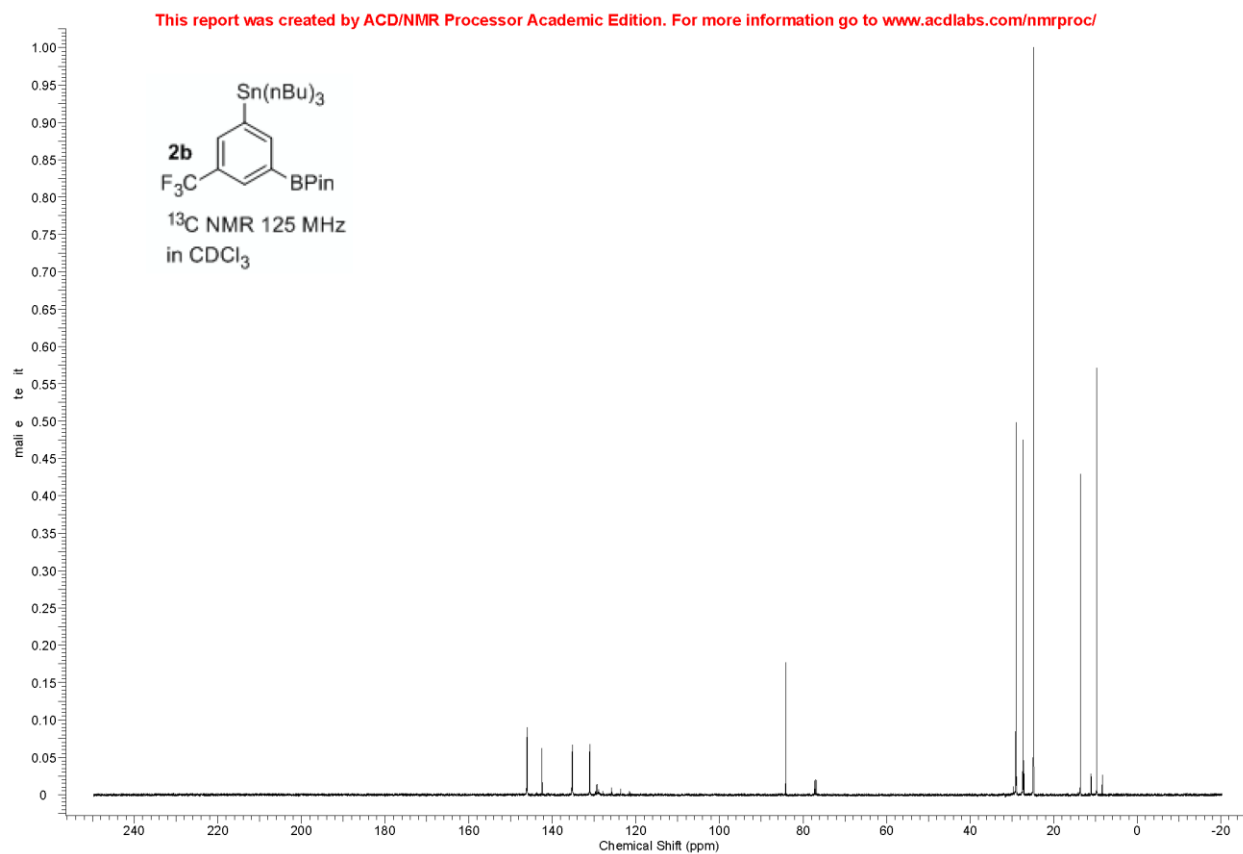


Figure 104 ^{19}F NMR of compound 2b

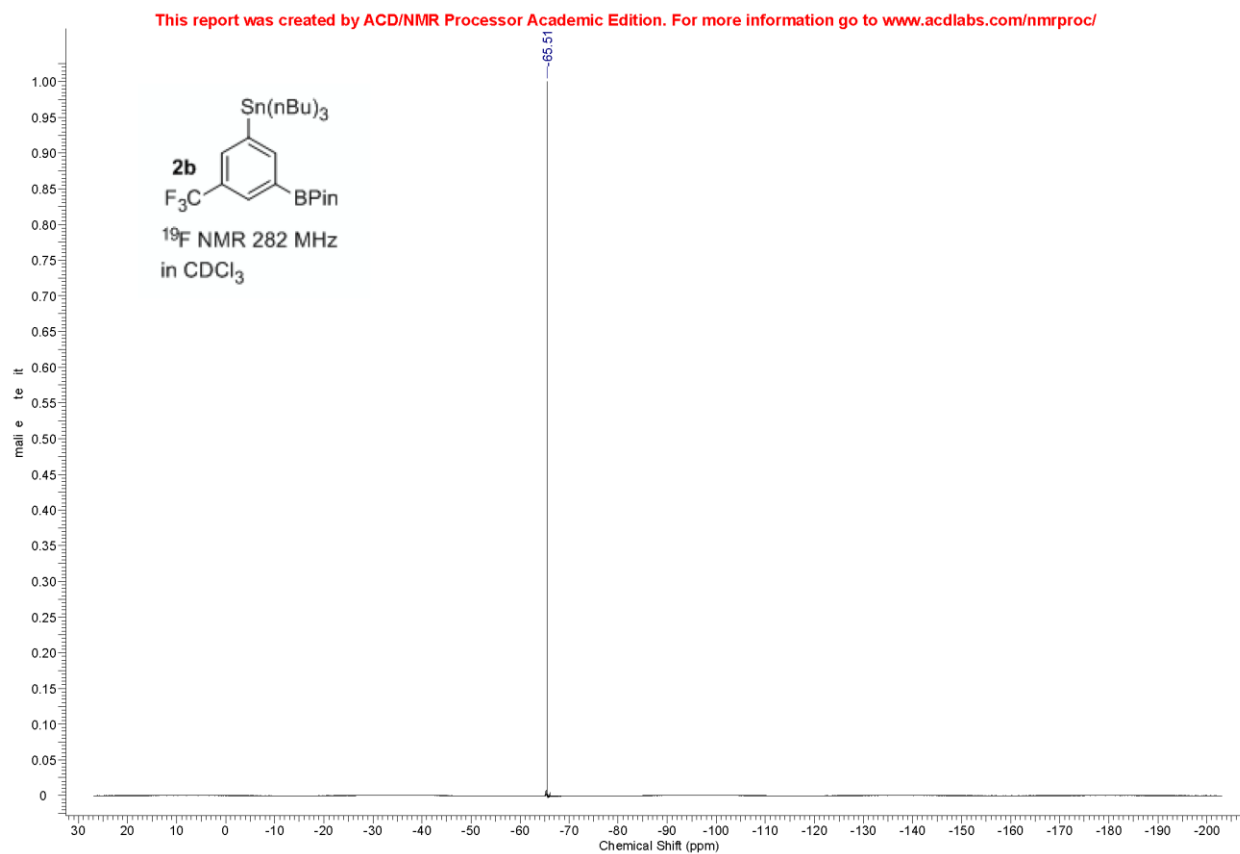


Figure 105 ^1H NMR of compound 2b

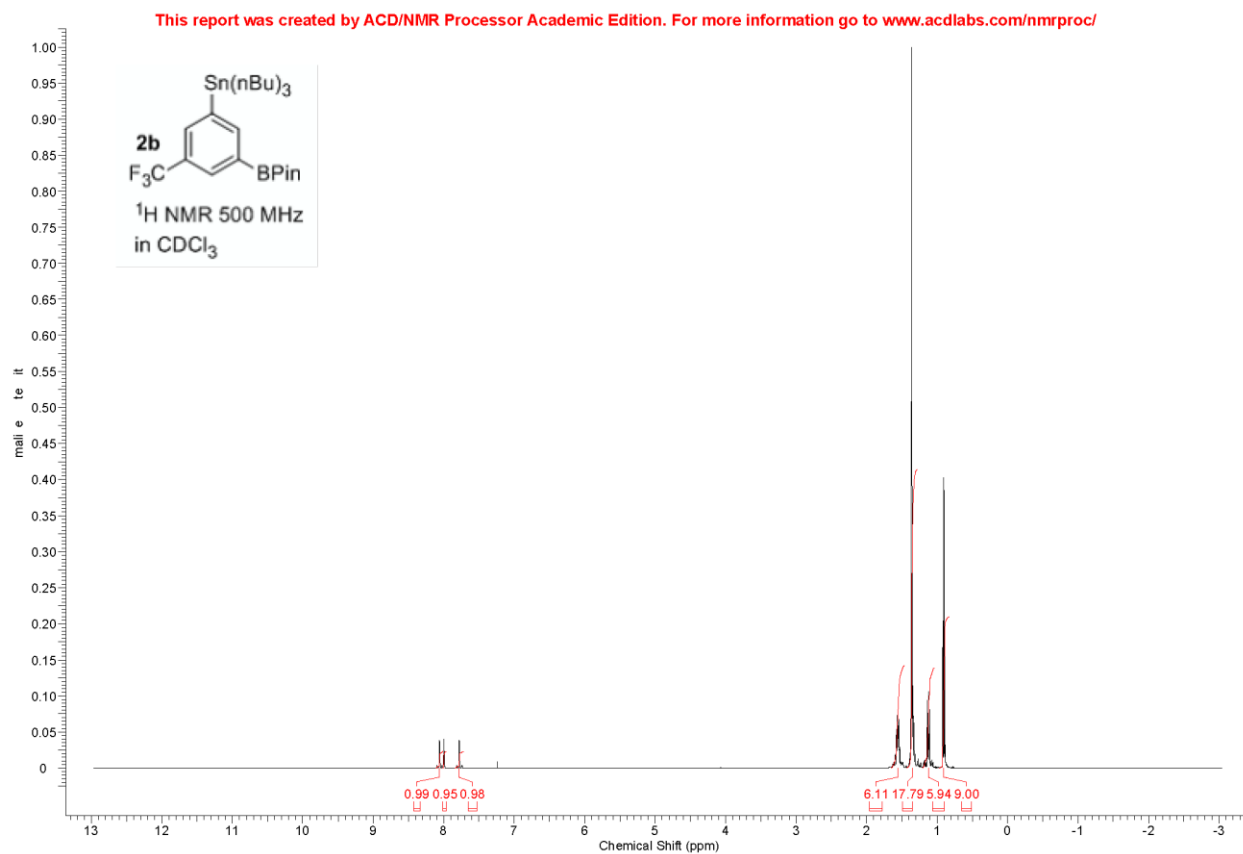


Figure 106 ^{119}Sn NMR of compound 2c

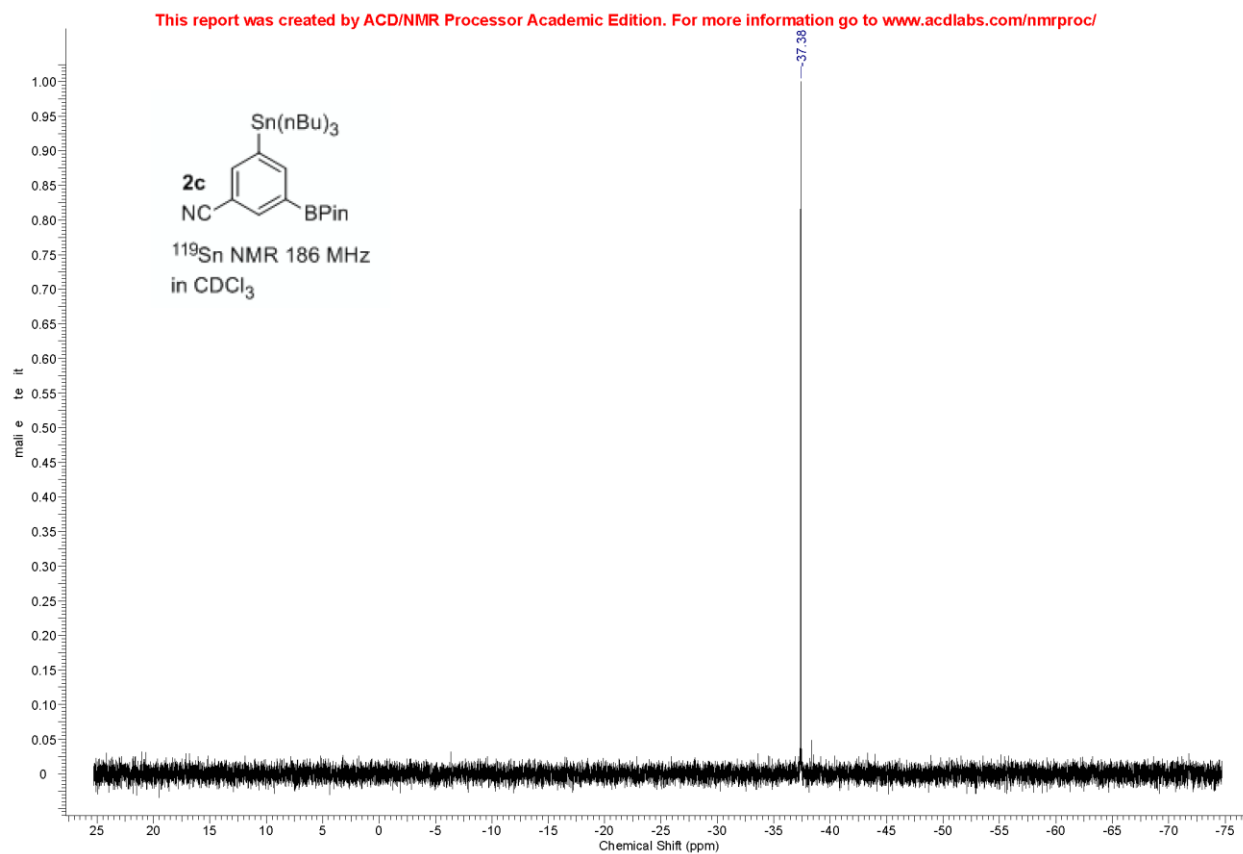


Figure 107 ^{11}B NMR of compound 2c

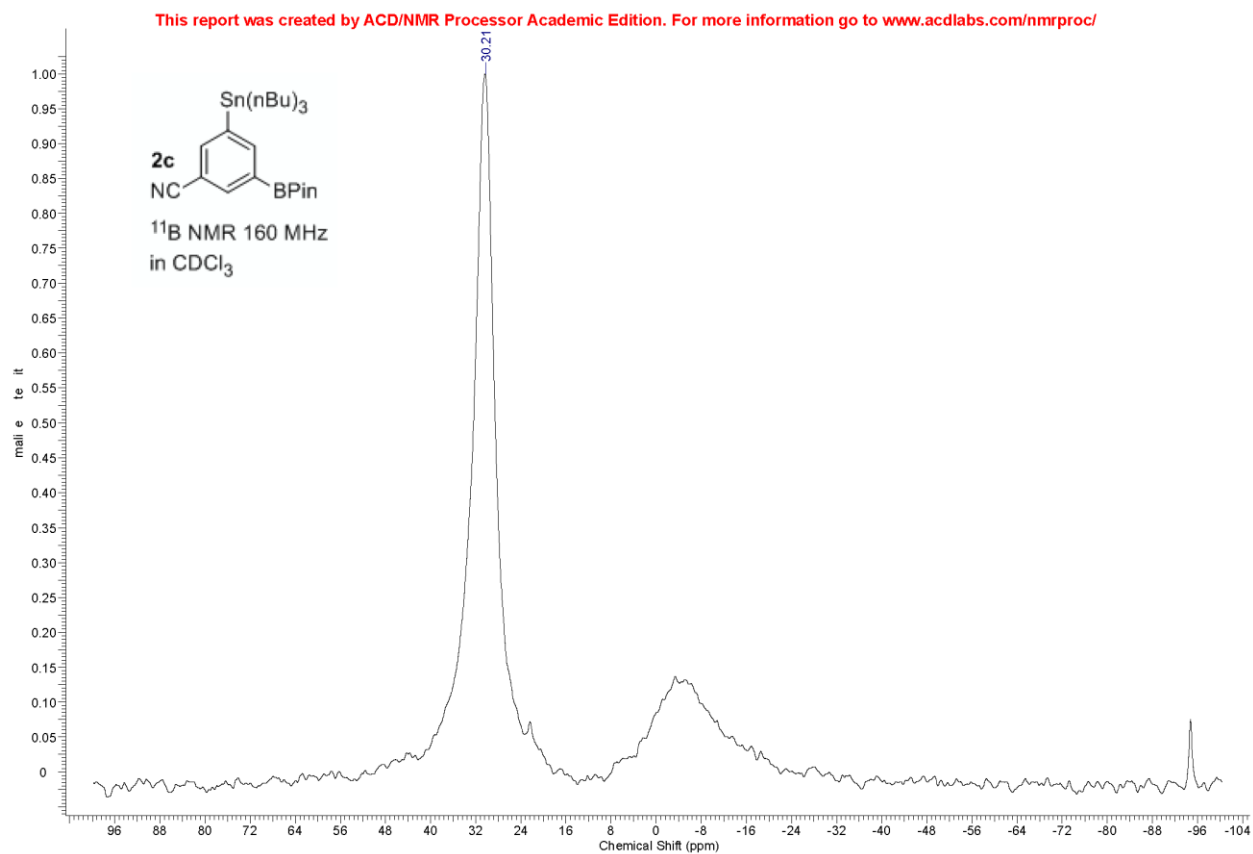


Figure 108 ^{13}C NMR of compound 2c

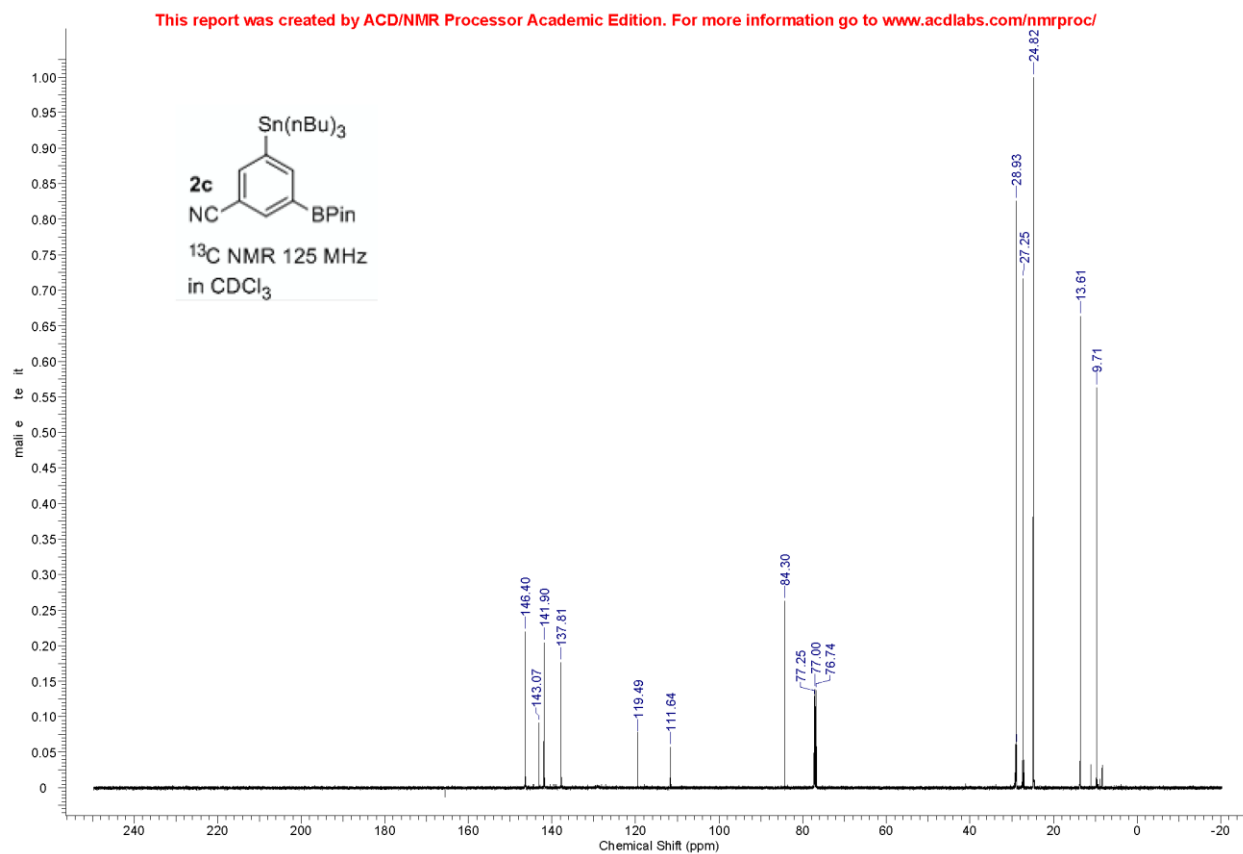


Figure 109 ^1H NMR of compound 2c

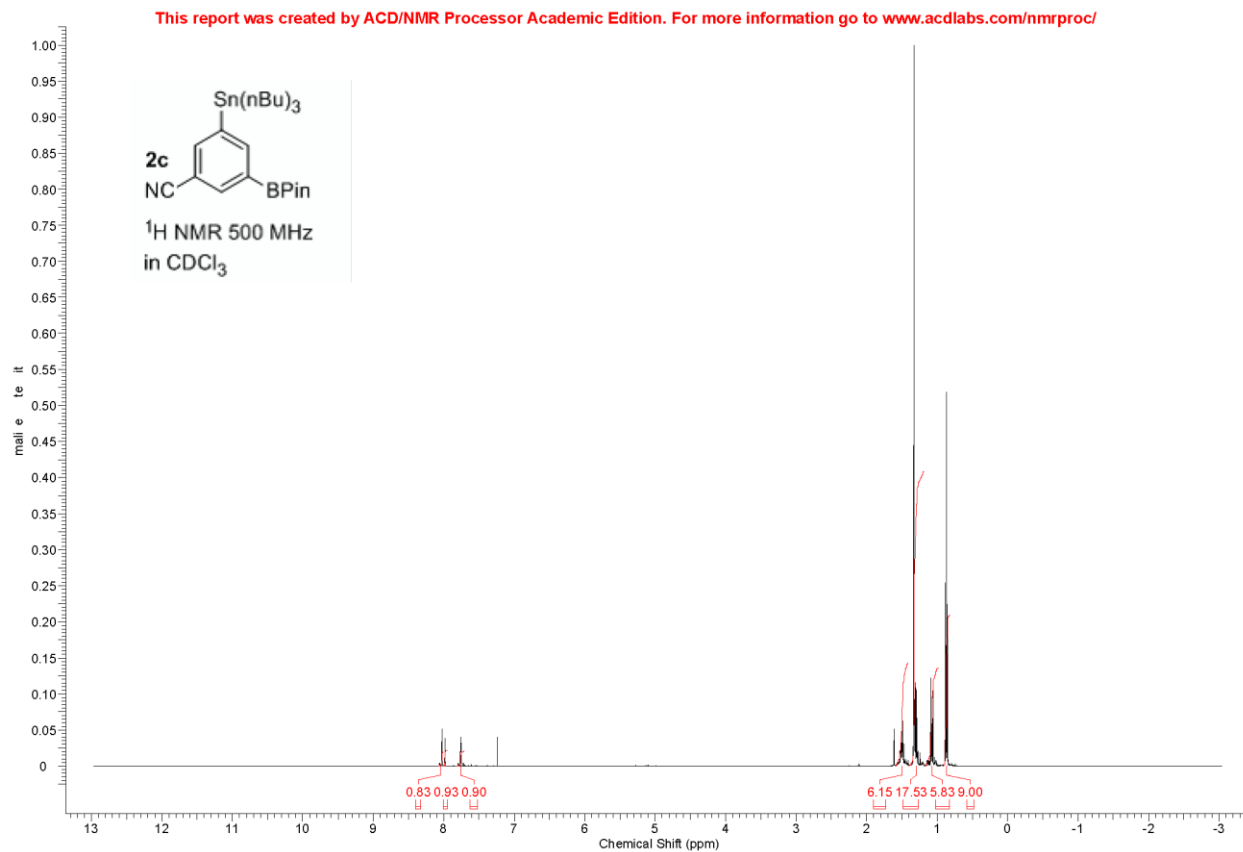


Figure 110 ^{119}Sn NMR of compound 2d

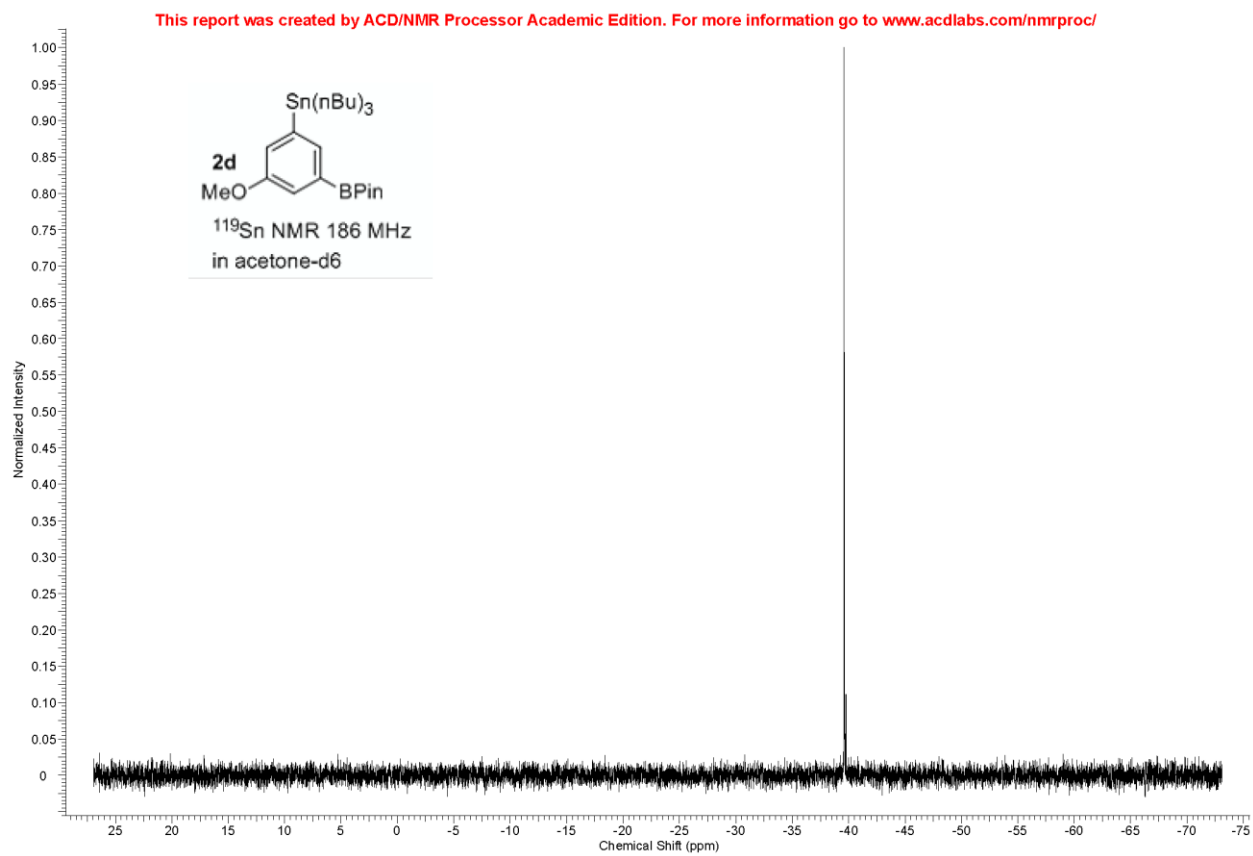


Figure 111 ^{11}B NMR of compound 2d

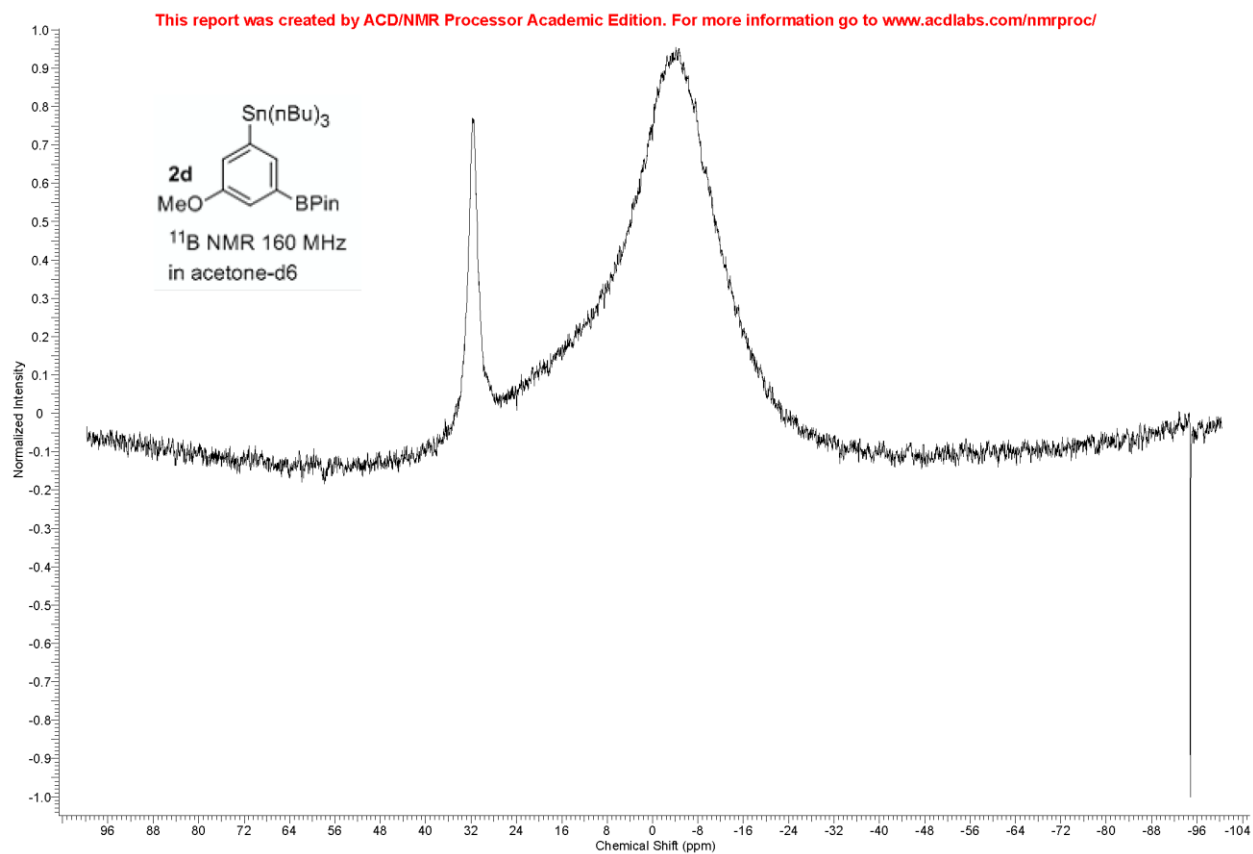


Figure 112 ^{13}C NMR of compound 2d

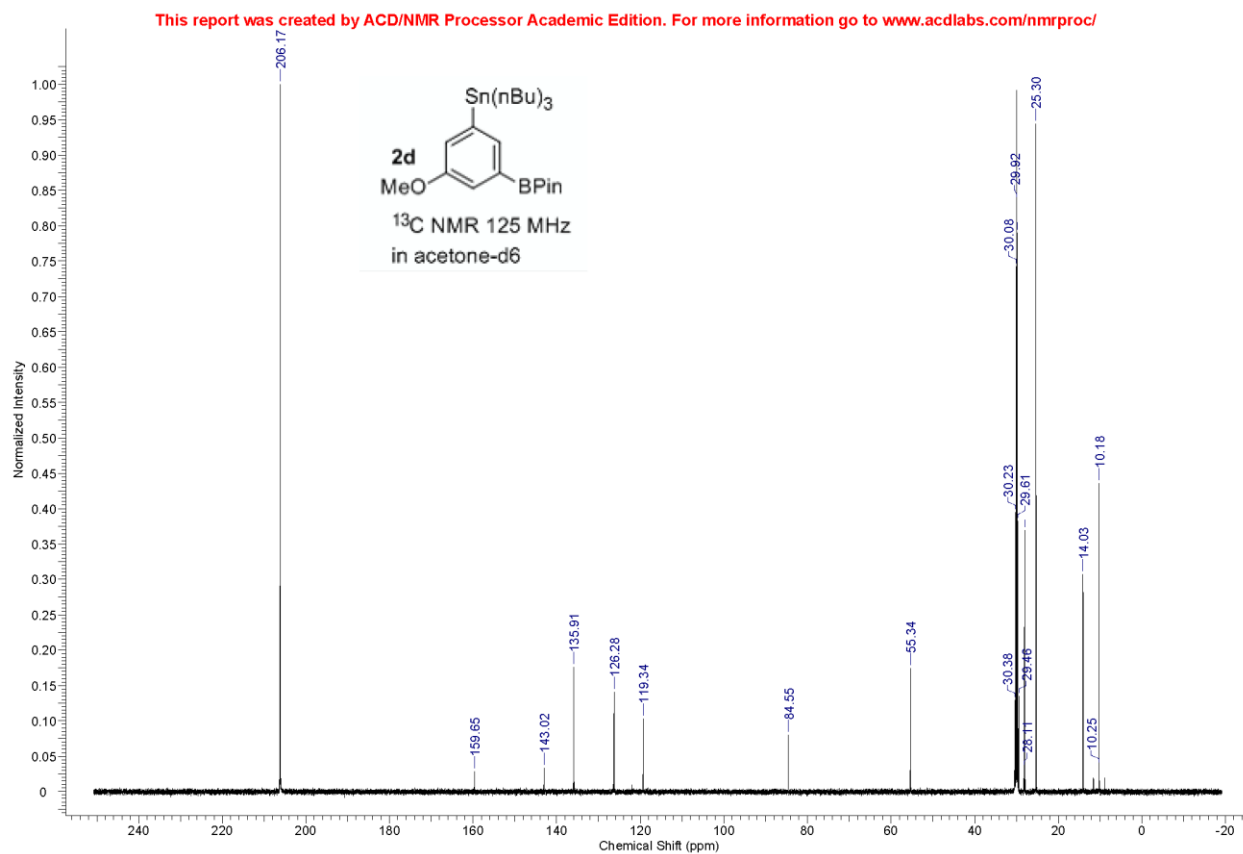


Figure 113 ^1H NMR of compound 2d

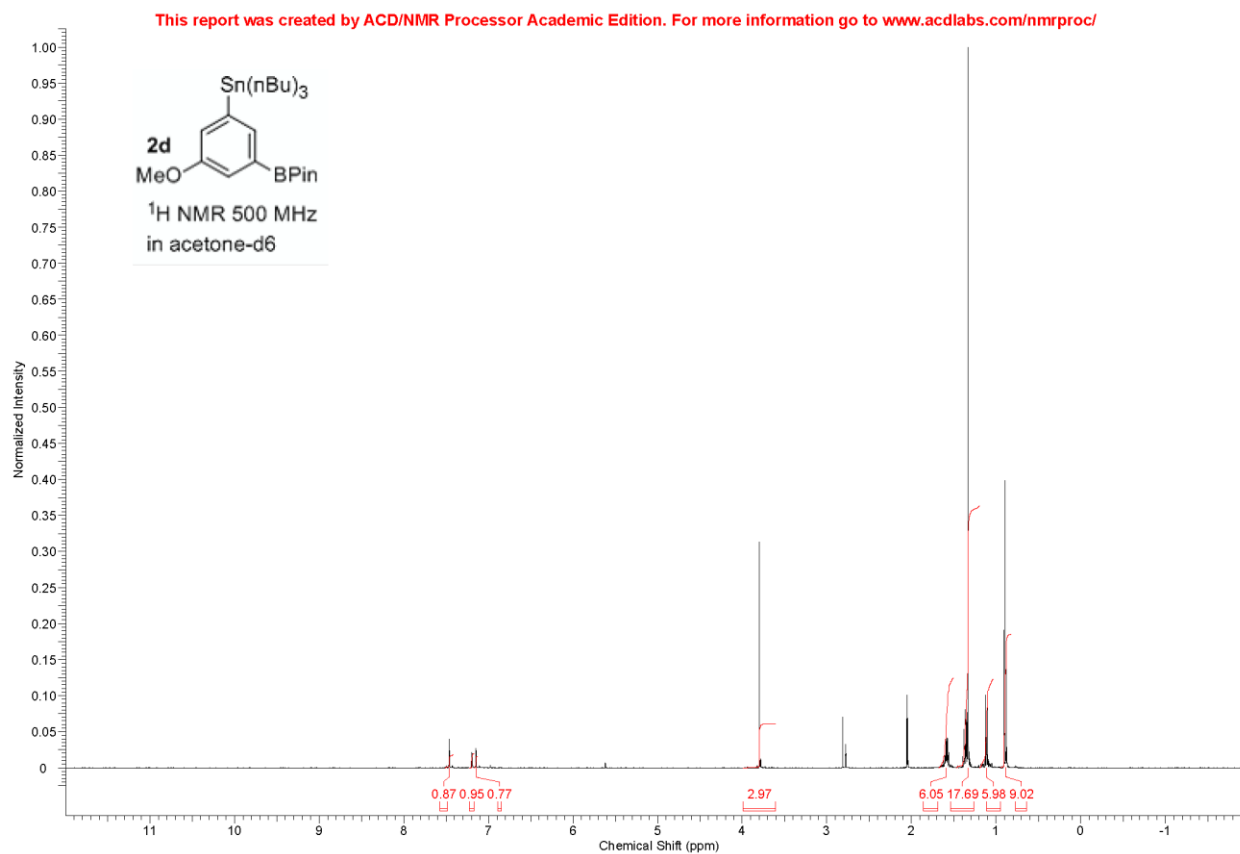


Figure 114 ^{119}Sn NMR of compound 2e

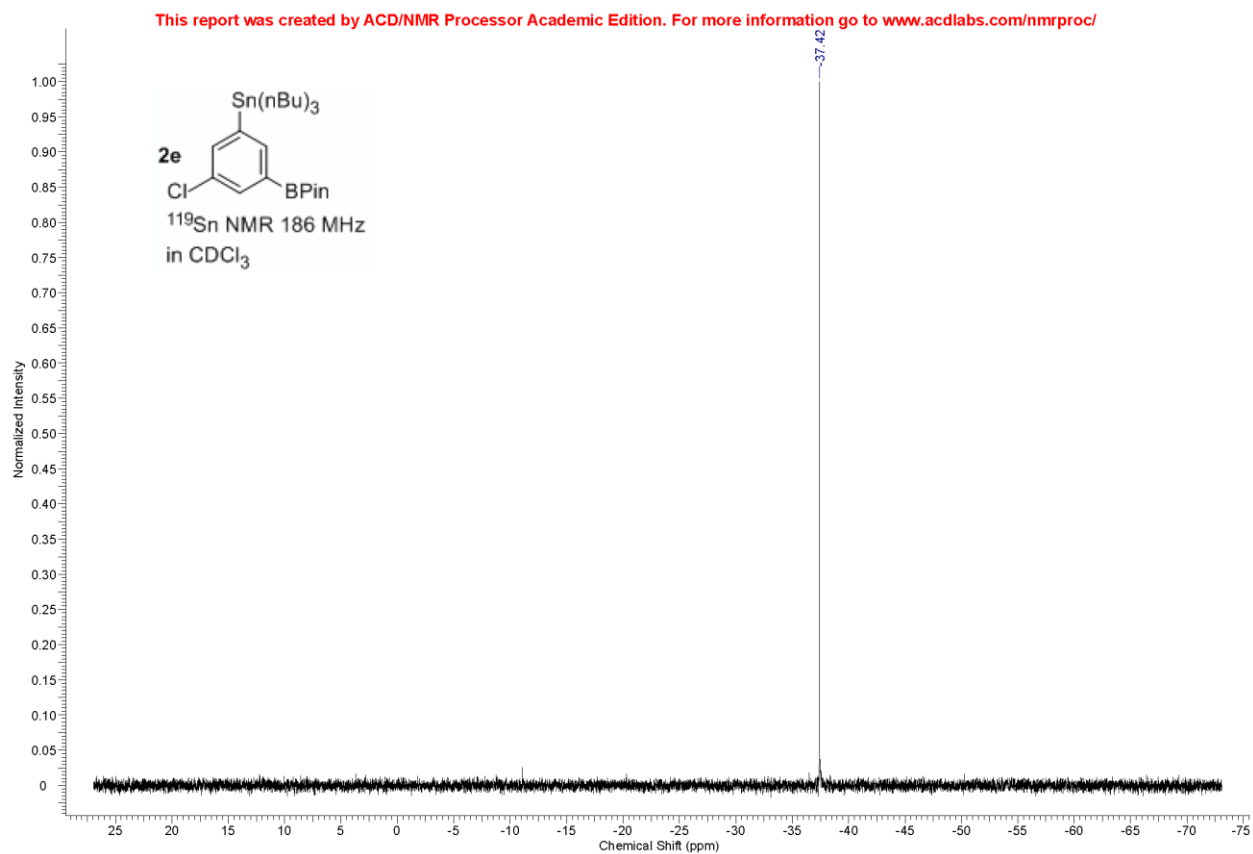


Figure 115 ^{11}B NMR of compound 2e

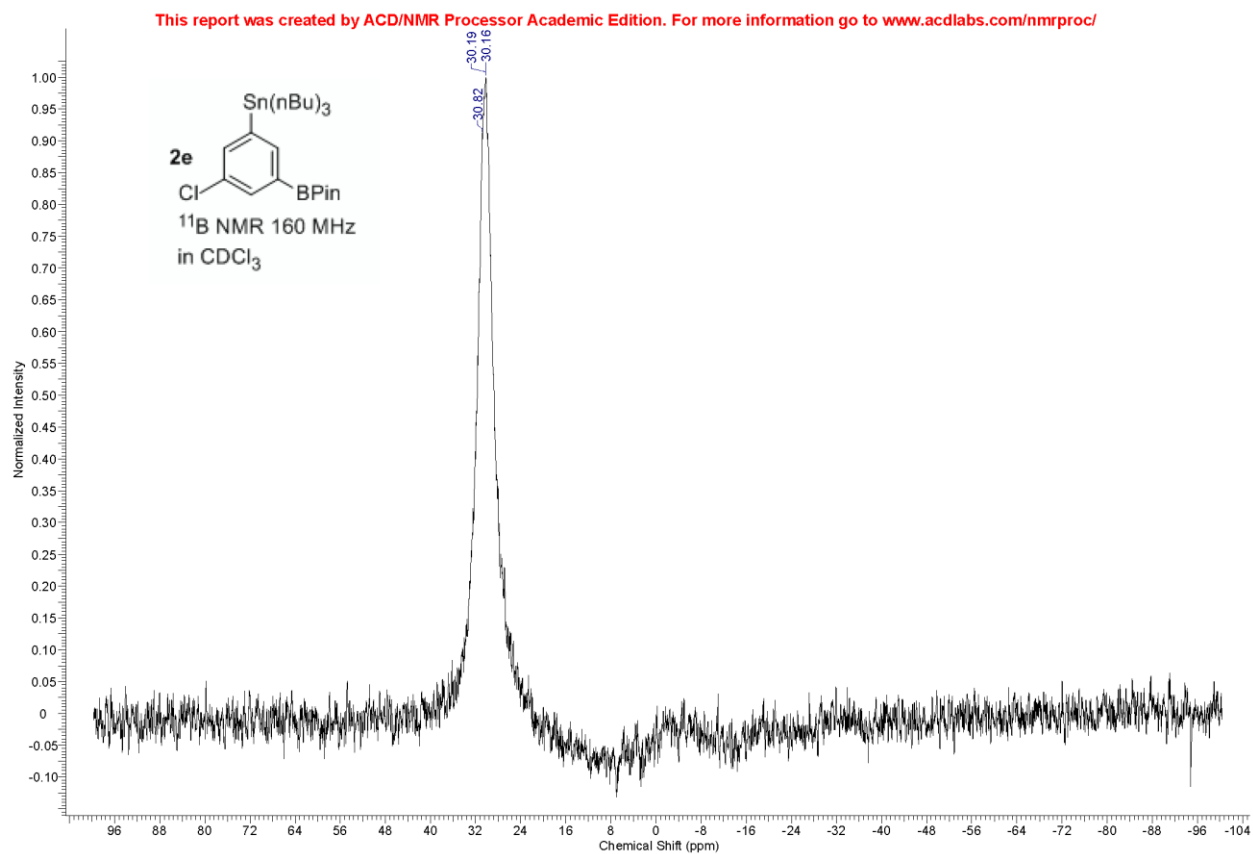


Figure 116 ^{13}C NMR of compound 2e

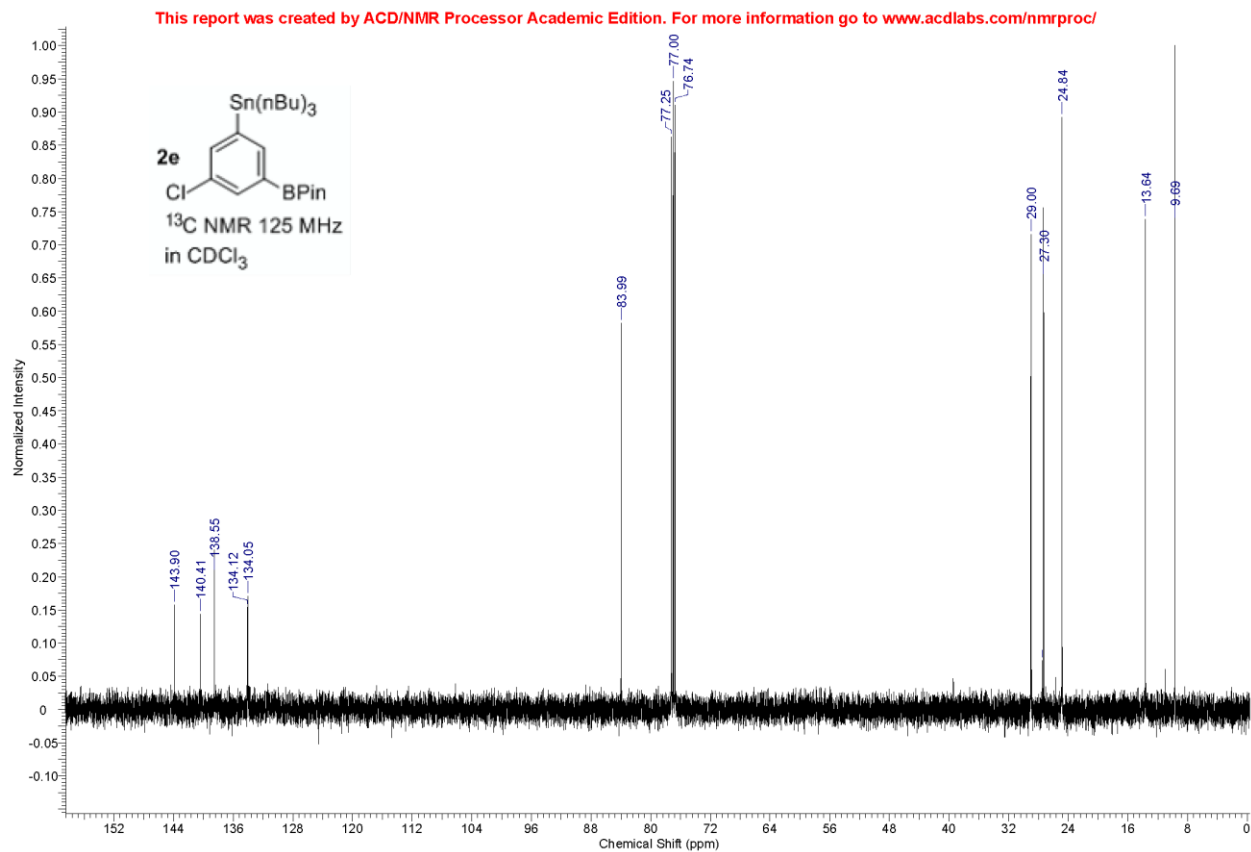


Figure 117 ^1H NMR of compound 2e

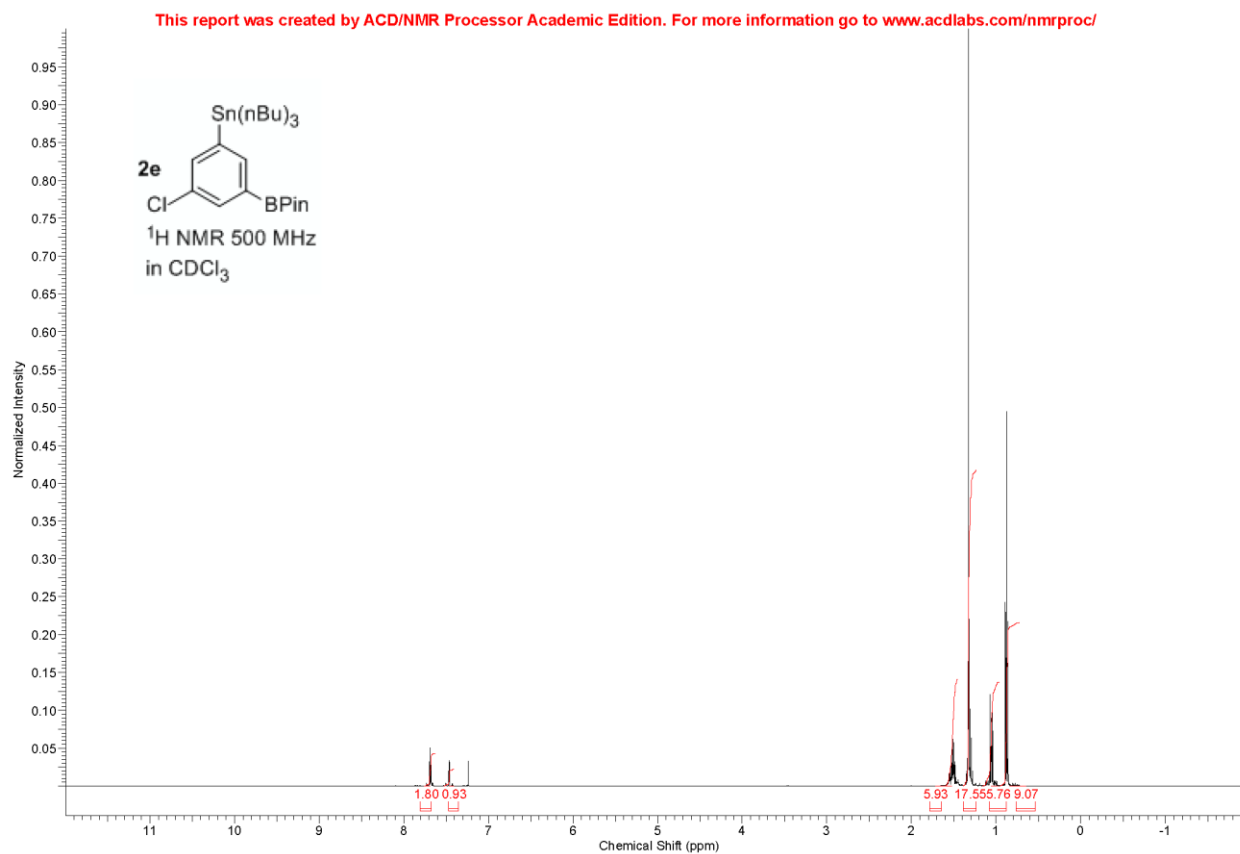


Figure 118 ^{119}Sn NMR of compound 2f

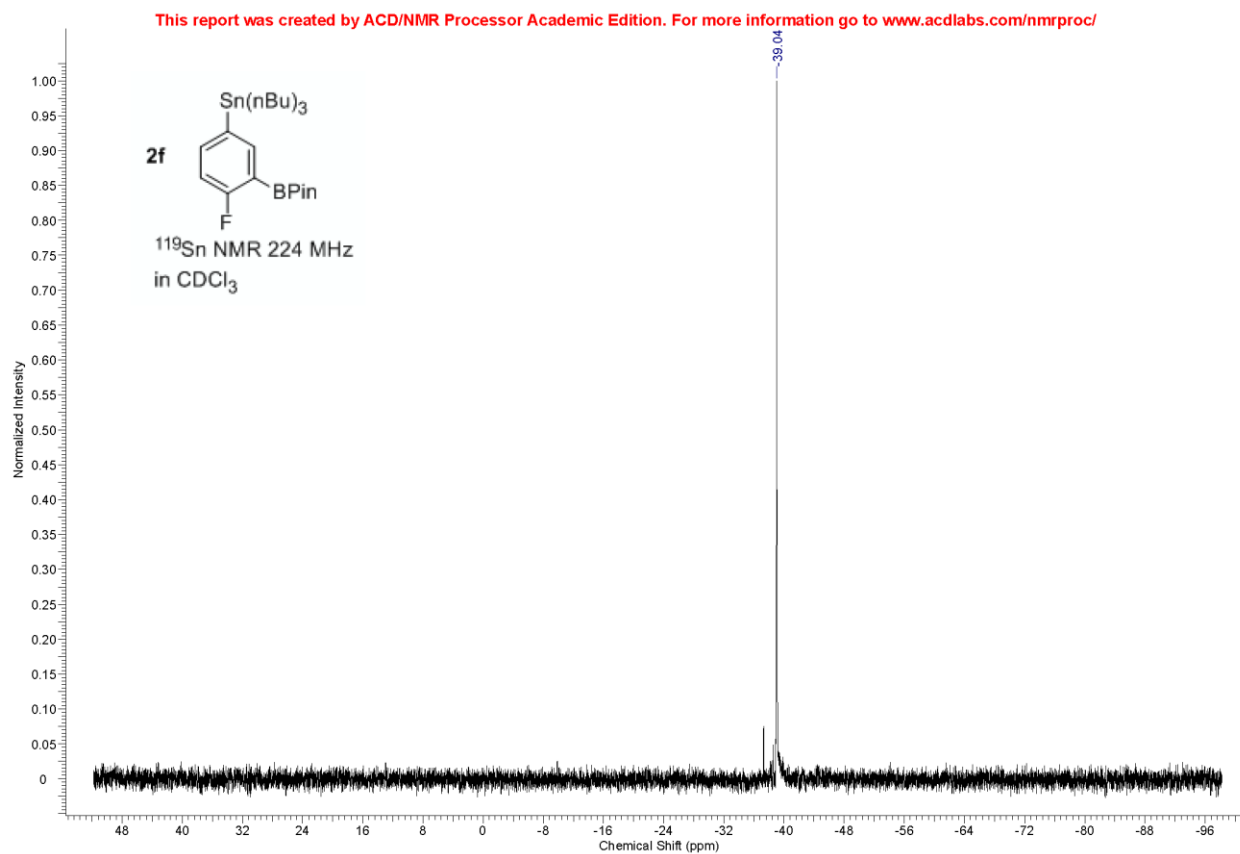


Figure 119 ^{11}B NMR of compound **2f**

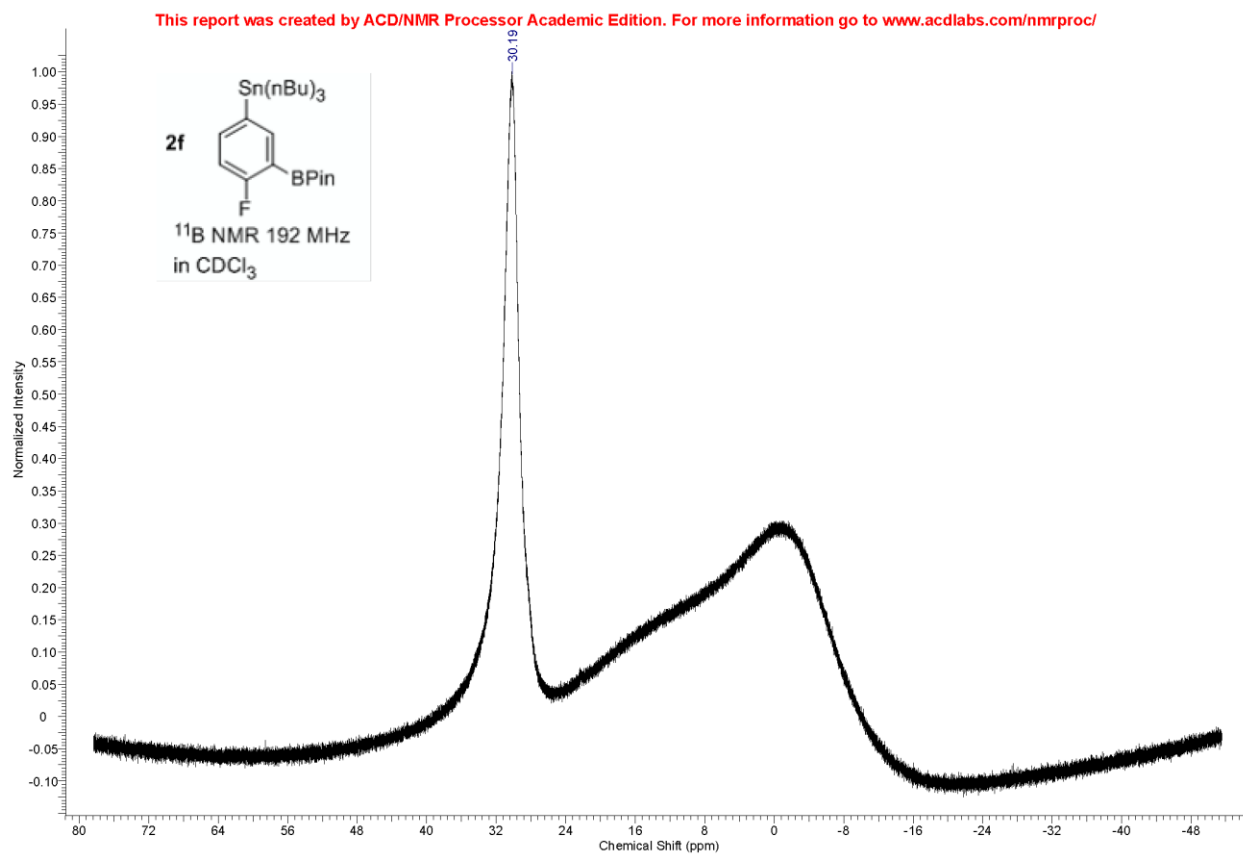


Figure 120 ^{13}C NMR of compound 2f

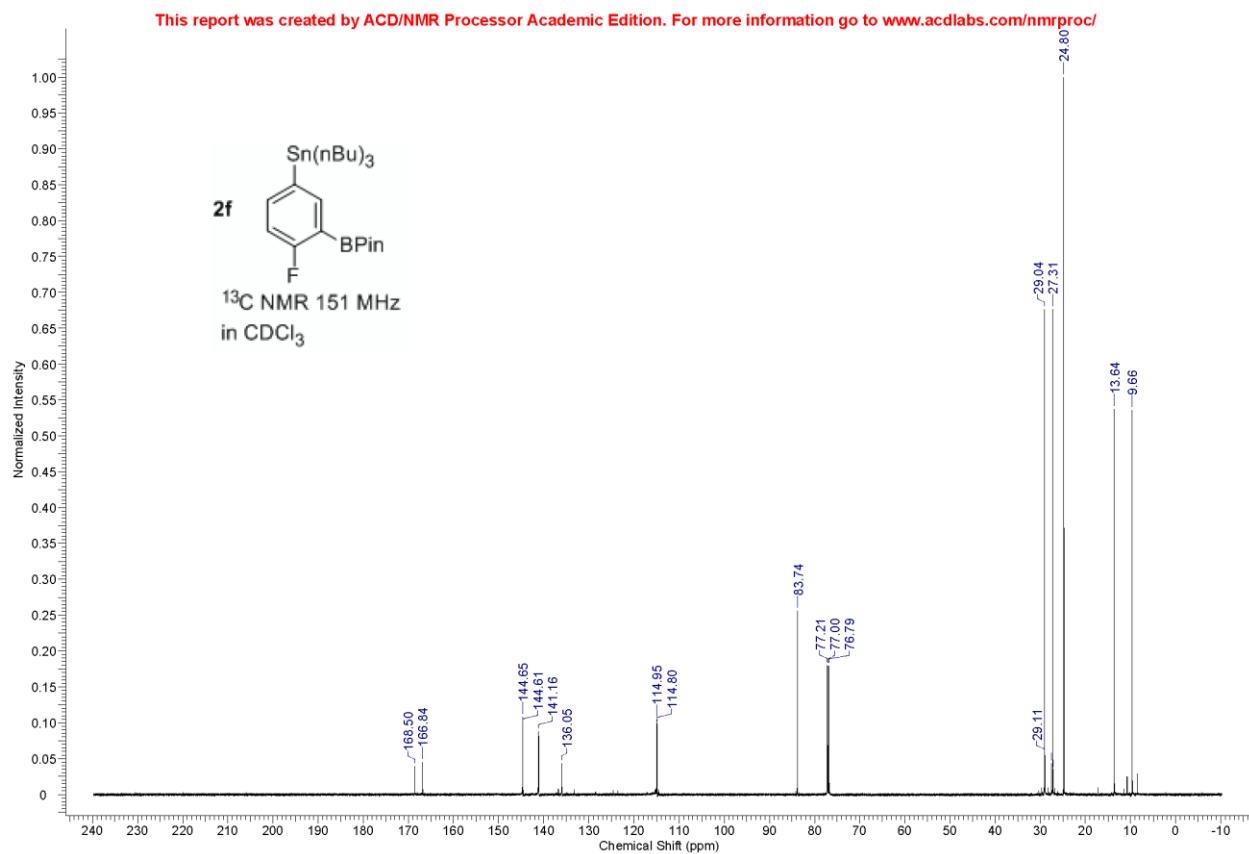


Figure 121 ^{19}F NMR of compound 2f

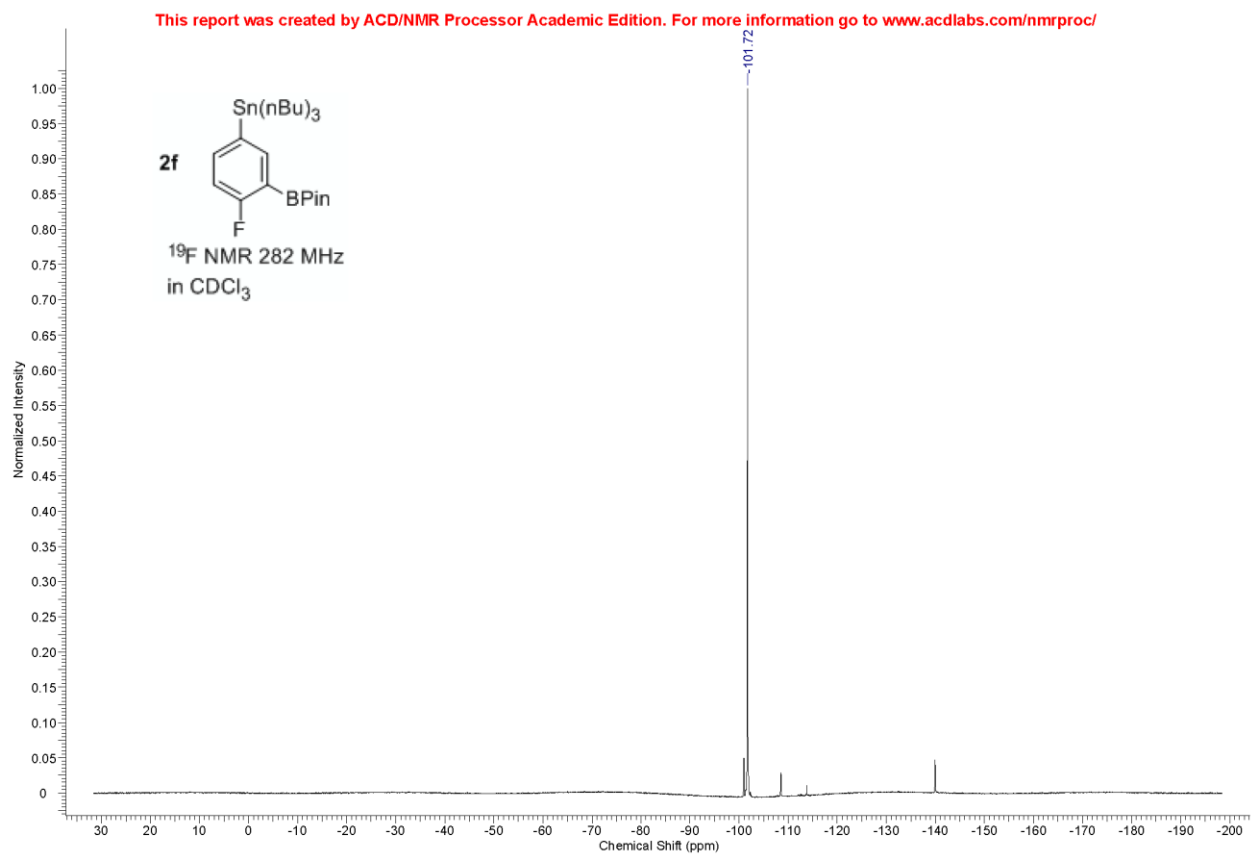


Figure 122 ^1H NMR of compound 2f

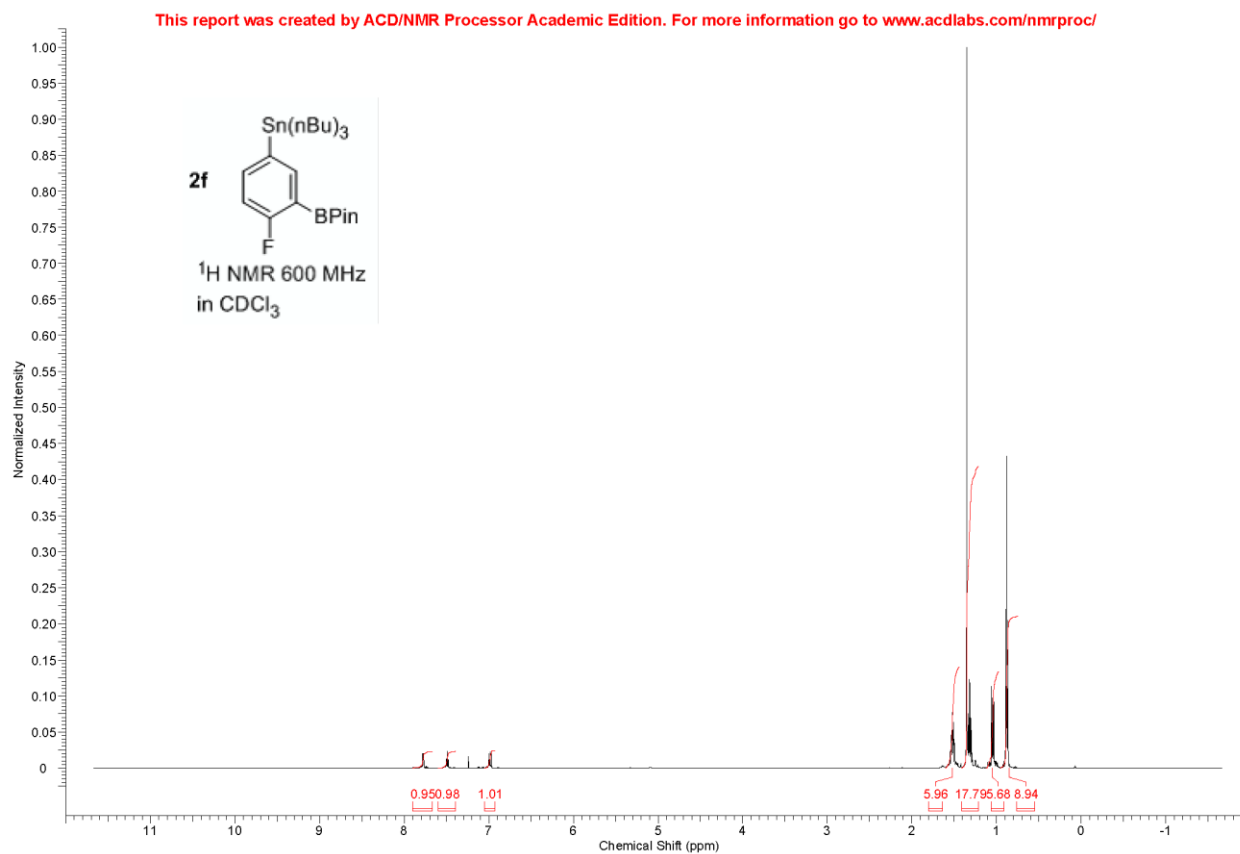


Figure 123 ^{119}Sn NMR of compound 4a

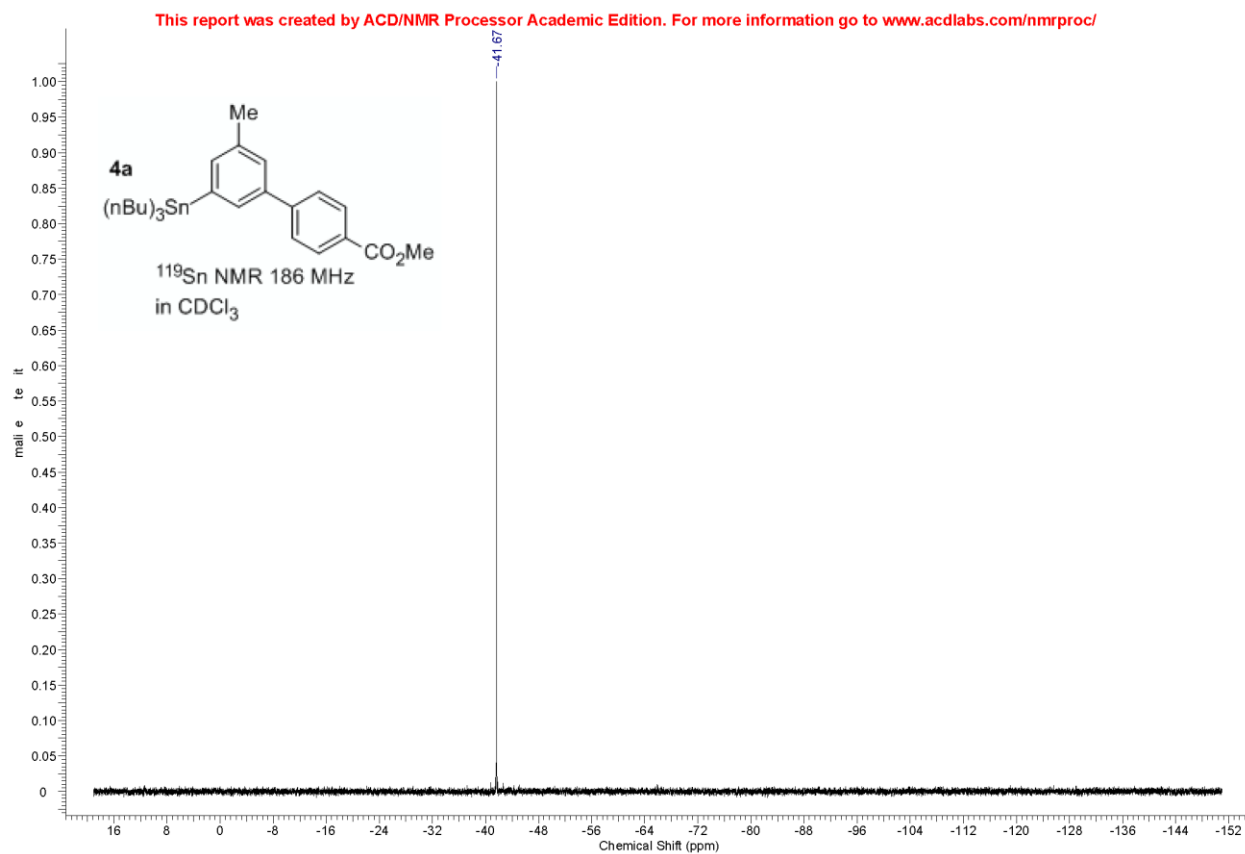


Figure 124 ^{13}C NMR of compound 4a

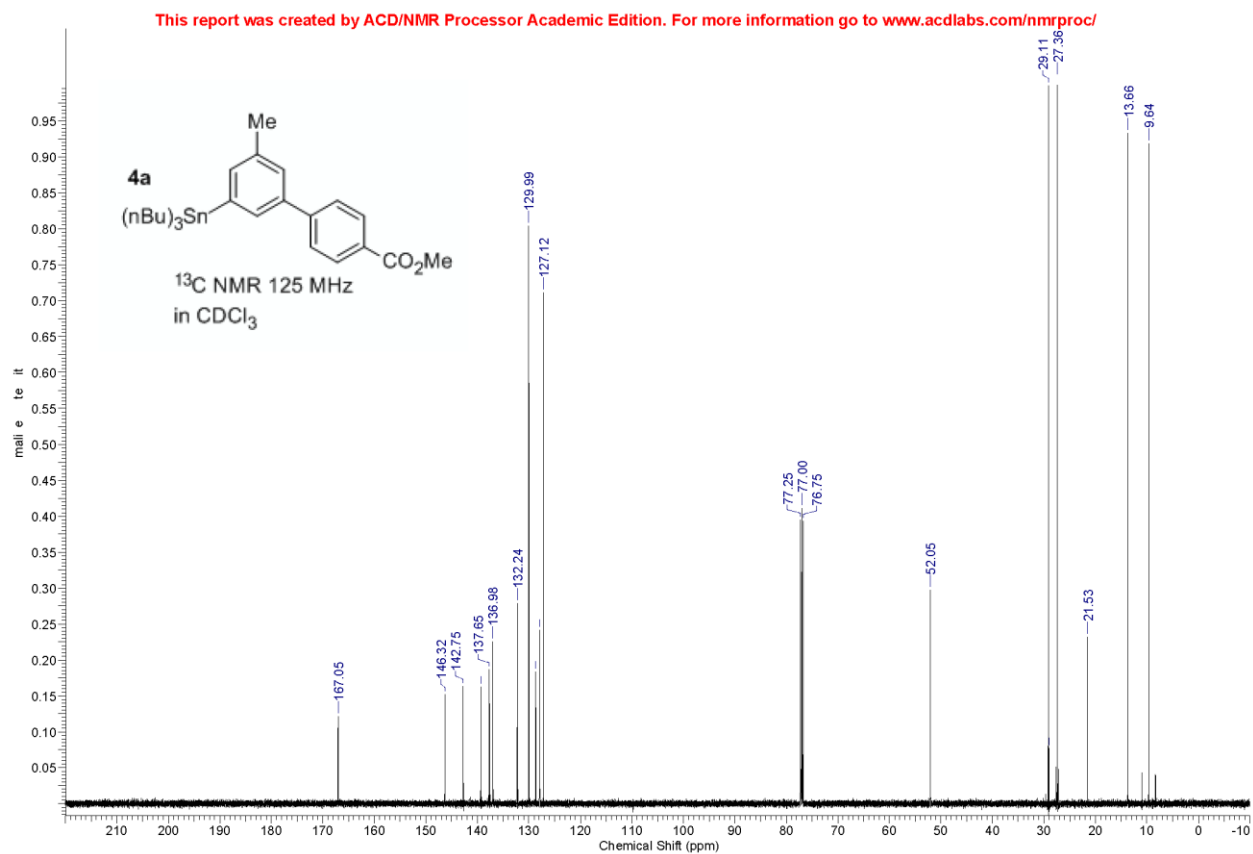


Figure 125 ^1H NMR of compound 4a

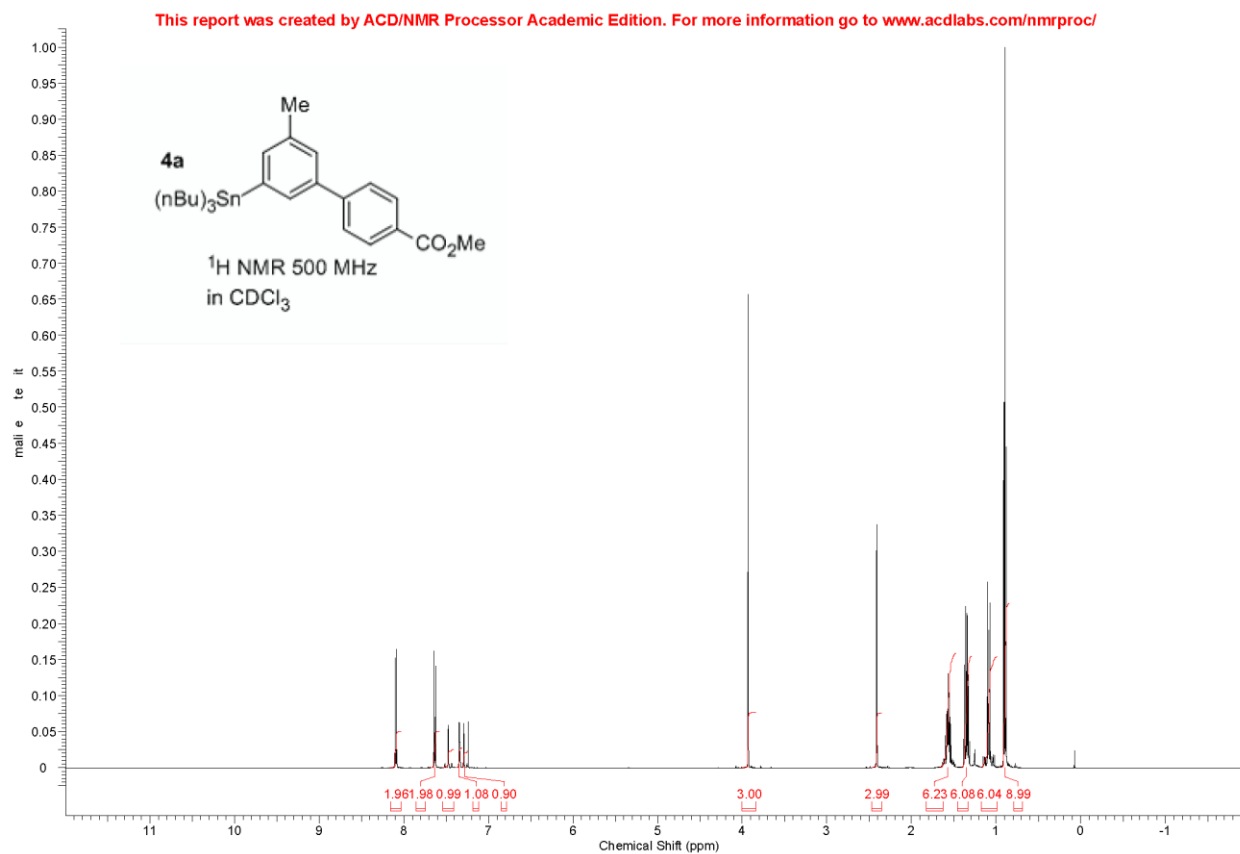


Figure 126 ^{119}Sn NMR of compound 4b

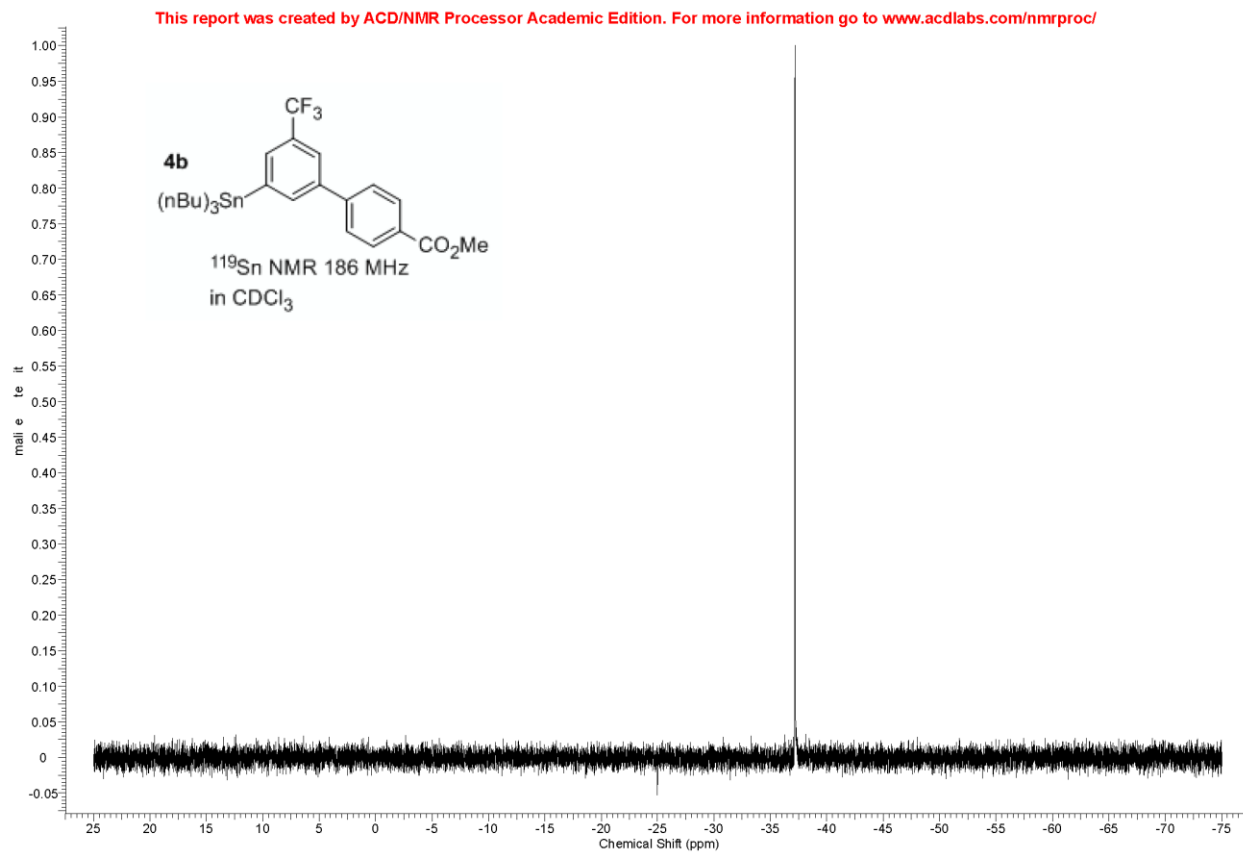


Figure 127 ^{13}C NMR of compound 4b

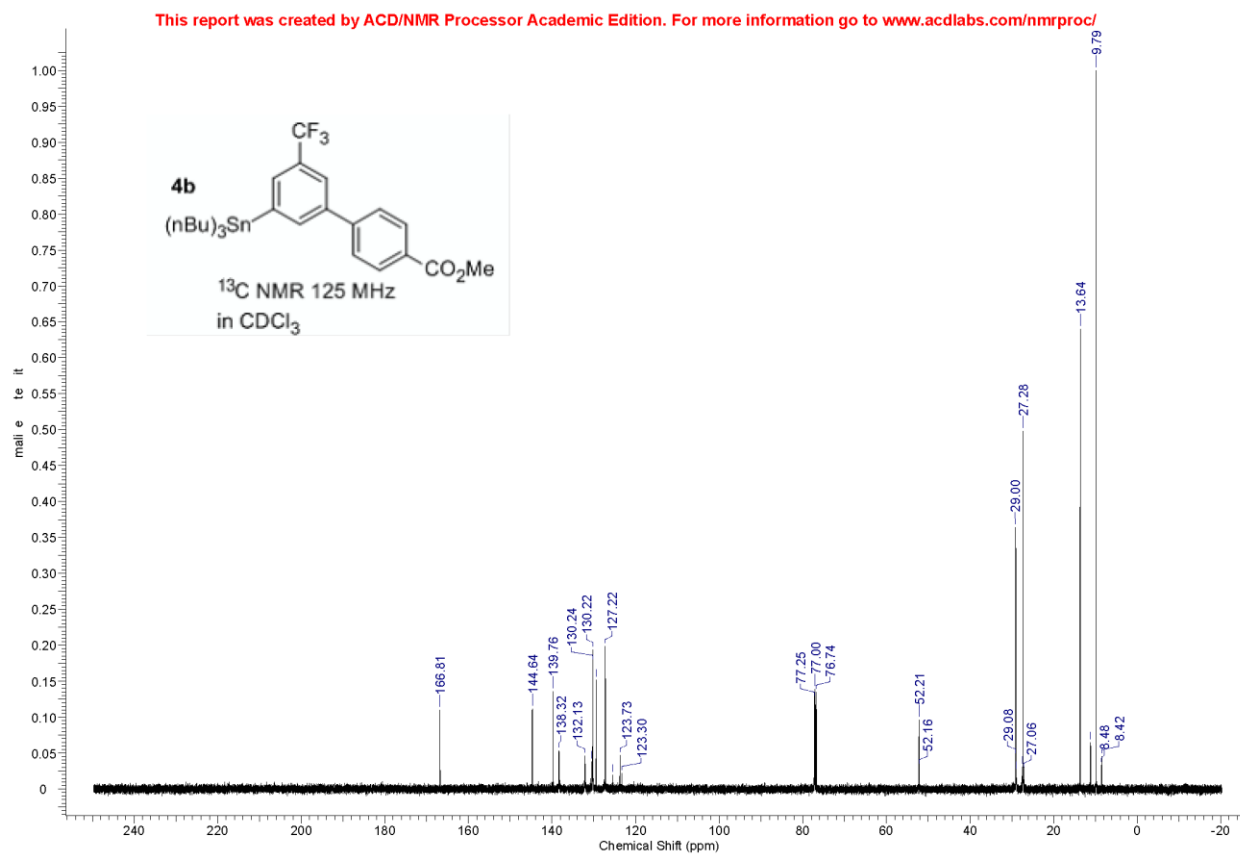


Figure 128 ^{19}F NMR of compound 4b

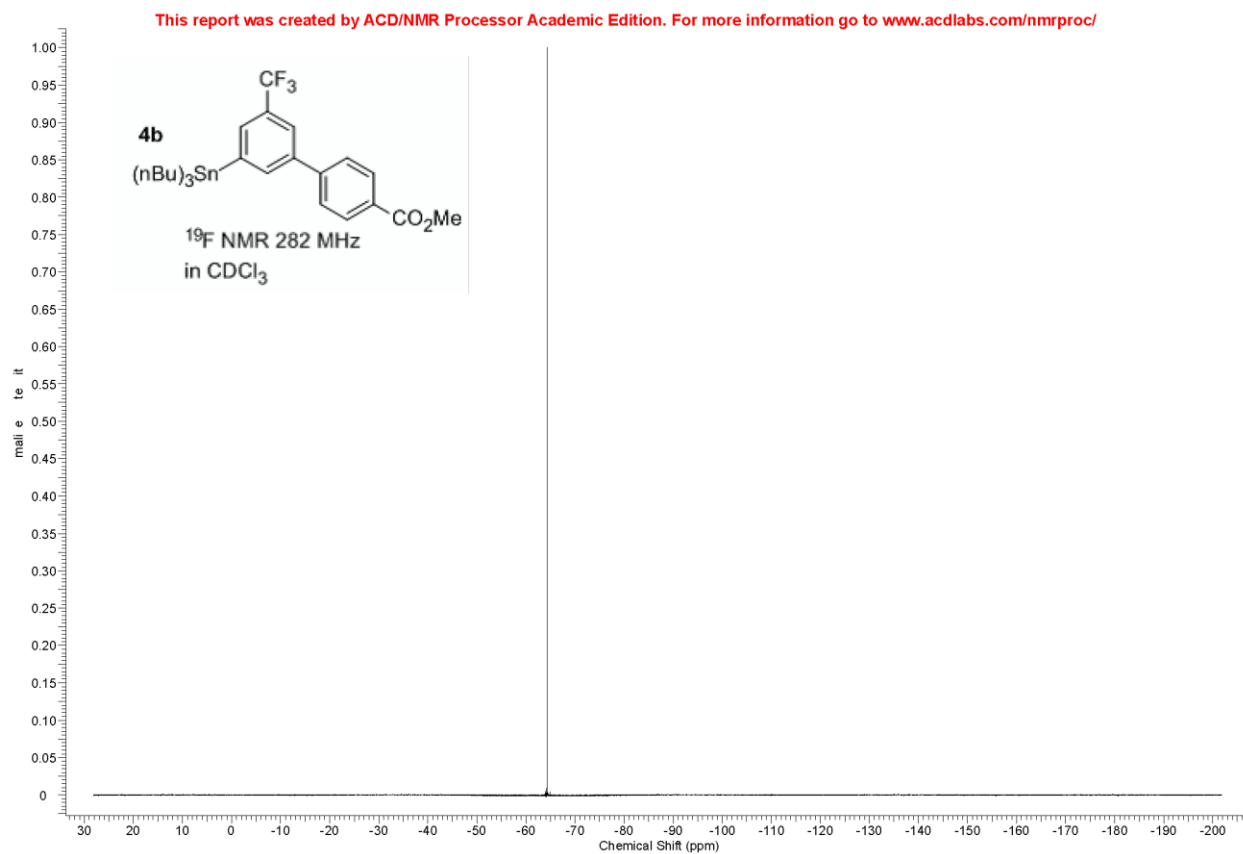


Figure 129 ^1H NMR of compound 4b

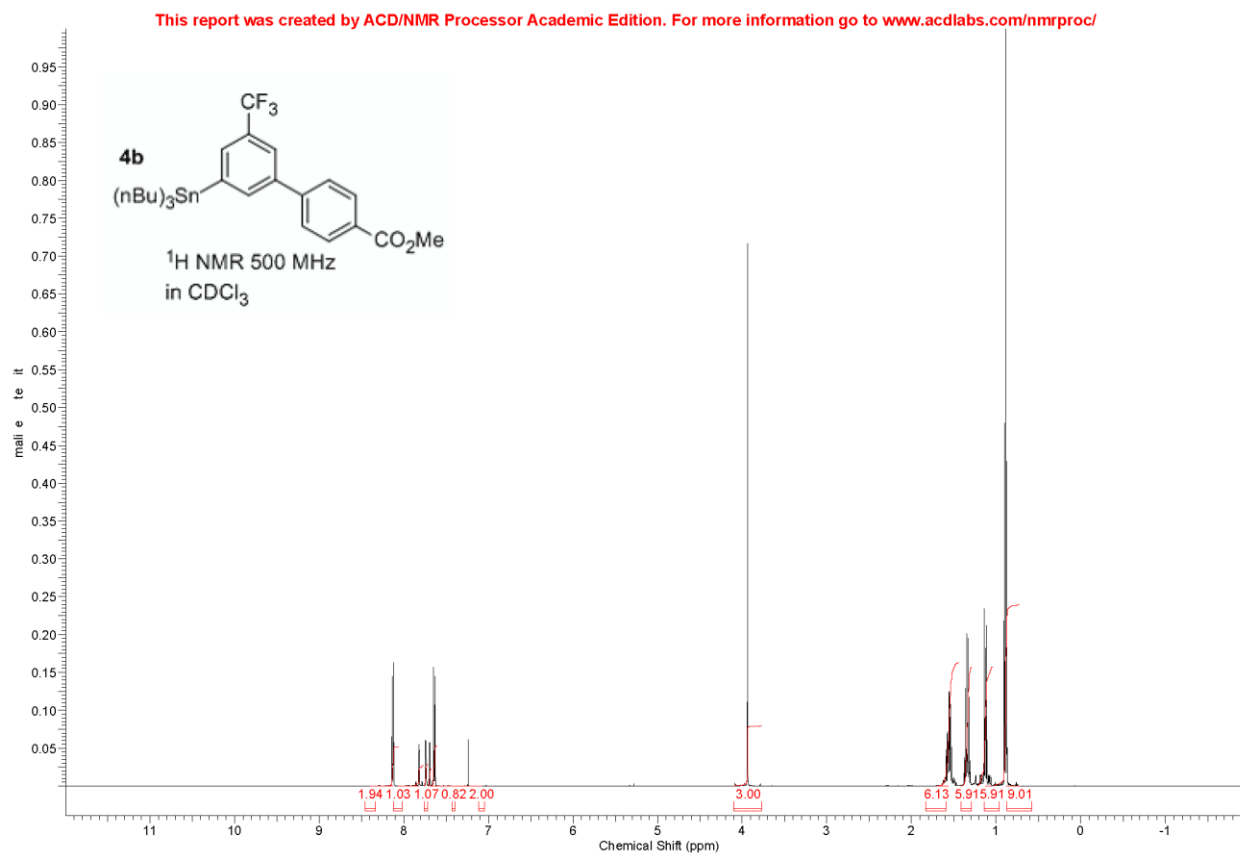


Figure 130 ^{119}Sn NMR of compound 4c

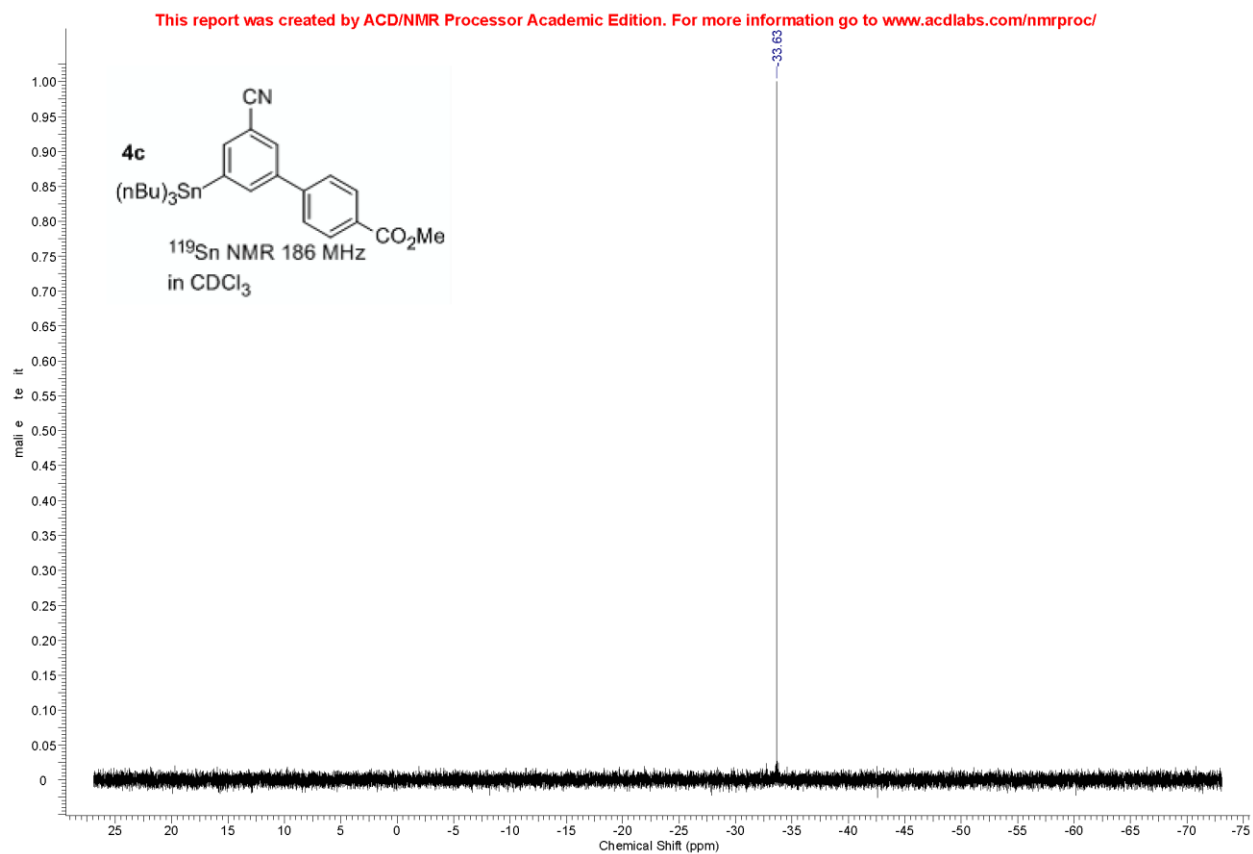


Figure 131 ^{13}C NMR of compound 4c

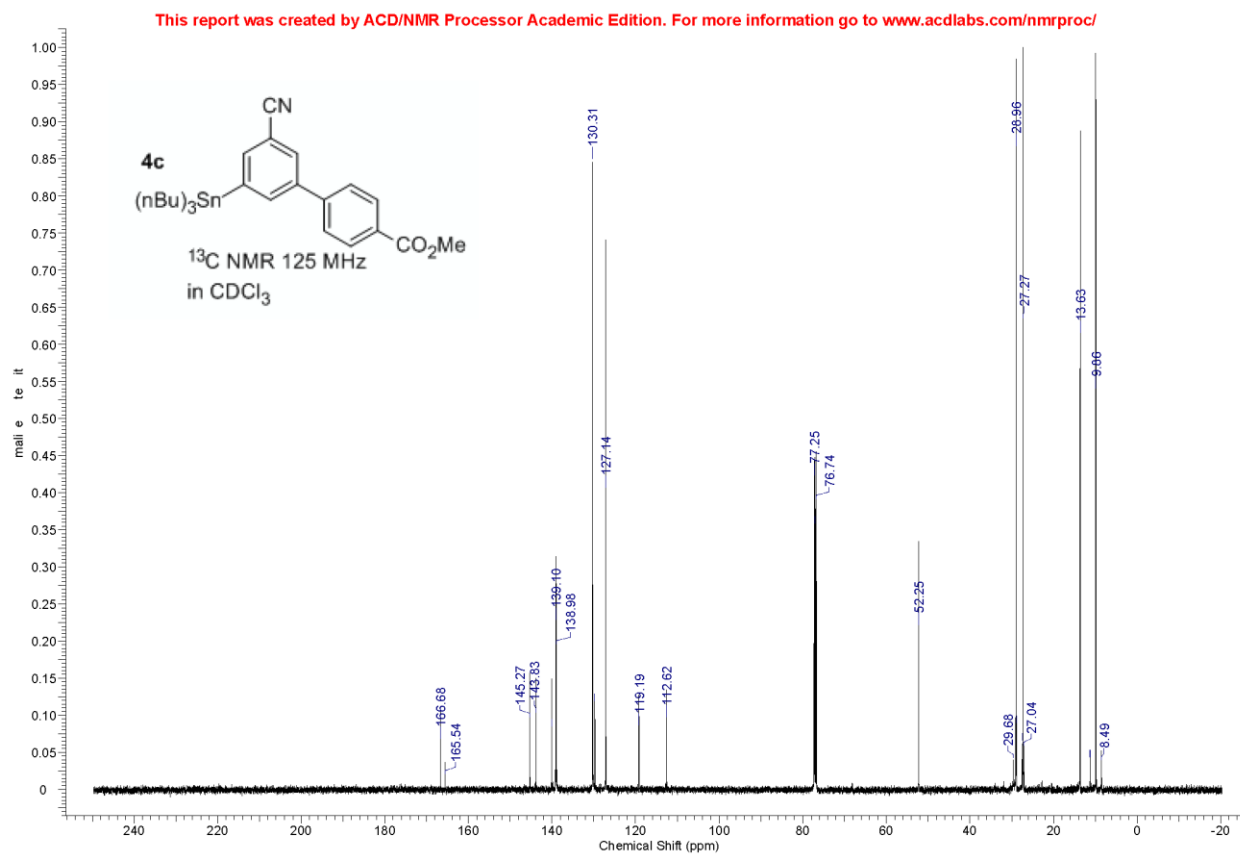


Figure 132 ^1H NMR of compound 4c

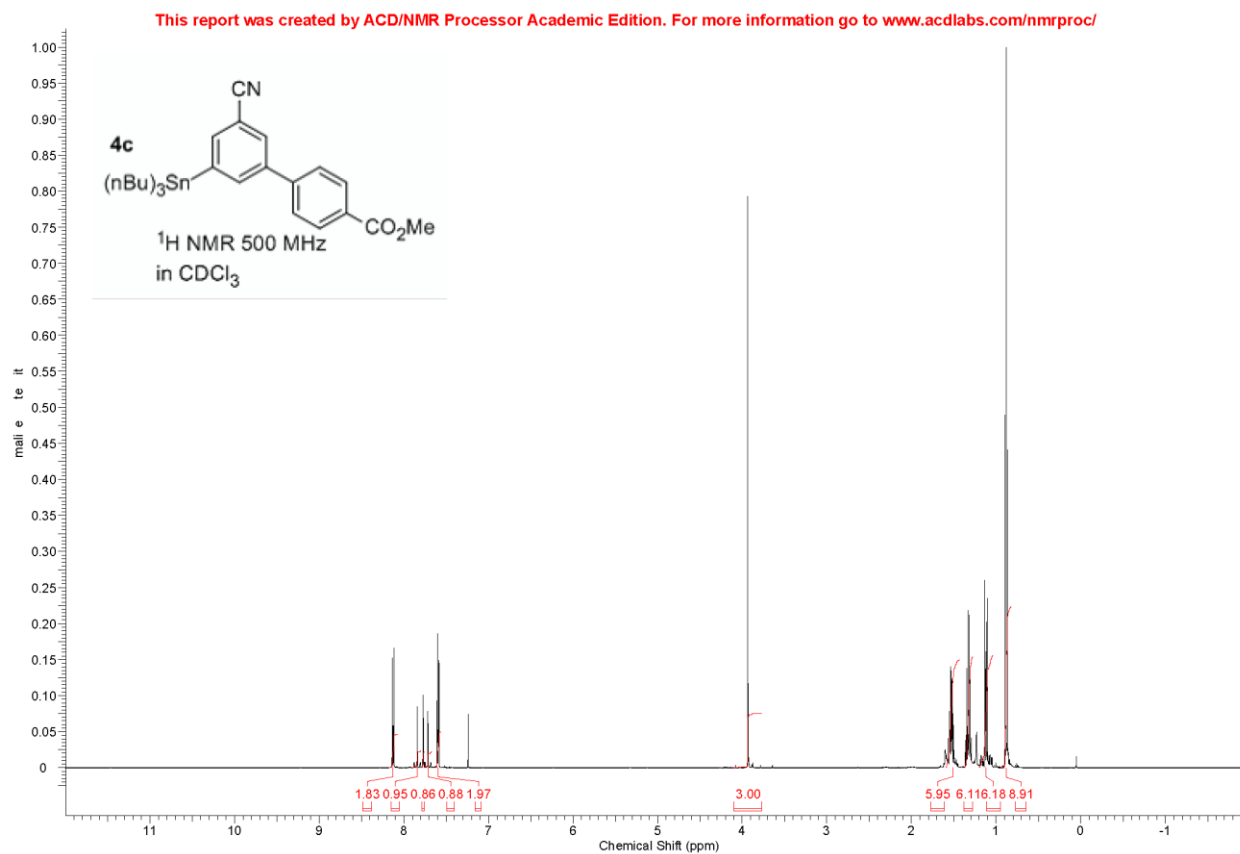


Figure 133 ^{119}Sn NMR of compound 4d

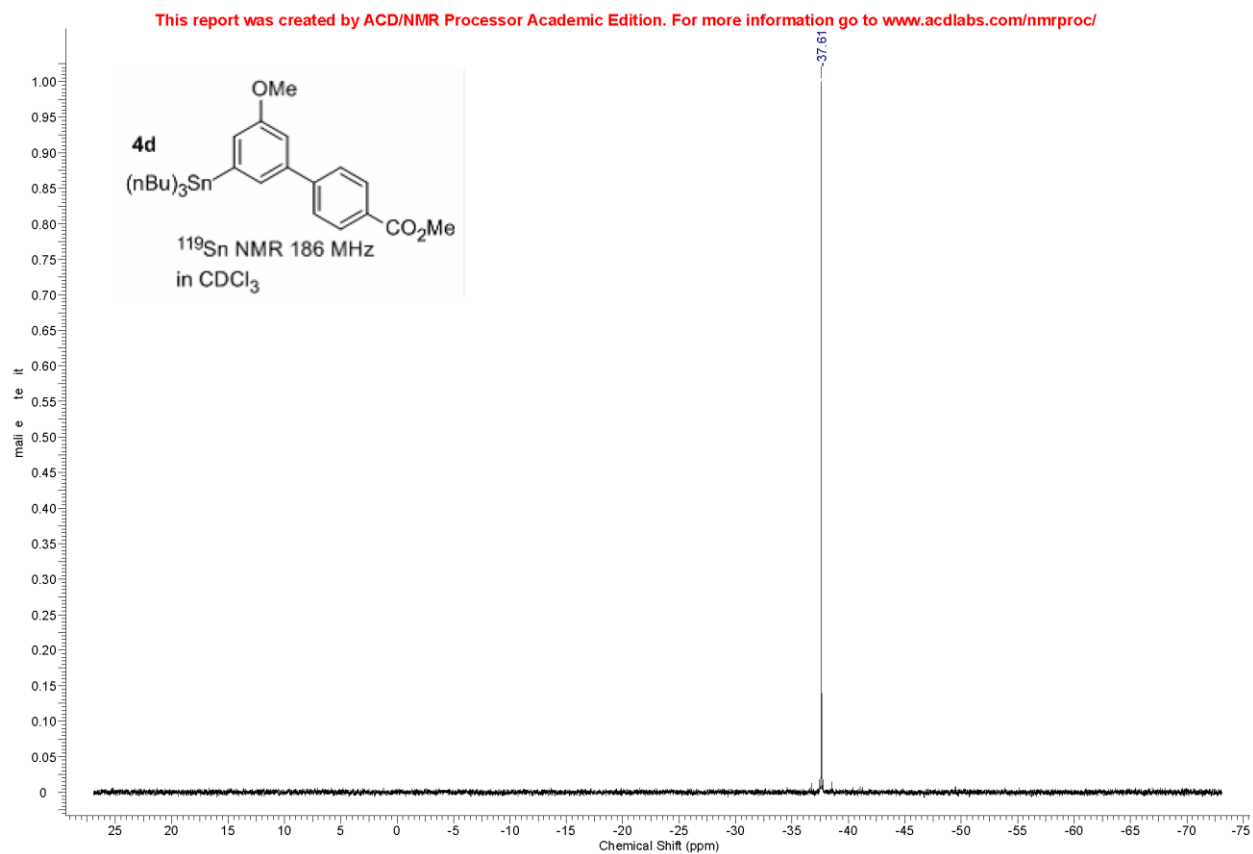


Figure 134 ^{13}C NMR of compound 4d

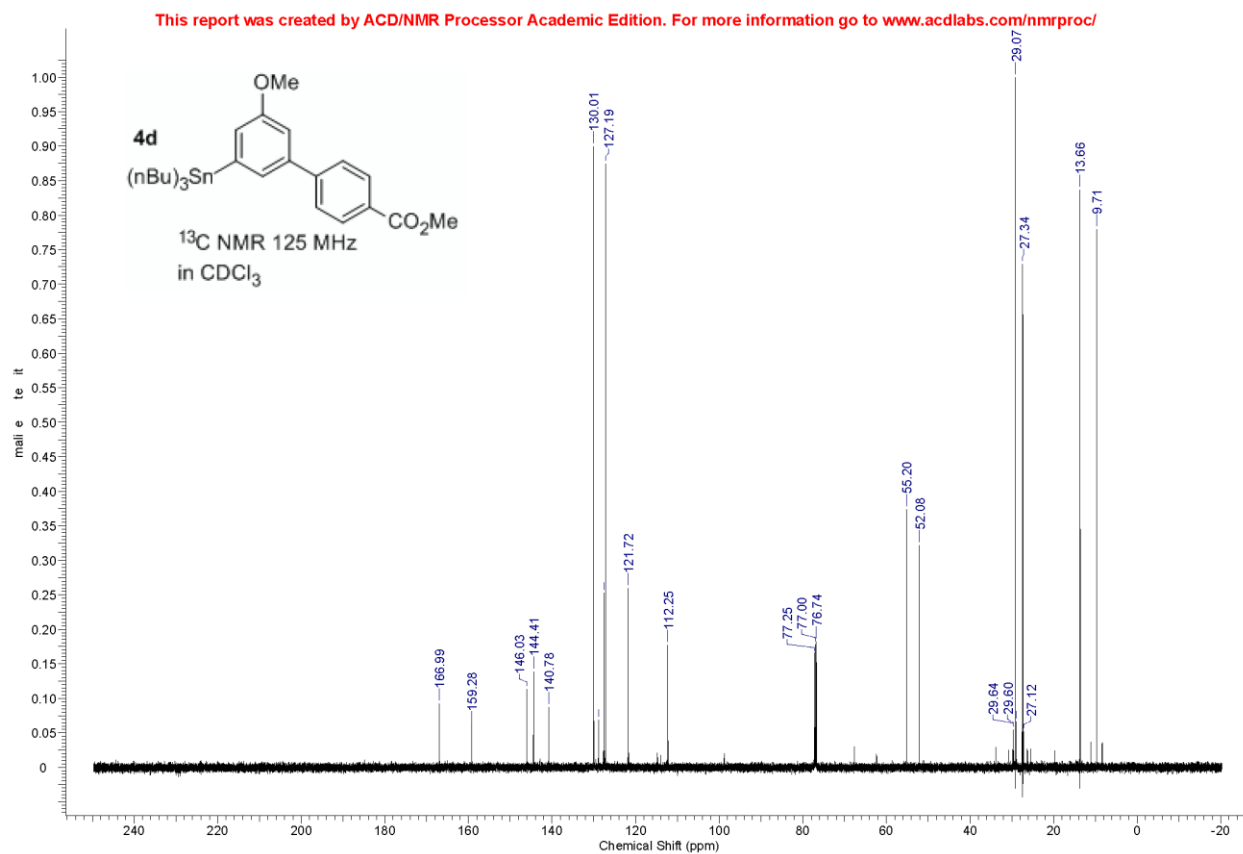


Figure 135 ^1H NMR of compound 4d

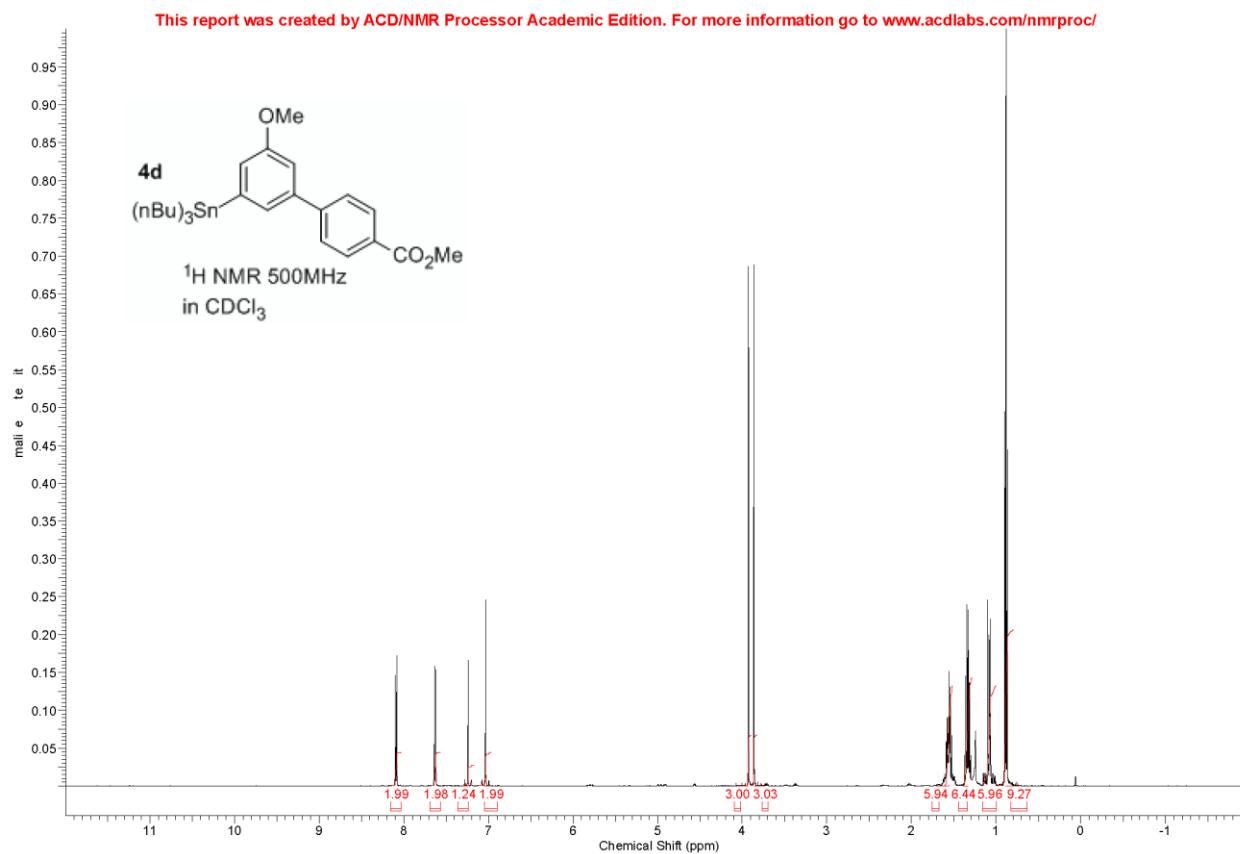


Figure 136 ^{119}Sn NMR of compound 4e

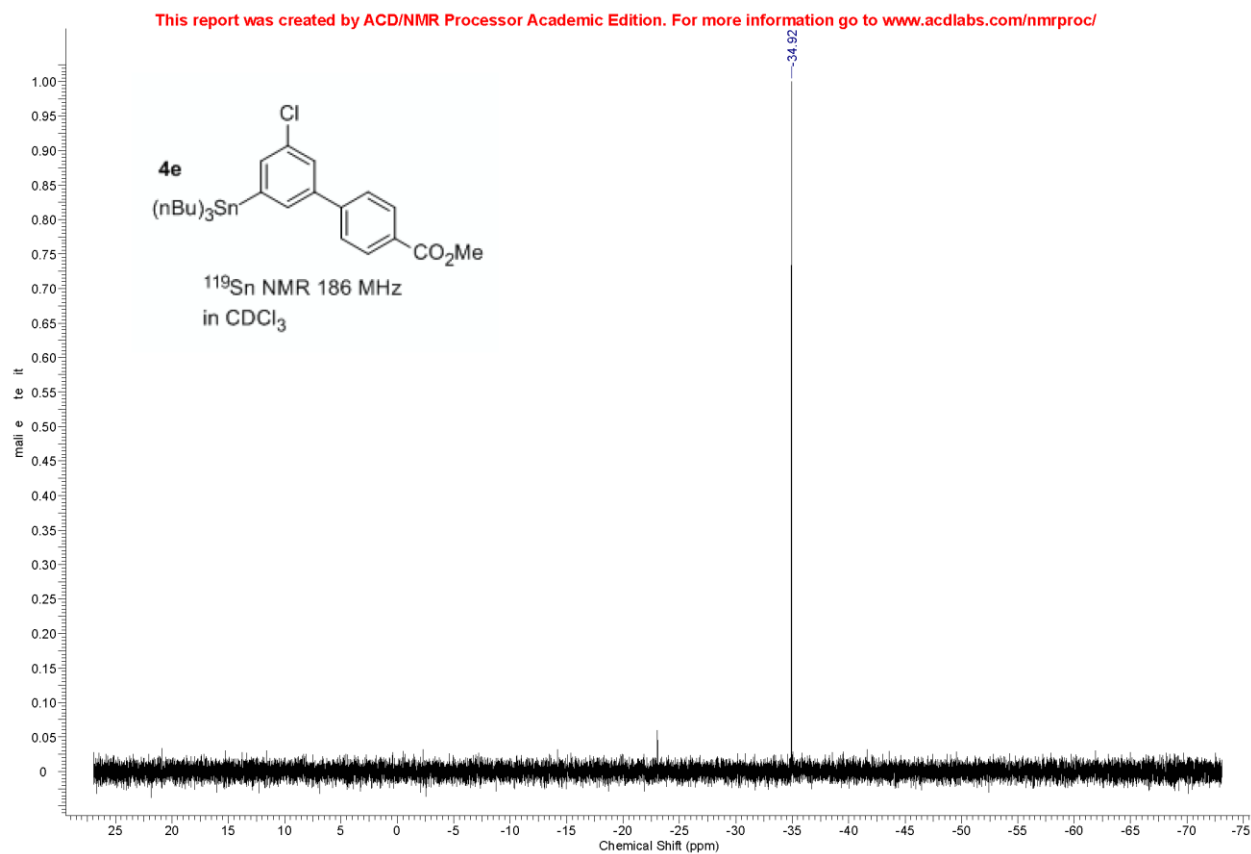


Figure 137 ^{13}C NMR of compound 4e

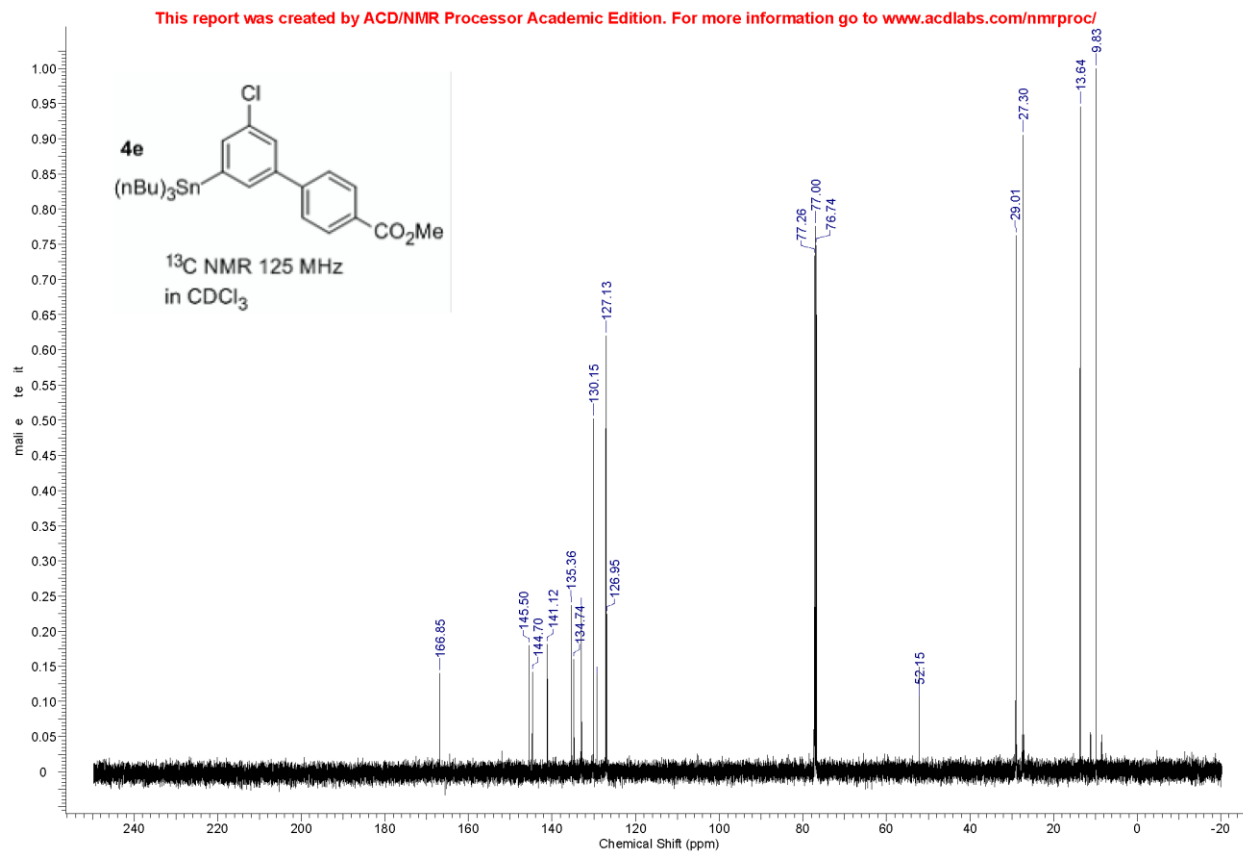


Figure 138 ^1H NMR of compound 4e

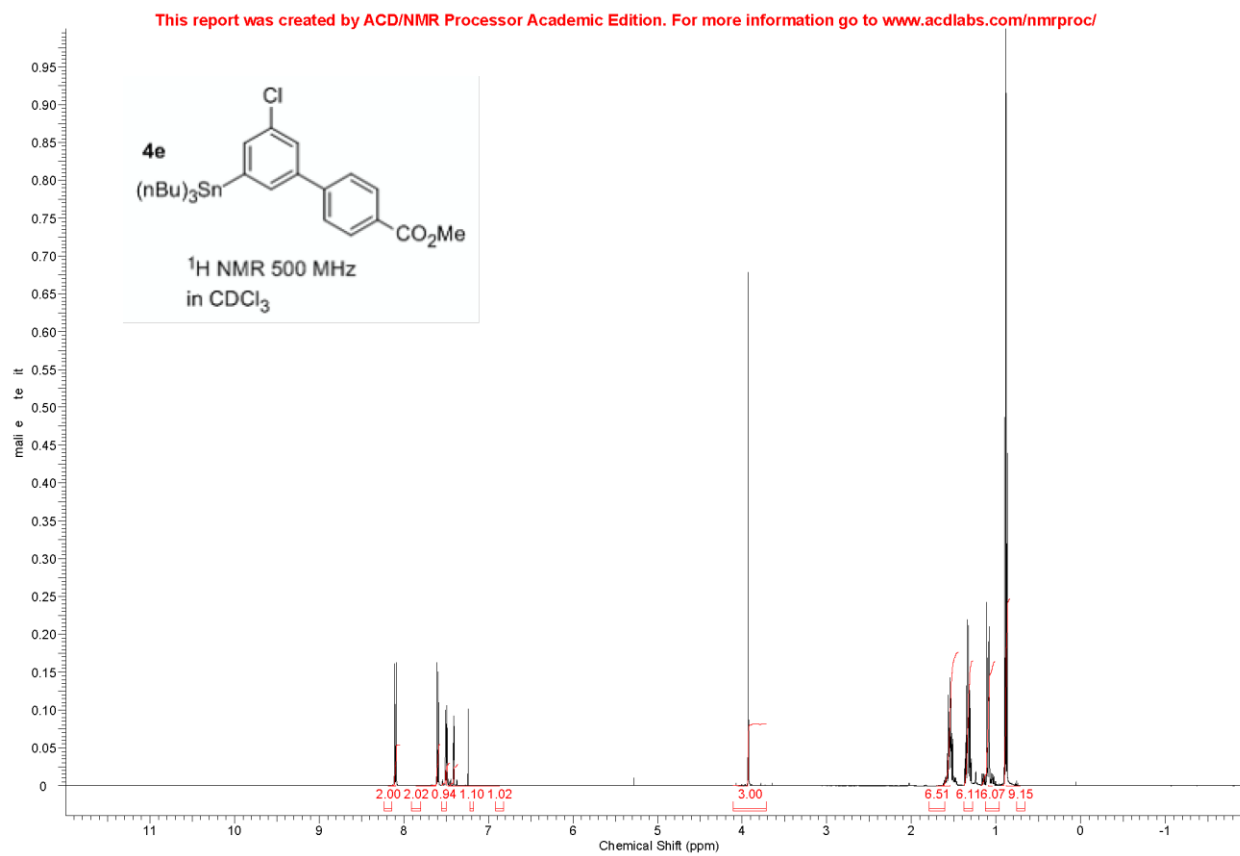


Figure 139 ^{119}Sn NMR of compound 4f

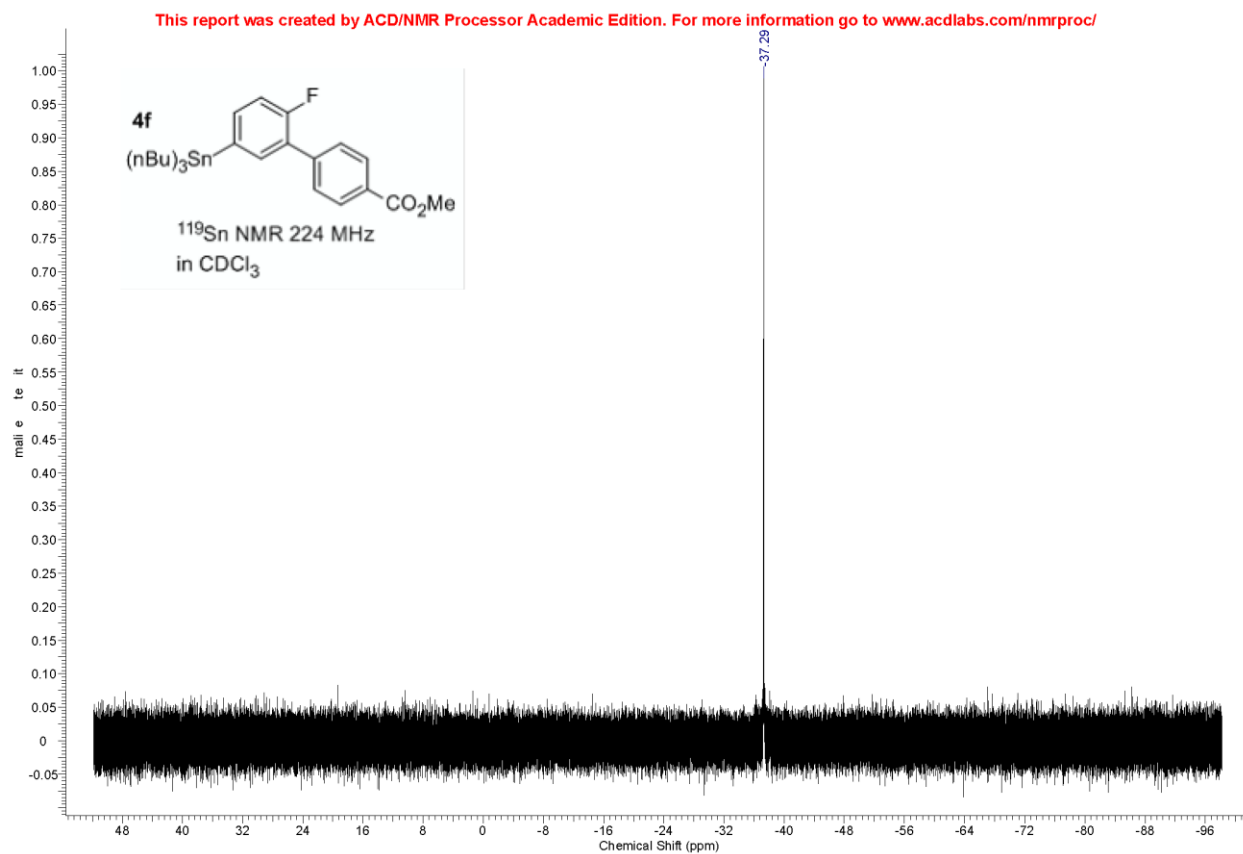


Figure 140 ^{13}C NMR of compound 4f

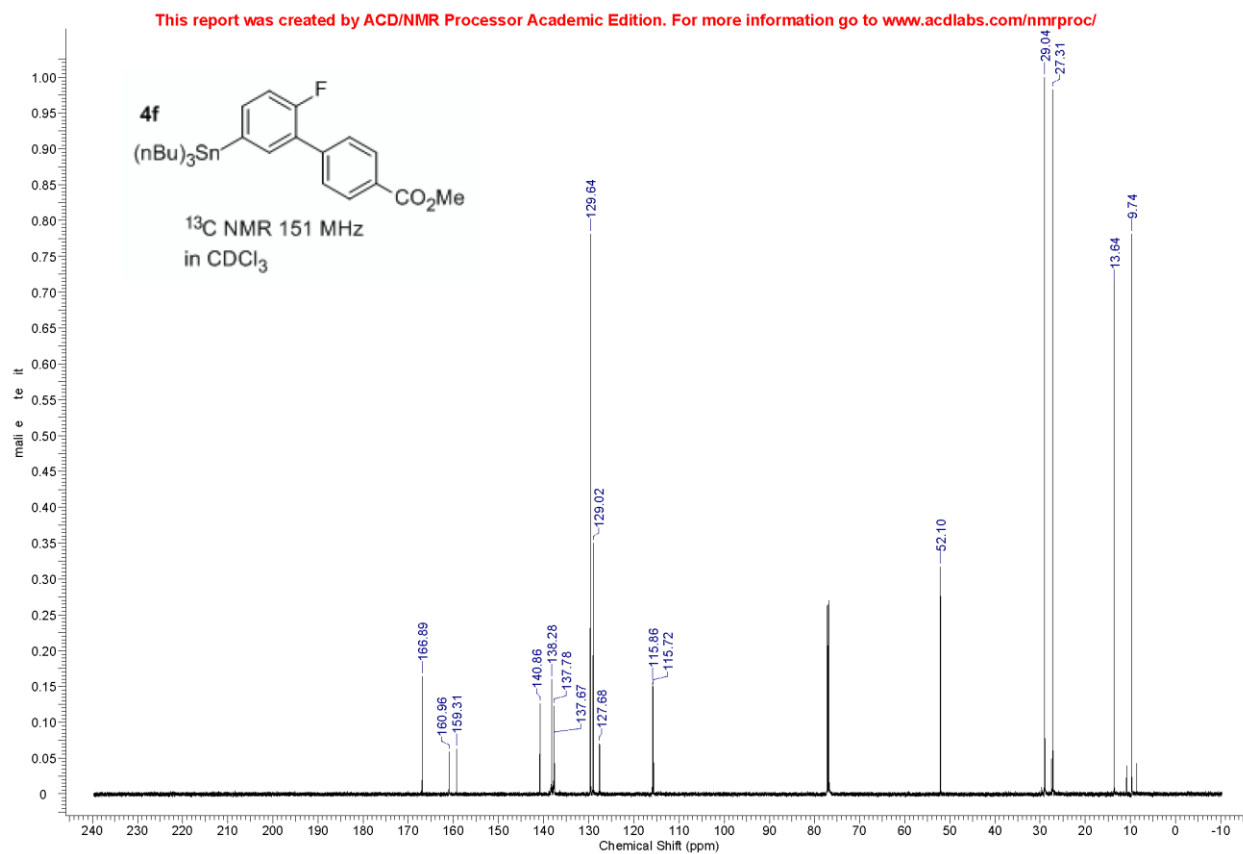


Figure 141 ^{19}F NMR of compound 4f

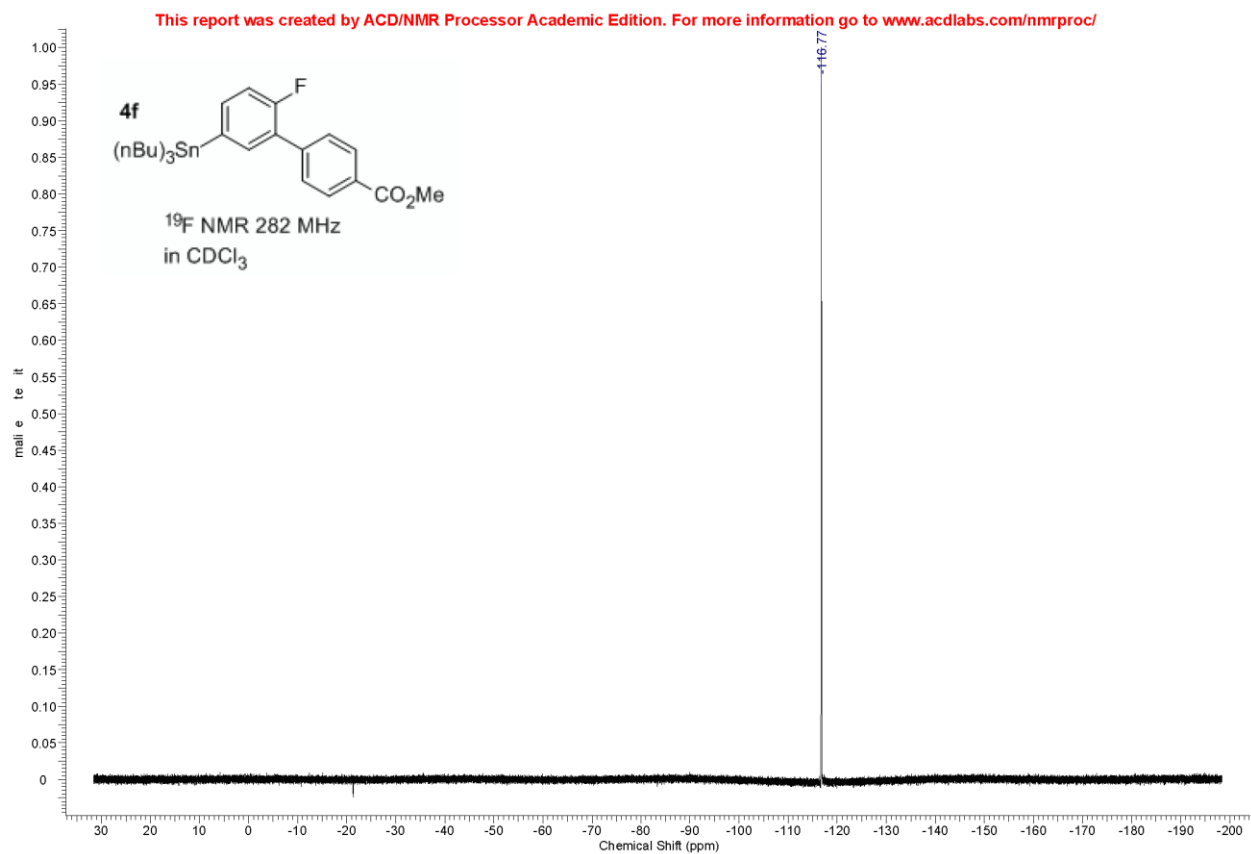


Figure 142 ^1H NMR of compound 4f

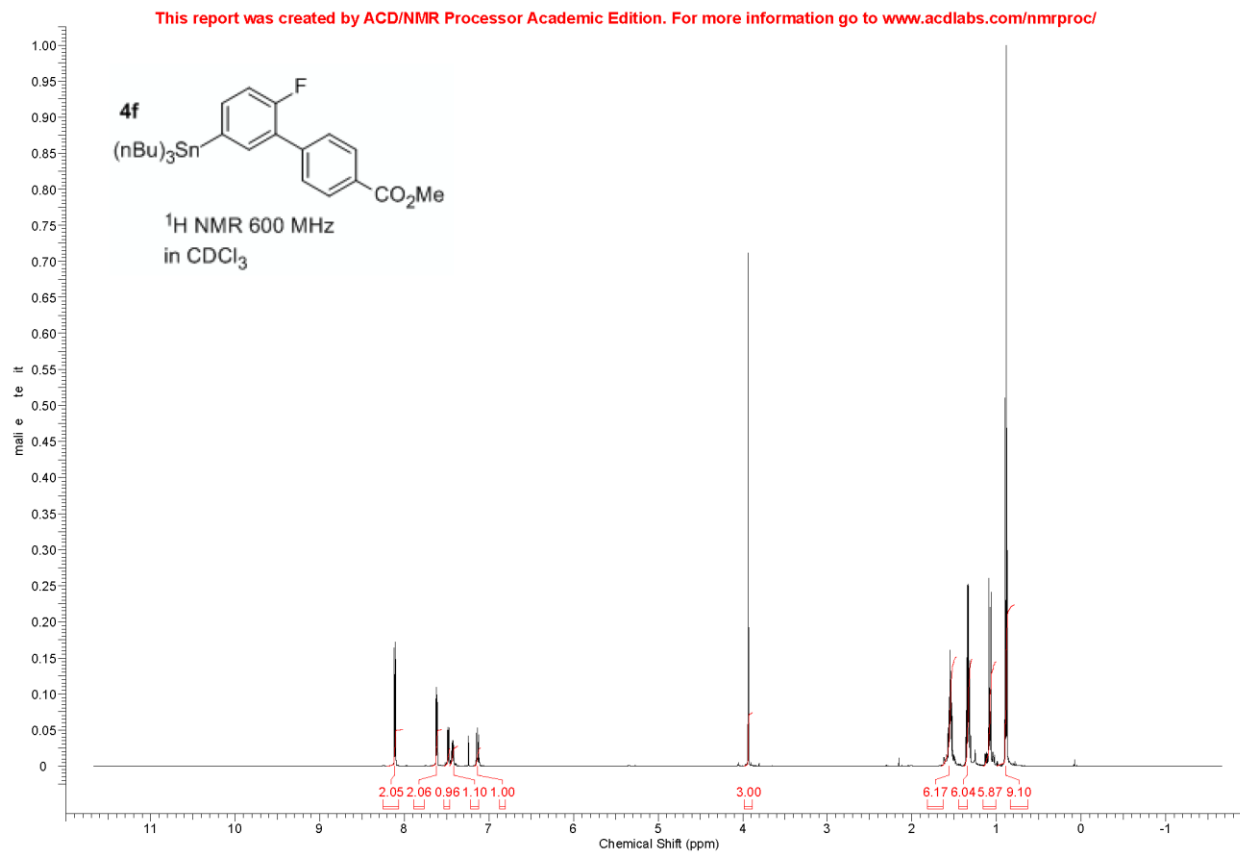


Figure 143 ^{119}Sn NMR of compound 5

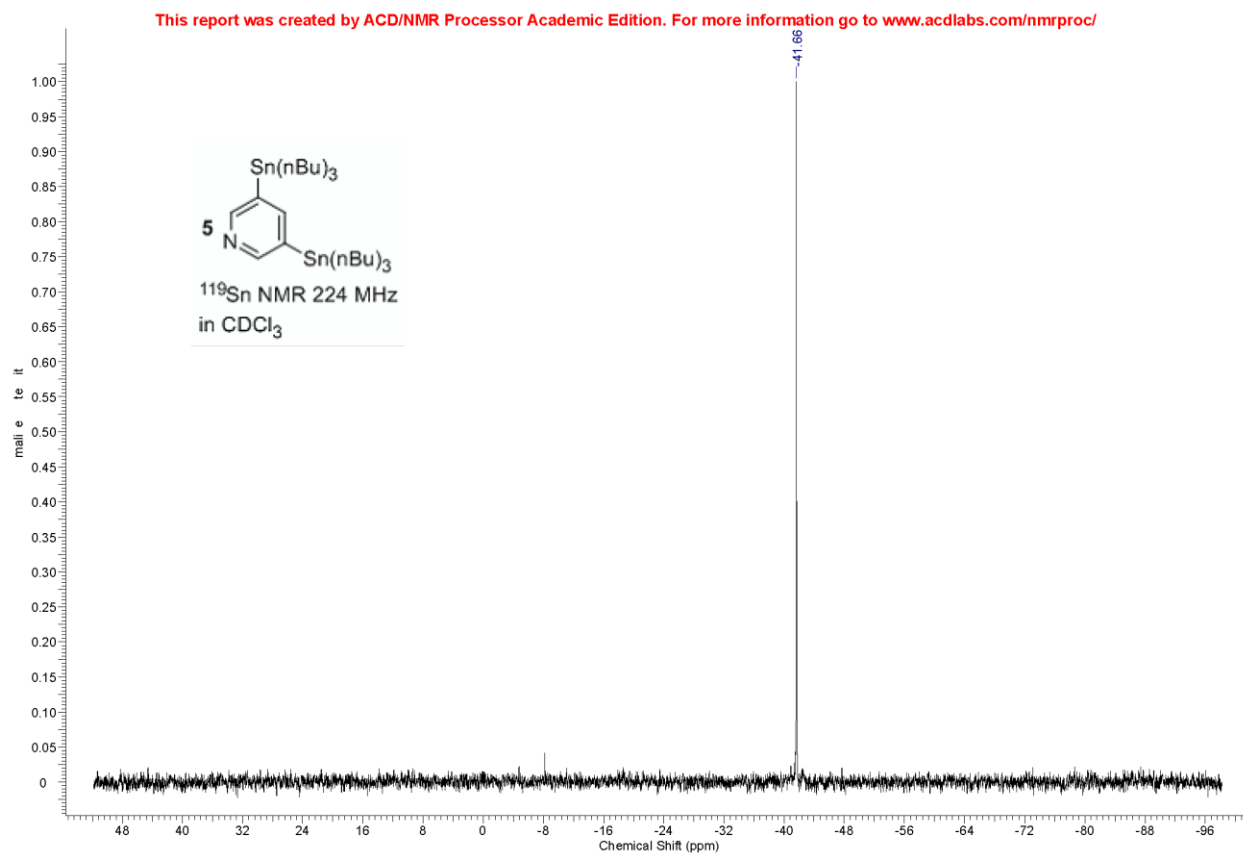


Figure 144 ^{13}C NMR of compound 5

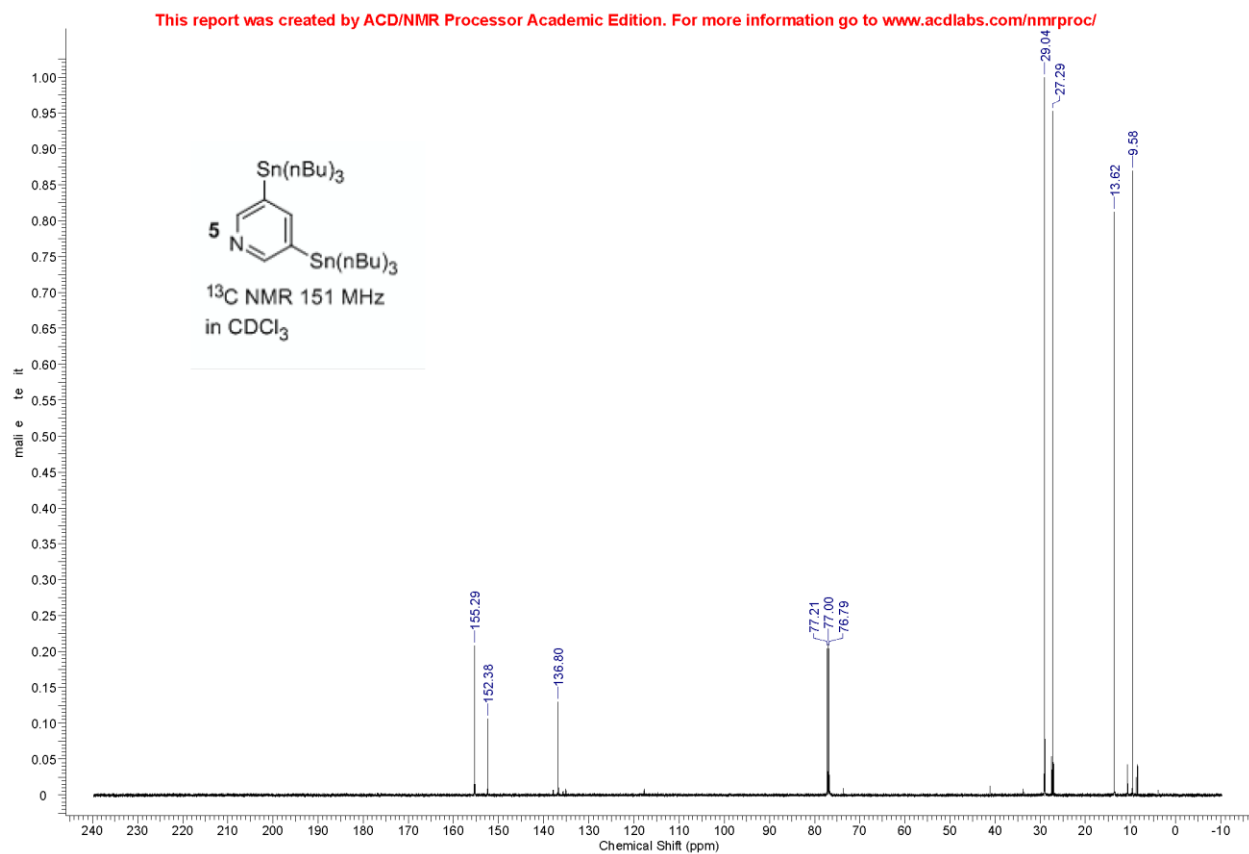


Figure 145 ^1H NMR of compound 5

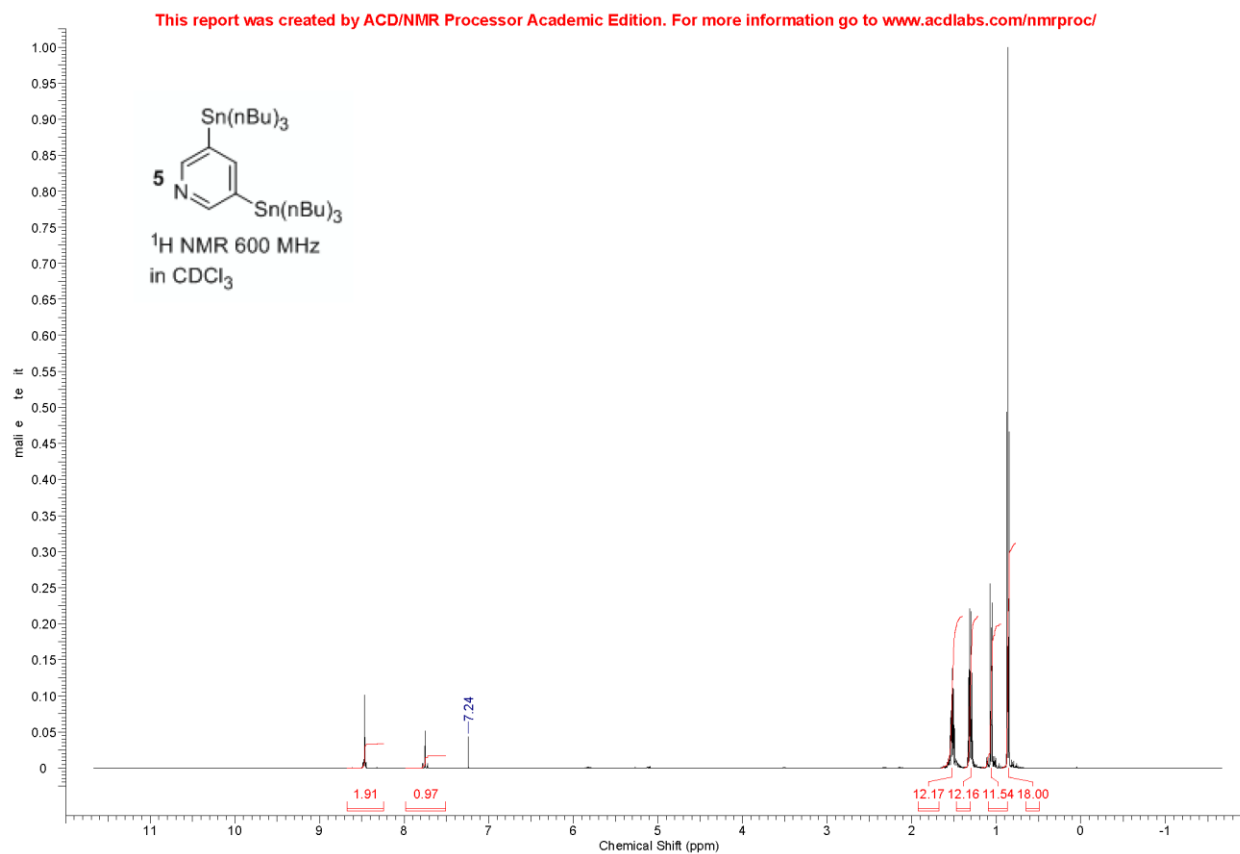


Figure 146 ^{119}Sn NMR of compound 7

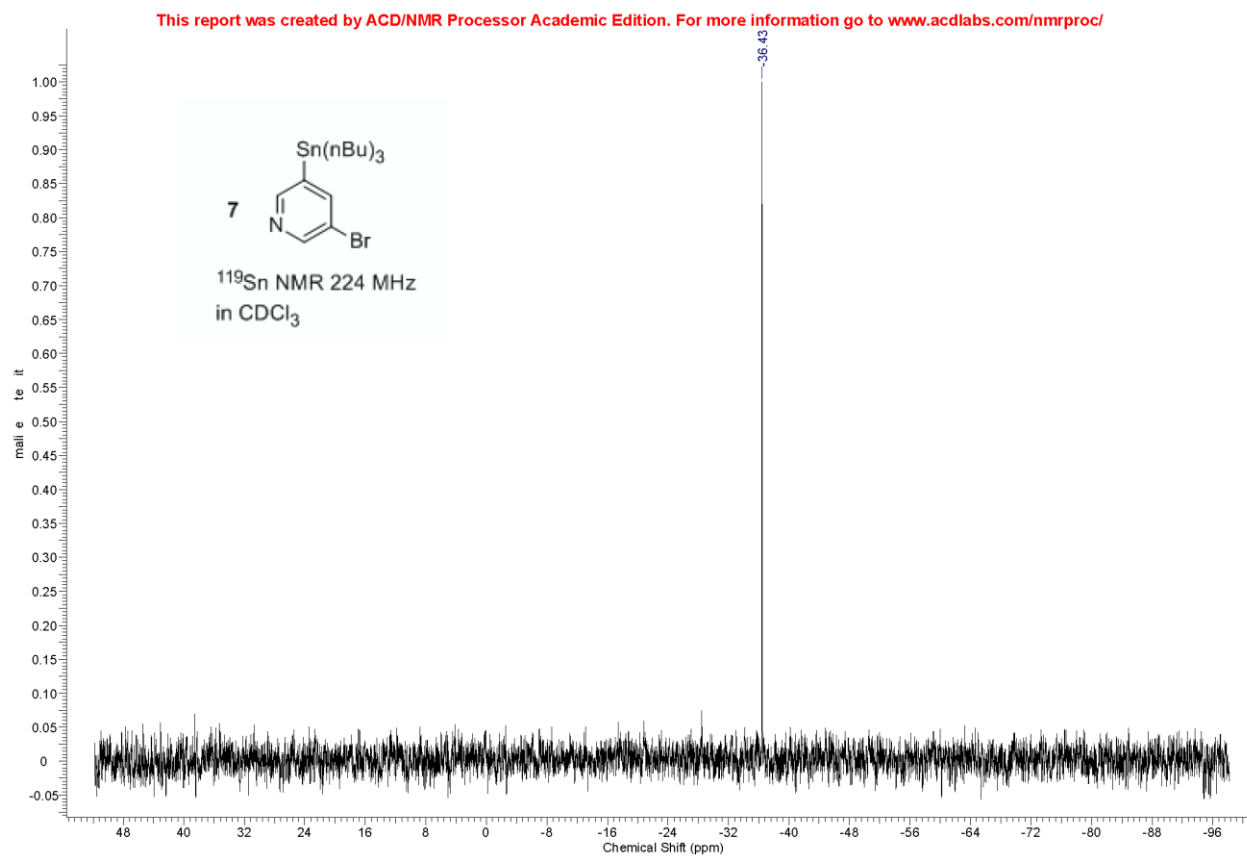


Figure 147 ^{13}C NMR of compound 7

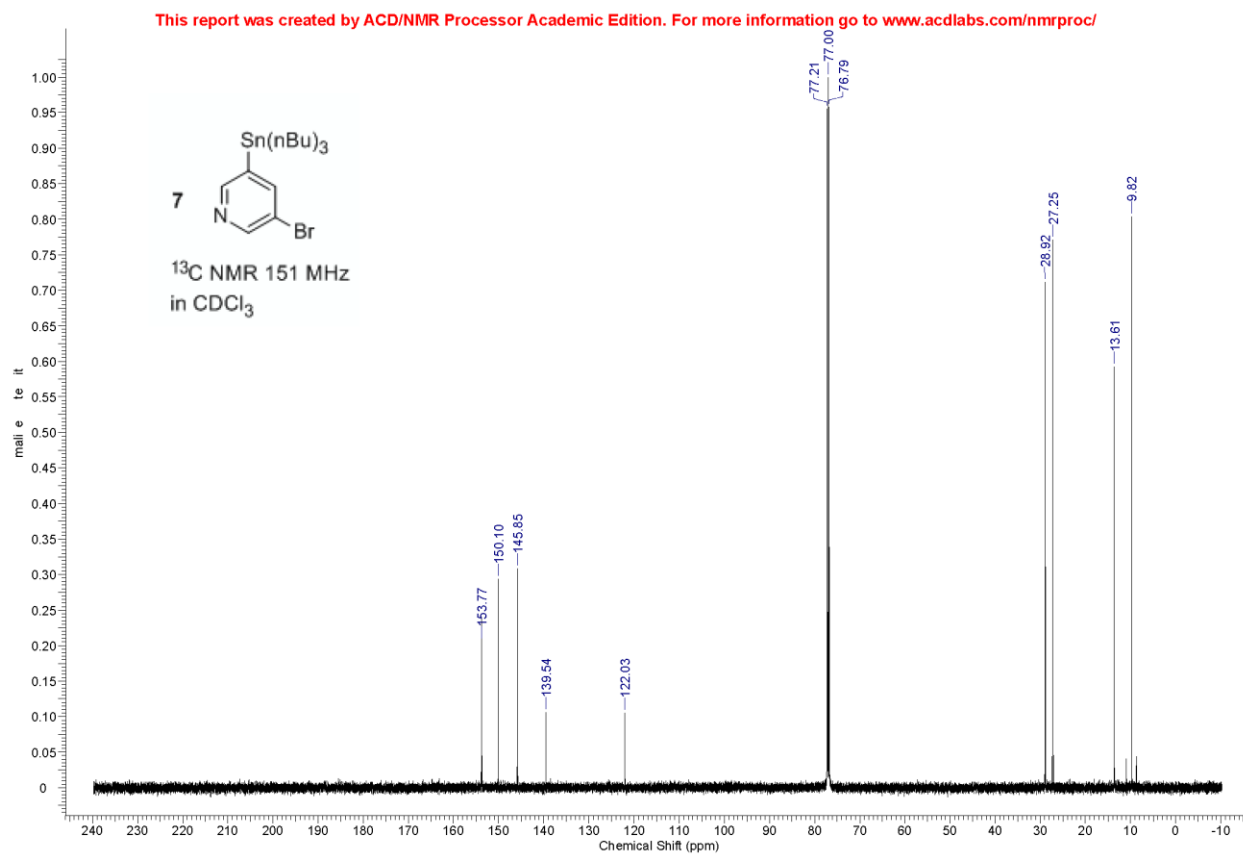


Figure 148 ^1H NMR of compound 7

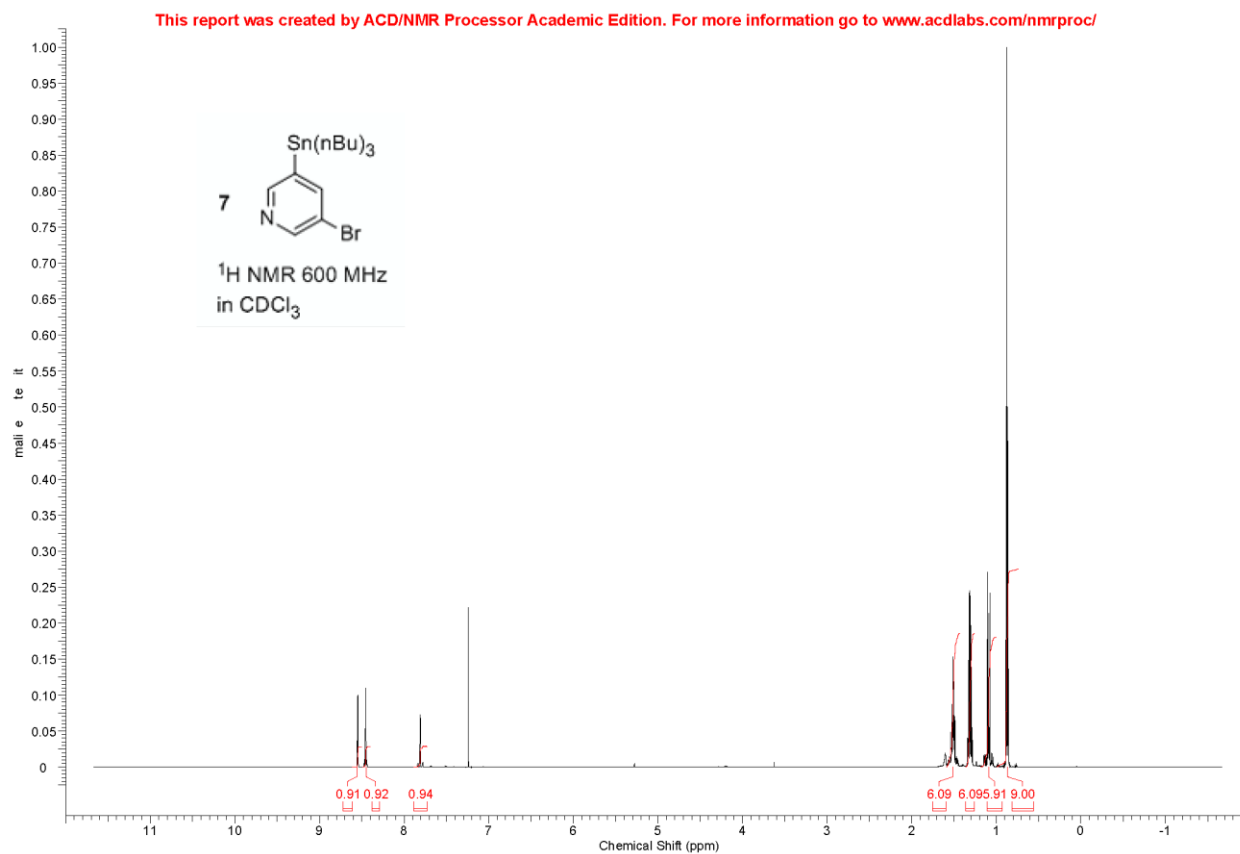


Figure 149 ^{13}C NMR of compound 11

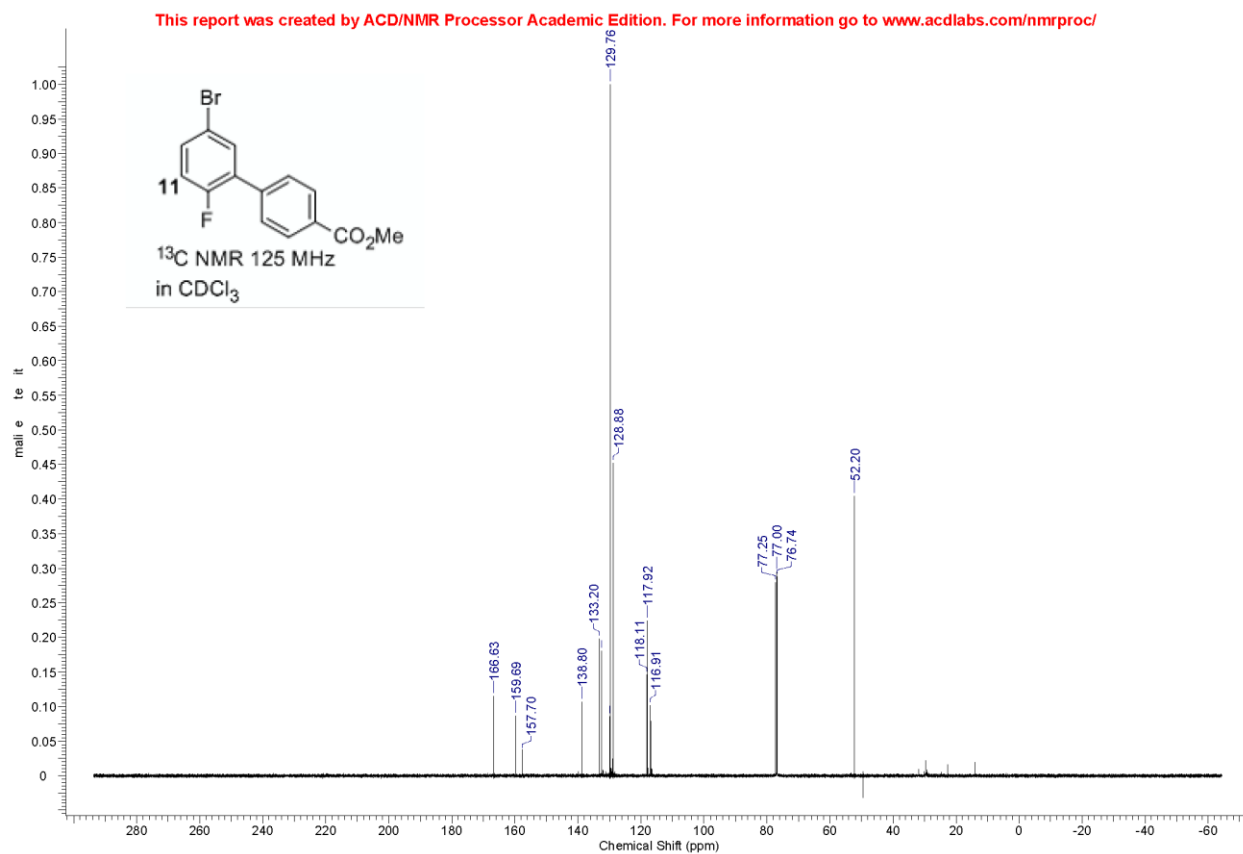


Figure 150 ^{19}F NMR of compound 11

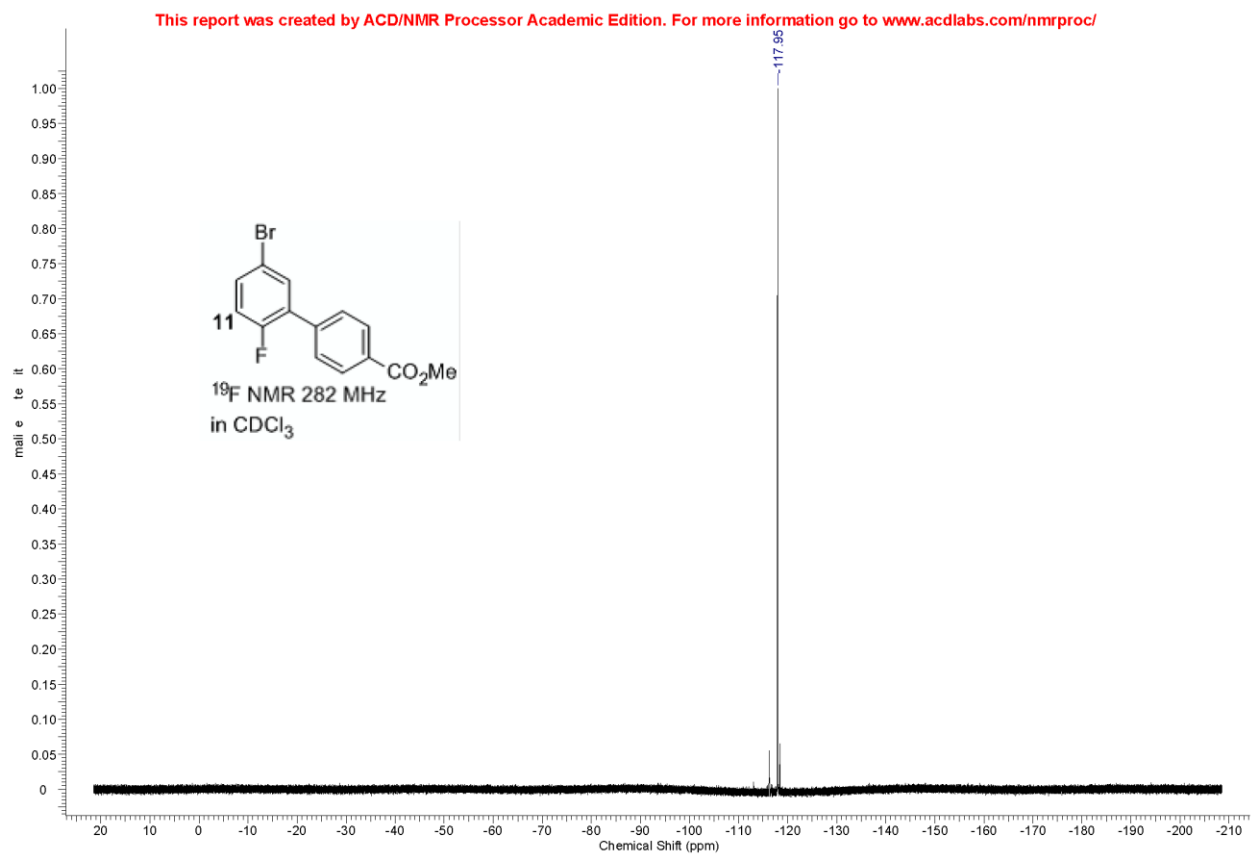


Figure 151 ^1H NMR of compound 11

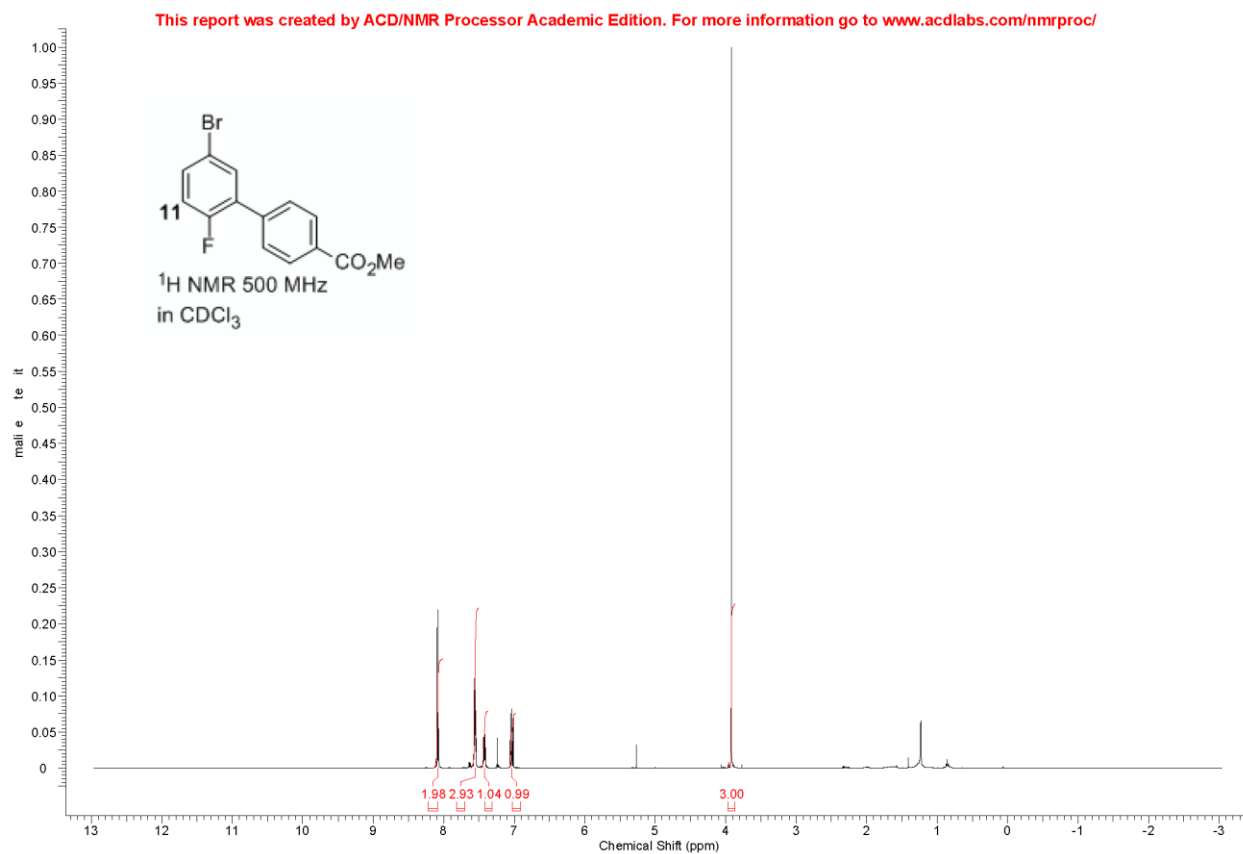


Figure 152 ^1H NMR of mixture of compounds **13d** and **13d'**

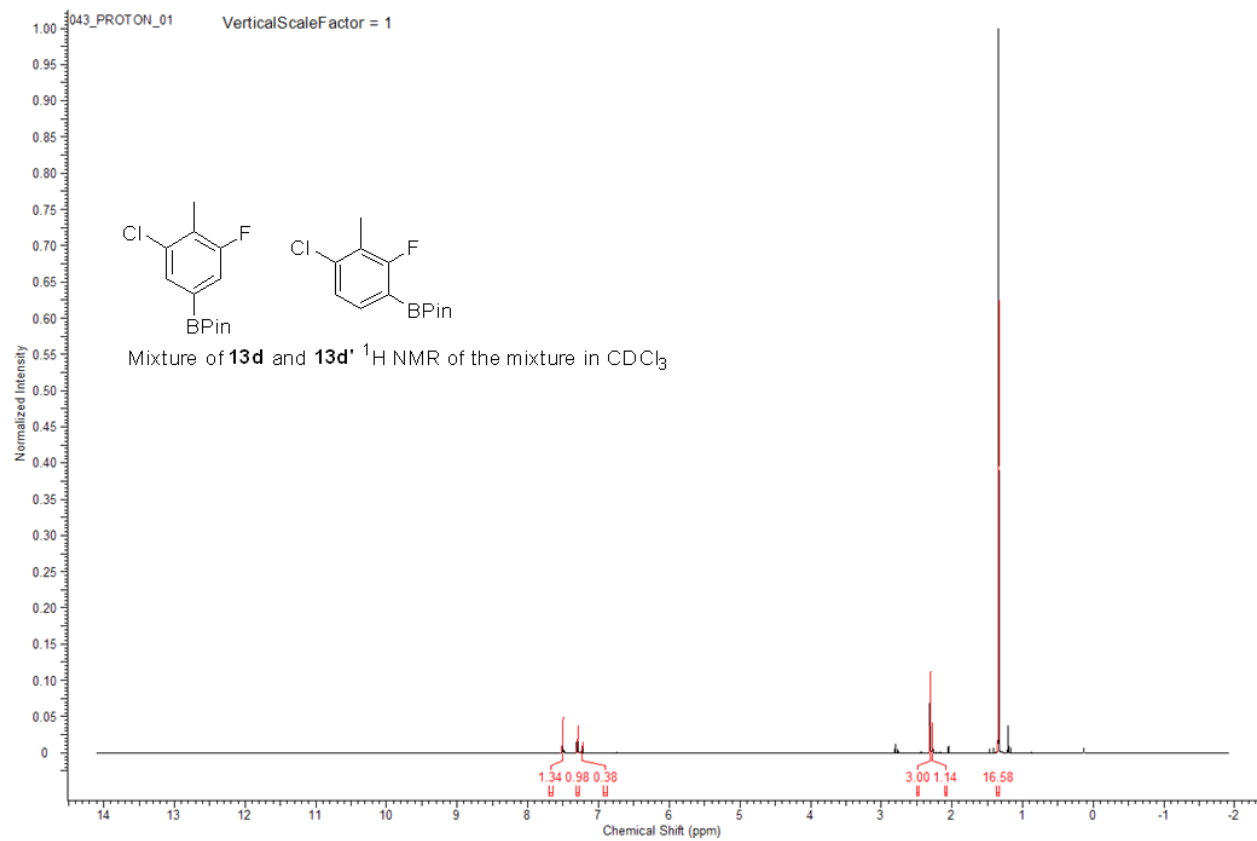


Figure 153 ^{11}B NMR of mixture of compounds **13d** and **13d'**

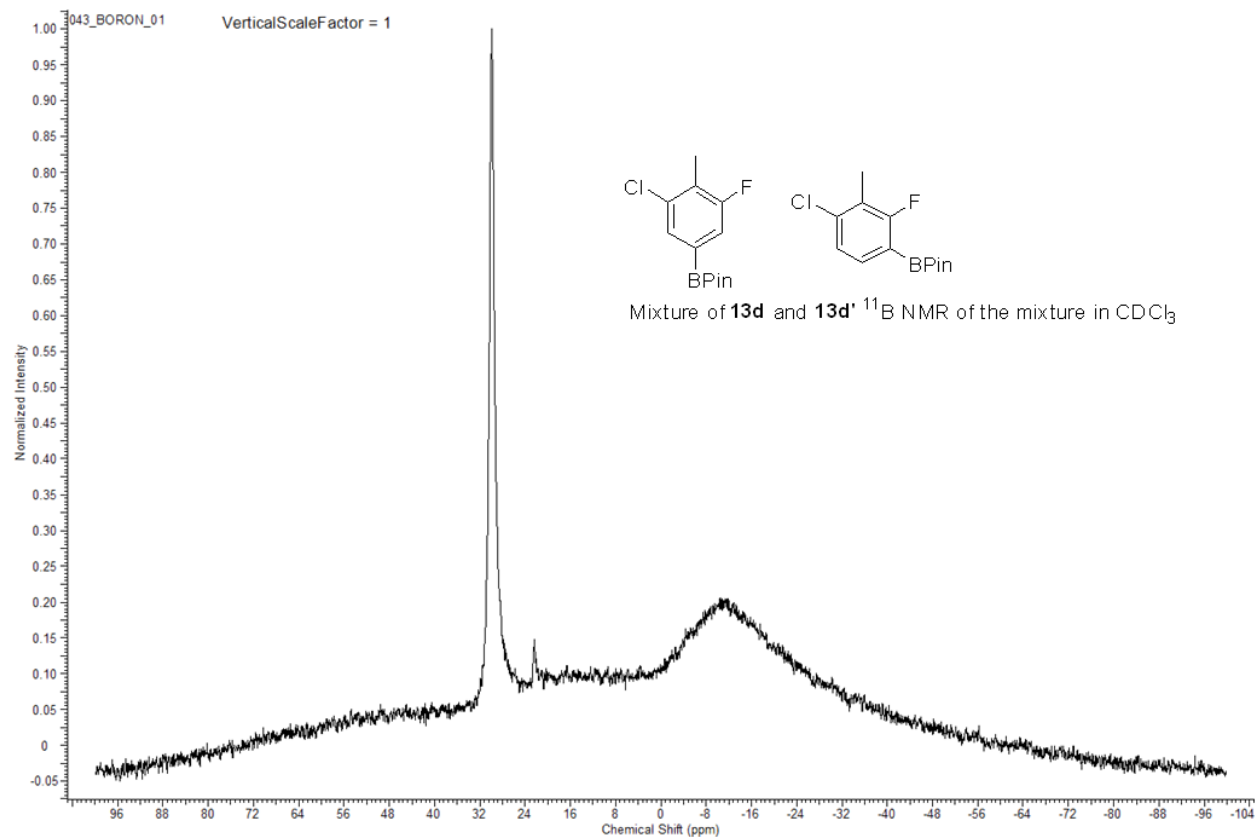


Figure 154 ^{13}C NMR of mixture of compounds 13d and 13d'

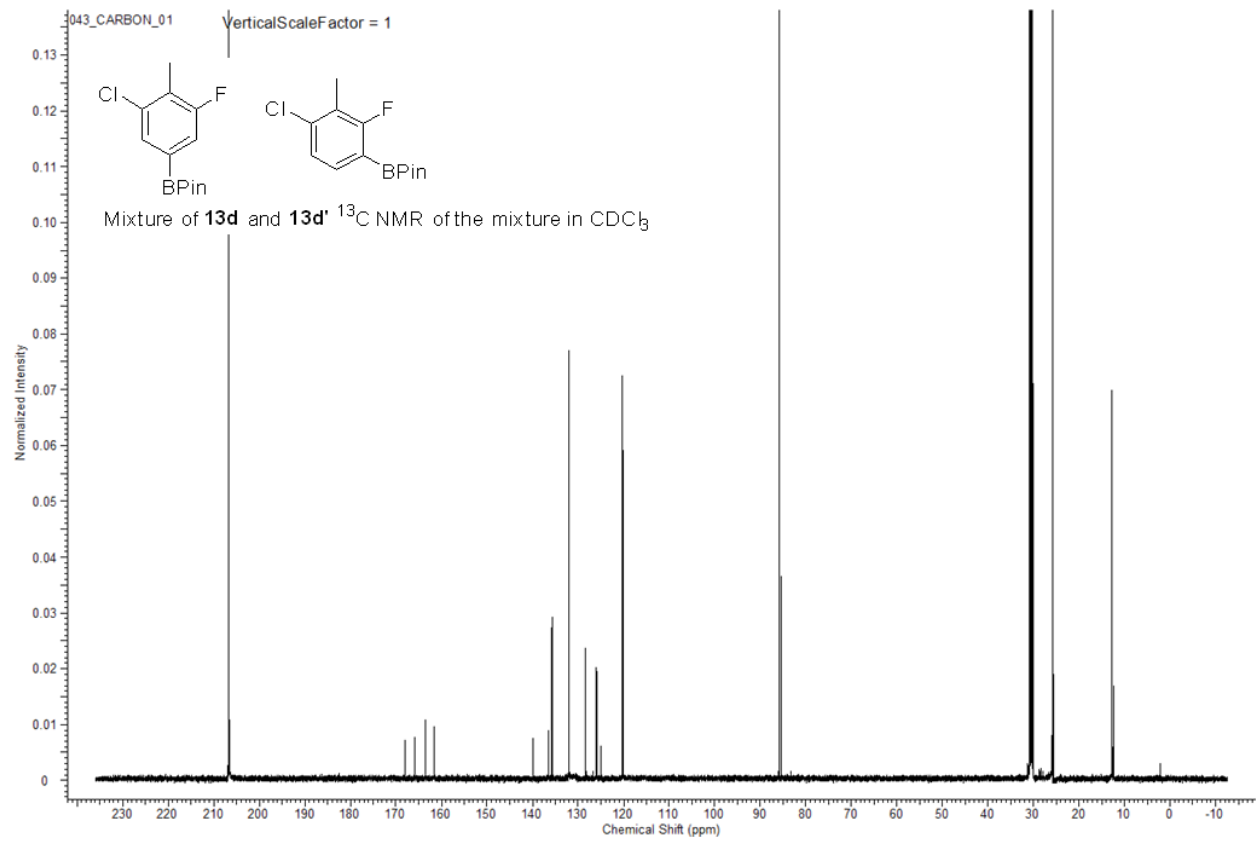


Figure 155 ^{19}F NMR of mixture of compounds **13d** and **13d'**

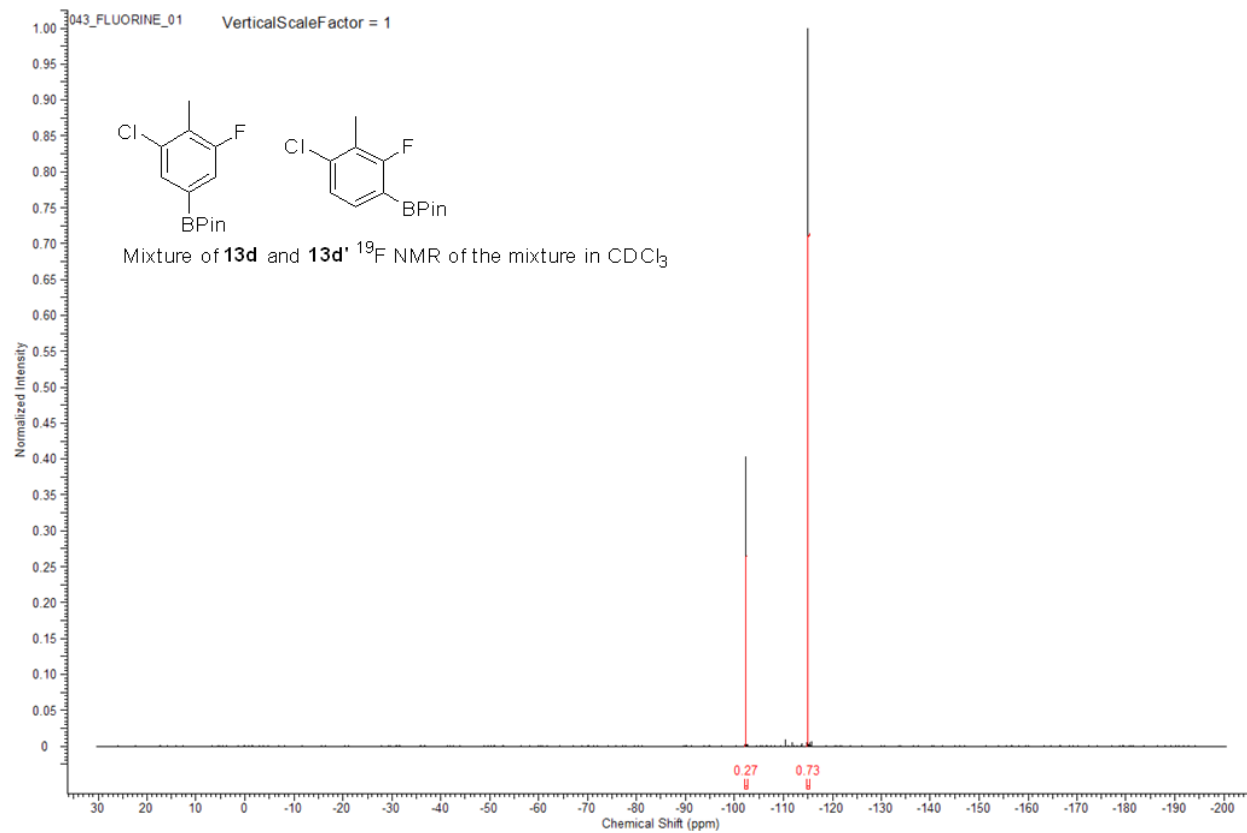


Figure 156 ^1H NMR of mixture of compounds **13e** and **13e'**

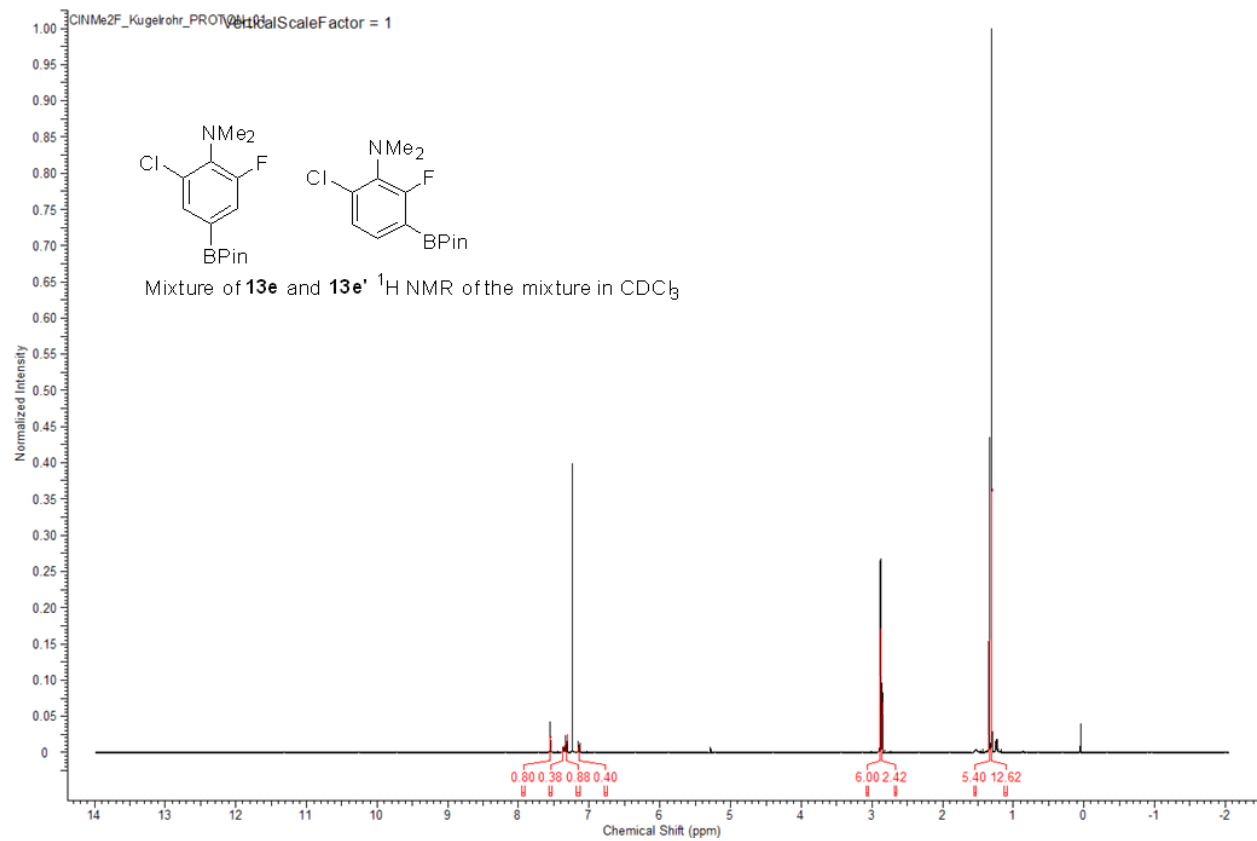


Figure 157 ^{11}B NMR of mixture of compounds **13e** and **13e'**

This report was created by ACD/NMR Processor Academic Edition. For more information go to www.acdlabs.com/nmrproc/

CINMe2F dtbpy THF 11B

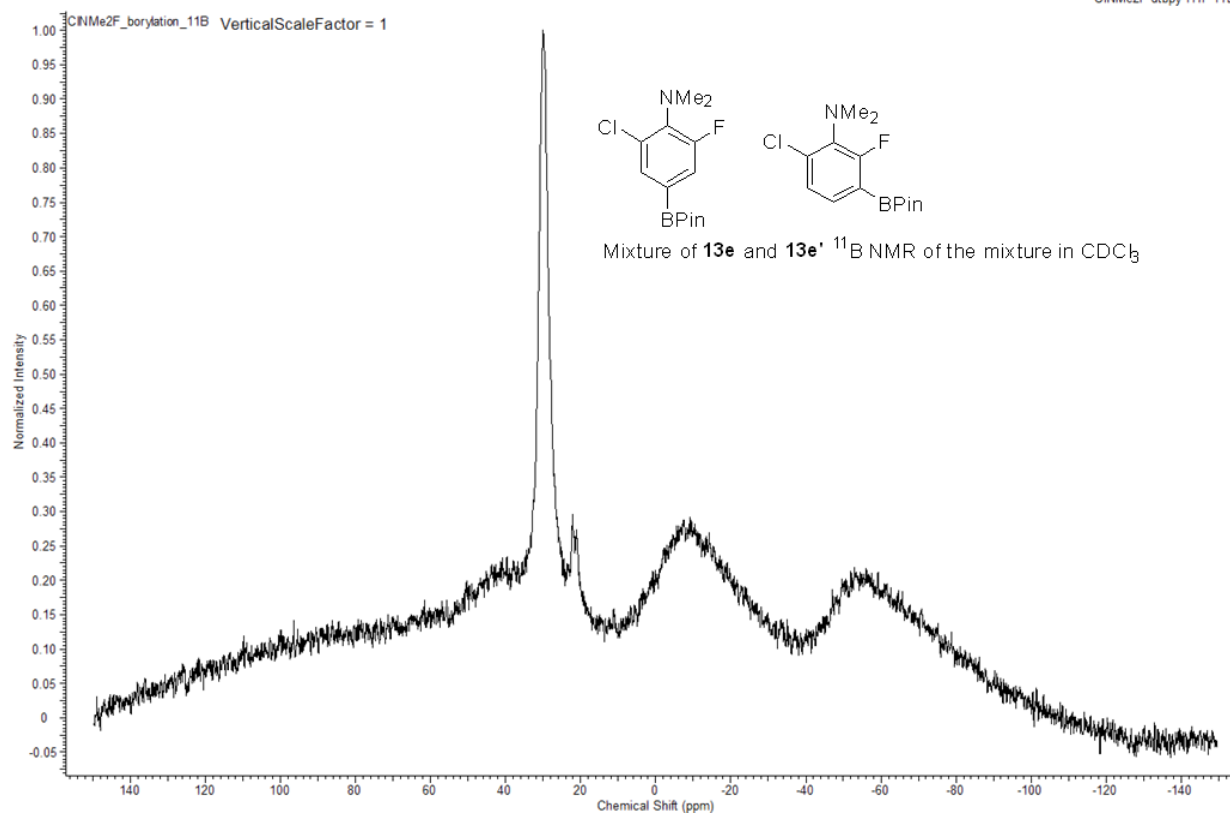


Figure 158 ^{13}C NMR of mixture of compounds **13e** and **13e'**

This report was created by ACD/NMR Processor Academic Edition. For more information go to www.acdlabs.com/nmrproc/

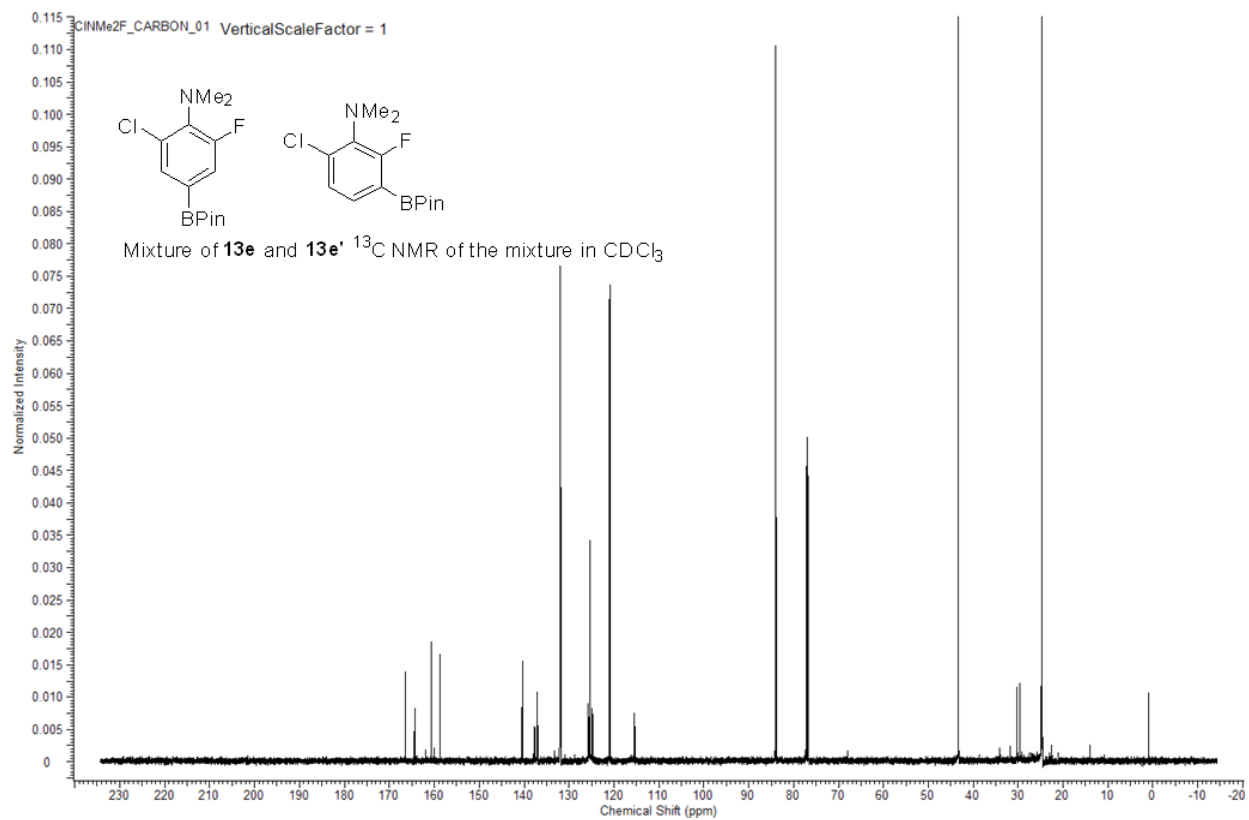


Figure 159 ^{19}F NMR of mixture of compounds **13e** and **13e'**

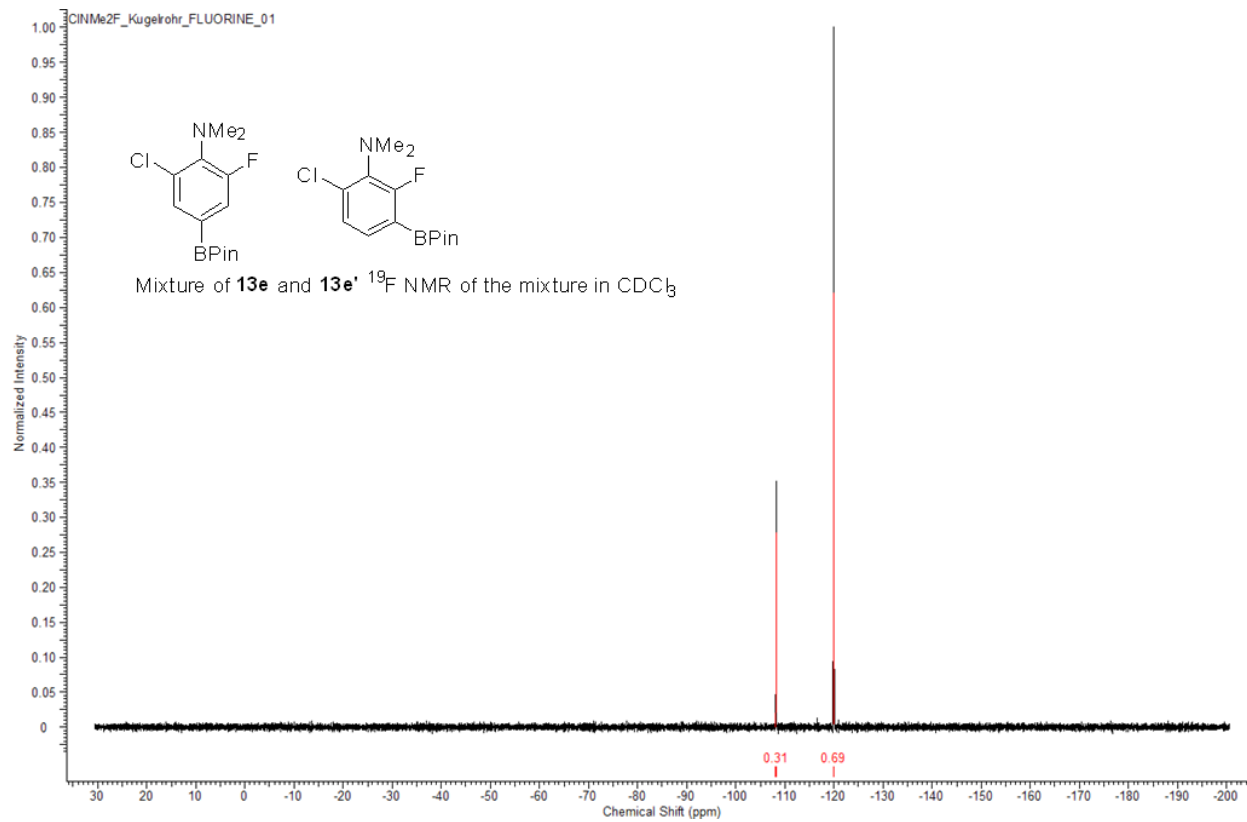


Figure 160 ^1H NMR of mixture of compounds **13f** and **13f'**

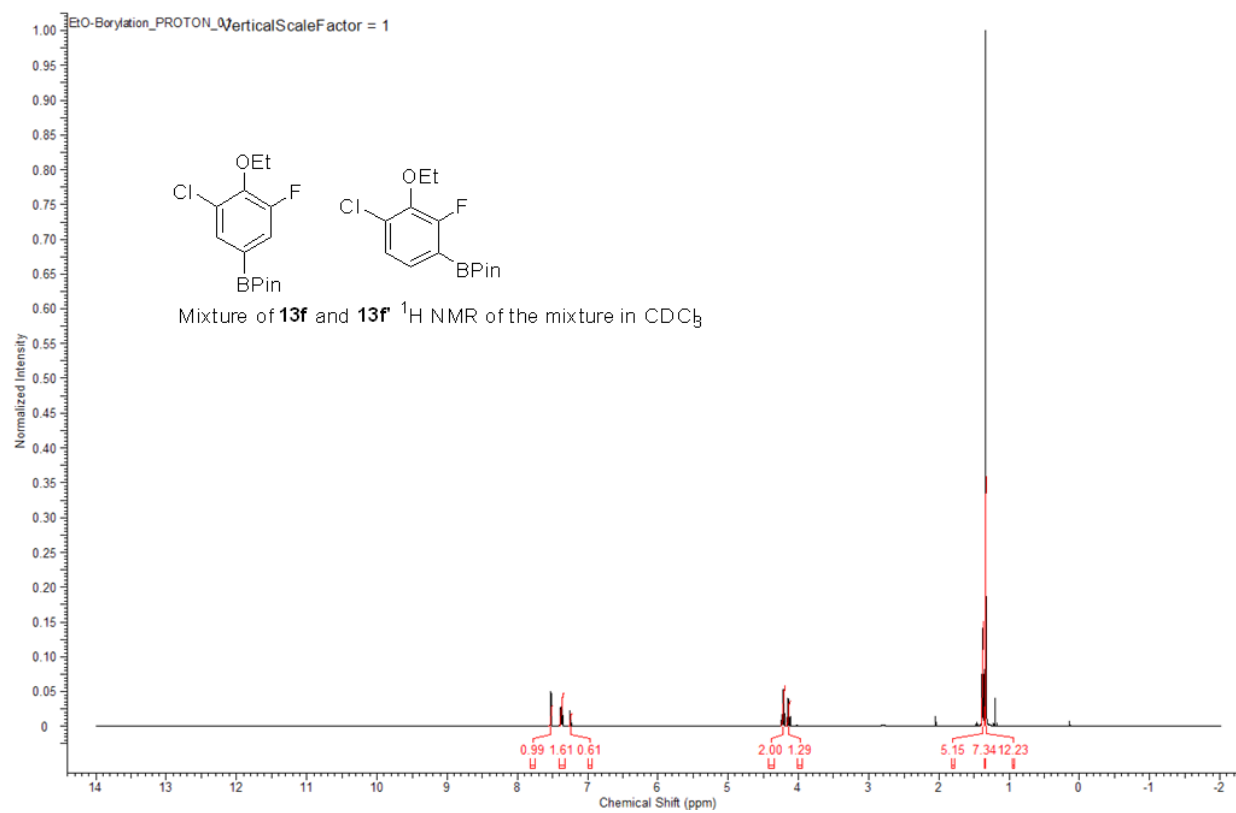


Figure 161 ^{11}B NMR of mixture of compounds **13f** and **13f'**

This report was created by ACD/NMR Processor Academic Edition. For more information go to www.acdlabs.com/nmrproc/

A24h 11B

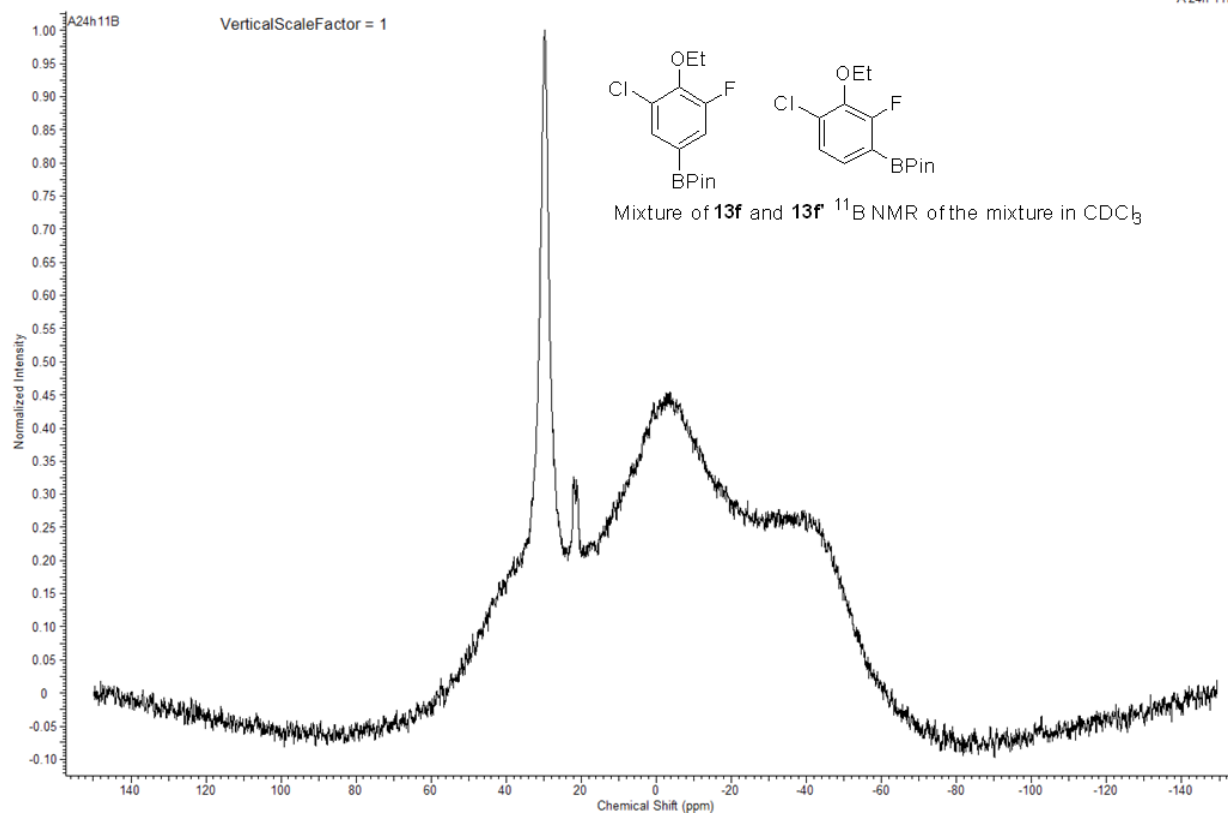


Figure 162 ^{13}C NMR of mixture of compounds **13f** and **13f'**

This report was created by ACD/NMR Processor Academic Edition. For more information go to www.acdlabs.com/nmrproc/

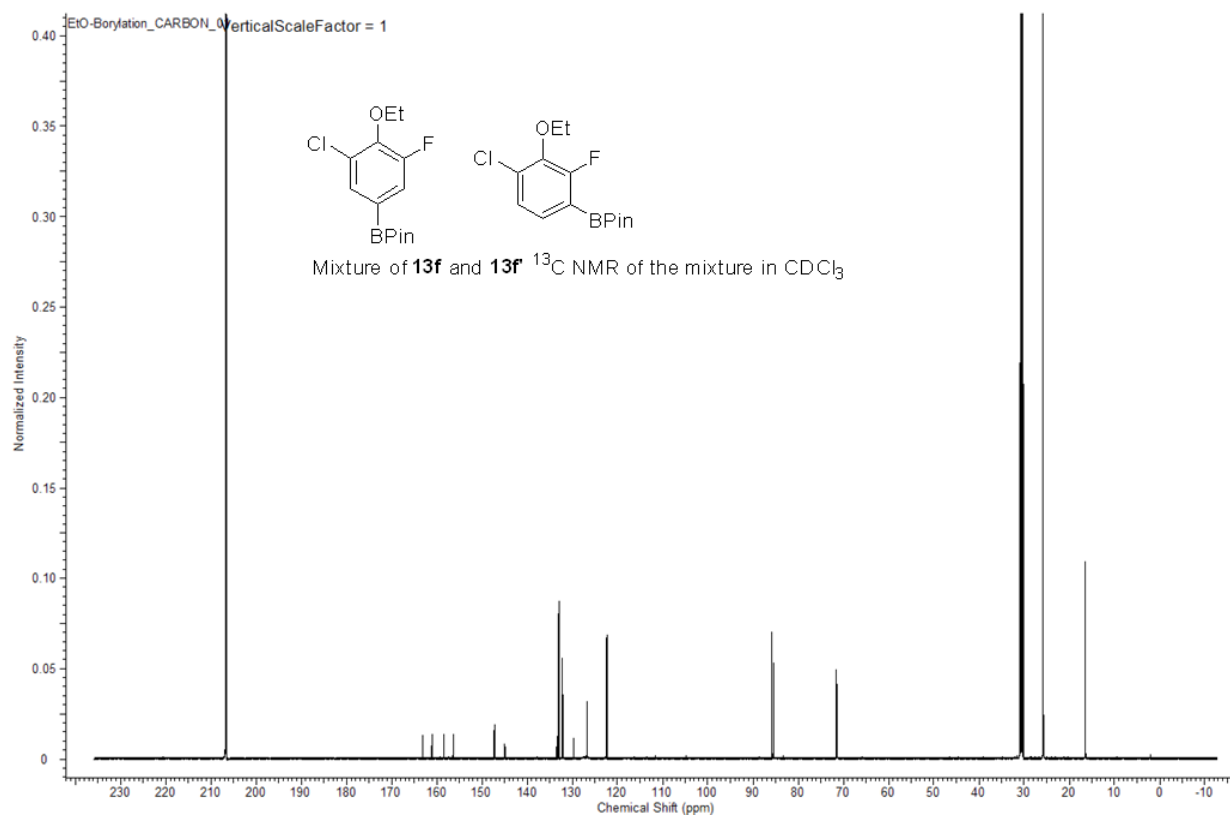


Figure 163 ^{19}F NMR of mixture of compounds **13f** and **13f'**

This report was created by ACD/NMR Processor Academic Edition. For more information go to www.acdlabs.com/nmrproc/

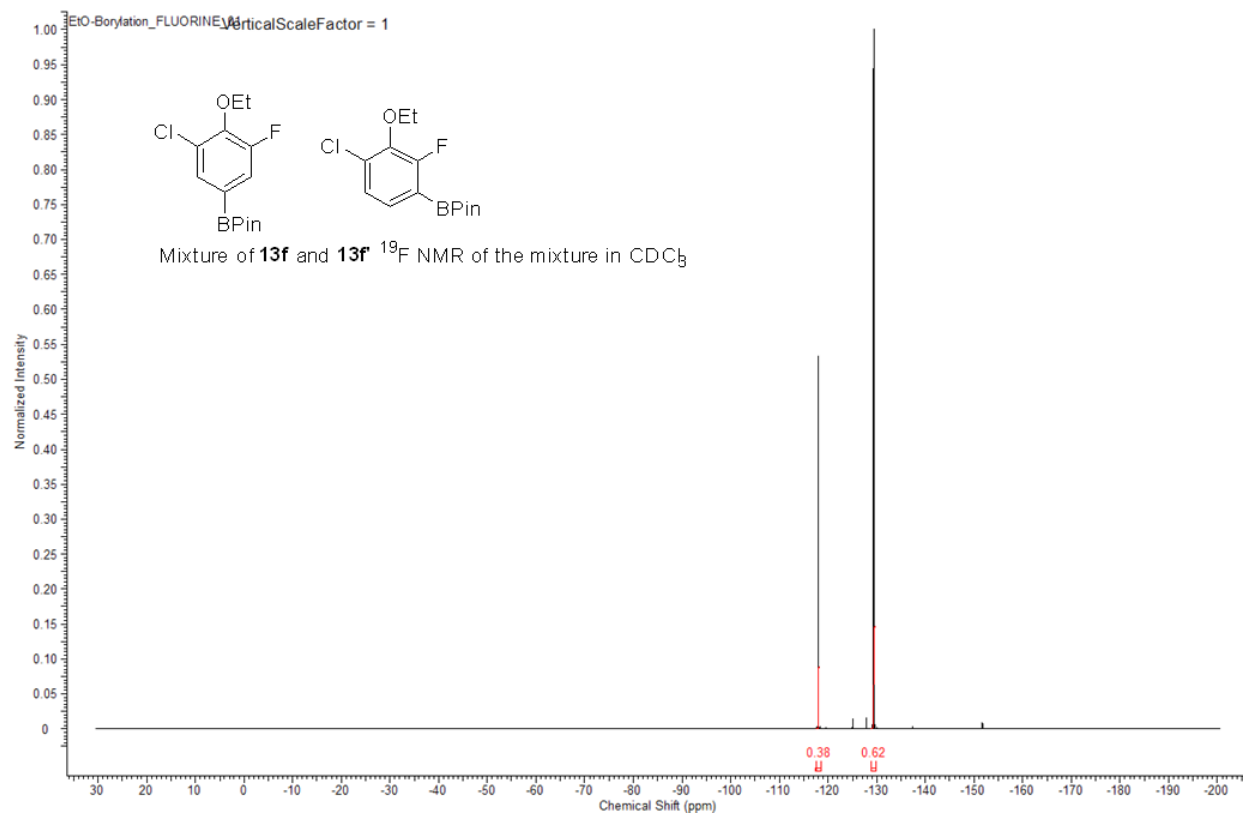


Figure 164 ^1H NMR of mixture of compounds **13a** and **13a'**

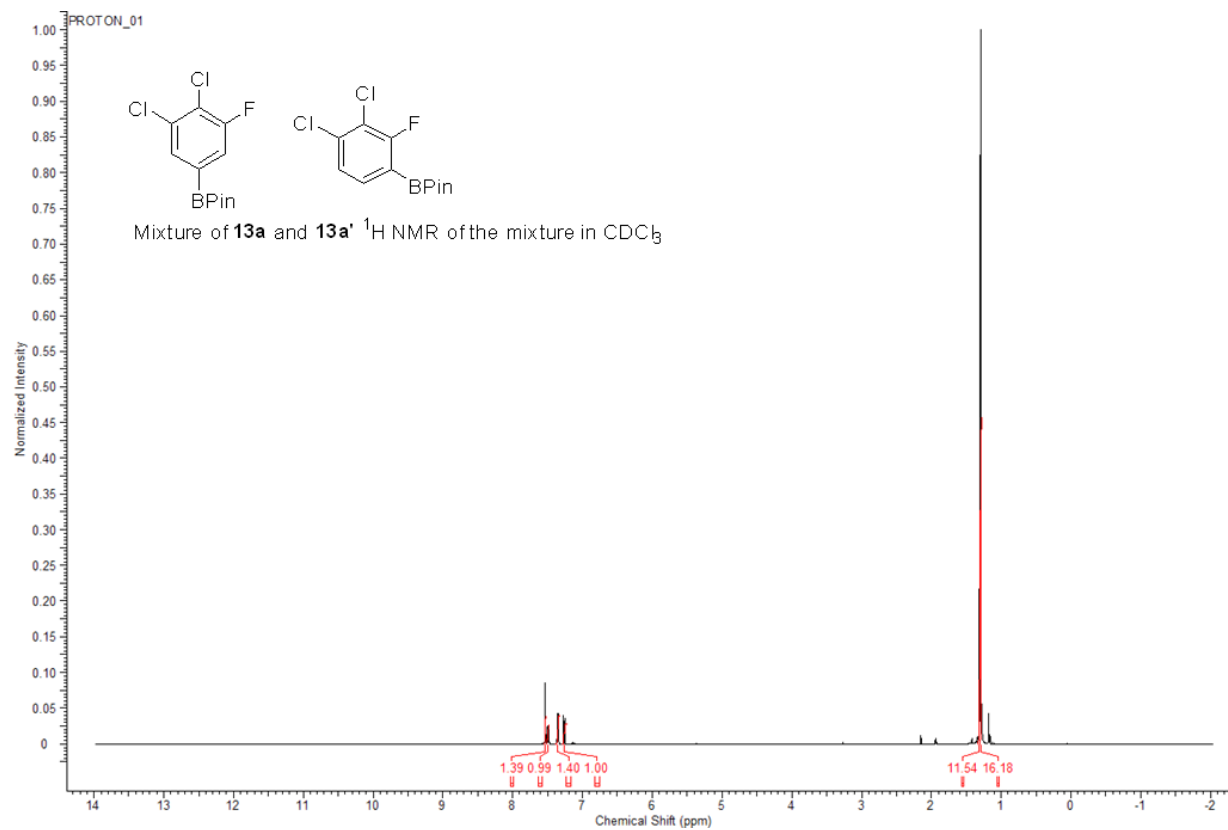


Figure 165 ^{11}B NMR of mixture of compounds **13a** and **13a'**

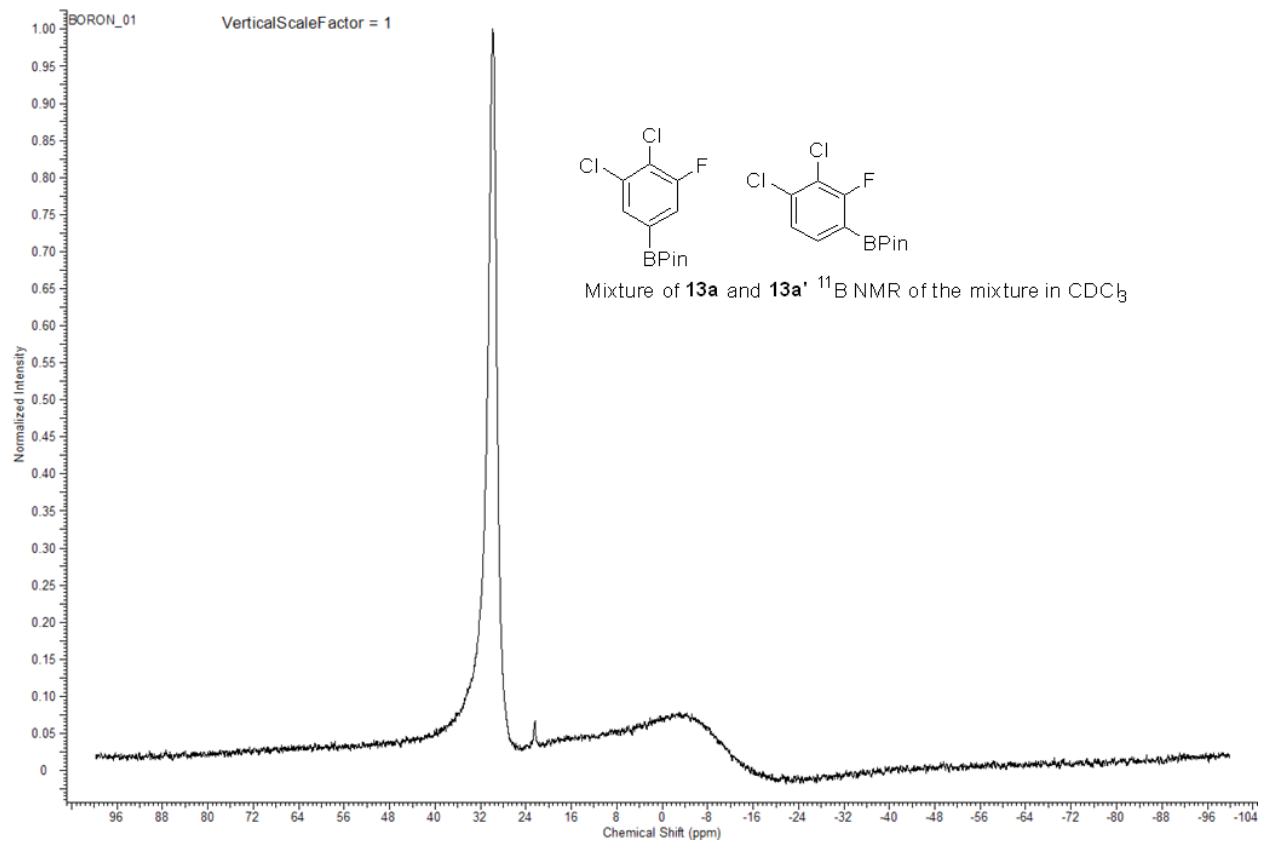


Figure 166 ^{13}C NMR of mixture of compounds **13a** and **13a'**

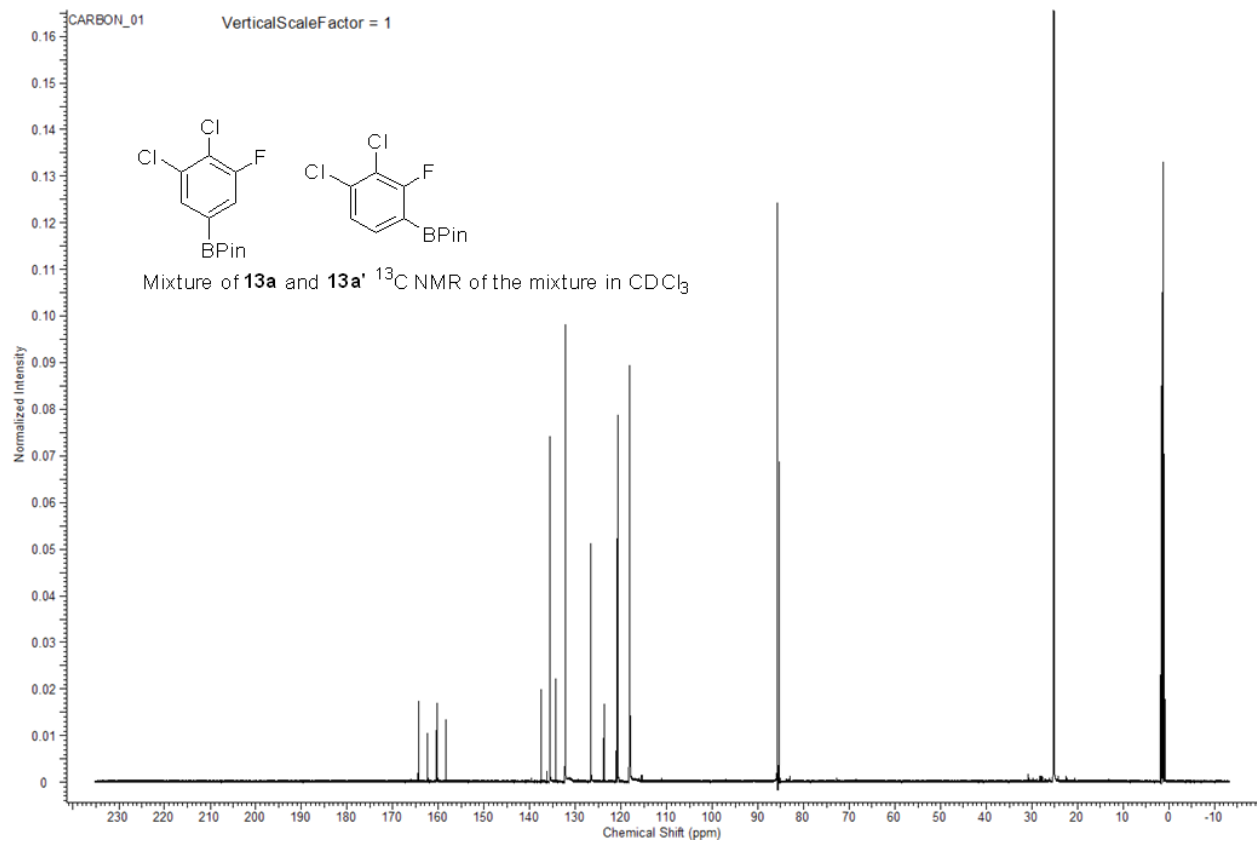


Figure 167 ^{19}F NMR of mixture of compounds **13a** and **13a'**

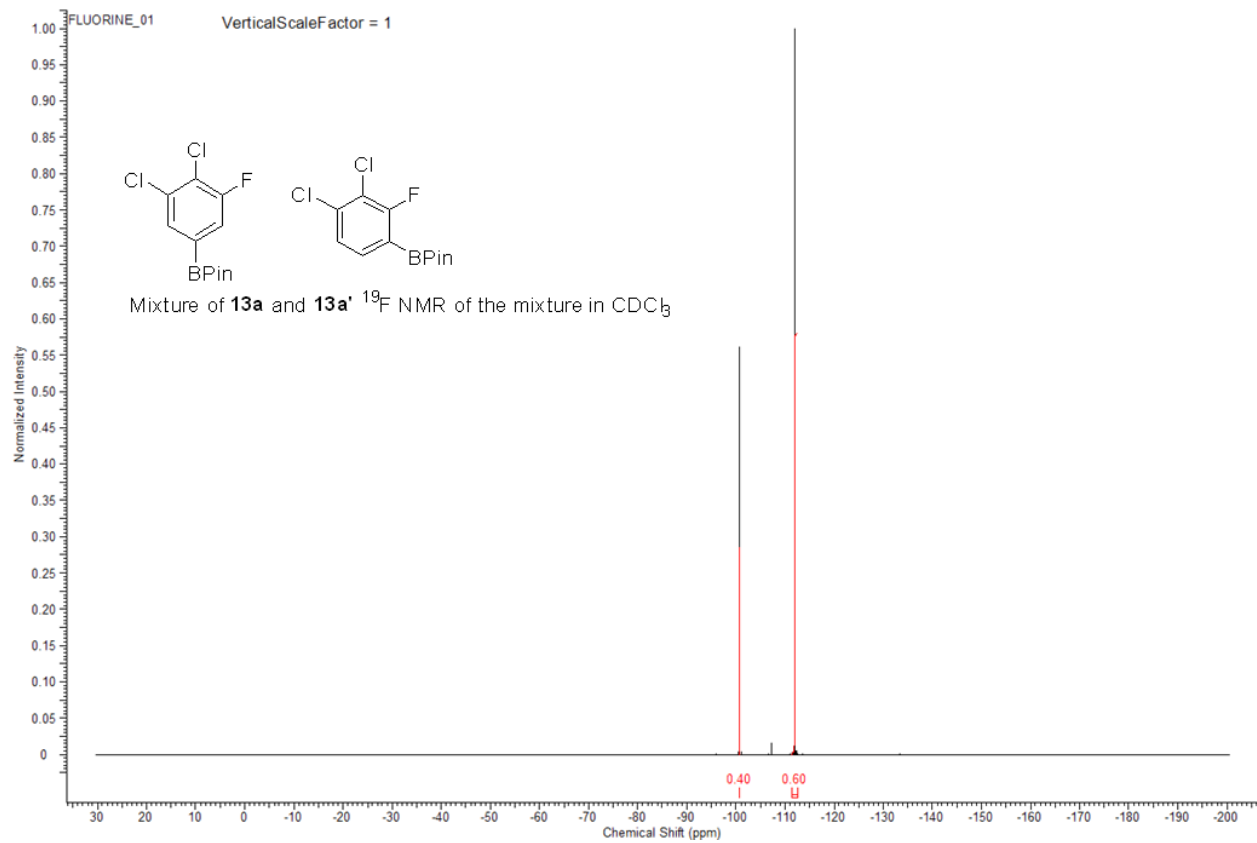


Figure 168 ^1H NMR of mixture of compounds **13c** and **13c'**

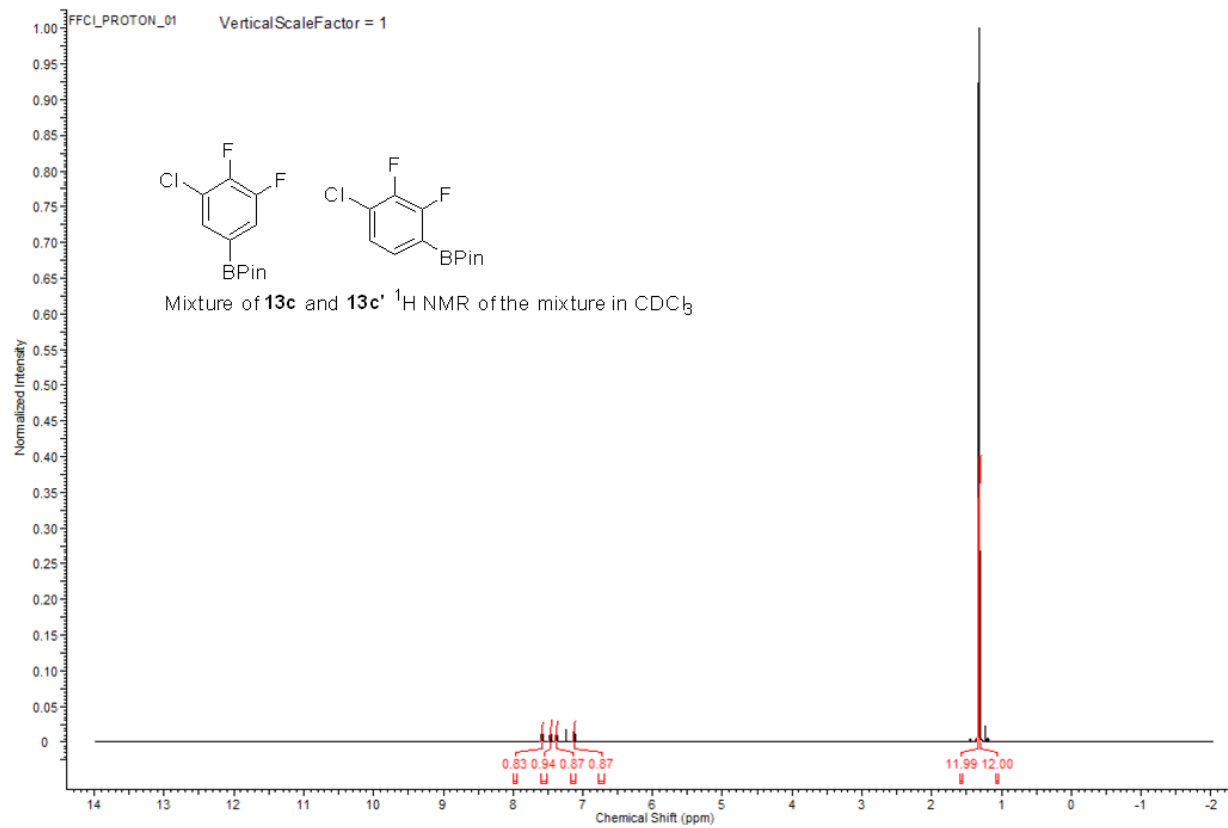


Figure 169 ^{11}B NMR of mixture of compounds **13c** and **13c'**

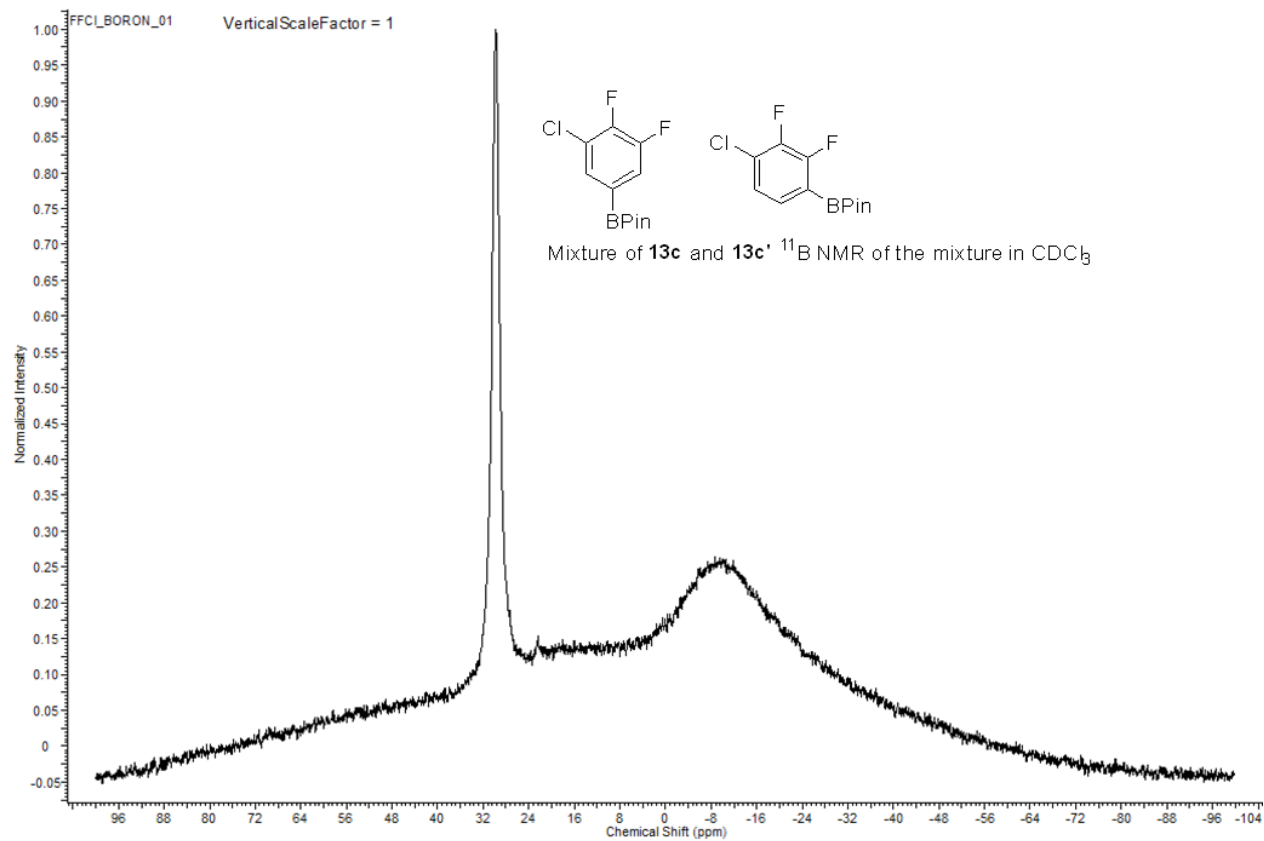


Figure 170 ^{13}C NMR of mixture of compounds **13c** and **13c'**

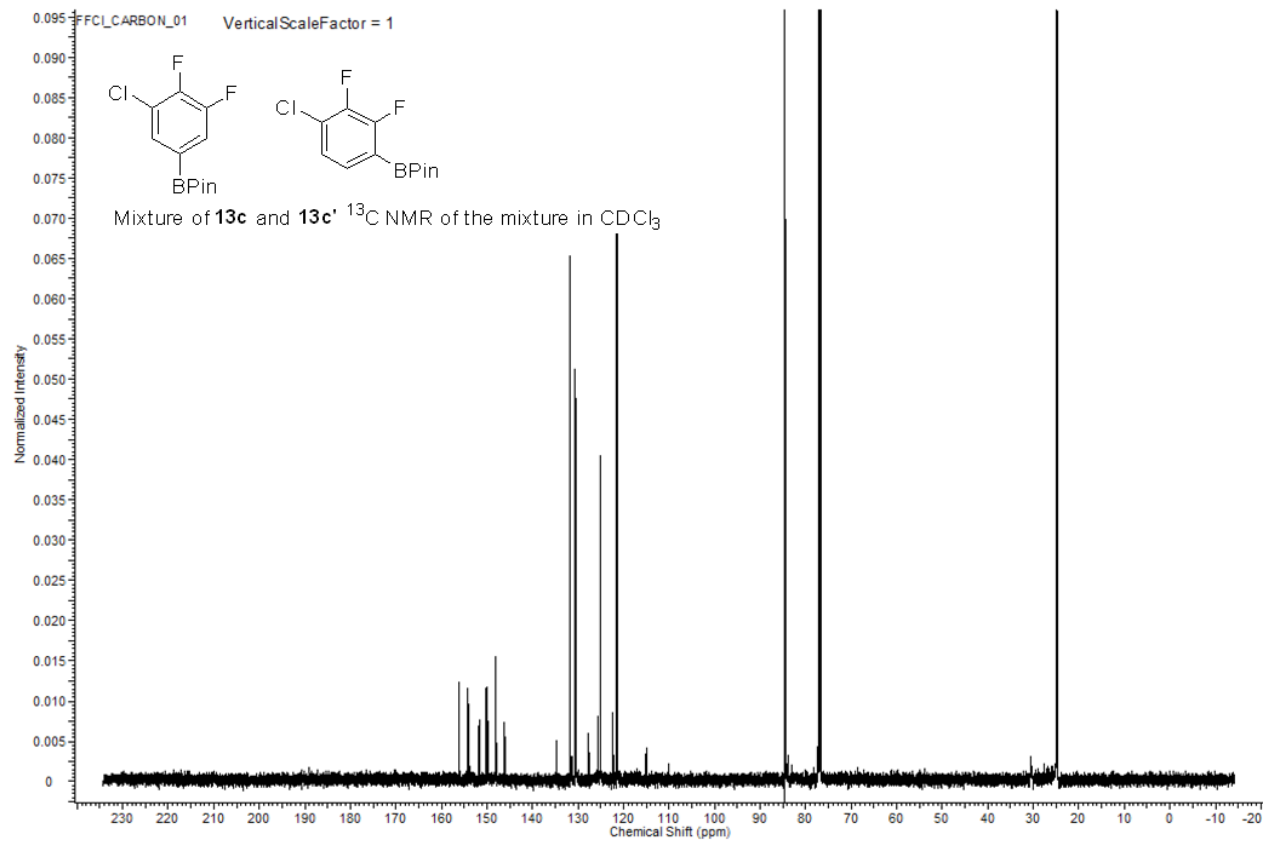


Figure 171 ^{19}F NMR of mixture of compounds **13c** and **13c'**

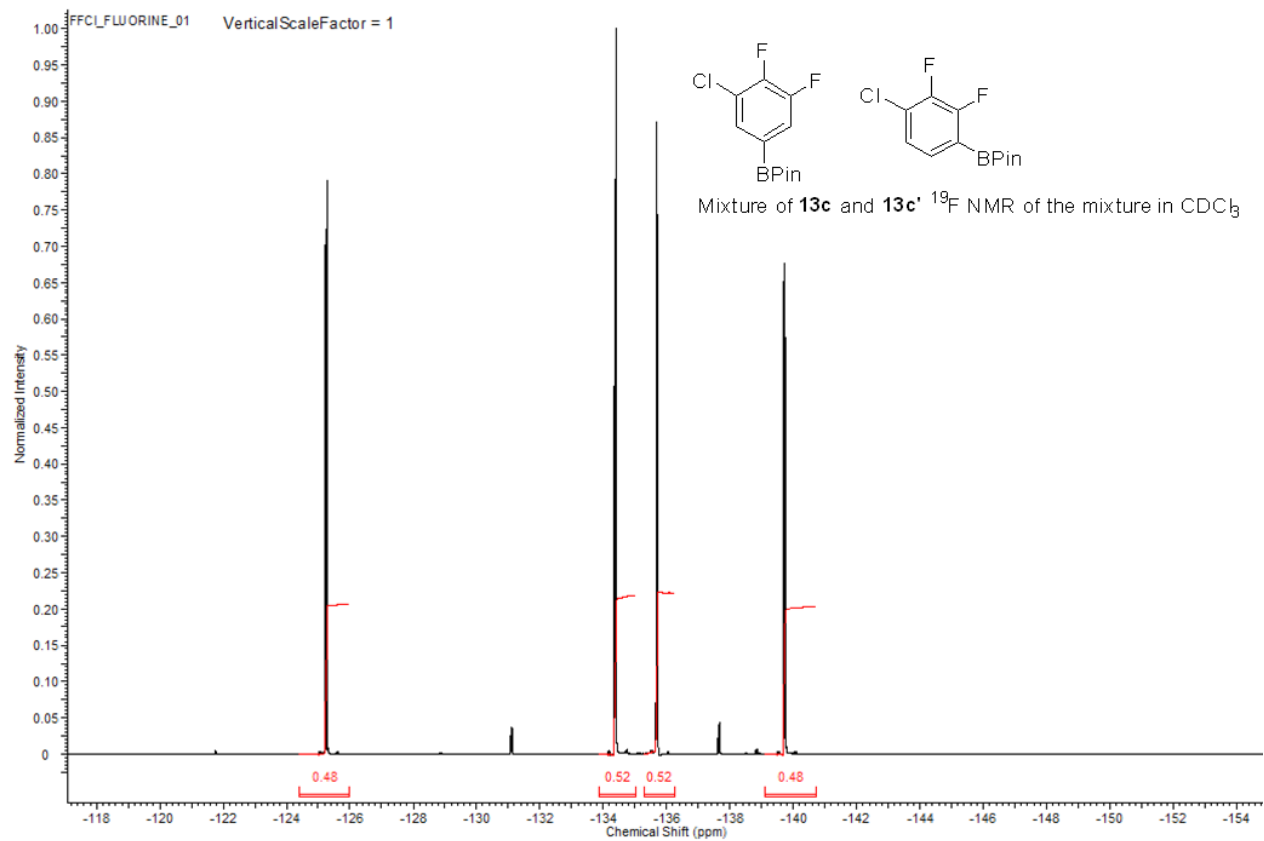


Figure 172 ^1H NMR of mixture of compounds **13b** and **13b'**

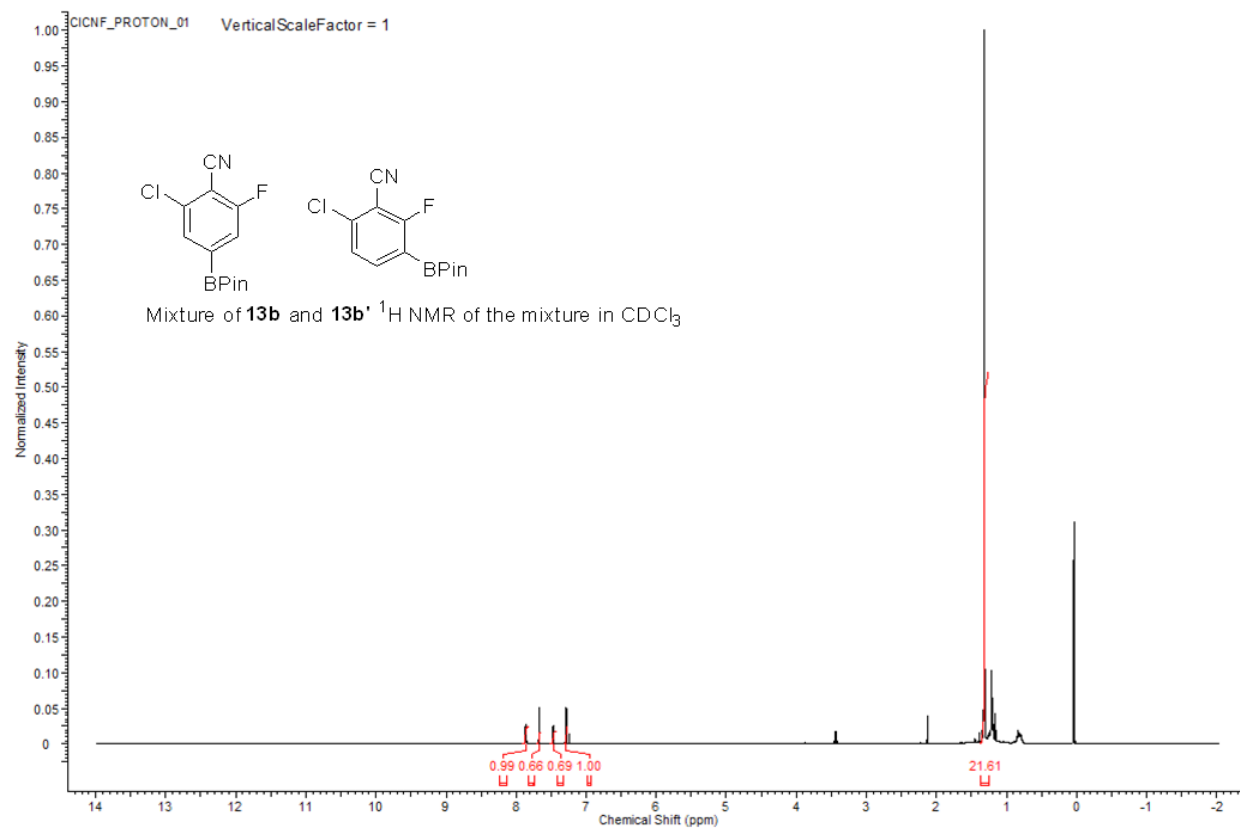


Figure 173 ^{11}B NMR of mixture of compounds **13b** and **13b'**

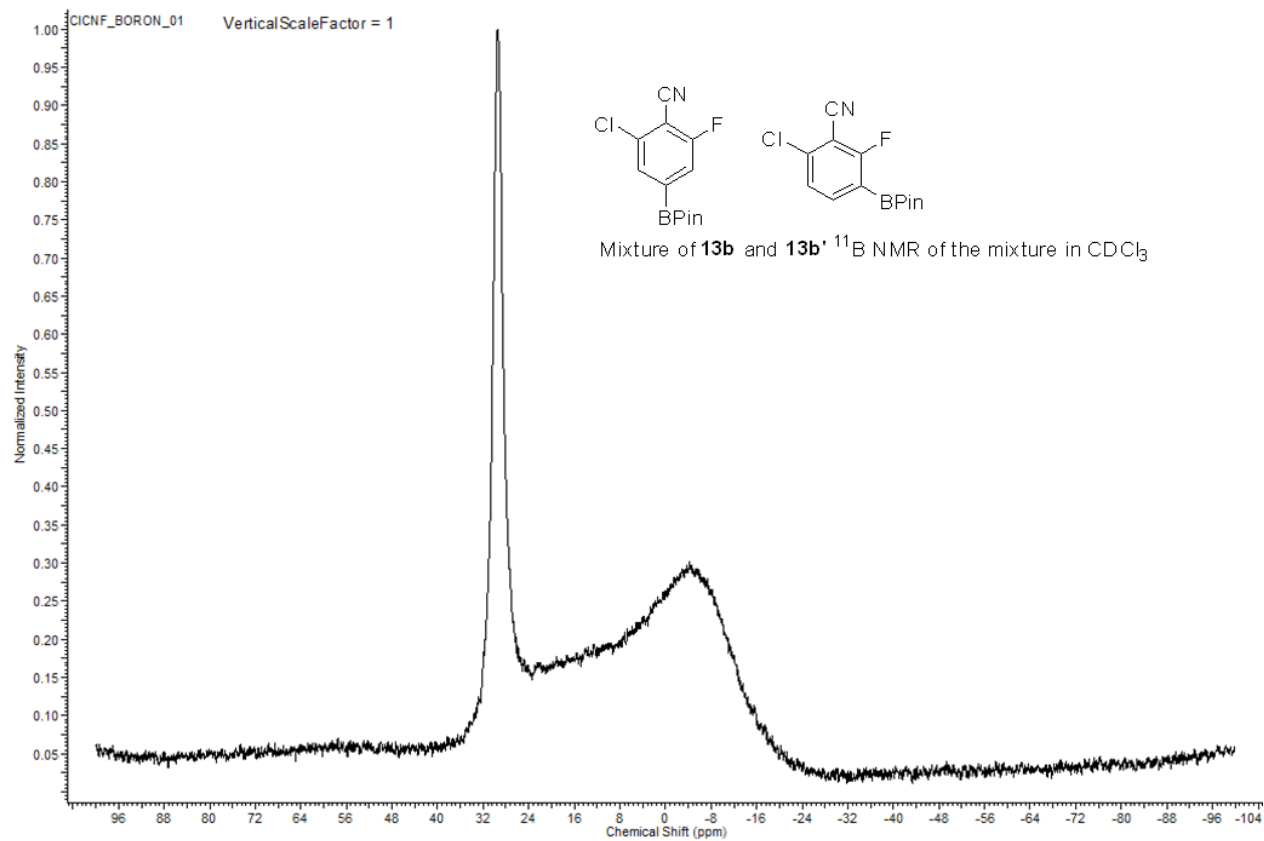


Figure 174 ^{13}C NMR of mixture of compounds **13b** and **13b'**

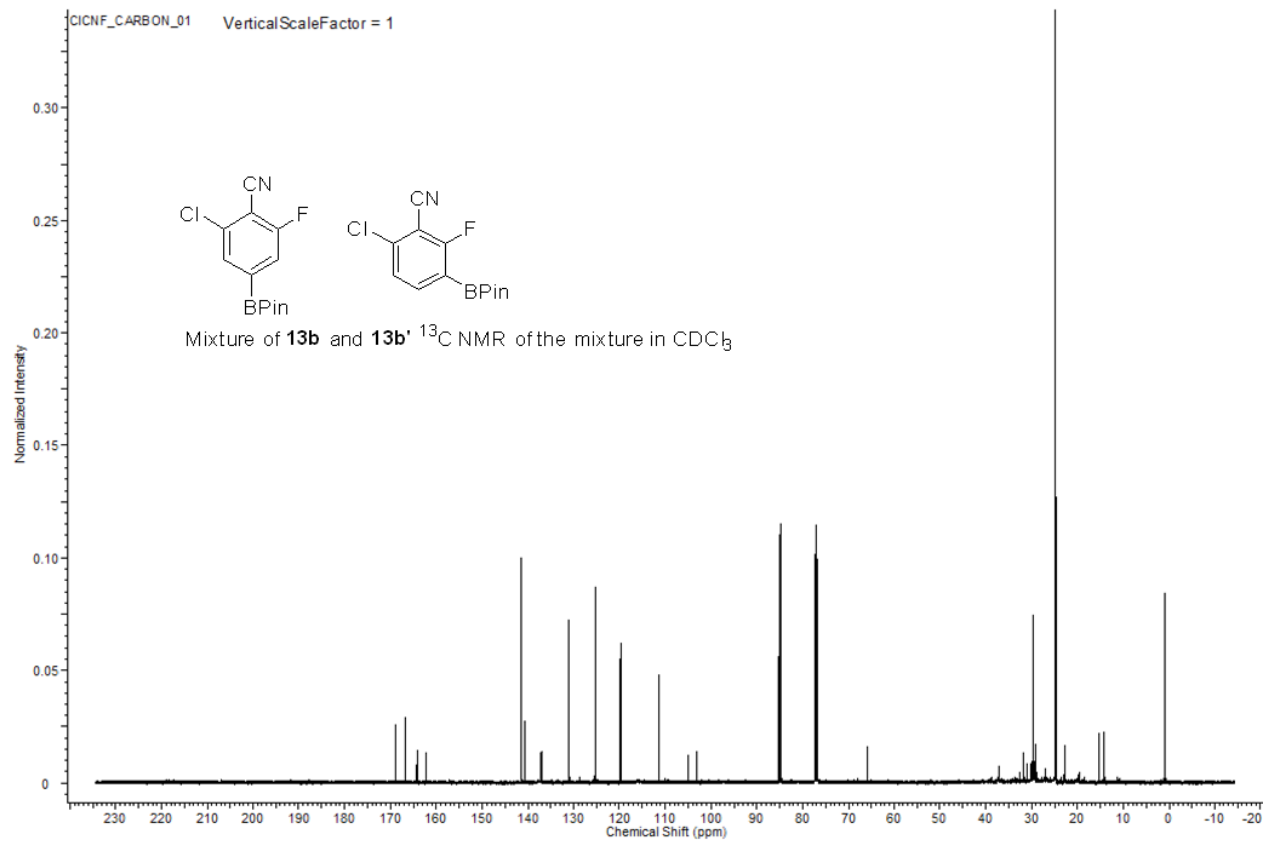


Figure 175 ^{19}F NMR of mixture of compounds **13b** and **13b'**

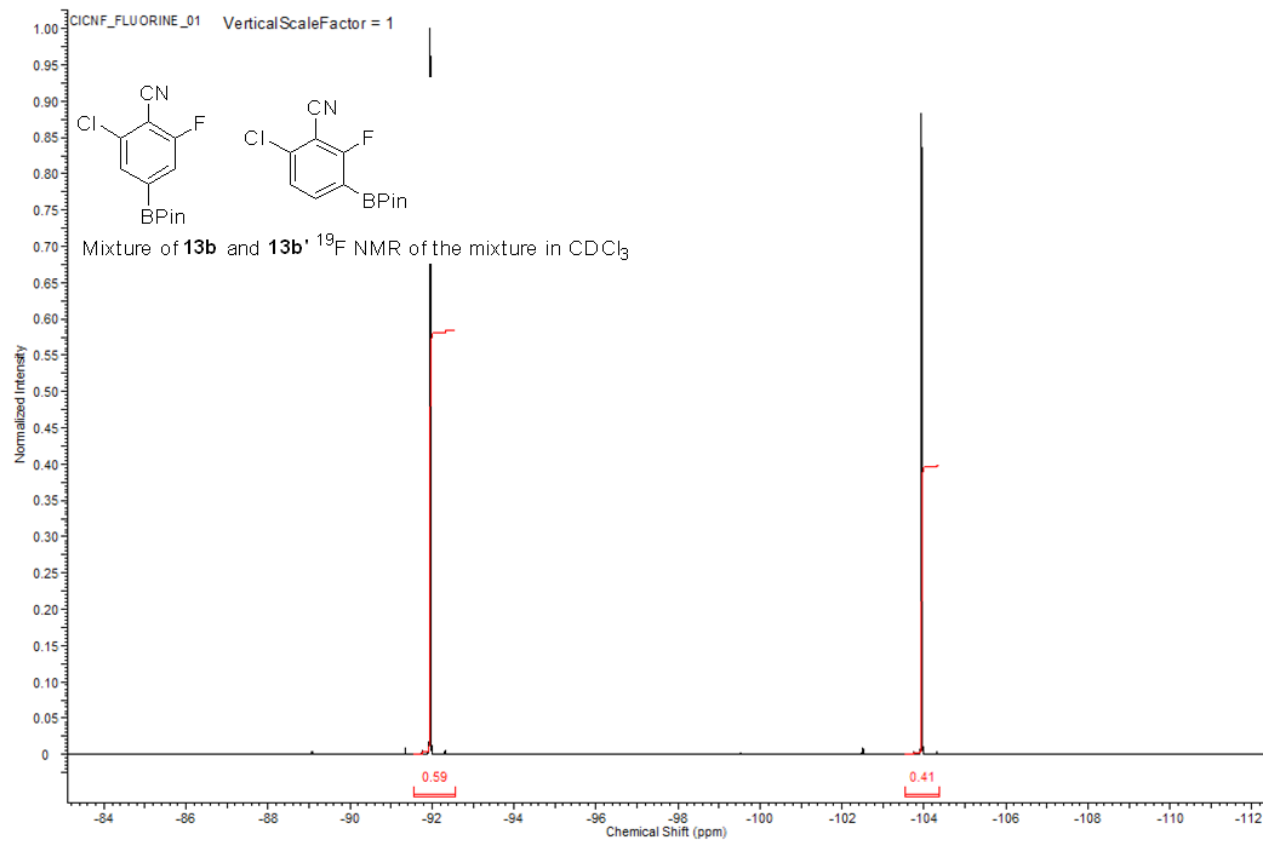


Figure 176 ^1H NMR of compound 14a

This report was created by ACD/NMR Processor Academic Edition. For more information go to www.acdlabs.com/nmrproc/

Acquisition Time (sec)	2.0447	Date	Sep 27 2013	Date Stamp	Sep 27 2013
File Name	C:\Users\lhao\Documents\Works\Down\UH-Dow-I-251\D1251F2_PROTON_01.fid			Frequency (MHz)	499.70
Nucleus	^1H	Number of Transients	32	Original Points Count	16384
Pulse Sequence	s2pul	Receiver Gain	30.00	Solvent	CHLOROFORM-d
Spectrum Offset (Hz)	2981.7954	Spectrum Type	STANDARD	Sweep Width (Hz)	8012.82
				Temperature (degree C)	AMBIENT TEMPERATURE

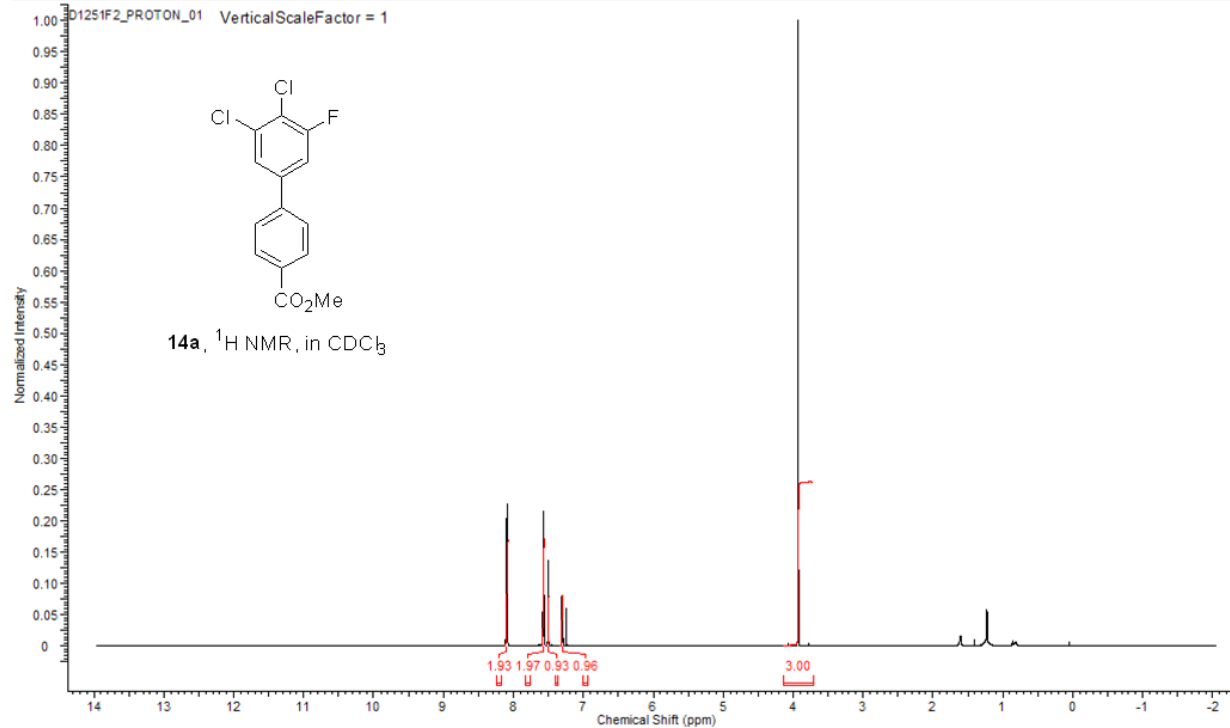


Figure 177 ^{13}C NMR of compound 14a

This report was created by ACD/NMR Processor Academic Edition. For more information go to www.acdlabs.com/nmrproc/

Acquisition Time (sec)	1.0486	Date	Sep 27 2013	Date Stamp	Sep 27 2013
File Name	C:\Users\lhao\Documents\Works\Down\UH-Dow-1-251\D1251F2_CARBON_01.fid\fid			Frequency (MHz)	125.66
Nucleus	^{13}C	Number of Transients	1024	Original Points Count	32768
Pulse Sequence	s2pul	Receiver Gain	30.00	Solvent	CHLOROFORM-d
Spectrum Offset (Hz)	13817.5771	Spectrum Type	STANDARD	Sweep Width (Hz)	31250.00
				Temperature (degree C)	AMBIENT TEMPERATURE

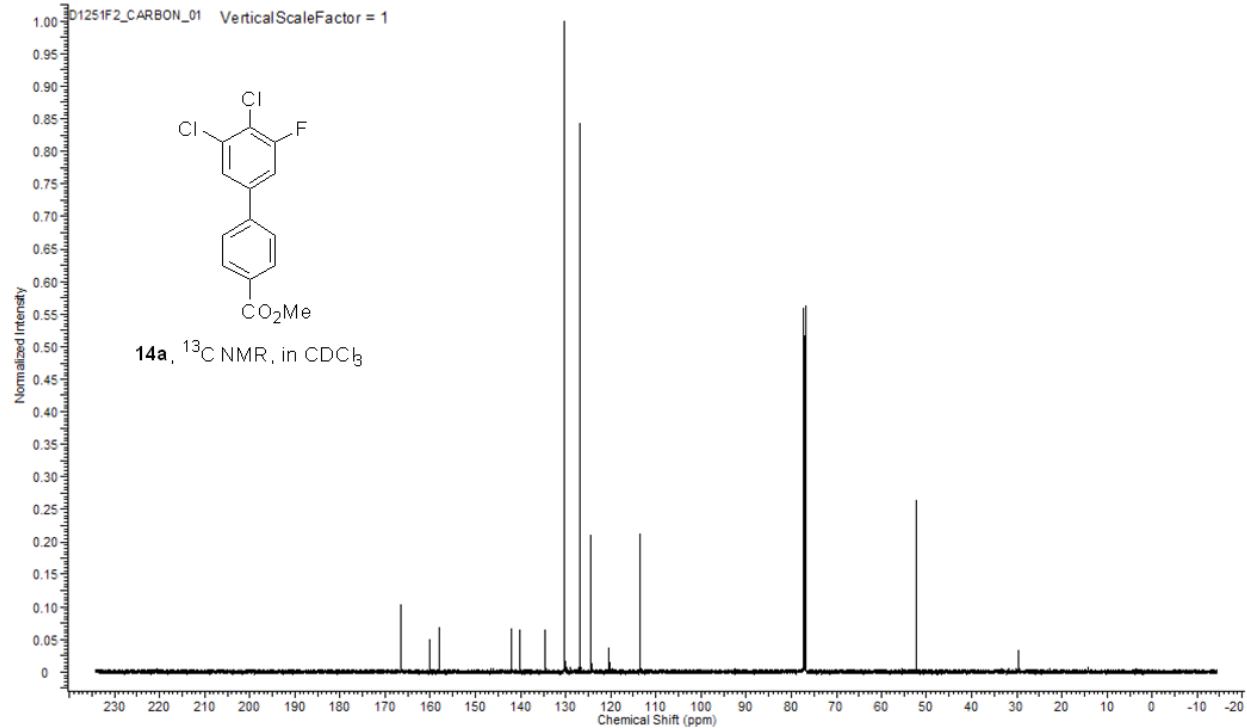


Figure 178 ^{19}F NMR of compound 14a

This report was created by ACD/NMR Processor Academic Edition. For more information go to www.acdlabs.com/nmrproc/

Acquisition Time (sec)	2.4117	Date	Sep 27 2013	Date Stamp	Sep 27 2013
File Name	C:\Users\yhao\Documents\Works\Down\UH-Dow-I-251\01251F2_FLUORINE_01.fid.tif			Frequency (MHz)	470.15
Nucleus	^{19}F	Number of Transients	32	Original Points Count	262144
Pulse Sequence	s2pul	Receiver Gain	58.00	Solvent	CH_2Cl_2
Spectrum Offset (Hz)	-39966.1367	Spectrum Type	STANDARD	Sweep Width (Hz)	108695.65
				Temperature (degree C)	AMBIENT TEMPERATURE

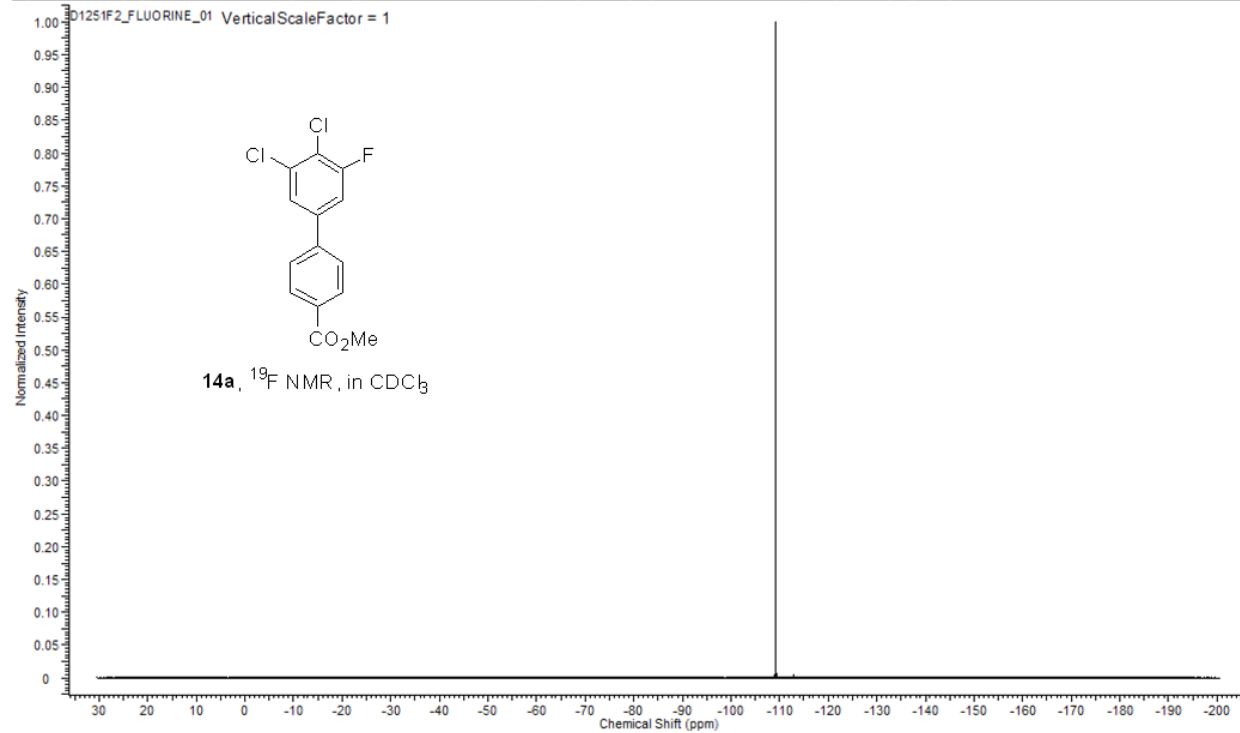


Figure 179 ^1H NMR of compound 14a'

This report was created by ACD/NMR Processor Academic Edition. For more information go to www.acdlabs.com/nmrproc/

Acquisition Time (sec)	2.0447	Date	Sep 27 2013	Date Stamp	Sep 27 2013
File Name	C:\Users\lhao\Documents\Works\Down\UH-Dow-I-251\D1251F3_PROTON_01.fid			Frequency (MHz)	499.70
Nucleus	^1H	Number of Transients	32	Original Points Count	16384
Pulse Sequence	s2pul	Receiver Gain	30.00	Solvent	CHLOROFORM-d
Spectrum Offset (Hz)	2982.2844	Spectrum Type	STANDARD	Sweep Width (Hz)	8012.82
				Temperature (degree C)	AMBIENT TEMPERATURE

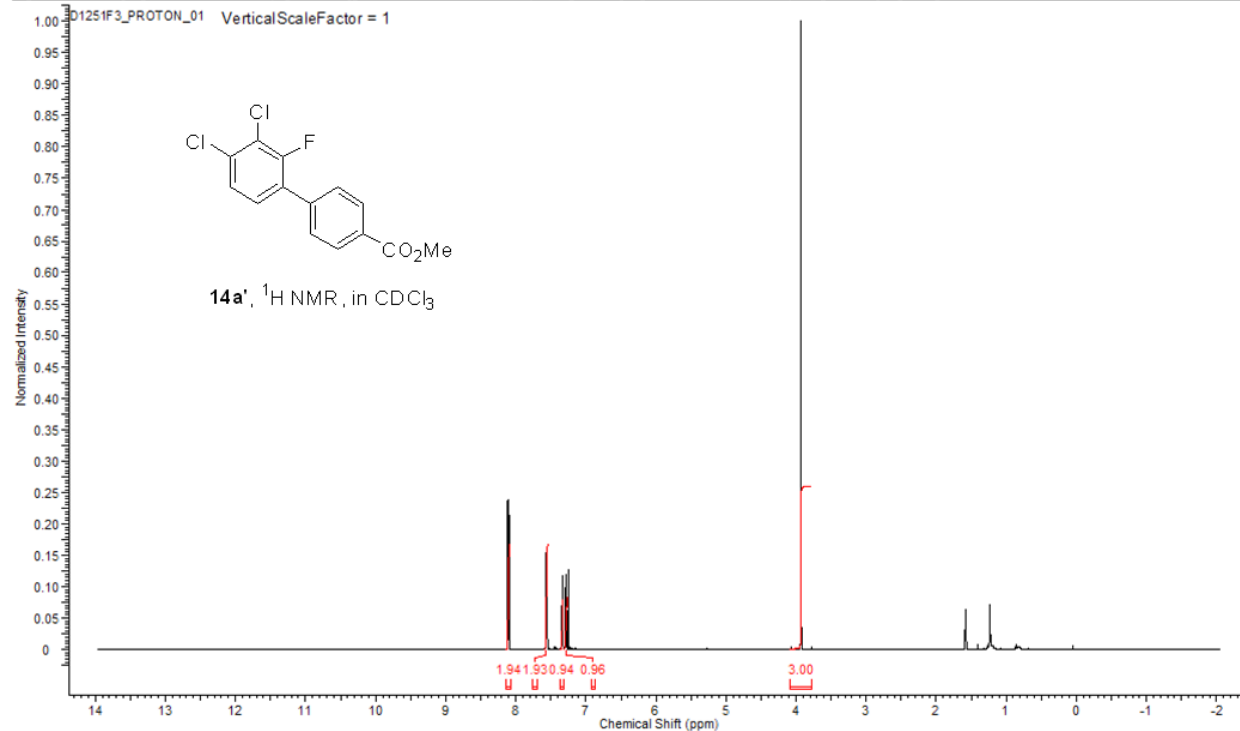


Figure 180 ^{13}C NMR of compound 14a'

This report was created by ACD/NMR Processor Academic Edition. For more information go to www.acdlabs.com/nmrproc/

Acquisition Time (sec)	1.0486	Date	Sep 27 2013	Date Stamp	Sep 27 2013
File Name	C:\Users\lhao\Documents\Works\Down\UH-Dow-I-251\01251F3_CARBON_01.fid			Frequency (MHz)	125.66
Nucleus	^{13}C	Number of Transients	1024	Original Points Count	32768
Pulse Sequence	s2pul	Receiver Gain	30.00	Solvent	CHLOROFORM-d
Spectrum Offset (Hz)	13818.5313	Spectrum Type	STANDARD	Sweep Width (Hz)	31250.00
				Temperature (degree C)	AMBIENT TEMPERATURE

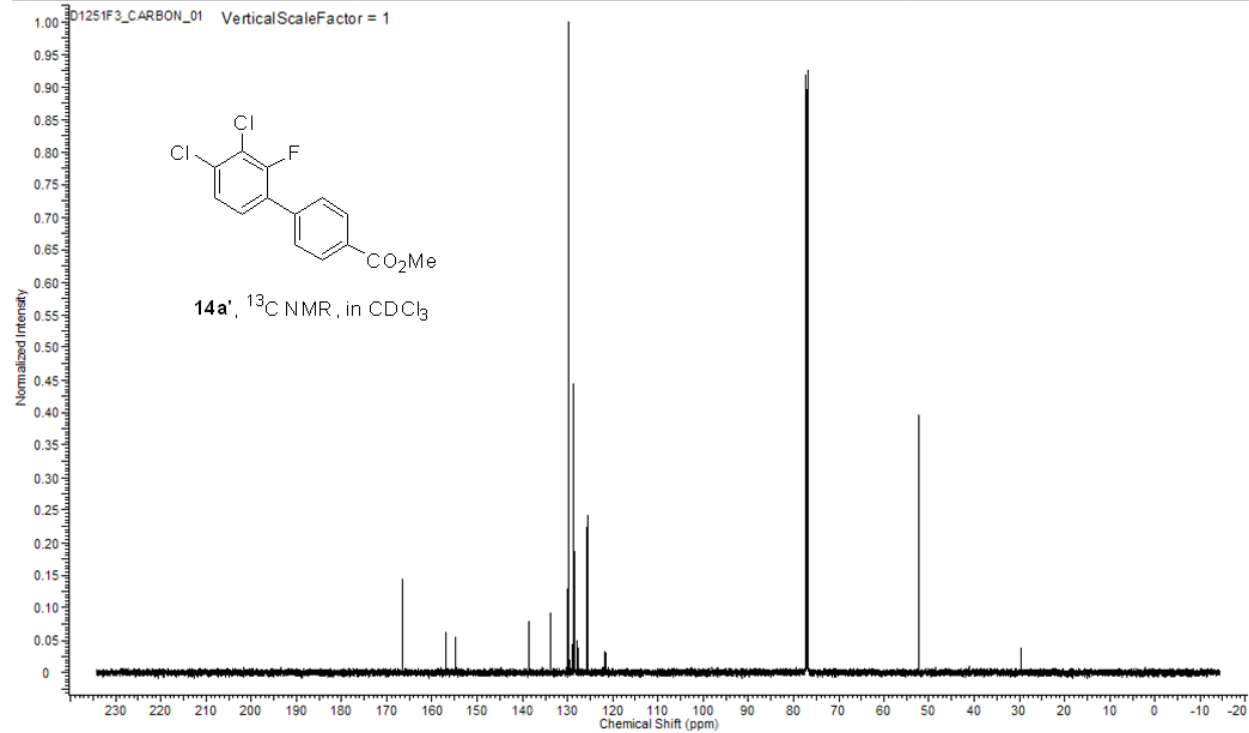


Figure 181 ^{19}F NMR of compound 14a'

This report was created by ACD/NMR Processor Academic Edition. For more information go to www.acdlabs.com/nmrproc/

Acquisition Time (sec)	2.4117	Date	Sep 27 2013	Date Stamp	Sep 27 2013		
File Name	C:\Users\lhao\Documents\Works\Down\UH-Dow-I-251\01251F3_FLUORINE_01.fid.tif	Frequency (MHz)	470.15	Points Count	262144		
Nucleus	^{19}F	Number of Transients	32	Original Points Count	262144		
Pulse Sequence	s2pul	Receiver Gain	60.00	Solvent	CH_2Cl_2		
Spectrum Offset (Hz)	-39966.1367	Spectrum Type	STANDARD	Sweep Width (Hz)	108695.65	Temperature (degree C)	AMBIENT TEMPERATURE

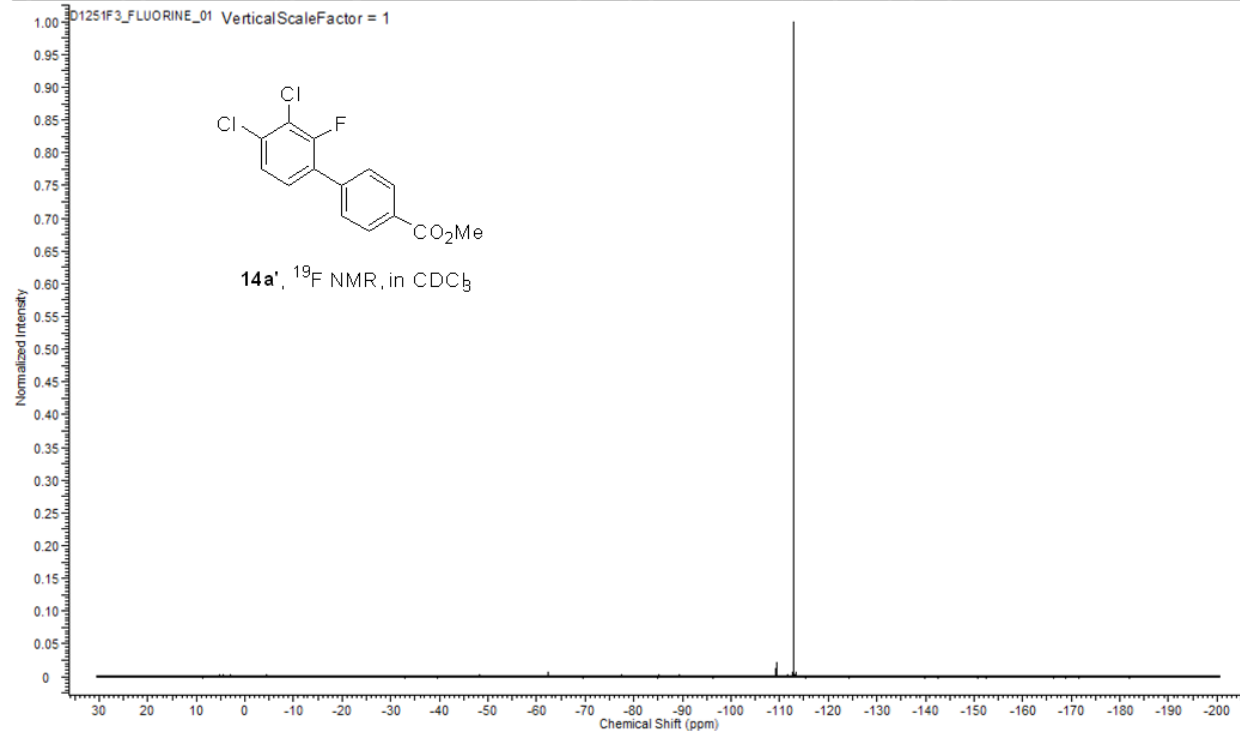


Figure 182 ^1H NMR of mixture of compounds 14b and 14b'

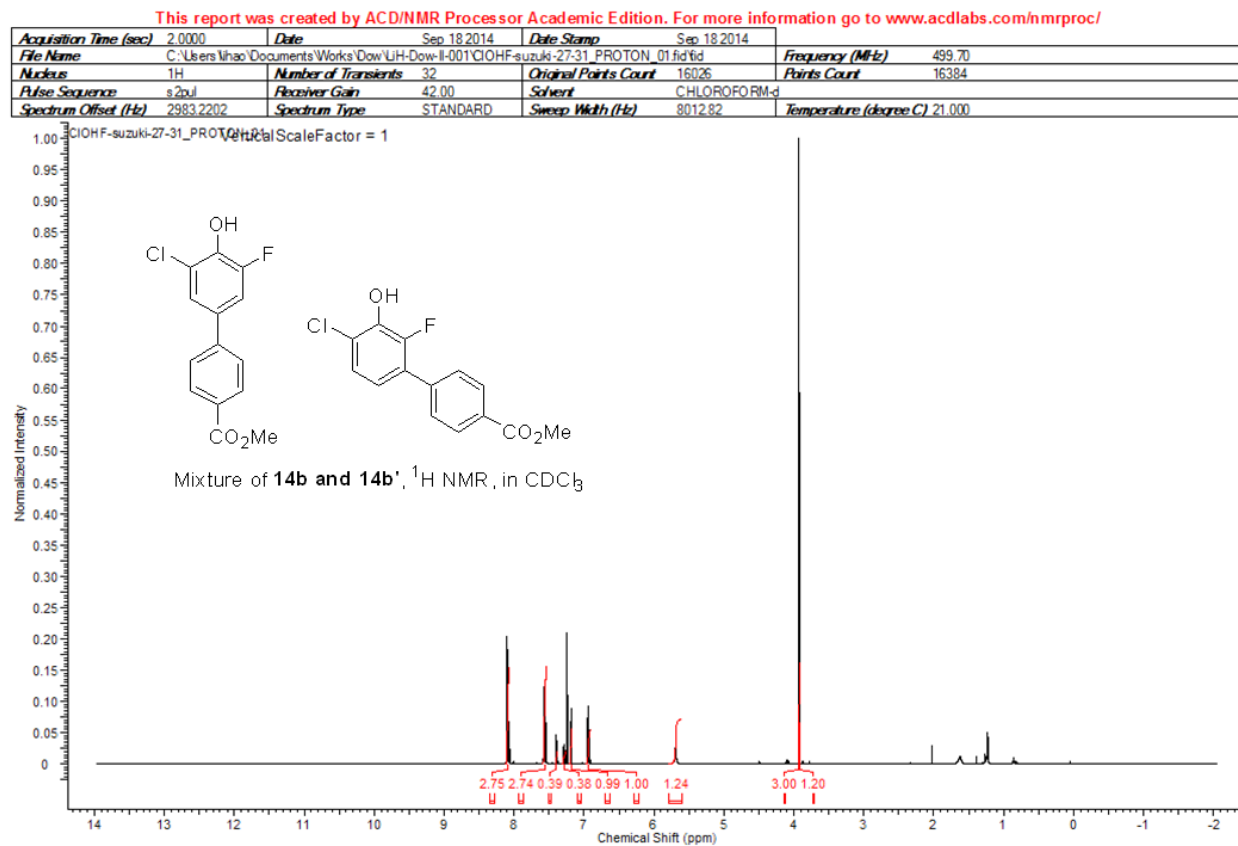


Figure 183 ^{19}F NMR of mixture of compounds 14b and 14b'

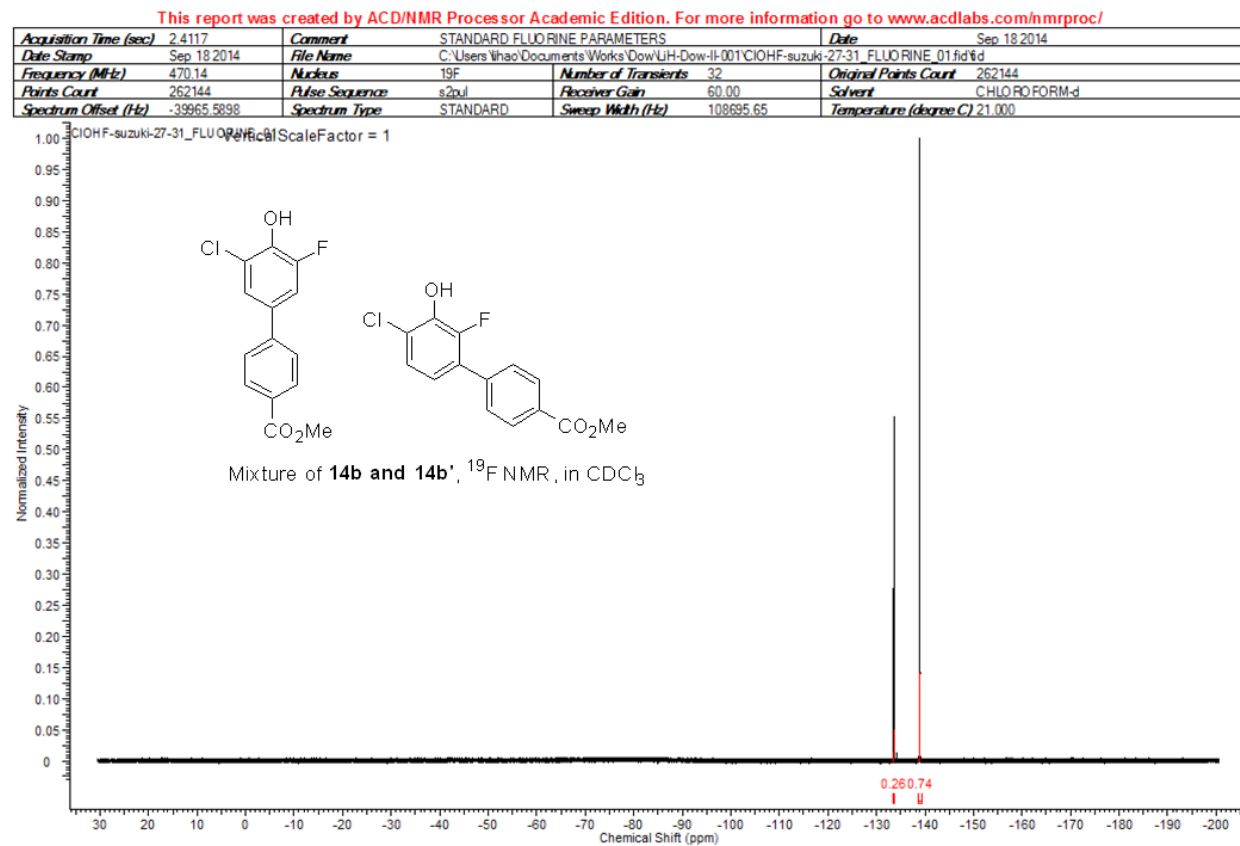


Figure 184 ^1H NMR of compound 14b'

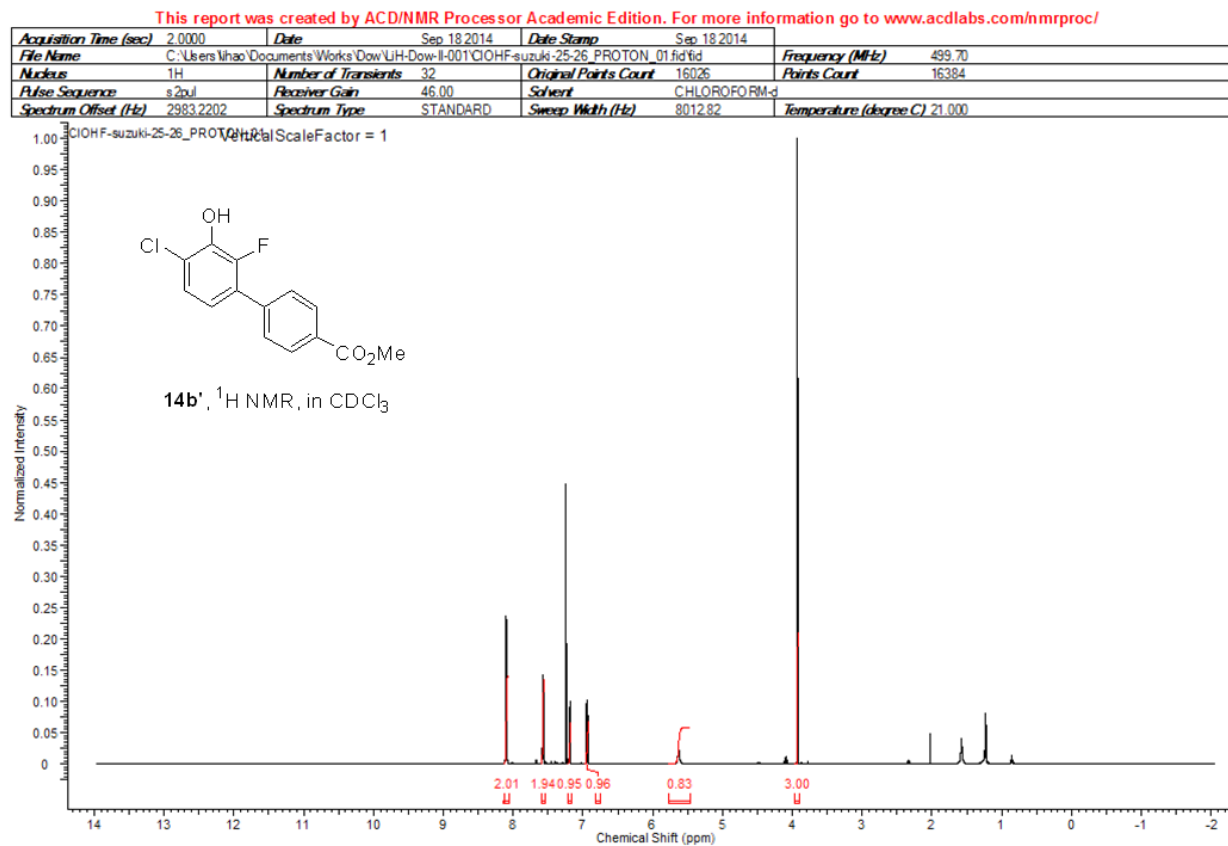


Figure 185 ^{13}C NMR of compound 14b'

This report was created by ACD/NMR Processor Academic Edition. For more information go to www.acdlabs.com/nmrproc/

Acquisition Time (sec)	1.0486	Date	Sep 18 2014	Date Stamp	Sep 18 2014
File Name	C:\Users\lhao\Documents\Works\Down\UH-Dow-II-001\ClOHF-suzuki-25-26_CARBON_01.fid			Frequency (MHz)	125.66
Nucleus	^{13}C	Number of Transients	1024	Original Points Count	32768
Pulse Sequence	s2pul	Receiver Gain	30.00	Solvent	CHLOROFORM-d
Spectrum Offset (Hz)	13821.3750	Spectrum Type	STANDARD	Sweep Width (Hz)	31250.00
				Temperature (degree C)	21.000

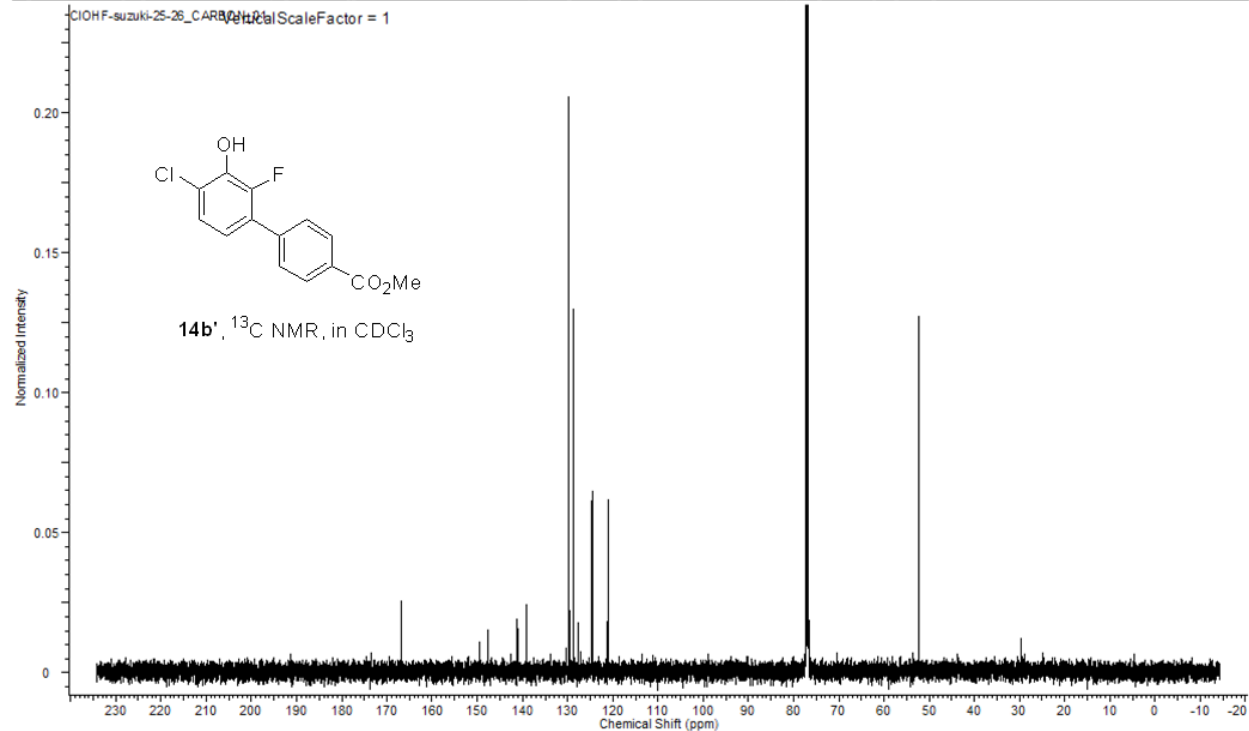


Figure 186 ^{19}F NMR of compound 14b'

This report was created by ACD/NMR Processor Academic Edition. For more information go to www.acdlabs.com/nmrproc/

Acquisition Time (sec)	2.4117	Comment	STANDARD FLUORINE PARAMETERS	Date	Sep 18 2014	
Date Stamp	Sep 18 2014	File Name	C:\Users\Yhao\Documents\Works\Down\UH-Dow-II-001\CIOHF-suzuki-25-26_FLUORINE_01.fid.tif			
Frequency (MHz)	470.14	Nucleus	^{19}F	Number of Transients	32	
Points Count	262144	Pulse Sequence	s2pul	Receiver Gain	60.00	
Spectrum Offset (Hz)	-39965.5898	Spectrum Type	STANDARD	Solvent	CHLOROFORM-d	
			Sweep Width (Hz)	108695.65	Temperature (degree C)	21.000

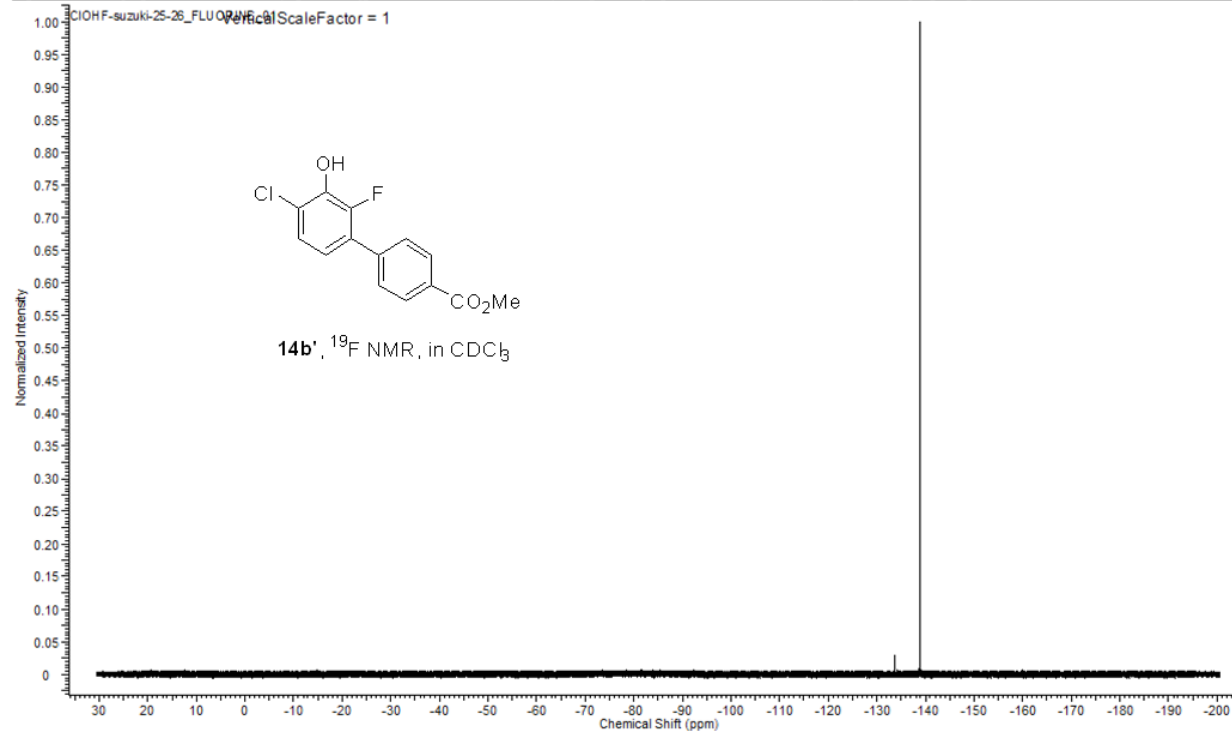


Figure 187 ^1H NMR of compound 14c

This report was created by ACD/NMR Processor Academic Edition. For more information go to www.acdlabs.com/nmrproc/

Acquisition Time (sec)	2.0447	Date	Nov 5 2013	Date Stamp	Nov 5 2013
File Name	C:\Users\lhao\Documents\Works\Down\UH-Dow-I-273\D1273F2_PROTON_01.fid			Frequency (MHz)	499.70
Nucleus	^1H	Number of Transients	64	Original Points Count	16384
Pulse Sequence	s2pul	Receiver Gain	30.00	Solvent	CHLOROFORM-d
Spectrum Offset (Hz)	2981.7954	Spectrum Type	STANDARD	Sweep Width (Hz)	8012.82
				Temperature (degree C)	AMBIENT TEMPERATURE

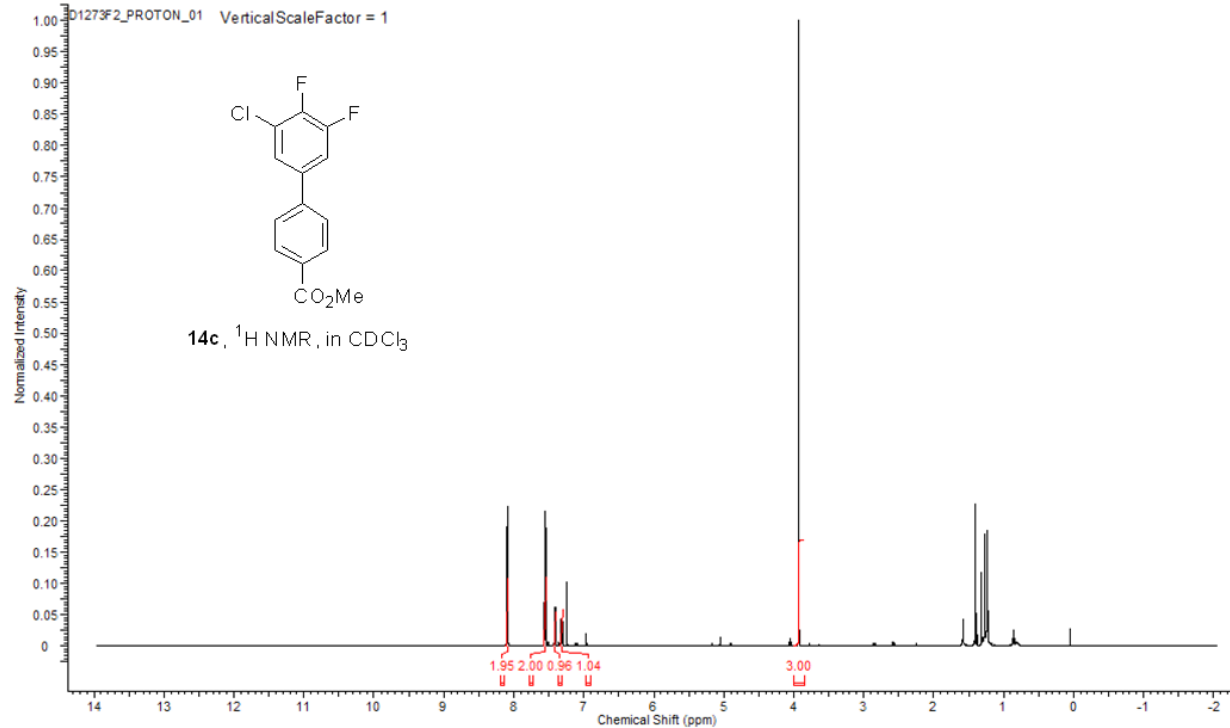


Figure 188 ^{13}C NMR of compound 14c

This report was created by ACD/NMR Processor Academic Edition. For more information go to www.acdlabs.com/nmrproc/

Acquisition Time (sec)	1.0486	Date	Nov. 6.2013	Date Stamp	Nov. 6.2013
File Name	C:\Users\yhao\Documents\Works\Down\UH-Dow-I-273\1273F2_CARBON_01.fid			Frequency (MHz)	125.66
Nucleus	^{13}C	Number of Transients	1024	Original Points Count	32768
Pulse Sequence	s2pul	Receiver Gain	30.00	Solvent	CHLOROFORM-d
Spectrum Offset (Hz)	13818.5313	Spectrum Type	STANDARD	Sweep Width (Hz)	31250.00
				Temperature (degree C)	AMBIENT TEMPERATURE

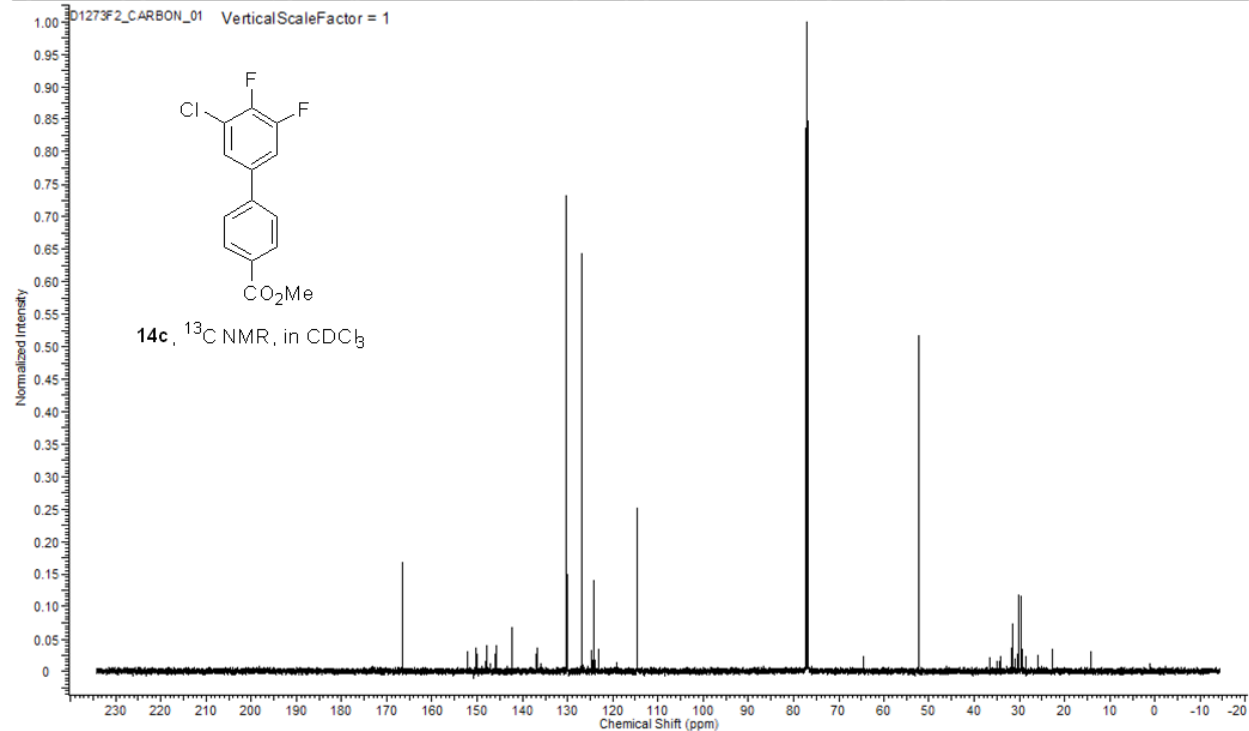


Figure 189 ^{19}F NMR of compound 14c

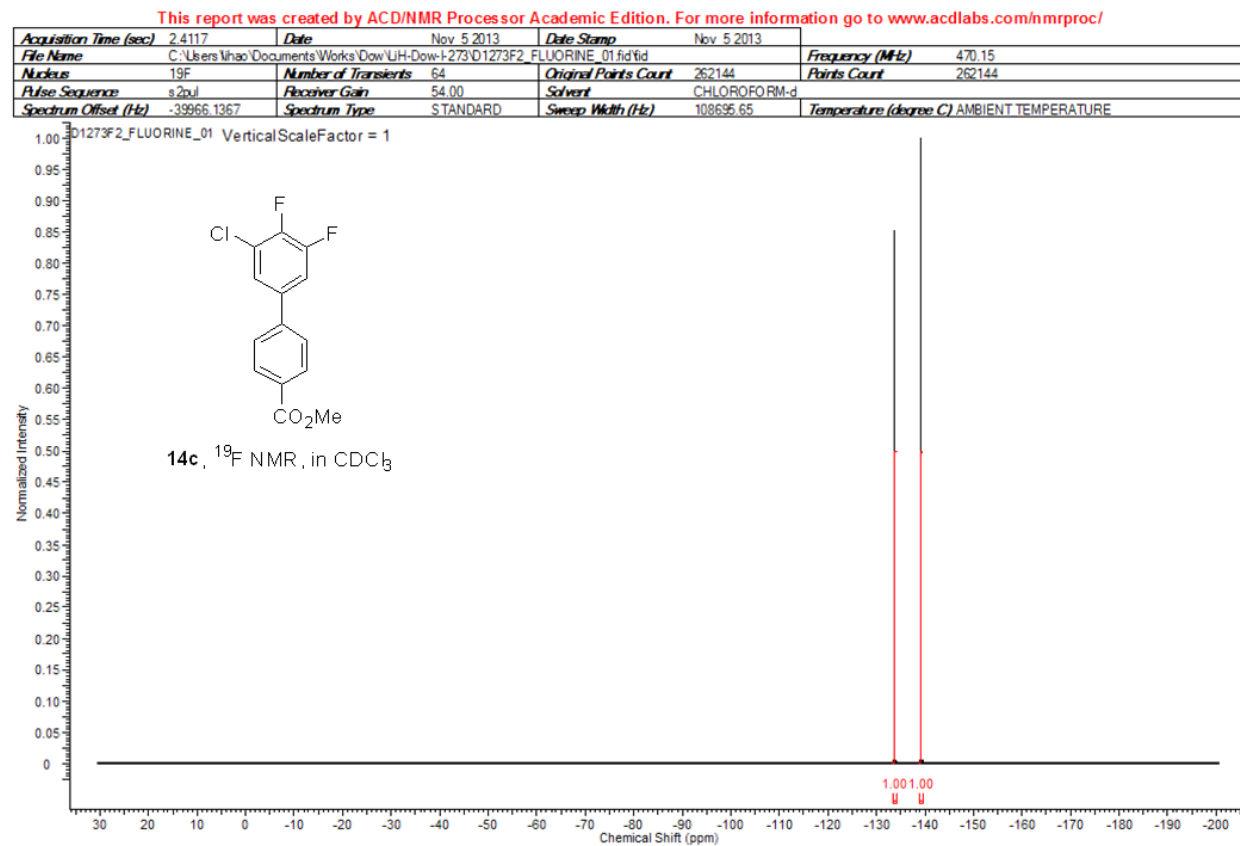


Figure 190 ^1H NMR of compound 14c'

This report was created by ACD/NMR Processor Academic Edition. For more information go to www.acdlabs.com/nmrproc/

Acquisition Time (sec)	2.0447	Date	Nov. 5.2013	Date Stamp	Nov. 5.2013
File Name	C:\Users\lhao\Documents\Works\Down\UH-Dow-I-273\1273F3_PROTON_01.fid			Frequency (MHz)	499.70
Nucleus	^1H	Number of Transients	64	Original Points Count	16384
Pulse Sequence	s2pul	Receiver Gain	42.00	Solvent	CHLOROFORM-d
Spectrum Offset (Hz)	2981.7954	Spectrum Type	STANDARD	Sweep Width (Hz)	8012.82
				Temperature (degree C)	AMBIENT TEMPERATURE

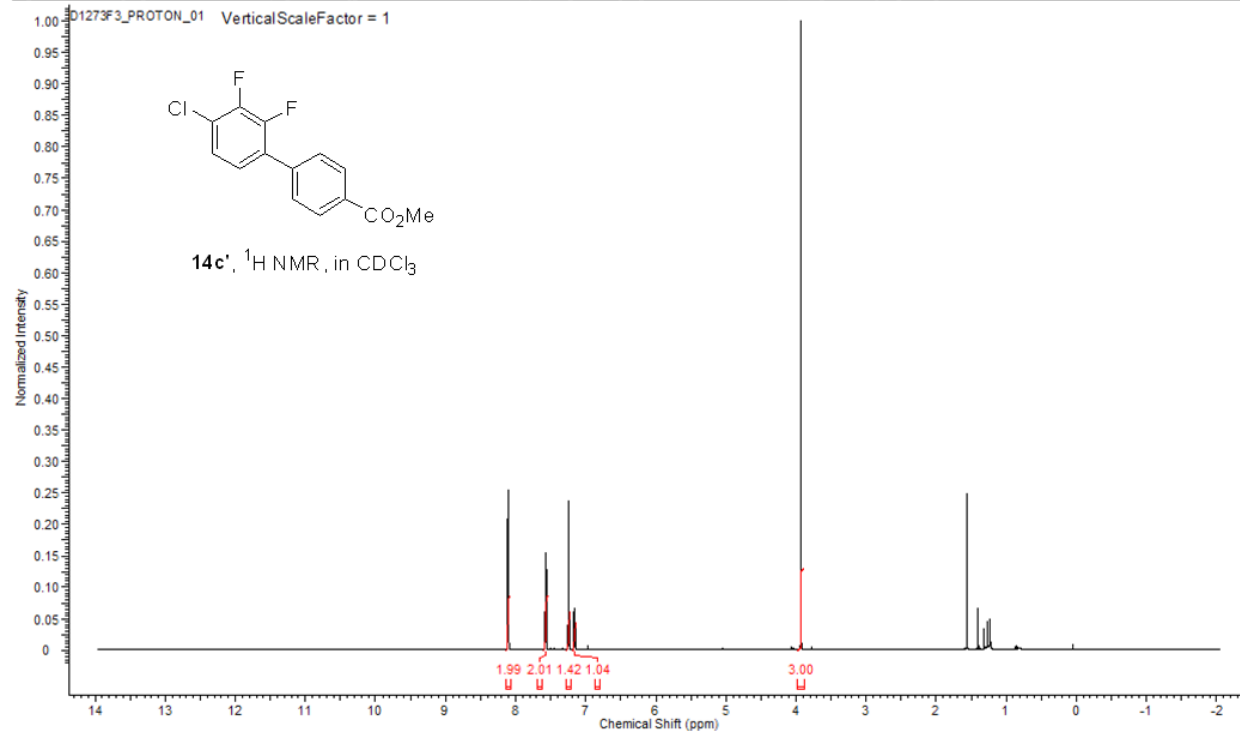


Figure 191 ^{13}C NMR of compound 14c'

This report was created by ACD/NMR Processor Academic Edition. For more information go to www.acdlabs.com/nmrproc/

Acquisition Time (sec)	1.0486	Date	Nov. 6.2013	Date Stamp	Nov. 6.2013
File Name	C:\Users\lhao\Documents\Works\Down\UH-Dow-I-273\1273F3_CARBON_01.fid			Frequency (MHz)	125.66
Nucleus	^{13}C	Number of Transients	1024	Original Points Count	32768
Pulse Sequence	s2pul	Receiver Gain	30.00	Solvent	CHLOROFORM-d
Spectrum Offset (Hz)	13818.5313	Spectrum Type	STANDARD	Sweep Width (Hz)	31250.00
				Temperature (degree C)	AMBIENT TEMPERATURE

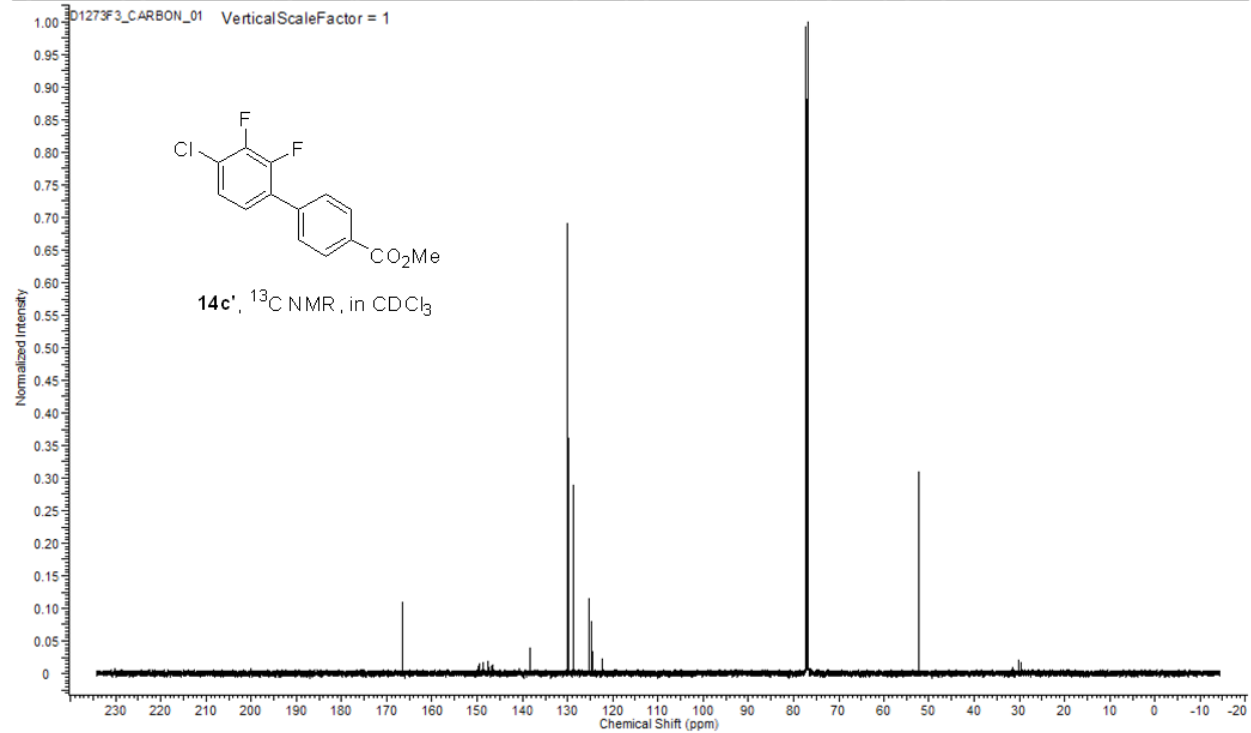


Figure 192 ^{19}F NMR of compound 14c'

This report was created by ACD/NMR Processor Academic Edition. For more information go to www.acdlabs.com/nmrproc/

Acquisition Time (sec)	2.4117	Date	Nov. 5. 2013	Date Stamp	Nov. 5. 2013
File Name	C:\Users\lhao\Documents\Works\Down\UH-Dow-I-273\1273F3_FLUORINE_01.fid\fid			Frequency (MHz)	470.15
Nucleus	^{19}F	Number of Transients	64	Original Points Count	262144
Pulse Sequence	s2pul	Receiver Gain	56.00	Solvent	CHLOROFORM-d
Spectrum Offset (Hz)	-39966.1367	Spectrum Type	STANDARD	Sweep Width (Hz)	108696.65
				Temperature (degree C)	AMBIENT TEMPERATURE

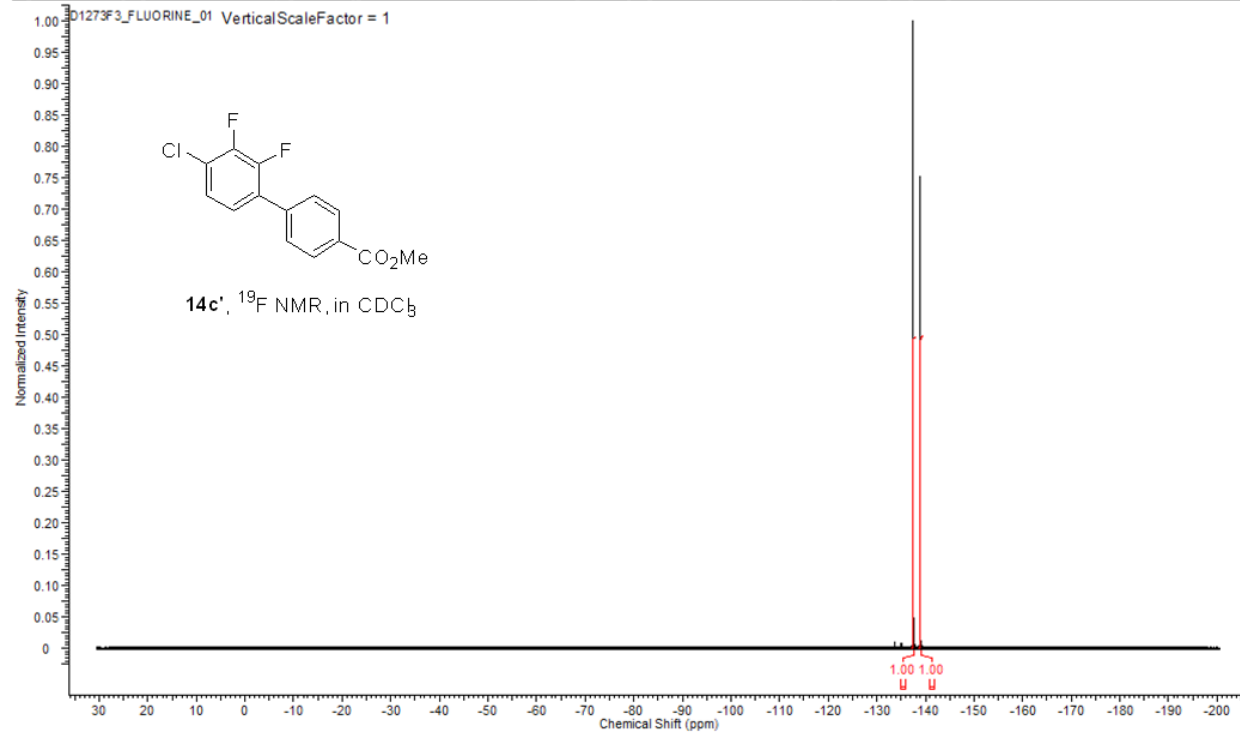


Figure 193 ^1H NMR of compound 14d

This report was created by ACD/NMR Processor Academic Edition. For more information go to www.acdlabs.com/nmrproc/

Acquisition Time (sec)	2.0447	Date	Nov 16 2013	Date Stamp	Nov 16 2013
File Name	C:\Users\yhao\Documents\Works\Down\UH-Dow-I-277\D1277_F3_PROTON_01.fid.tif			Frequency (MHz)	499.70
Nucleus	^1H	Number of Transients	128	Original Points Count	16384
Pulse Sequence	s2pul	Receiver Gain	48.00	Solvent	CHLOROFORM-d
Spectrum Offset (Hz)	2981.7954	Spectrum Type	STANDARD	Sweep Width (Hz)	8012.82
				Temperature (degree C)	AMBIENT TEMPERATURE

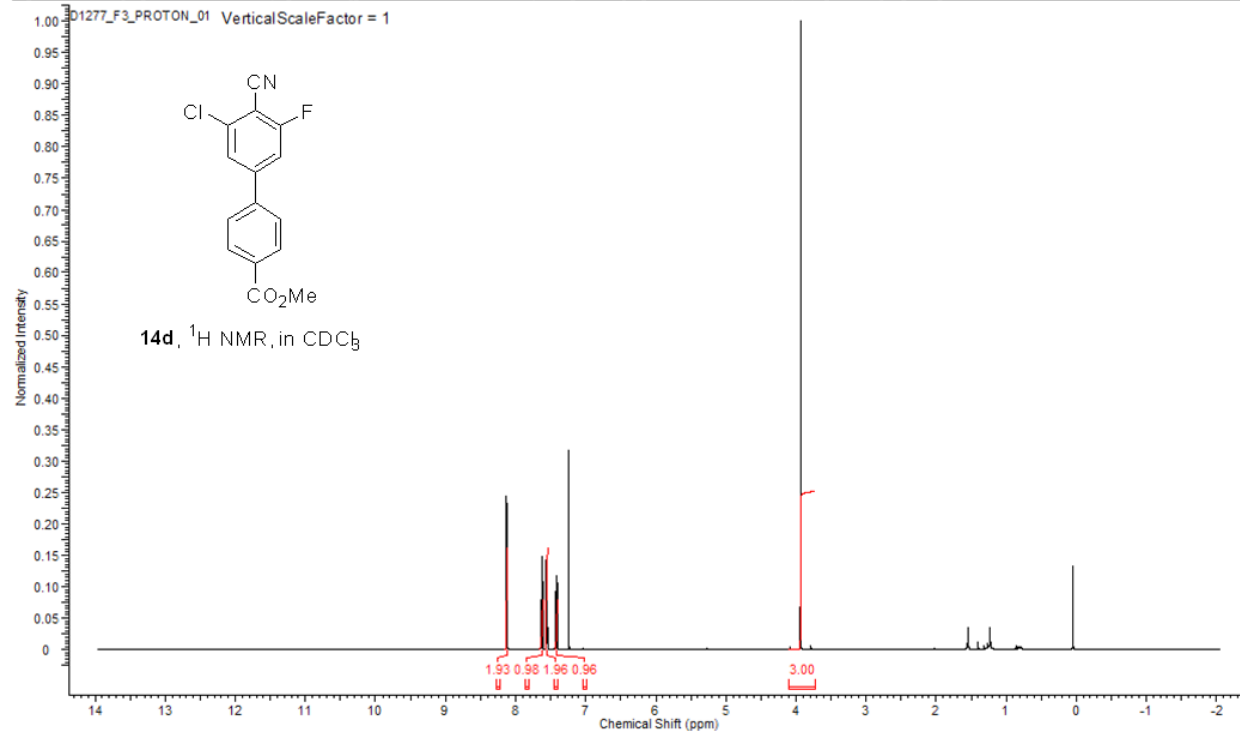


Figure 194 ^{13}C NMR of compound 14d

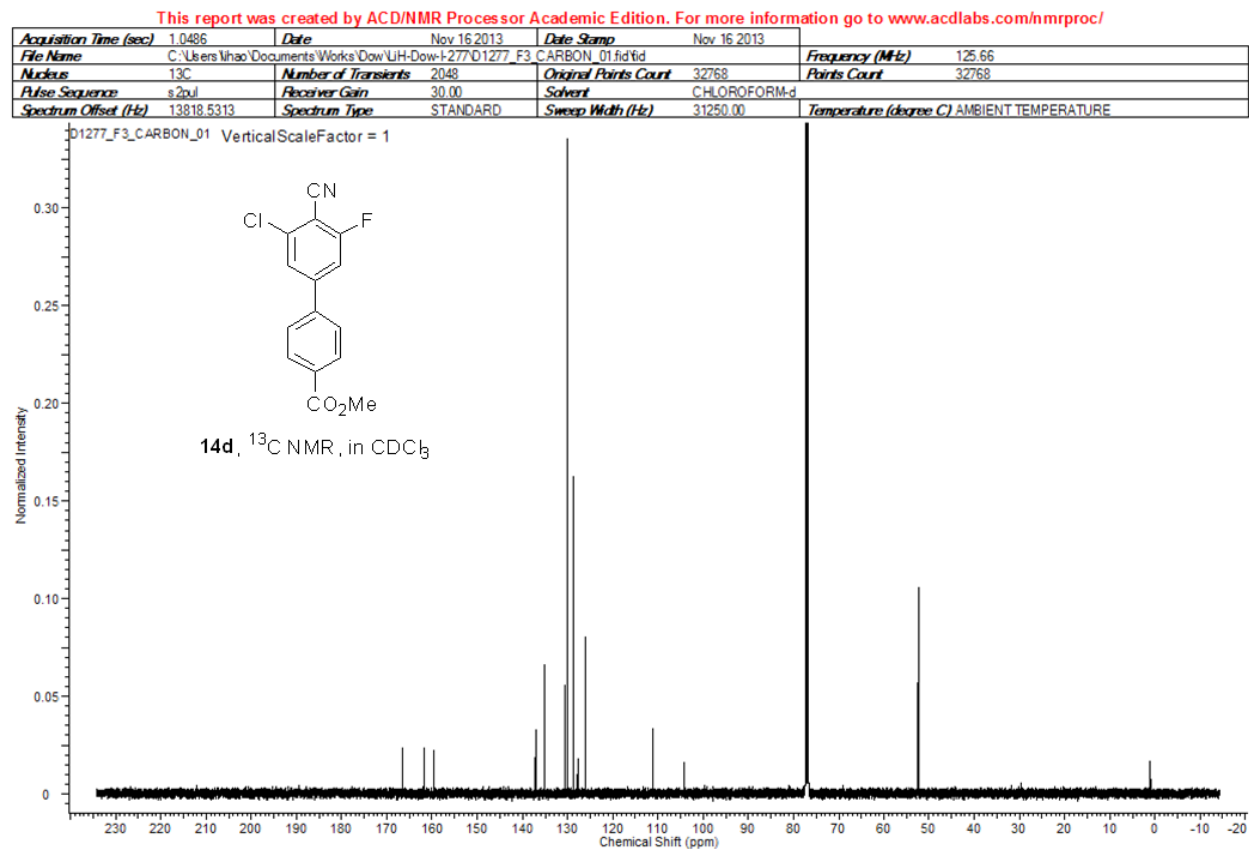


Figure 195 ^{19}F NMR of compound 14d

This report was created by ACD/NMR Processor Academic Edition. For more information go to www.acdlabs.com/nmrproc/

Acquisition Time (sec)	2.4117	Date	Nov 16 2013	Date Stamp	Nov 16 2013
File Name	C:\Users\yhao\Documents\Works\Down\UH-Dow-1-277\D1277_F3_FLUORINE_01.fid\fid			Frequency (MHz)	470.15
Nucleus	^{19}F	Number of Transients	128	Original Points Count	262144
Pulse Sequence	s2pul	Receiver Gain	60.00	Solvent	CHLOROFORM-d
Spectrum Offset (Hz)	-39966.1367	Spectrum Type	STANDARD	Sweep Width (Hz)	108695.65
				Temperature (degree C)	AMBIENT TEMPERATURE

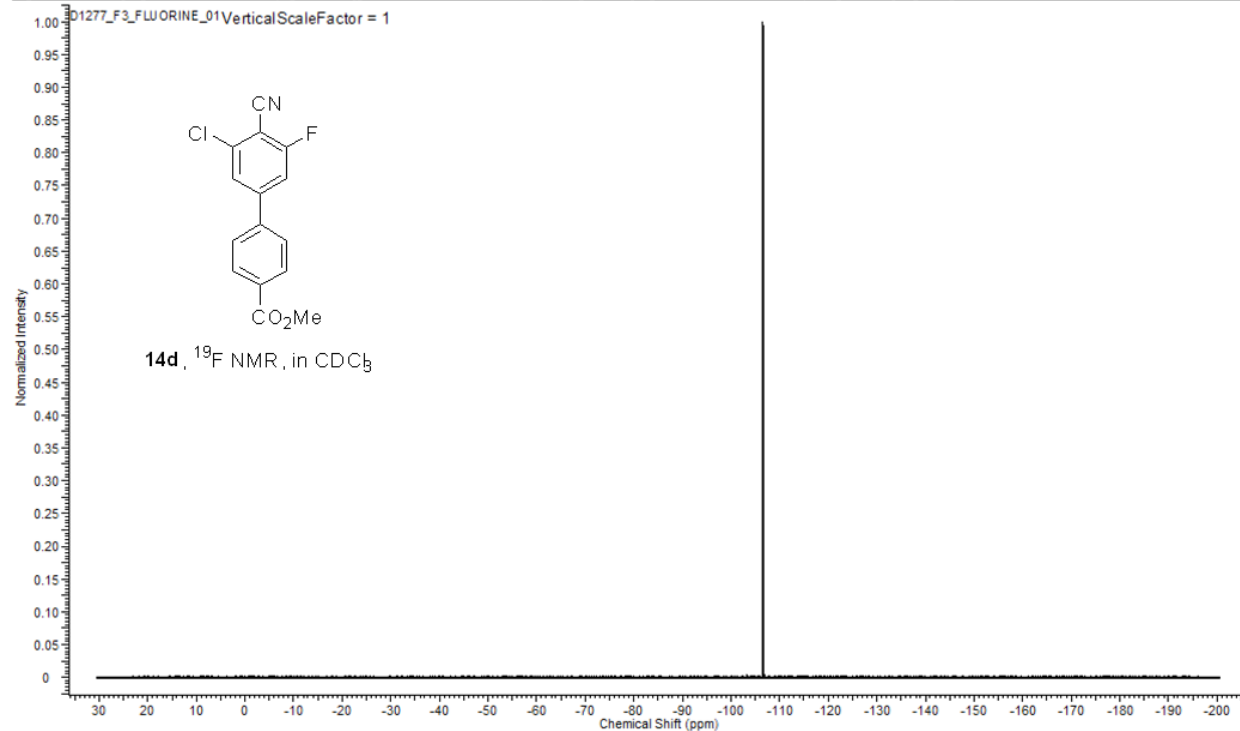


Figure 196 ^1H NMR of compound 14d'

This report was created by ACD/NMR Processor Academic Edition. For more information go to www.acdlabs.com/nmrproc/

Acquisition Time (sec)	2.0447	Date	Nov 16 2013	Date Stamp	Nov 16 2013
File Name	C:\Users\yhao\Documents\Works\Down\UH-Dow-I-277\01277_F2_PROTON_01.fid.tif			Frequency (MHz)	499.70
Nucleus	^1H	Number of Transients	128	Original Points Count	16384
Pulse Sequence	s2pul	Receiver Gain	46.00	Solvent	CHLOROFORM-d
Spectrum Offset (Hz)	2981.7954	Spectrum Type	STANDARD	Sweep Width (Hz)	8012.82
				Temperature (degree C)	AMBIENT TEMPERATURE

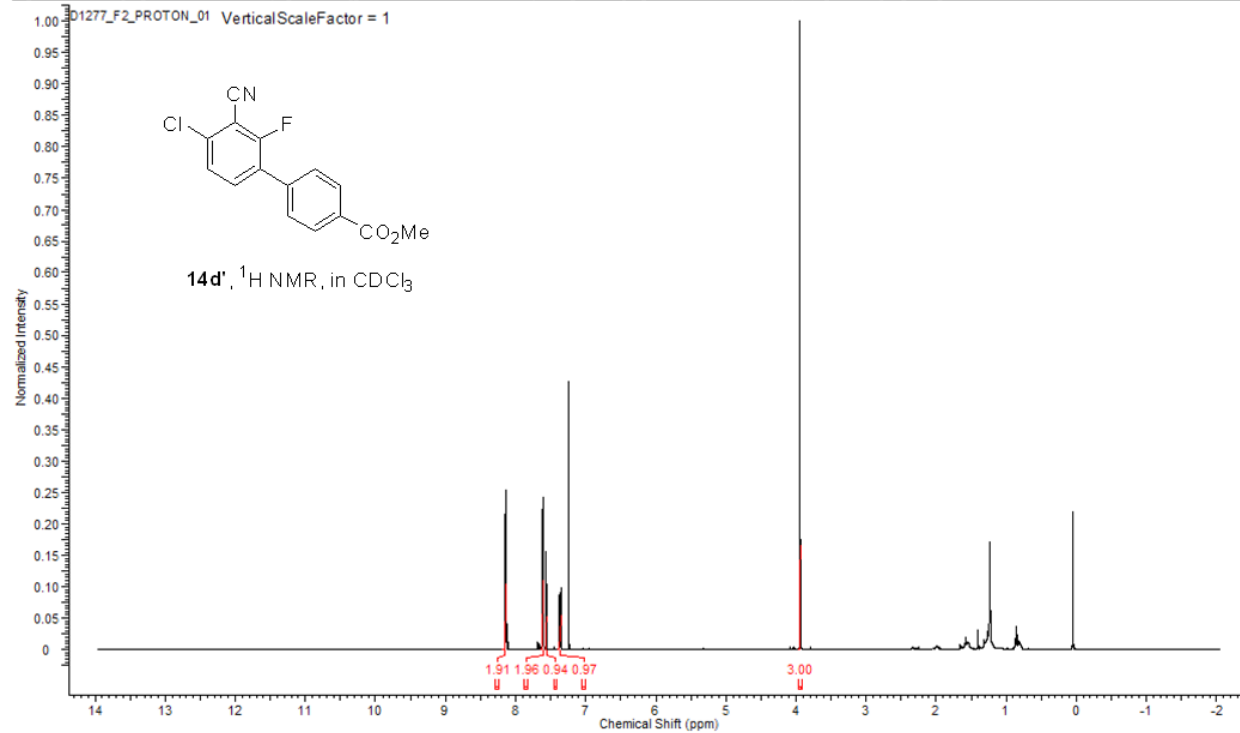


Figure 197 ^{13}C NMR of compound 14d'

This report was created by ACD/NMR Processor Academic Edition. For more information go to www.acdlabs.com/nmrproc/

Acquisition Time (sec)	1.0486	Date	Nov 16 2013	Date Stamp	Nov 16 2013
File Name	C:\Users\lhao\Documents\Works\Down\277\1277_F2 CARBON_01.fid.tif			Frequency (MHz)	125.66
Nucleus	^{13}C	Number of Transients	2048	Original Points Count	32768
Pulse Sequence	s2pul	Receiver Gain	30.00	Solvent	CHLOROFORM-d
Spectrum Offset (Hz)	13819.4854	Spectrum Type	STANDARD	Sweep Width (Hz)	31250.00
				Temperature (degree C)	AMBIENT TEMPERATURE

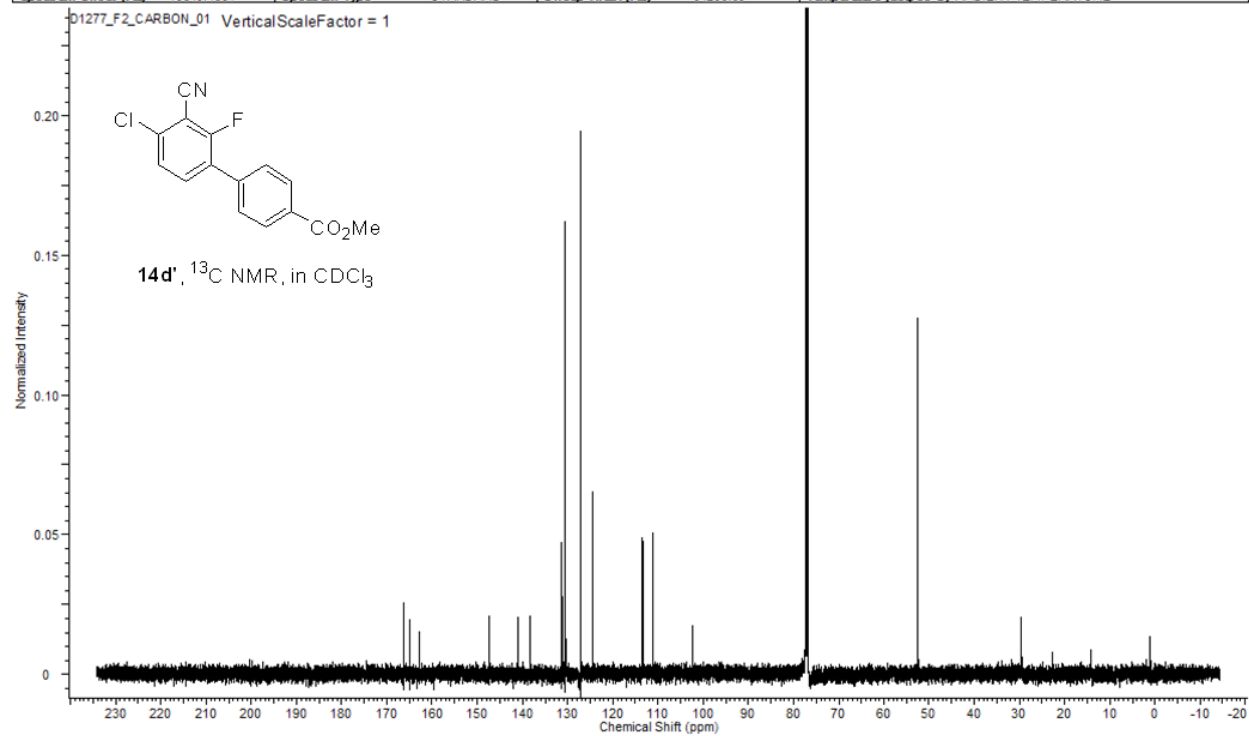


Figure 198 ^{19}F NMR of compound 14d'

This report was created by ACD/NMR Processor Academic Edition. For more information go to www.acdlabs.com/nmrproc/

Acquisition Time (sec)	2.4117	Date	Nov 16 2013	Date Stamp	Nov 16 2013
File Name	C:\Users\yhao\Documents\Works\Down\UH-Dow-1-277\D1277_F2_FLUORINE_01.fid\fid			Frequency (MHz)	470.15
Nucleus	^{19}F	Number of Transients	128	Original Points Count	262144
Pulse Sequence	s2pul	Receiver Gain	60.00	Solvent	CH_2Cl_2
Spectrum Offset (Hz)	-39966.1367	Spectrum Type	STANDARD	Sweep Width (Hz)	108695.65
				Temperature (degree C)	AMBIENT TEMPERATURE

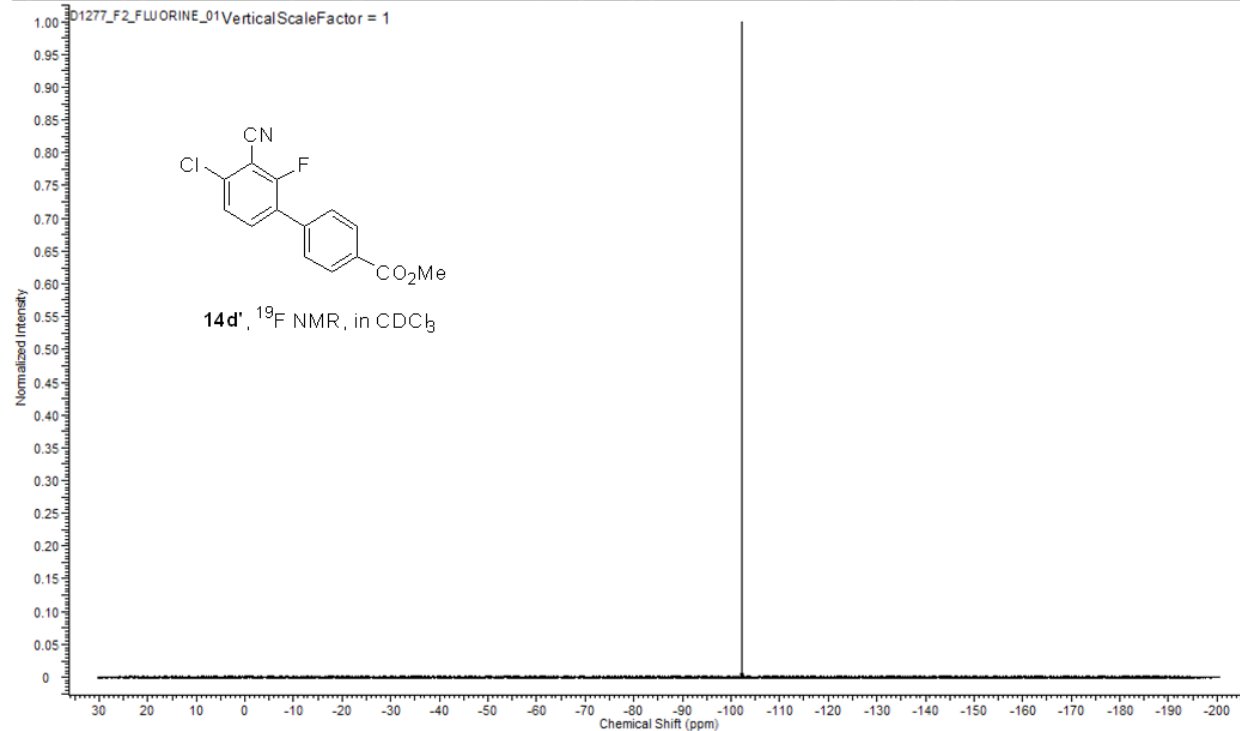


Figure 199 ^1H NMR of mixture of compounds **14e** and **14e'**

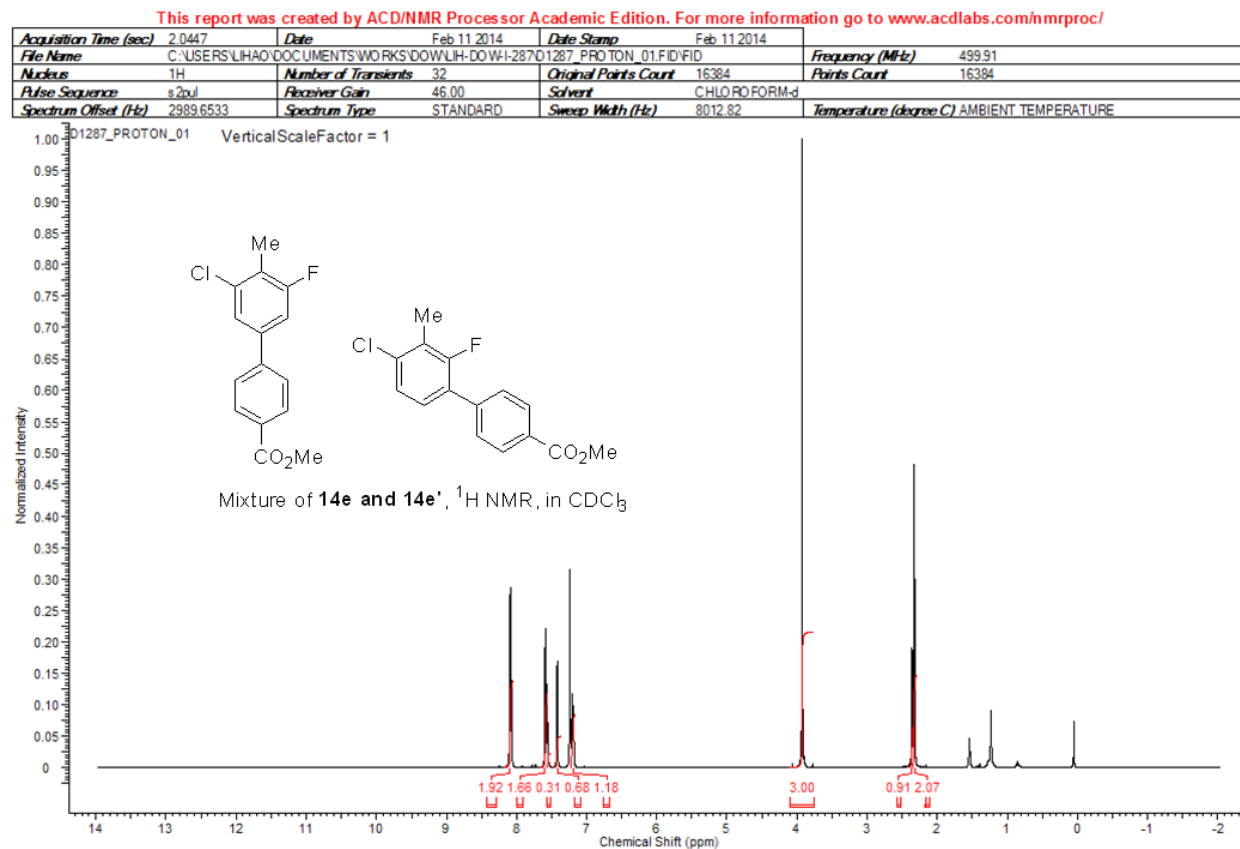


Figure 200 ^{13}C NMR of mixture of compounds 14e and 14e'

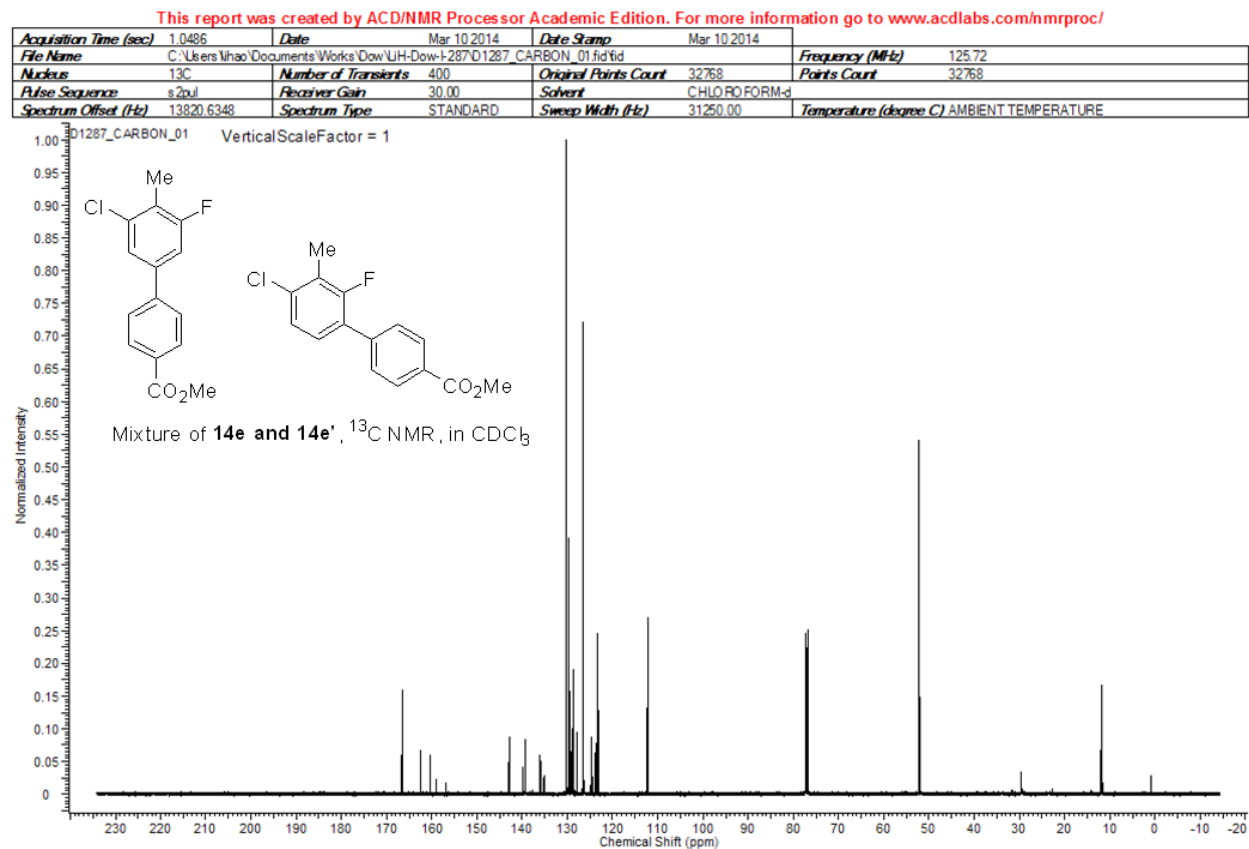


Figure 201 ^{19}F NMR of mixture of compounds 14e and 14e'

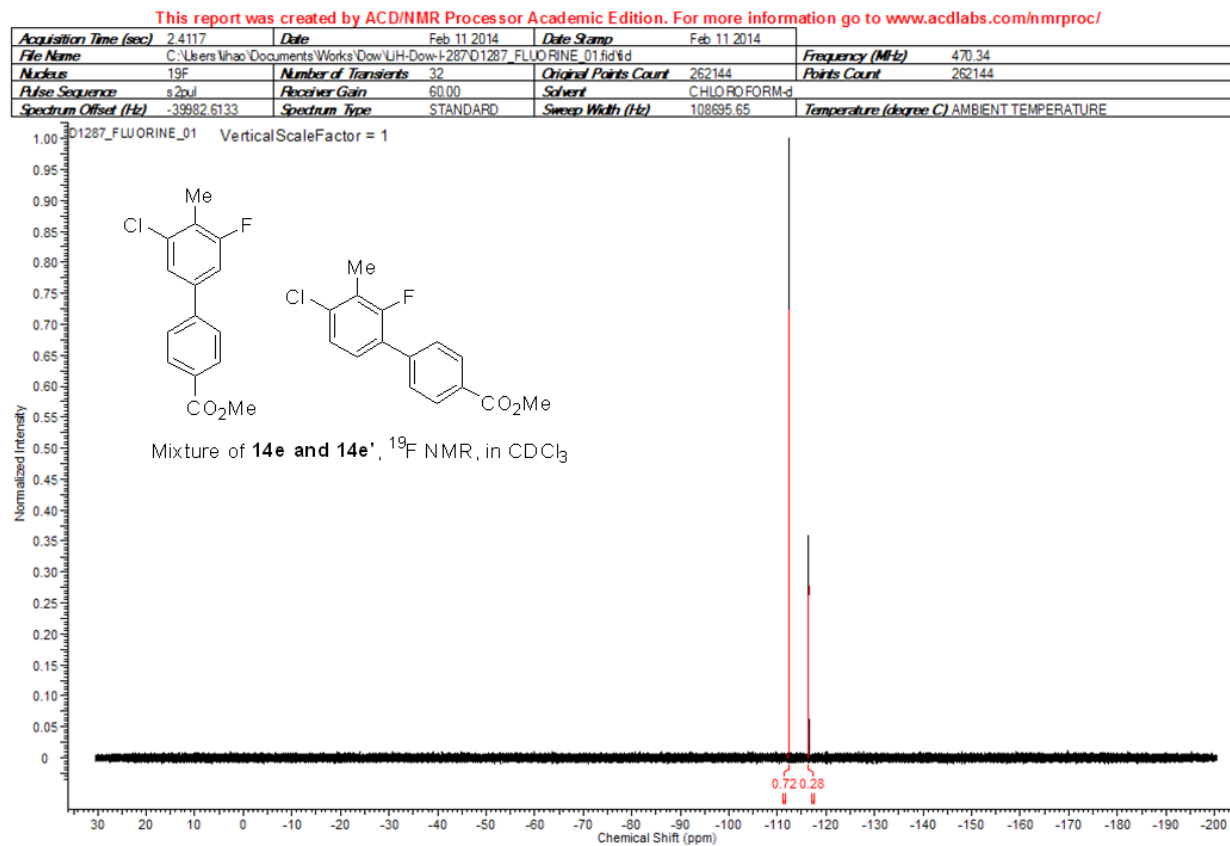


Figure 202 ^1H NMR of mixture of compounds 14f and 14f'

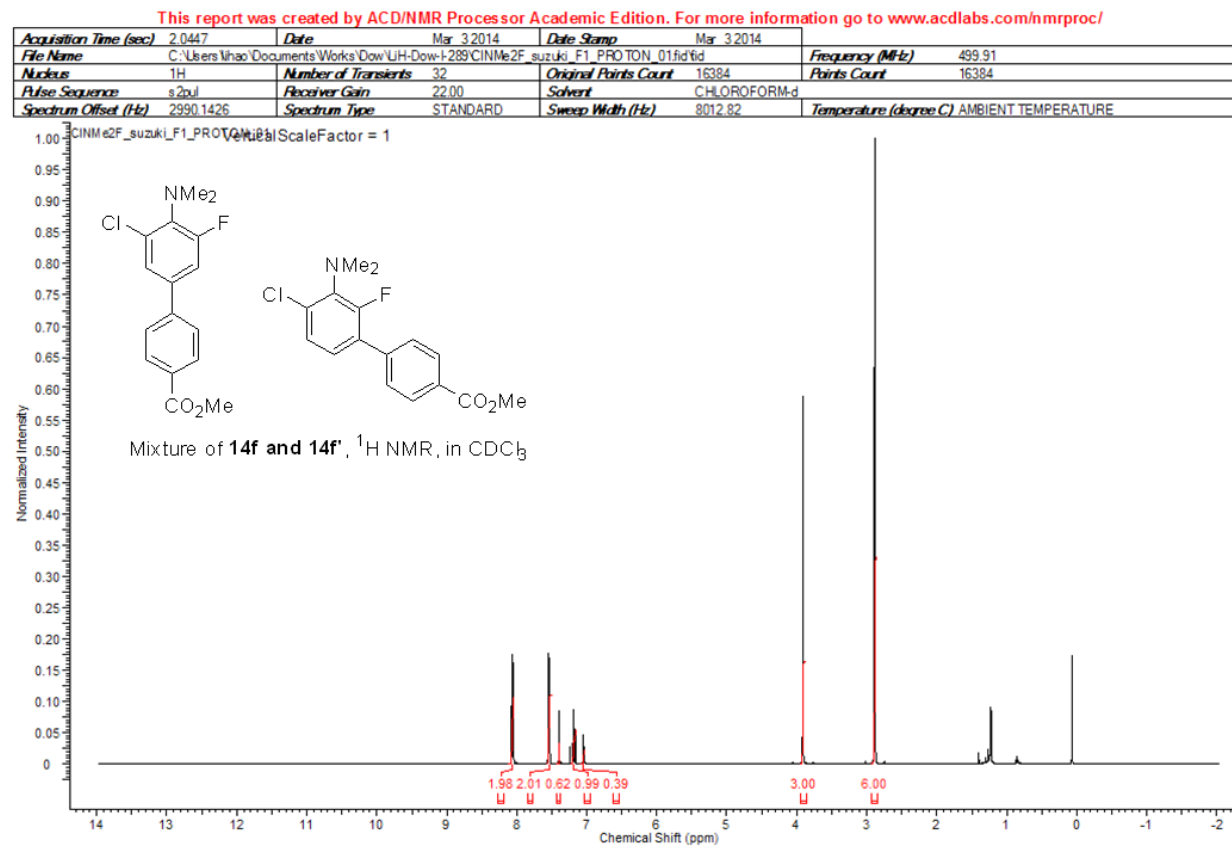


Figure 203 ^{13}C NMR of mixture of compounds 14f and 14f'

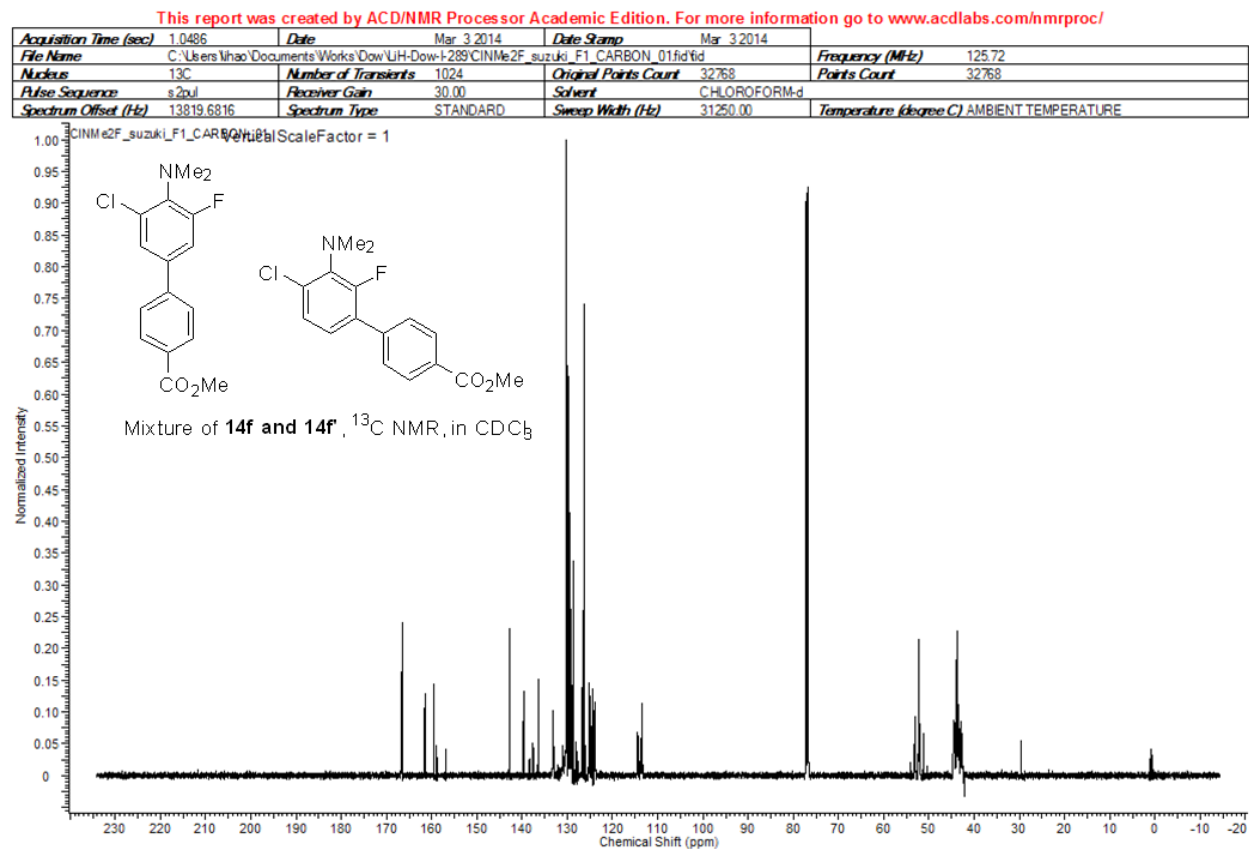


Figure 204 ^{19}F NMR of mixture of compounds **14f** and **14f'**

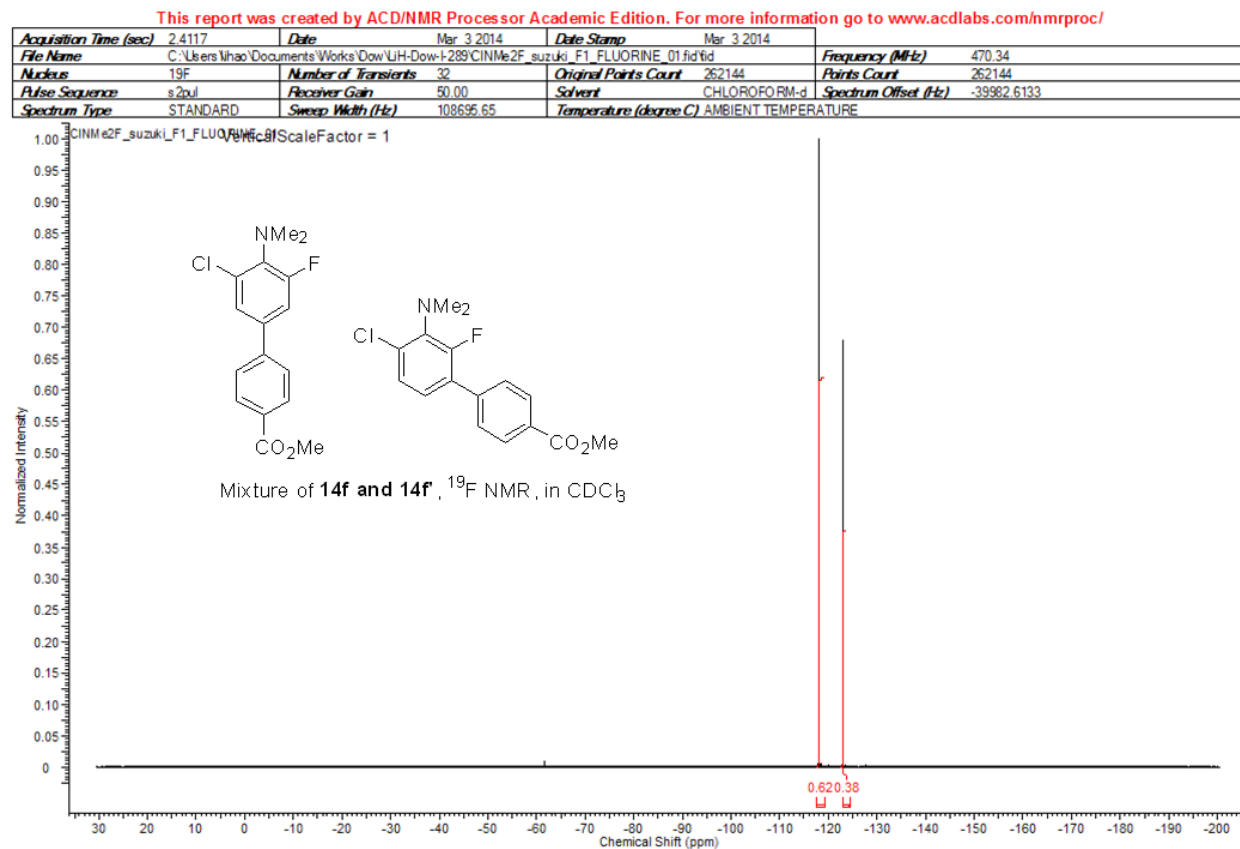


Figure 205 ^1H NMR of mixture of compounds 17a and 18a

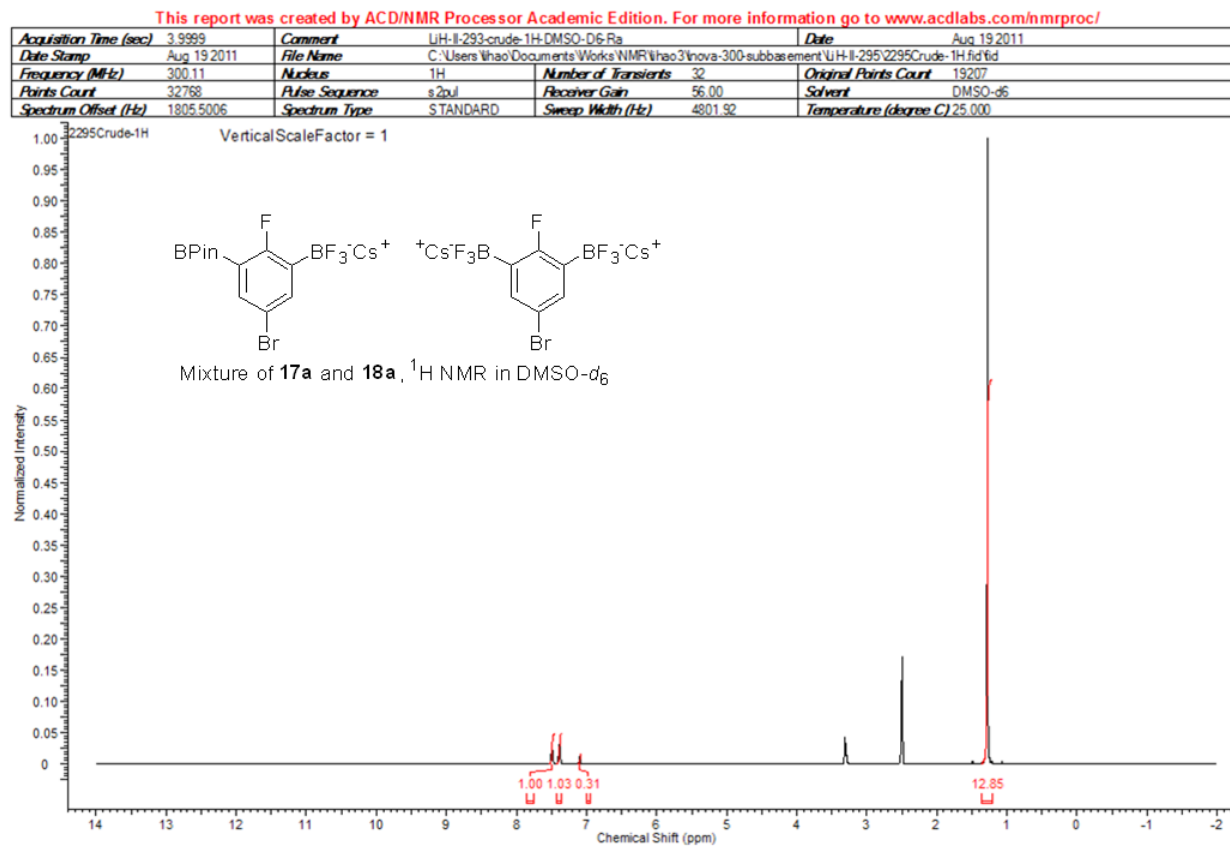


Figure 206 ^{11}B NMR of mixture of compounds 17a and 18a

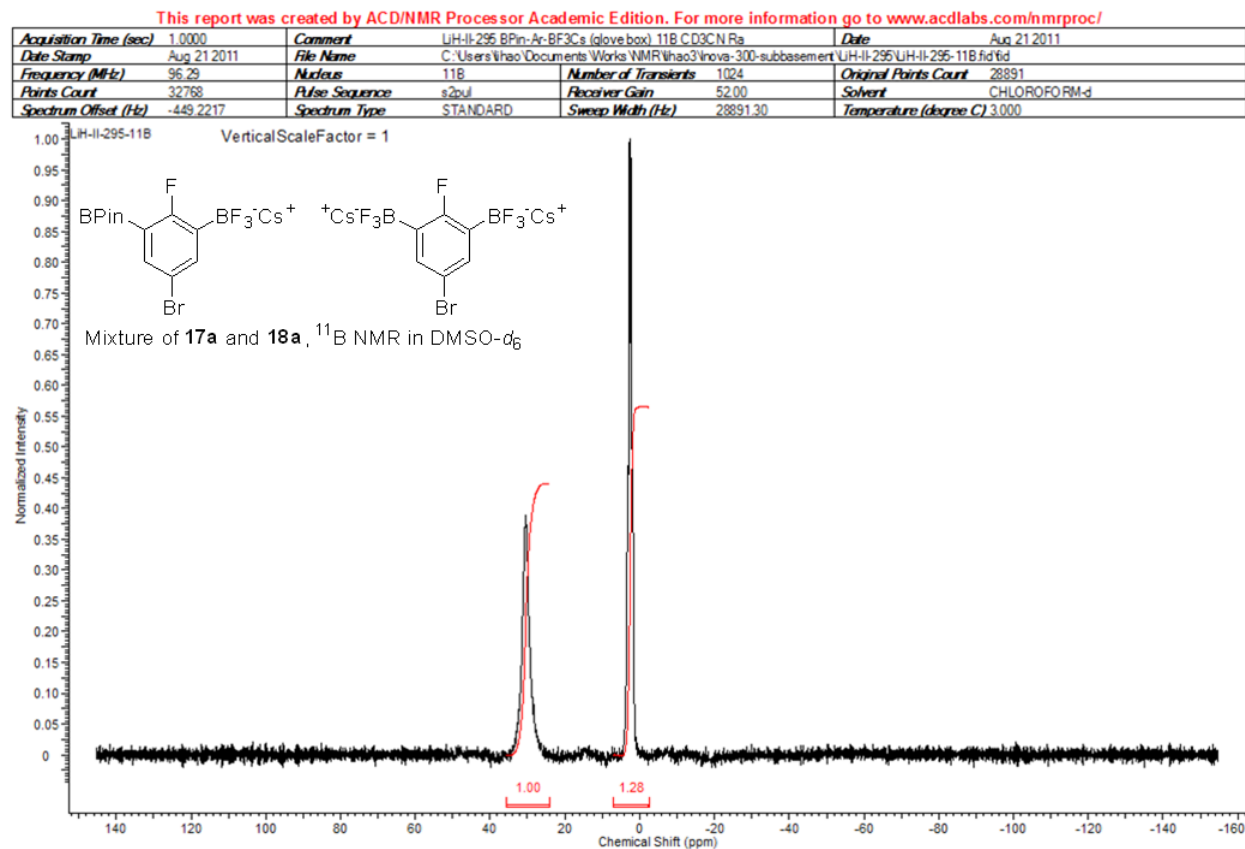


Figure 207 ^{19}F NMR of mixture of compounds 17a and 18a

This report was created by ACD/NMR Processor Academic Edition. For more information go to www.acdlabs.com/nmrproc/

Acquisition Time (sec)	3.0000	Comment	UH-II-295 BPIn-Ar-BF ₃ CS (glove box) 19F CD ₃ CN F8		Date	Aug 21 2011	
Date Stamp	Aug 21 2011	File Name	C:\Users\Wbao\Documents\Works\NMR\Wbao3\inova-300-subbase\UH-II-295\UH-II-295-19F.fid.tif		Original Points Count	194805	
Frequency (MHz)	282.36	Nucleus	19F	Number of Transients	124		
Points Count	262144	Pulse Sequence	s2pul	Receiver Gain	60.00	Solvent	CHLOROFORM-d
Spectrum Offset (Hz)	-26956.3848	Spectrum Type	STANDARD	Sweep Width (Hz)	64935.07	Temperature (degree C)	25.000

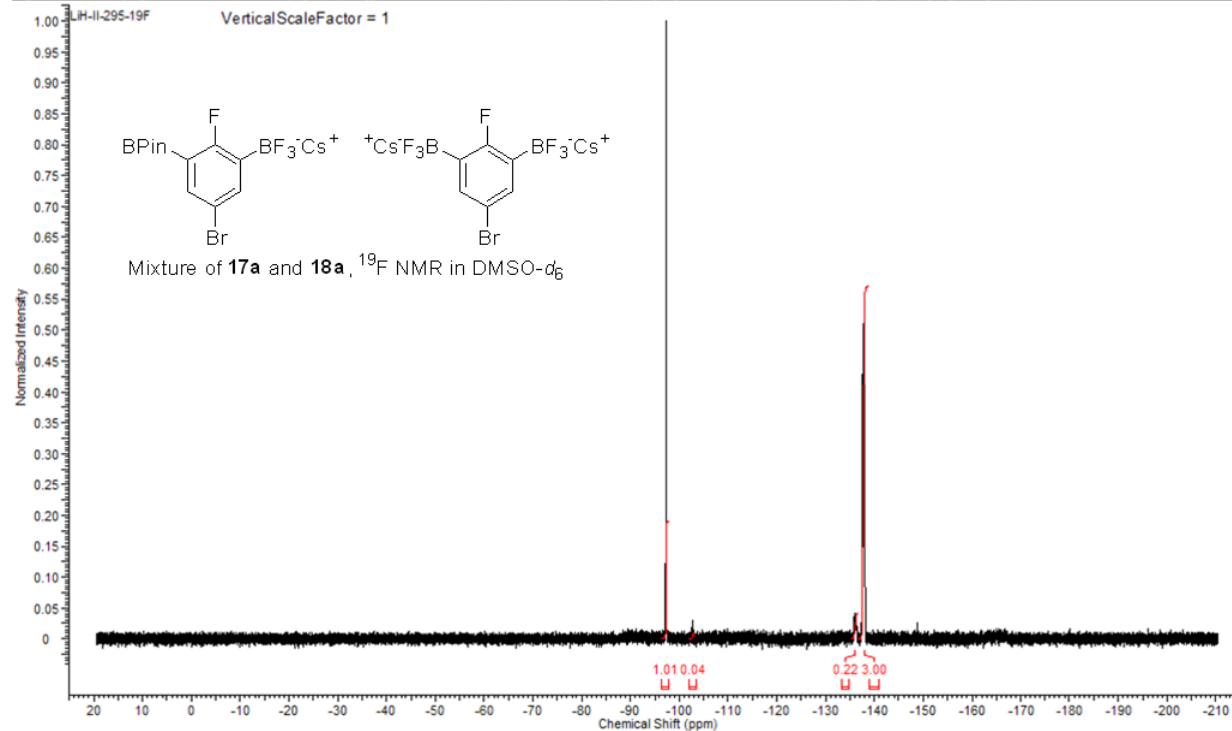


Figure 208 ^1H NMR of compound 17b

This report was created by ACD/NMR Processor Academic Edition. For more information go to www.acdlabs.com/nmrproc/

Acquisition Time (sec)	4.0000	Comment	UH-III-112.1H in DMSO-d6 on Mut	Date	Jan 23 2012
Date Stamp	Jan 23 2012	File Name	C:\Users\lhao\Documents\Works\NMR\lhao3\UnityPlus 500-NEW_room88\UH-III-112\UH-III-112.1H.fid		
Frequency (MHz)	499.74	Nucleus	^1H	Number of Transients	32
Points Count	32768	Pulse Sequence	s2pul	Receiver Gain	39.00
Spectrum Offset (Hz)	2499.7559	Spectrum Type	STANDARD	Sweep Width (Hz)	8000.00
				Solvent	DMSO-d6
				Temperature (degree C)	AMBIENT TEMPERATURE

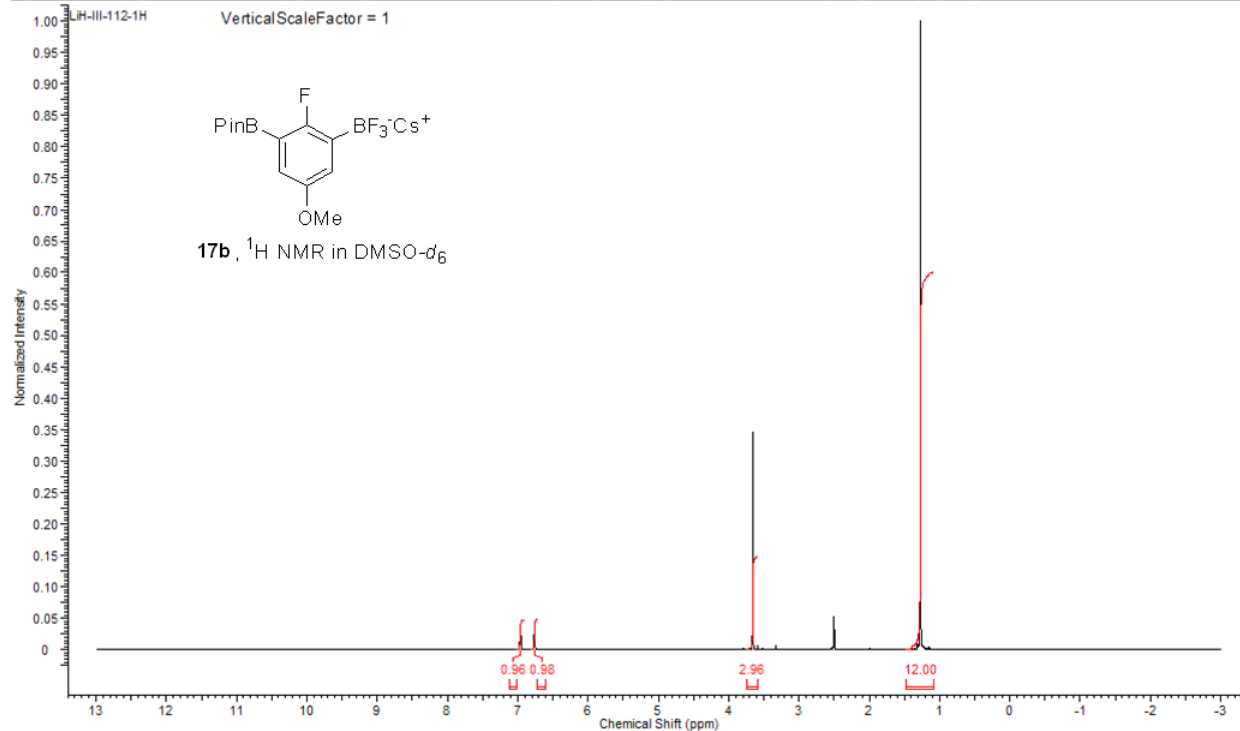


Figure 209 ^{13}C NMR of compound 17b

This report was created by ACD/NMR Processor Academic Edition. For more information go to www.acdlabs.com/nmrproc/

Acquisition Time (sec)	1.2896	Comment	UH-III-112-13C in DMSO-d6 on Mut		Date	Jan 23 2012	
Date Stamp	Jan 23 2012	File Name	C:\Users\Wao\Documents\Works\NMR\hao3\UnityPlus500-NEW_room88\UH-III-112\UH-III-112-13C.fid.tif				
Frequency (MHz)	125.68	Nucleus	^{13}C	Number of Transients	256	Original Points Count	54299
Points Count	65536	Pulse Sequence	s2p1	Receiver Gain	60.00	Solvent	DMSO-d6
Spectrum Offset (Hz)	20330.9551	Spectrum Type	STANDARD	Sweep Width (Hz)	42105.26	Temperature (degree C)	AMBIENT TEMPERATURE

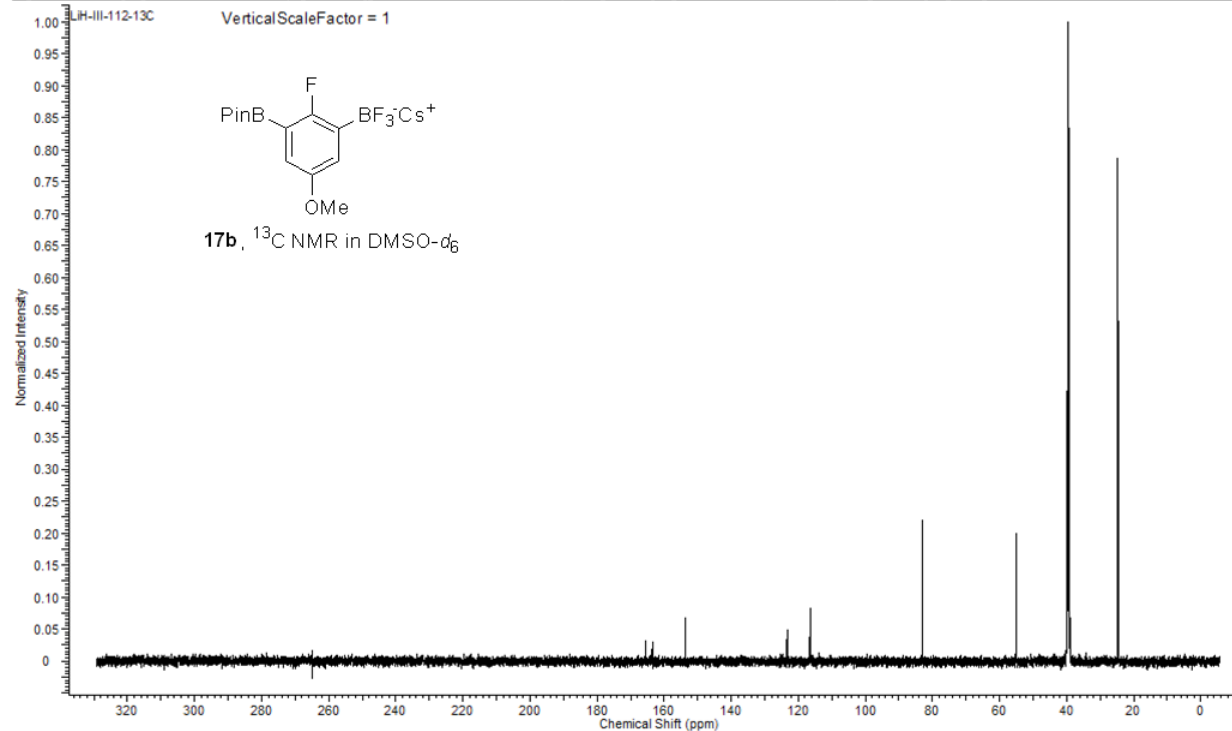


Figure 210 ^1H NMR of compound 19a

This report was created by ACD/NMR Processor Academic Edition. For more information go to www.acdlabs.com/nmrproc/

Acquisition Time (sec)	3.9999	Comment	UH-III-059 final 1H in CD3CN on Isis		Date	Oct 18 2011	
Date Stamp	Oct 18 2011	File Name	C:\Users\yhao\Documents\Works\NMR\yhao3\leis-600\UH-III-059\UH-III-059-final-1H.fid.tif				
Frequency (MHz)	599.81	Nucleus	1H	Number of Transients	32	Original Points Count	38387
Points Count	65536	Pulse Sequence	s2bul	Receiver Gain	46.00	Solvent	ACETONITRILE-d3
Spectrum Offset (Hz)	3598.9912	Spectrum Type	STANDARD	Sweep Width (Hz)	9596.93	Temperature (degree C)	25.000

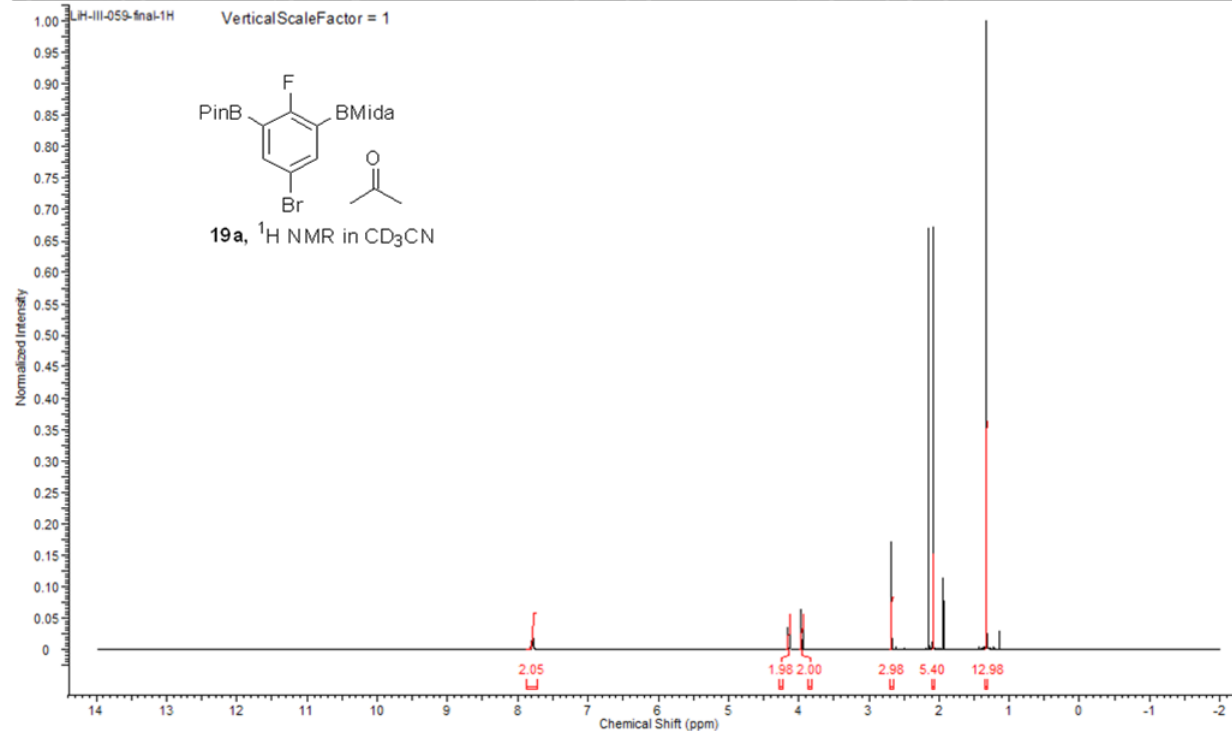


Figure 211 ^{13}C NMR of compound 19a

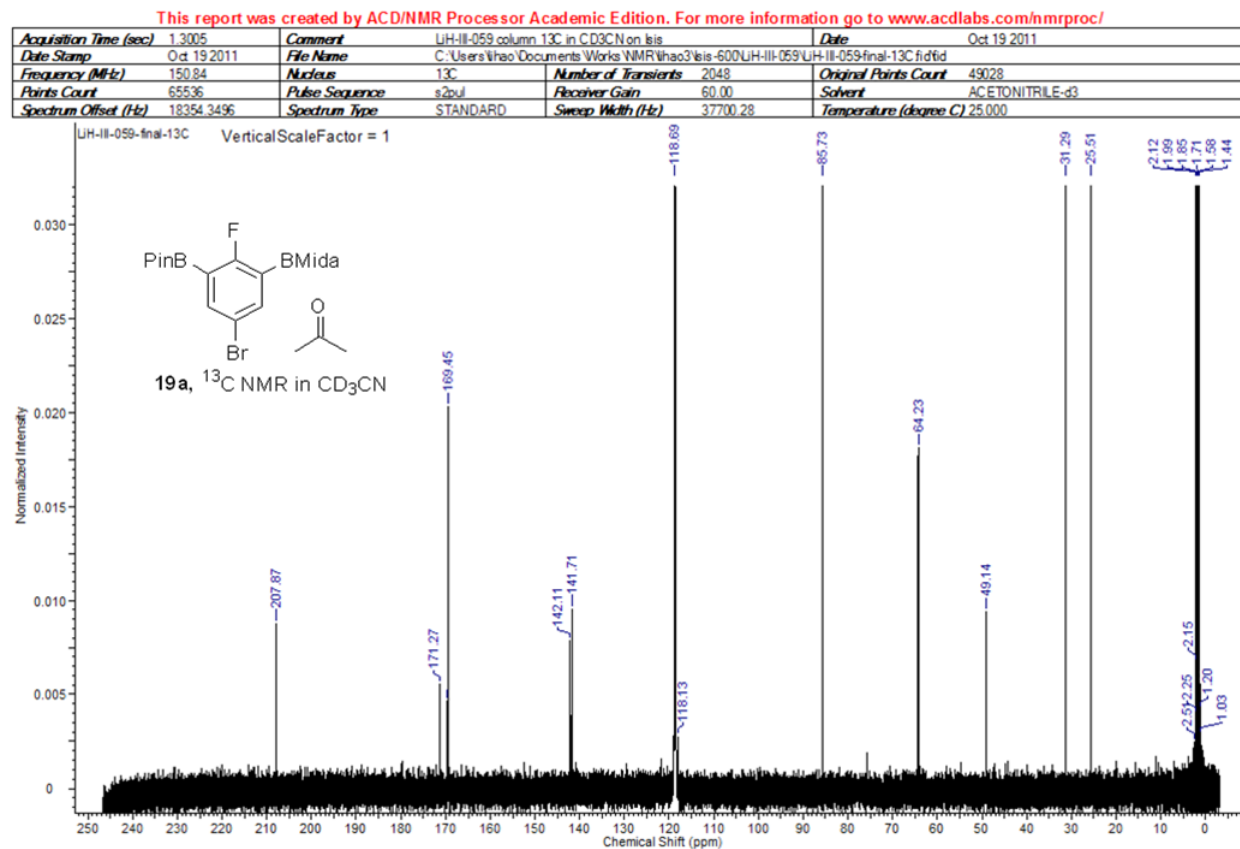


Figure 212 ^1H NMR of compound 19b

This report was created by ACD/NMR Processor Academic Edition. For more information go to www.acdlabs.com/nmrproc/

Acquisition Time (sec)	3.9999	Comment	UH-III-118 Prod. 1H in CD ₃ CN on Isis	Date	Feb. 2. 2012
Date Stamp	Feb. 2. 2012	File Name	C:\Users\Wihao\Documents\Works\NMR\Wihao3\Isis-600\UH-III-118\UH-III-118-1H.fid\fid		
Frequency (MHz)	599.81	Nucleus	¹ H	Number of Transients	32
Points Count	65536	Pulse Sequence	s2pul	Receiver Gain	34.00
Spectrum Offset (Hz)	3598.6982	Spectrum Type	STANDARD	Sweep Width (Hz)	9596.93
				Solvent	ACETONITRILE-d3
				Temperature (degree C)	25.000

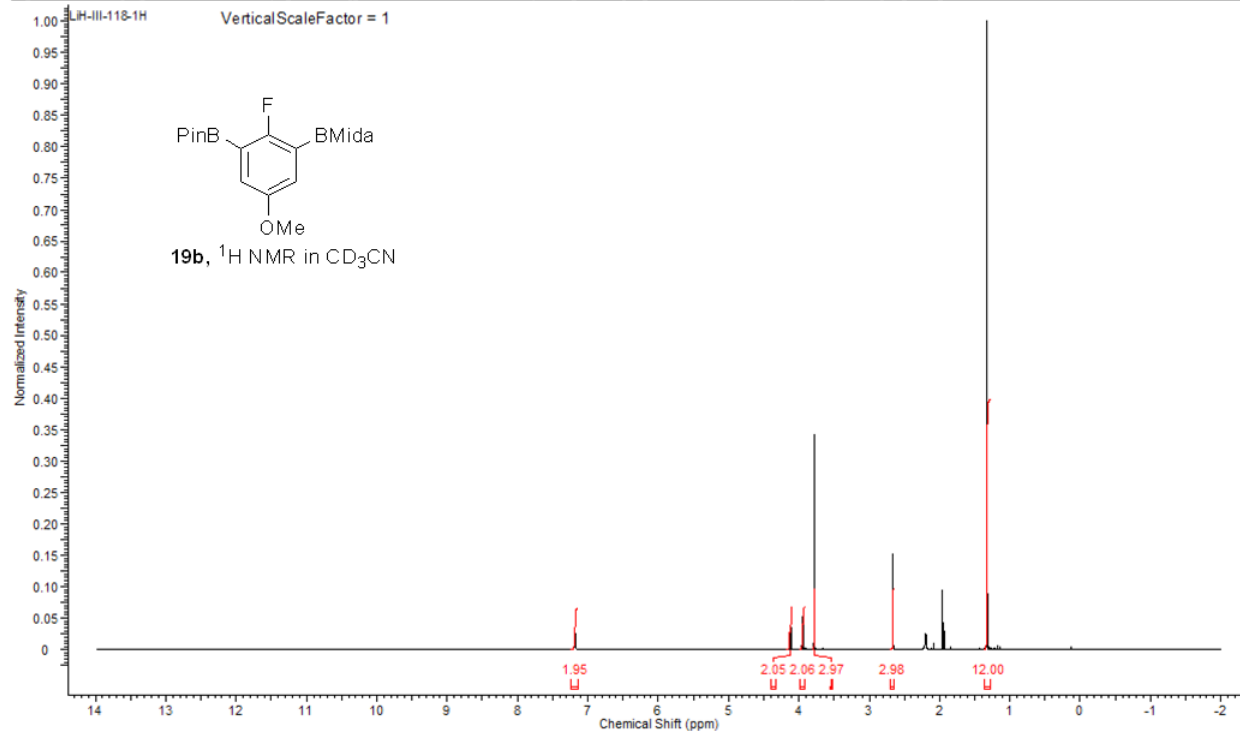


Figure 213 ^{11}B NMR of compound 19b

This report was created by ACD/NMR Processor Academic Edition. For more information go to www.acdlabs.com/nmrproc/

Acquisition Time (sec)	1.0000	Comment	UH-III-118-118 in CD ₃ CN on Ra	Date	Feb. 2. 2012
Date Stamp	Feb. 2. 2012	File Name	C:\Users\Yihao\Documents\Works\NMR\Yihao3\Yinova-300-subbasement\UH-III-118\UH-III-118.fid\fid		
Frequency (MHz)	96.55	Nucleus	^{11}B	Number of Transients	128
Points Count	32768	Pulse Sequence	s2pu1	Receiver Gain	48.00
Spectrum Offset (Hz)	-388.8262	Spectrum Type	STANDARD	Sweep Width (Hz)	28891.30
				Solvent	CHLOROFORM-d
				Temperature (degree C)	25.000

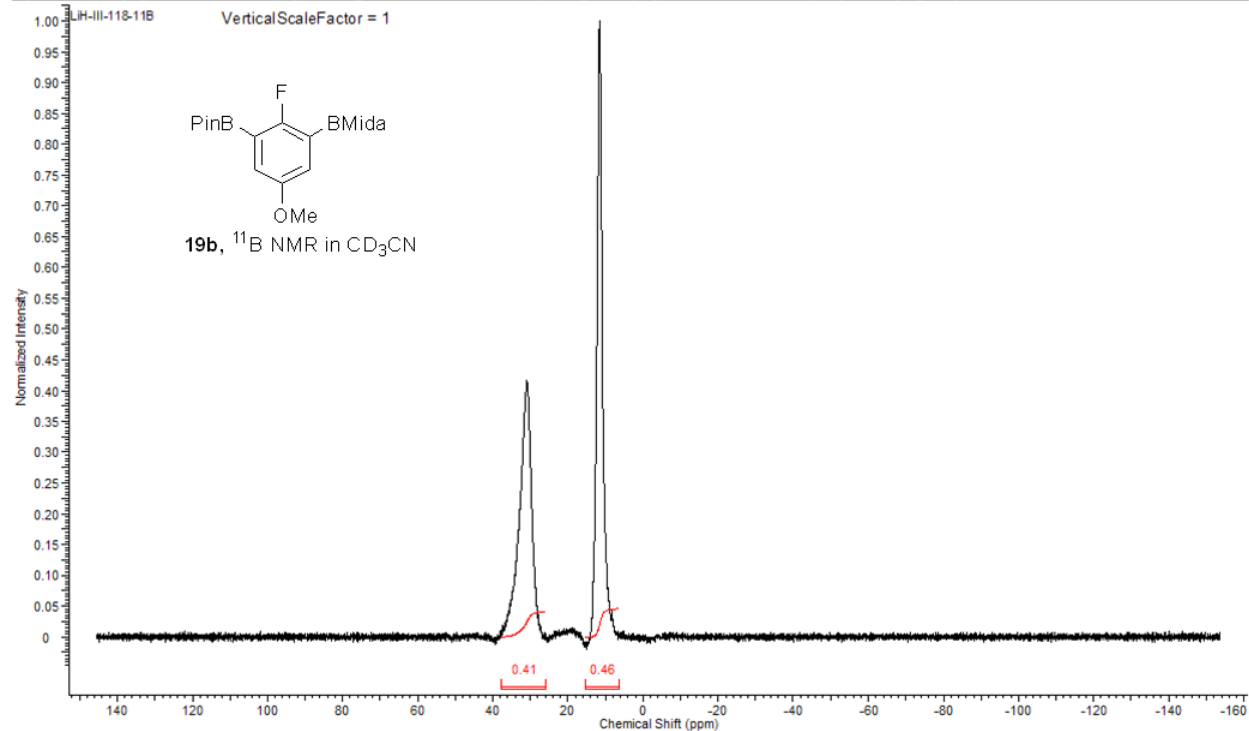


Figure 214 ^{13}C NMR of compound 19b

This report was created by ACD/NMR Processor Academic Edition. For more information go to www.acdlabs.com/nmrproc/

Acquisition Time (sec)	1.3005	Comment	LIH-III-118 Prod 13C in CD3CN on Isis	Date	Feb 22012
Date Stamp	Feb 2 2012	File Name	C:\Users\Yihao\Documents\Works\NMR\Yihao3\Isis-600\UH-III-118\UH-III-118-13C.fid.tif		
Frequency (MHz)	150.84	Nucleus	^{13}C	Number of Transients	1024
Points Count	65536	Pulse Sequence	s2pul	Receiver Gain	30.00
Spectrum Offset (Hz)	15643.8418	Spectrum Type	STANDARD	Sweep Width (Hz)	36199.09
				Solvent	ACETONITRILE-d3
				Temperature (degree C)	25.000

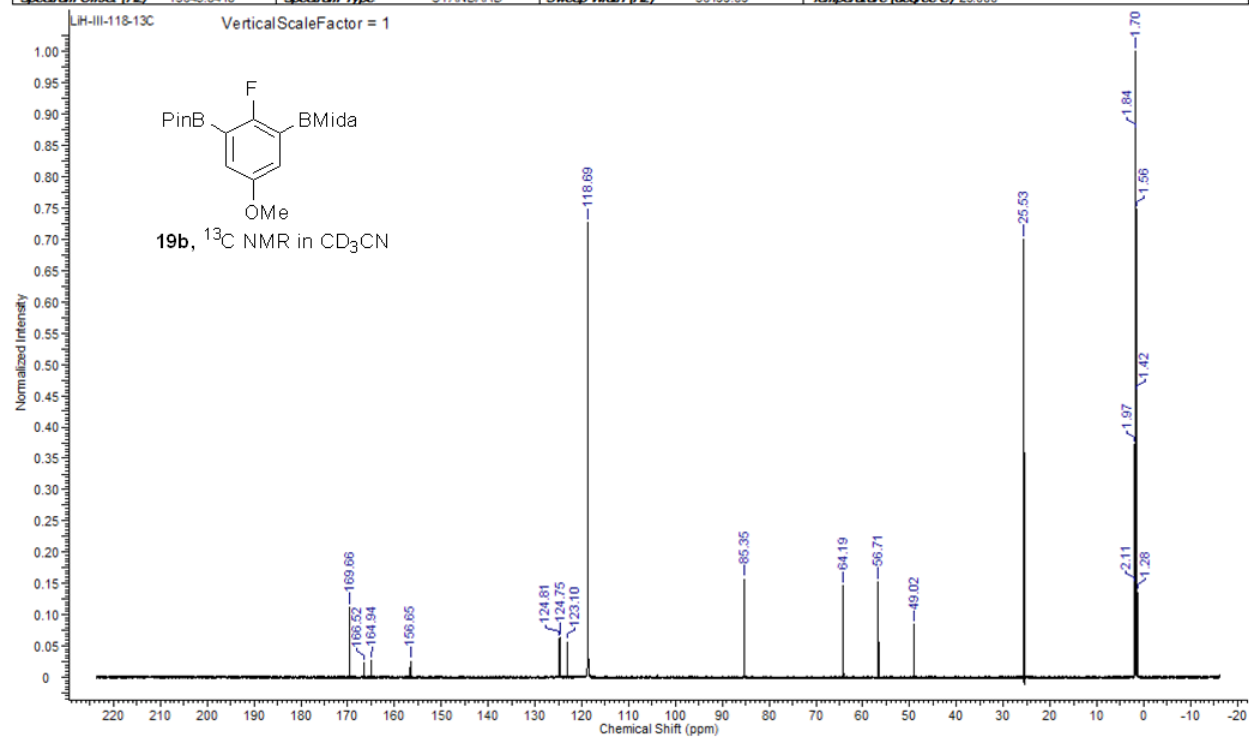
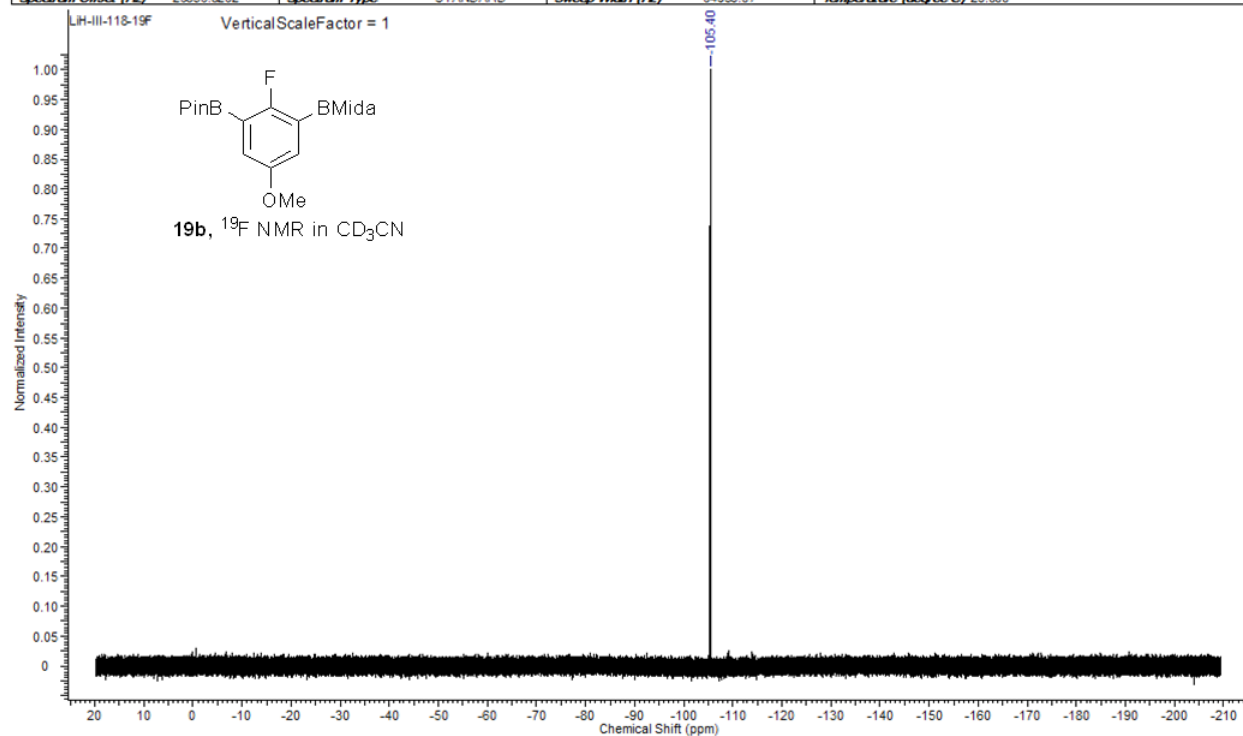


Figure 215 ^{19}F NMR of compound 19b

This report was created by ACD/NMR Processor Academic Edition. For more information go to www.acdlabs.com/nmrproc/

Acquisition Time (sec)	3.0000	Comment	UH-III-118-19F in CD3CN on Ra	Date	Feb. 2 2012	
Date Stamp	Feb. 2 2012	File Name	C:\Users\Nhao\Documents\Works\NMR\Nhao3\Inova-300-subbasement\UH-III-118\UH-III-118-19F.fid.tif			
Frequency (MHz)	283.14	Nucleus	^{19}F	Number of Transients	32	
Points Count	262144	Pulse Sequence	s.pul	Receiver Gain	60.00	
Spectrum Offset (Hz)	-26836.8262	Spectrum Type	STANDARD	Solvent	CHLOROFORM-d	
			Sweep Width (Hz)	64935.07	Temperature (degree C)	25.000



REFERENCES

REFERENCES

- ¹ Iverson, C. N.; Smith, M. R. *J Am Chem Soc* **1999**, *121*, 7696-7697.
- ² (a) Smith, M. R.; Cho, J. Y.; Tse, M. K.; Holmes, D.; Maleczka, R. E. Jr. *Science* **2002**, *295*, 305–308. (b) Ishiyama, T.; Takagi, J.; Ishida, K.; Miyaura, N.; Anastasi, N. R.; Hartwig, J. F. *J. Am. Chem. Soc.* **2002**, *124*, 390–391. (c) Mkhaliid, I. A. I.; Barnard, J. H.; Marder, T. B.; Murphy, J. M.; Hartwig, J. F. *Chem. Rev.* **2010**, *110*, 890–931.
- ³ (a) Vanchura, B. A.; Preshlock, S. M.; Roosen, P. C.; Kallepalli, V. A.; Staples, R. J.; Maleczka, R. E.; Singleton, D. A.; Smith, M. R. *Chem Commun* **2010**, *46*, 7724-7726. (b) Tajuddin, H.; Harrisson, P.; Bitterlich, B.; Collings, J. C.; Sim, N.; Batsanov, A. S.; Cheung, M. S.; Kawamorita, S.; Maxwell, A. C.; Shukla, L.; Morris, J.; Lin, Z. Y.; Marder, T. B.; Steel, P. G. *Chem Sci* **2012**, *3*, 3505-3515.
- ⁴ (a) Chotana, G. A.; Rak, M. A.; Smith, M. R. *J Am Chem Soc* **2005**, *127*, 10539-10544. (b) Maleczka, R. E.; Shi, F.; Holmes, D.; Smith, M. R. *J Am Chem Soc* **2003**, *125*, 7792-7793.
- ⁵ Maleczka and Smith groups unpublished results
- ⁶ (a) ACS catalysis paper (b) Dow computational paper (c) Smith, M. R. III; Maleczka, R. E. Jr.; Li, H.; Jayasundara, C.; Oppenheimer, J.; Sabasovs, D. US 20150065743 A1, **2015**.
- ⁷ Maleczka and Smith groups unpublished results
- ⁸ Suzuki, A. *Angew Chem Int Edit* **2011**, *50*, 6722-6737.
- ⁹ Hall, D. G. *Boronic Acids: Preparation and Applications in Organic Synthesis, Medicine and Materials, 2nd ed.*; Wiley-VCH: Weinheim, 2011.
- ¹⁰ Stille, J. K. *Angew Chem Int Edit* **1986**, *25*, 508-523.
- ¹¹ Miyaura, N.; Suzuki, A. *Chem Rev* **1995**, *95*, 2457-2483.
- ¹² (a) One early example of chemoselective Suzuki coupling of iodobromobenzene. Hensel, V.; Schluter, A. D. *Liebigs Ann-Recl* **1997**, 303-309. More examples: (b) Wu, X. F.; Anbarasan, P.; Neumann, H.; Beller, M. *Angew Chem Int Edit* **2010**, *49*, 7316-7319. (c) Aranyos, A.; Old, D. W.; Kiyomori, A.; Wolfe, J. P.; Sadighi, J. P.; Buchwald, S. L. *J Am Chem Soc* **1999**, *121*, 4369-4378. (d) Cho, G. Y.; Remy, P.; Jansson, J.; Moessner, C.; Bolm, C. *Org Lett* **2004**, *6*, 3293-3296. (e) Mosrin, M.; Knochel, P. *Chem-Eur J* **2009**, *15*, 1468-1477.

- ¹³ Grob, J. E.; Dechantsreiter, M. A.; Tichkule, R. B.; Connolly, M. K.; Honda, A.; Tomlinson, R. C.; Hamann, L. G. *Org Lett* **2012**, *14*, 5578-5581.
- ¹⁴ Lhermitte, F.; Carboni, B. *Synlett* **1996**, 377-379.
- ¹⁵ Coleman, R. S.; Walczak, M. C. *Org. Lett.* **2005**, *7*, 2289-2291.
- ¹⁶ Snieckus, V.; Kalinin, A. V.; Scherer, S. *Angew. Chem. Int. Ed.* **2003**, *42*, 33993404.
- ¹⁷ Burke, M. D.; Lee, S. J.; Gray, K. C.; Paek, J. S. *J. Am. Chem. Soc.* **2008**, *130*, 466-468.
- ¹⁸ (a) Yamamoto, Y.; Seko, T.; Nemoto, H. *J. Org. Chem.* **1989**, *54*, 4734-4736. (b) vonderSaal, W.; Engh, R. A.; Eichinger, A.; Gabriel, B.; Kuczniarz, R.; Sauer, J. *Arch. Pharm.* **1996**, *329*, 73-82.
- ¹⁹ (a) Linshoeft, J.; Heinrich, A. C. J.; Segler, S. A. W.; Gates, P. J.; Staubitz, A. *Org Lett* **2012**, *14*, 5644-5647. (b) Heinrich, A. C. J.; Thiedemann, B.; Gates, P. J.; Staubitz, A. *Org Lett* **2013**, *15*, 4666-4669.
- ²⁰ (a) Qiu, D.; Wang, S. A.; Tang, S. B.; Meng, H.; Jin, L.; Mo, F. Y.; Zhang, Y.; Wang, J. B. *J Org Chem* **2014**, *79*, 1979-1988. (b) Takenak, H.; Ohta, Y.; Taguchi, Y.; Ueda, S.; Ishino, Y.; Nakashima, H.; Uehara, K.; Kirihata, M. Chiral 4-boronophenylalanine (bpa) derivative and method for producing same, and method for producing 18f-labeled bpa using said derivative WO2014061508 A1. (c) Wang, J. B.; Qiu, D.; Ye, Y. X.; Deng, Y. F.; Zhang, Y. Synthesis method of aryltin compounds from aromatic amine, distannane and alkyl nitrite CN 103665026 A. (d) Qiu, D.; Meng, H.; Jin, L.; Wang, S.; Tang, S. B.; Wang, X.; Mo, F. Y.; Zhang, Y.; Wang, J. B. *Angew Chem Int Edit* **2013**, *52*, 11581-11584.
- ²¹ (a) Roush, W. R.; Tortosa, M.; Yakelis, N. A. *J. Am. Chem. Soc.* **2008**, *130*, 2722-2723. (b) Coleman, R. S.; Walczak, M. C.; Campbell, E. L. *J. Am. Chem. Soc.* **2005**, *127*, 16038-16039. (c) Coleman, R. S.; Walczak, M. C. *J. Org. Chem.* **2006**, *71*, 9841-9844. (d) Coleman, R. S.; Lu, X. L.; Modolo, I. *J. Am. Chem. Soc.* **2007**, *129*, 3826-3827.
- ²² Coleman, R. S.; Lu, X. L. *Chem. Comm.* **2006**, 423-425.
- ²³ (a) Braga, A. A. C.; Morgon, N. H.; Ujaque, G.; Maseras, F. *J. Am. Chem. Soc.* **2005**, *127*, 9298-9307. (b) Hartwig, J. F.; Carrow, B. P. *J. Am. Chem. Soc.* **2011**, *133*, 2116-2119.
- ²⁴ (a) *Chemistry of Tin*; Smith, P. J., Ed.; Blackie Academic & Professional: New York, 1998. (b) Davies A. G. In *Organotin Chemistry*; VCH: New York, 1997.
- ²⁵ (a) Smith, M. R.; Cho, J. Y.; Tse, M. K.; Holmes, D.; Maleczka, R. E. Jr. *Science* **2002**, *295*, 305-308. (b) Ishiyama, T.; Takagi, J.; Ishida, K.; Miyaura, N.; Anastasi, N. R.; Hartwig, J. F. *J. Am. Chem. Soc.* **2002**, *124*, 390-391. (c) Mkhaliid, I. A. I.; Barnard, J. H.; Marder, T. B.; Murphy, J. M.; Hartwig, J. F. *Chem. Rev.* **2010**, *110*, 890-931.

²⁶ For an example of Ir-catalyzed borylation on arylsilanes see Reus, C.; Liu, N. W.; Bolte, M.; Lerner, H. W.; Wagner, M. *J Org Chem* **2012**, *77*, 3518-3523.

²⁷ Hartwig, J. F.; Boller, T. M.; Murphy, J. M.; Hapke, M.; Ishiyama, T.; Miyaura, N. *J Am Chem Soc* **2005**, *127*, 14263

²⁸ (a) Gosmini, C.; Fillon, H.; Périchon, J. *J. Am. Chem. Soc.* **2003**, *125*, 3867–3870. (b) Gosmini, C.; Périchon, J. *Org. Biomol. Chem.* **2005**, *3*, 216–217.

²⁹ (a) Bolm, C.; Rudolph, J.; Schmidt, F. *Adv. Synth. Catal.* **2004**, *346*, 867–872. (b) Rudolph, J.; Schmidt, F.; Bolm, C. *Synthesis* **2005**, 840–842. (c) Bolm, C.; Schmidt, F.; Rudolph, J. *Synthesis* **2006**, 3625–3630. (d) Bolm, C.; Schmidt, F.; Stemmler, R. T.; Rudolph, J. *Chem. Soc. Rev.* **2006**, *35*, 454–470. (e) Bolm, C.; Schmidt, F.; Rudolph, J. *Adv. Synth. Catal.* **2007**, *349*, 703–708. For mechanism discussions see: (f) Maseras, F.; Jimeno, C.; Sayalero, S.; Fjermestad, T.; Colet, G.; Pericas, M. A. *Angew. Chem. Int. Ed.* **2008**, *47*, 1098–1101. (g) Partyka, D. V. *Chem. Rev.* **2011**, *111*, 1529–1595.

³⁰ At the time of this work, few commercial suppliers had TIOEt in stock and thus this base was not screened in Table 3. When this base was finally secured, its use in the reaction of **2f** via the procedure of Linshoeft, J.; Heinrich, A. C. J.; Segler, S. A. W.; Gates, P. J.; Staubitz, A. *Org Lett* **2012**, *14*, 5644. gave **4f** in 47% isolated yield.

³¹ (a) Fried, J.; Sabo, E. F. *J Am Chem Soc* **1953**, *75*, 2273-2274. (b) Fried, J.; Sabo, E. F. *J Am Chem Soc* **1954**, *76*, 1455-1456.

³² Purser, S.; Moore, P. R.; Swallow, S.; Gouverneur, V. *Chem Soc Rev* **2008**, *37*, 320-330.

³³ Wang, J.; Sanchez-Rosello, M.; Acena, J. L.; del Pozo, C.; Sorochinsky, A. E.; Fustero, S.; Soloshonok, V. A.; Liu, H. *Chem Rev* **2014**, *114*, 2432-2506.

³⁴ Lee, E.; Kamlet, A. S.; Powers, D. C.; Neumann, C. N.; Boursalian, G. B.; Furuya, T.; Choi, D. C.; Hooker, J. M.; Ritter, T. *Science* **2011**, *334*, 639-642.

³⁵ Hagmann, W. K. *J Med Chem* **2008**, *51*, 4359-4369.

³⁶ Laali, K. K.; Gettwert, V. J. *J Fluorine Chem* **2001**, *107*, 31-34.

³⁷ Shimizu, M.; Hiyama, T. *Angew Chem Int Edit* **2005**, *44*, 214-231.

³⁸ (a) Rozen, S. *Accounts Chem Res* **2005**, *38*, 803-812. (b) Singh, R. P.; Shreeve, J. M. *Accounts Chem Res* **2004**, *37*, 31-44. (c) Lal, G. S.; Pez, G. P.; Syvret, R. G. *Chem Rev* **1996**, *96*, 1737-1755. (d) Ma, J. A.; Cahard, D. *Chem Rev* **2004**, *104*, 6119-6146.

³⁹ (a) Lyons, T. W.; Sanford, M. S. *Chem Rev* **2010**, *110*, 1147-1169. (b) Wang, X. S.; Mei, T. S.; Yu, J. Q. *J Am Chem Soc* **2009**, *131*, 7520-+. (c) Hull, K. L.; Anani, W. Q.; Sanford, M. S. *J Am Chem Soc* **2006**, *128*, 7134-7135.

⁴⁰ Examples of such borylations: (a) Newby, J. A.; Blaylock, D. W.; Witt, P. M.; Pastre, J. C.; Zacharova, M. K.; Ley, S. V.; Browne, D. L. *Org Process Res Dev* **2014**, *18*, 1211-1220. (b) Oppenheimer, J. Methods of isolating 4-chloro-2-fluoro-3-substituted-phenylboronic acids. US 20130030213 A1, **2013**.

⁴¹ Examples of reactions utilizing benzyne generated in this way: (a) Soorukram, D.; Qu, T.; Barrett, A. G. M. *Org Lett* **2008**, *10*, 3833-3835. (b) Riggs, J. C.; Ramirez, A.; Cremeens, M. E.; Bashore, C. G.; Candler, J.; Wirtz, M. C.; Coe, J. W.; Collum, D. B. *J Am Chem Soc* **2008**, *130*, 3406-3412.

⁴² Del Grosso, A.; Carrillo, J. A.; Ingleson, M. J. *Chem Commun* **2015**, *51*, 2878-2881.

⁴³ Knochel, P. Metallic amidoborates for functionalizing organic compounds WO2012085169 A1, **2012**

⁴⁴ Erb, W.; Hellal, A.; Albin, M.; Rouden, J.; Blanchet, J. *Chem-Eur J* **2014**, *20*, 6608-6612.

⁴⁵ Furukawa, T.; Tobisu, M.; Chatani, N. *J Am Chem Soc* **2015**, *137*, 12211-12214.

⁴⁶ Iverson, C. N.; Smith, M. R. *J Am Chem Soc* **1999**, *121*, 7696-7697.

⁴⁷ (a) Smith, M. R.; Cho, J. Y.; Tse, M. K.; Holmes, D.; Maleczka, R. E. Jr. *Science* **2002**, *295*, 305-308. (b) Ishiyama, T.; Takagi, J.; Ishida, K.; Miyaura, N.; Anastasi, N. R.; Hartwig, J. F. *J. Am. Chem. Soc.* **2002**, *124*, 390-391. (c) Mkhali, I. A. I.; Barnard, J. H.; Marder, T. B.; Murphy, J. M.; Hartwig, J. F. *Chem. Rev.* **2010**, *110*, 890-931.

⁴⁸ (a) Kawamorita, S.; Ohmiya, H.; Hara, K.; Fukuoka, A.; Sawamura, M. *J Am Chem Soc* **2009**, *131*, 5058-5059. (b) Ishiyama, T.; Isou, H.; Kikuchi, T.; Miyaura, N. *Chem Commun* **2010**, *46*, 159-161. (c) Boebel, T. A.; Hartwig, J. F. *J Am Chem Soc* **2008**, *130*, 7534-7535. (d) Roosen, P. C.; Kallepalli, V. A.; Chattopadhyay, B.; Singleton, D. A.; Maleczka, R. E.; Smith, M. R. *J Am Chem Soc* **2012**, *134*, 11350-11353. (e) Preshlock, S. M.; Plattner, D. L.; Maligres, P. E.; Krska, S. W.; Maleczka, R. E.; Smith, M. R. *Angew Chem Int Edit* **2013**, *52*, 12915-12919.

⁴⁹ Previous computational studies showed the transition state of C-H activation exhibits a significant proton transfer characteristics, and experimental studies also suggest more acidic C-H bonds are favored for Ir catalyzed C-H activation/borylation: (a) Vanchura, B. A.; Preshlock, S. M.; Roosen, P. C.; Kallepalli, V. A.; Staples, R. J.; Maleczka, R. E.; Singleton, D. A.; Smith, M. R. *Chem Commun* **2010**, *46*, 7724-7726. (b) Tajuddin, H.; Harrisson, P.; Bitterlich, B.; Collings, J. C.; Sim, N.; Batsanov, A. S.; Cheung, M. S.; Kawamorita, S.; Maxwell, A. C.; Shukla, L.; Morris, J.; Lin, Z. Y.; Marder, T. B.; Steel, P. G. *Chem Sci* **2012**, *3*, 3505-3515.

⁵⁰ We also included Hunig's base as one of the solvent in the screening, due to its excellent performance in literature for borylation reactions: Preshlock, S. M.; Ghaffari, B.; Maligres, P. E.; Krska, S. W.; Maleczka, R. E.; Smith, M. R. *J Am Chem Soc* **2013**, *135*, 7572-7582.

⁵¹ N-Ir-N angle for Ir(Bpin)₃dtbpy(coe) complex is 74.7°, ref 2(b). Is that of box actually known?

⁵² (a) Chan, K. S.; Tse, A. K. S. *Synthetic Communications* **1993**, *23*, 1929-1934. (b) Iyoda, M.; Otsuka, H.; Sato, K.; Nisato, N.; Oda, M. *B Chem Soc Jpn* **1990**, *63*, 80-87. (c) Furue, M.; Maruyama, K.; Oguni, T.; Naiki, M.; Kamachi, M. *Inorg Chem* **1992**, *31*, 3792-3795. (d) McFarland, S. A.; Lee, F. S.; Cheng, K. A. W. Y.; Cozens, F. L.; Schepp, N. P. *J Am Chem Soc* **2005**, *127*, 7065-7070.

⁵³ Li, H.; Oppenheimer, J.; Smith, M. R.; Maleczka, R. E. *Tetrahedron Lett* **2016**, *57*, 2231-2232.

⁵⁴ Synthesis and characterization of these compounds are also described in Smith, M. R. III.; Maleczka, R. E. Jr.; Li, H.; Jayasundara, C.; Oppenheimer, J.; Sabasovs, D. Methods for the selective borylation of arenes, including arenes substituted with an electron-withdrawing group. US2015/65743 A1, **2015**.

⁵⁵ Synthesis and characterization of 2e' was also described in: Vrudhula, V. M. R. P.; Pan, S.; Rajamani, R.; Macor, J. E.; Bronson, J. J.; Dzierba, C. D.; Nara, S. J.; Karatholuvhu, M. S.; aryl ether-base kinase inhibitors. US2013/237555 A1, **2013**.

⁵⁶ Synthesis and characterization of 2f' was also described in: Epp, J. B.; Schmitzer, P. R.; Guentensperger, K. A.; Lo, W. C.; Siddall, T. L. 2-(Substituted phenyl)-6-amino-5-alkoxy, thioalkoxy and aminoalkyl-4-pyrimidinecarboxylates and their use as herbicides. Patent: US2009/62125 A1, **2009**.

⁵⁷ (a) Synthesis and characterization of a compound structurally similar to 2g was also described in: Matsuo, y.; Hisada, S.; Nakamura, Y.; Ahmed, F.; Walker, J. R.; Huntley, R. 1,5-Naphthyridine derivatives and melk inhibitors containing the same. WO2013/109388 A2, **2013**. (b) Synthesis and characterization of 2g' was also described in: Newby, J. A.; Blaylock, D. W.; Witt, P. M.; Pastre, J. C.; Zacharova, M. K.; Ley, S. V.; Browne, D. L. *Org Process Res Dev* **2014**, *18*, 1211-1220.

⁵⁸ Synthesis and characterization of a compound structurally similar to 2a was also described in: Sott, R.; Hawner, C.; Johansen, J. E. *Tetrahedron* **2008**, *64*, 4135-4142.

⁵⁹ Synthesis and characterization of 2c was also described in: Akama, T.; Balko, T. W.; Defauw, J. M.; Plattner, J. J.; White, W. H.; Winkle, J. R.; Zhang, Y.-K.; Zhou, Y. Boron-containing small molecules. US2013/131016 A1, **2013**. Synthesis and characterization of 2c' was also described in: ref. 33

⁶⁰ Synthesis and characterization of 2d' was also described in: ref. 34(b)

⁶¹ (a) Wang, C. Y.; Glorius, F. *Angew Chem Int Edit* **2009**, *48*, 5240-5244. (b) Tobisu, M.; Chatani, N. *Angew Chem Int Edit* **2009**, *48*, 3565-3568.

⁶² (a) Iwadate, N.; Suginome, M. *Org Lett* **2009**, *11*, 1899-1902. (b) Noguchi, H.; Hojo, K.; Suginome, M. *J Am Chem Soc* **2007**, *129*, 758-759. (c) Noguchi, H.; Shioda, T.; Chou, C. M.; Suginome, M. *Org Lett* **2008**, *10*, 377-380.

⁶³ Molander, G. A.; Sandrock, D. L. *J Am Chem Soc* **2008**, *130*, 15792-+.

⁶⁴ (a) Gillis, E. P.; Burke, M. D. *J Am Chem Soc* **2007**, *129*, 6716-+. (b) Gillis, E. P.; Burke, M. D. *J Am Chem Soc* **2008**, *130*, 14084-+. (c) Lee, S. J.; Gray, K. C.; Paek, J. S.; Burke, M. D. *J Am Chem Soc* **2008**, *130*, 466-+.

⁶⁵ See Molander, G. A.; Sandrock, D. L. *J. Am. Chem. Soc.* **2008**, *130*, 15793 and references cited therein.

⁶⁶ Matteson, D. S.; Kim, G. Y. *Org. Lett.* **2002**, *4*, 2153.